

Doctoral theses at NTNU, 2021:120

Ingrid Vikøren Mo

# Towards block polysaccharides: Terminal activation of chitin and chitosan oligosaccharides by dioxyamines and dihydrazides and the preparation of block structures

**NTNU**  
Norwegian University of Science and Technology  
Thesis for the Degree of  
Philosophiae Doctor  
Faculty of Natural Sciences  
Department of Biotechnology and Food Science



Norwegian University of  
Science and Technology



Ingrid Vikøren Mo

# **Towards block polysaccharides: Terminal activation of chitin and chitosan oligosaccharides by dioxyamines and dihydrazides and the preparation of block structures**

Thesis for the Degree of Philosophiae Doctor

Trondheim, April 2021

Norwegian University of Science and Technology  
Faculty of Natural Sciences  
Department of Biotechnology and Food Science



Norwegian University of  
Science and Technology

**NTNU**

Norwegian University of Science and Technology

Thesis for the Degree of Philosophiae Doctor

Faculty of Natural Sciences

Department of Biotechnology and Food Science

© Ingrid Vikøren Mo

ISBN 978-82-326-6212-8 (printed ver.)

ISBN 978-82-326-6507-5 (electronic ver.)

ISSN 1503-8181 (printed ver.)

ISSN 2703-8084 (online ver.)

Doctoral theses at NTNU, 2021:120

Printed by NTNU Grafisk senter

## Acknowledgements

First and foremost, I would like to thank my main supervisor, Professor Bjørn. E. Christensen, for giving me the opportunity to work on this project. Thank you for always having an open-door policy and for being available for discussions, for your interest in new results and for sharing your knowledge and experience with me.

I would also like to thank my co-supervisor Associate Professor Christophe Schatz at Laboratoire de Chimie des Polymères Organiques, University of Bordeaux for his expertise and enthusiasm leading up to fruitful discussions, either on Skype or with physical presence in Bordeaux/Trondheim, and for giving me the opportunity to do some of the work abroad.

Further, I would like to thank all the co-authors for their contributions to the papers included in this thesis with a special thanks to Marianne Ø. Dalheim and Amalie Solberg. I am utterly grateful for all the good discussions in group meetings and collaborations in the lab but also for all the fun we have had on our travels around the world.

Ann-Sissel T. Ulset, Wenche I. Strand and Olav A. Aarstad are thanked for invaluable technical assistance in the laboratory, and Kåre A. Kristiansen is thanked for running the mass spectrometry (MS) analysis and for teaching me the little I know about MS.

All my colleagues at the Department of Biotechnology and Food Science and especially the Biopolymers and Biomaterials group are thanked for creating a good working environment, both scientifically and socially. A special thanks to the girls in “hus-til-hus” who have given me lots of inspiration during these years, including a lot of fun. Also, I would like to express my gratitude to my friends in Trondheim for making the PhD-life bearable through song, dinners and concerts, and the rest of my friends around the country for all the support and love.

I would also like to express my gratitude to my parents, my sister (also my flatmate during the PhD years), my brother and the rest of my family for their encouragement, care, and support, even from a long distance. Mum and dad are also thanked for giving me shelter during the last months of thesis writing. My grandfather is especially thanked for his huge interest in my project (which he never will understand), and for being my proudest supporter. Finally, a big thanks to Eirik, for your love and patience the past year and for laughs and cheering words.

*If you want to go fast, go alone. If you want to go far, go together.*

## **Preface**

This thesis is submitted as a partial fulfilment of the requirements for the academic title *Philosophiae Doctor* at the Norwegian University of Science and Technology (NTNU).

The work of this thesis has been carried out at the Department of Biotechnology and Food Science at NTNU under the supervision of Professor Bjørn E. Christensen. A part of the work was carried out at Laboratoire de Chimie des Polymères Organiques (LCPO) at the University of Bordeaux, France under the supervision of Associate Professor Christophe Schatz.

The thesis consists of a general introduction to the subject of matter, the scope of thesis, a summary and general discussion of the results presented in the three appended papers and appendices, and finally concluding remarks.

## Summary

Polysaccharides are highly abundant and due to the large variation in chemical compositions, they possess a range of intrinsic properties, biological functions, and industrial applications. In the context of block copolymers, polysaccharide-containing structures are attracting increasing interest since they also serve as more sustainable alternatives to copolymers exclusively composed of synthetic polymers. *Block polysaccharides* represent a new class of engineered block polymers, exclusively composed of terminally linked oligo- or polysaccharides. Terminal coupling of blocks will, in contrast to the traditional lateral substitution, retain the intrinsic polysaccharide properties, as it does not perturbate the chain structure. Such block polysaccharides can be relevant for a wide range of applications in e.g. the biomedical and (bio)material fields.

Chitin is the second most abundant polysaccharide found in nature after cellulose and is the major structural component of the exoskeleton of crustaceans and insects. Chitin is a water-insoluble high molecular weight unbranched homopolysaccharide composed of  $\beta$ -1,4-linked *N*-acetylglucosamine (GlcNAc, A) residues, whereas its de-*N*-acetylated derivative, chitosan, has high water-solubility at acidic pH due to the positively charged amino groups ( $pK_a$  approx. 6.5) of the glucosamine (GlcN, D) residues. Chitin and chitosan are particularly interesting in the context of block polysaccharides due to their high abundance, biocompatibility, biodegradability, self-assembling properties (chitin) and positive charge (chitosan).

In the work of this thesis the terminal activation of chitin and chitosan oligomers by a dioxyamine (O,O'-1,3-propanediylbishydroxylamine, PDHA) and a dihydrazide (adipic acid dihydrazide, ADH) using reductive amination with  $\alpha$ -picoline borane (PB) as the reductant was studied in detail. In **Paper I** and **Paper II** the chemistry and kinetics of the reducing end activation of chitooligosaccharides (CHOS) were investigated. A simple *pseudo* first order model was introduced to obtain kinetic data which enable simulation of reactions under different conditions as a tool to develop preparative protocols. Activated CHOS were also purified and thoroughly characterised.

In contrast to other “click” reagents, oxyamines and hydrazides can react directly with the reducing end aldehyde of carbohydrates without an intermediate reaction step. PDHA and ADH can therefore serve as linkers between two polysaccharide blocks for the preparation of AB-type antiparallel block structures. The attachment of a second block to the free end of the linkers was therefore studied in detail in **Paper II**.

Preparation of parallel block polysaccharides or more complex block structures (e.g. ABC-type) additionally require functionalisation of the non-reducing end (NRE). Only a few and highly polysaccharide specific NRE functionalisation methods are available. Chitin can, however, be selectively oxidised by

periodate to obtain a dialdehyde in the NRE residue. The aldehydes can subsequently be activated by PDHA or ADH which enable conjugation of the reducing end of other polysaccharides to the NRE of chitin. Periodate oxidation and subsequent activation chitin oligomers and the preparation of water-soluble chitin-based block polymers by end-coupling of chitin oligomers were studied in **Paper III**.

$D_nXA$  oligomers ( $X = D$  or  $A$ ), prepared by enzymatic degradation of chitosan using chitinase B, and  $A_nM$  or  $D_nM$  oligomers ( $M = 2,5$ -anhydro- $D$ -mannose), prepared by nitrous acid depolymerisation of chitosan, were used in this study. First, activation (amination) of the reducing end by PDHA and ADH was studied.  $D_nXA$  oligomers were shown to have very low reactivity towards the linkers as compared to glucose (Glc) terminated oligomers (obtained from dextran or  $\beta$ -1,3-glucan), but a notably higher reactivity compared to CHOS terminating in  $D$  residues. The yields and type of conjugates (Schiff bases and/or  $N$ -glycosides) formed with  $D_nXA$  were highly linker dependent, whereas the kinetics was highly pH dependent (in the pH range 3.0-5.0). The best compromise between yield and rates was obtained at pH 4.0.  $A_nM$  and  $D_nM$  oligomers were in contrast highly reactive towards PDHA and ADH at all pH values and, due to the pending aldehyde of the  $M$  residue, only Schiff bases (oximes and hydrazones, respectively) were formed in high yields. The kinetics was also independent of the fraction of acetylated residues ( $F_A$ ) of the oligomers.

PB was introduced as the reducing agent for the reductive amination reactions. This reducing agent has lower HSE concerns compared to sodium cyanoborohydride ( $NaCNBH_3$ ) and has proven efficient for reductive amination reactions with carbohydrates. Unreacted  $A_nM$  and  $D_nM$  were rapidly reduced by both PB and  $NaCNBH_3$  and the reductive amination of these oligomers therefore needs to be performed in two consecutive steps. The reduction of  $A_nM$ - or  $D_nM$ -based conjugates formed with PDHA and ADH was fast compared to conjugates formed with the other oligomers and clearly fastest at low pH (3.0). Moreover, hydrazones were faster reduced than oximes. Unreacted  $D_nXA$  oligomers and oligomers terminating in Glc residues were in contrast essentially stable towards the reducing agents. Reductive amination of these oligomers can therefore be performed as conventional one pot. The one pot reductive amination reactions with  $D_nXA$  oligomers were however, limited by extremely slow kinetics, especially with ADH. Hence, the kinetics of these reactions needs to be improved by high concentrations of linkers and PB, higher temperatures and longer reaction times. The reduction of  $D_nXA$ -based conjugates by  $NaCNBH_3$  yielded a different and unidentified type of conjugates, and this reducing agent is therefore not applicable for these oligomers.

The preparation of chitin- and chitosan-based diblock structures was demonstrated by attaching a second oligomer block to the free end of the linkers. An increased reactivity for the free end of both linkers was observed after activation of the first block, which facilitates the use of PDHA and ADH for the preparation of block polysaccharides. To exploit the particularly high reactivity of the  $M$  residues for the preparation



of diblock structures,  $A_nM$  and  $D_nM$  oligomers can be used as the second block. However, to prevent the rapid reduction of unreacted oligomers, an excess of the activated block is recommended to obtain high amination yields prior to reduction. Due to the low reactivity observed for CHOS terminating in A or D residues, such oligomers (e.g.  $D_nXA$ ) should on the other hand be used as the first block for the preparation of block structures. To improve the kinetics of the diblock formation, an excess of the activated block is recommended, also for these preparative protocols. However, this approach requires subsequent purification of the diblocks, and even though gel filtration chromatography was proven useful for the shorter blocks used in this study, other purification methods need to be considered.

A pH dependent degradation of the M residue was observed for the  $D_nM$  oligomers during isolation and purification, but activation of the oligomers prior to isolation preserved the M residue. De-*N*-acetylation of  $A_nM$ -based diblocks was also shown to be an alternative approach for the preparation of chitosan-based diblock structures.

The low water-solubility of chitin limits its applications. The preparation of water-soluble chitin-based diblocks was therefore attempted by conjugating water-insoluble  $A_nM$  oligomers to ADH activated dextran which is highly water-soluble. The results were inconclusive but suggested that the high reactivity of the M residue promotes conjugation to the free end of ADH without the dextran block being able to increase the water-solubility of chitin block. However, very recent (unpublished) results suggest that water-insoluble  $A_nM$  can react with PDHA in DMAc/LiCl. Hence, this solvent can serve as an alternative for the preparation of chitin-based diblock structures with longer water-insoluble chitin blocks.

The vicinal diol in the NRE residue of  $A_nM$  oligomers can be selectively oxidised by periodate to form a dialdehyde. The subsequent activation of oxidised  $A_nM$  by PDHA and ADH revealed a high reactivity of both these aldehydes towards the linkers and the reactivity was even higher than for the pending aldehyde of the M residue. Such oxidised and activated  $A_nM$  oligomers can serve as precursors for more complex block polysaccharides (e.g. ABA- or ABC-type). By reacting oxidised  $A_nM$  oligomers with a sub-stoichiometric amount of PDHA, a discrete distribution of 'polymerised' oligomers was formed. These chitin-based block polysaccharides were, in contrast to chitins of the same length, water-soluble.

## List of papers

### Paper I

**Mo, I. V.**, Feng, Y., Dalheim, M. Ø., Solberg, A., Aachmann, F. L., Schatz, C., Christensen, B. E. (2020). *Activation of enzymatically produced chitoooligosaccharides by dioxyamines and dihydrazides*. Carbohydrate Polymers, 232, 115748.

### Paper II

**Mo, I. V.**, Dalheim, M. Ø., Aachmann, F. L., Schatz, C., Christensen, B. E. (2020). *2,5-anhydro-D-mannose end-functionalised chitin oligomers activated by dioxyamines or dihydrazides as precursors of diblock oligosaccharides*. Biomacromolecules, 21(7), p. 2884-2895.

### Paper III

**Mo, I. V.**, Schatz, C., Christensen, B. E. (2020). *Functionalisation of the non-reducing end of chitin: A new approach to form complex block polysaccharides and soluble chitin-based block polymers*. Manuscript in preparation.

## Symbols and abbreviations

$\alpha$	Degree of scission
A (residue)	<i>N</i> -acetylglucosamine, GlcNAc
ADH	Adipic acid dihydrazide
AmAc	Ammonium acetate
ChiB	Chitinase B from <i>Serratia marcescens</i>
CHOS	Chitooligosaccharides
D (residue)	Glucosamine, GlcN
DP	Degree of polymerisation
DP <sub>n</sub>	Number average degree of polymerisation
F <sub>A</sub>	Fraction of <i>N</i> -acetylated (GlcNAc, A) residues
F <sub>D</sub>	Fraction of de- <i>N</i> -acetylated (GlcN, D) residues
GFC	Gel filtration chromatography
Glc	Glucose
GlcN	Glucosamine, D residue
GlcNAc	<i>N</i> -acetylglucosamine, A residue
HMF	5-hydroxymethyl-2-furfural
HONO	Nitrous acid
NaCNBH <sub>3</sub>	Sodium cyanoborohydride
NMR	Nuclear magnetic resonance
M (residue)	2,5-anhydro-D-mannose
M <sub>n</sub>	Number average molecular weight
M <sub>w</sub>	Weight average molecular weight
MS	Mass spectrometry
PB	$\alpha$ -picoline borane, pic-BH <sub>3</sub>
PDHA	O,O'-1,3-propanediylbishydroxylamine dihydrochloride
pK <sub>a</sub>	Acid dissociation constant

## Contents

<b>Acknowledgements .....</b>	<b>I</b>
<b>Preface.....</b>	<b>II</b>
<b>Summary.....</b>	<b>III</b>
<b>List of papers .....</b>	<b>VI</b>
<b>Symbols and abbreviations .....</b>	<b>VII</b>
<b>1. Introduction.....</b>	<b>1</b>
1.1 General background .....	1
1.2 Block copolymers .....	1
1.2.1 Synthetic block copolymers .....	1
1.2.2 Polysaccharide-containing block copolymers.....	2
1.2.3 Block polysaccharides.....	3
1.3 End functionalisation of polysaccharides and block coupling strategies .....	4
1.3.1 Reducing end functionalisation of polysaccharides .....	4
1.3.2 Non-reducing end functionalisation of polysaccharides .....	4
1.3.3 Block coupling strategies .....	5
1.3.4 Our block coupling strategy .....	7
1.4 Reductive amination .....	8
1.4.1 Reductive amination of carbohydrates.....	9
1.4.2 Kinetic modelling of reductive amination reactions with carbohydrates.....	10
1.5 Periodate oxidation .....	13
1.6 Chitin and chitosan .....	15
1.6.1 Structure and chemical properties.....	15
1.6.2 Preparation of chitooligosaccharides (CHOS).....	16
1.6.3 Applications .....	20
1.7 Dextran.....	21

1.8 $\beta$ -1,3-glucan .....	21
1.9 Purification and characterisation of oligosaccharides .....	22
1.9.1 Gel filtration chromatography (GFC) .....	22
1.9.2 Nuclear magnetic resonance (NMR).....	22
1.9.3 Mass spectrometry (MS).....	24
<b>2. Scope of the thesis .....</b>	<b>25</b>
<b>3. Summary of results and discussion .....</b>	<b>26</b>
3.1 Reducing end activation of $D_nXA$ oligomers prepared by enzymatic degradation .....	26
3.1.1 Preparation of $D_nXA$ oligomers .....	26
3.1.2 Activation of $D_nXA$ oligomers by PDHA and ADH: the amination step .....	27
3.1.3 Comparison to CHOS with D residues at the reducing end .....	30
3.1.4 Activation of $D_nXA$ oligomers by PDHA and ADH: the reduction step .....	30
3.1.5 Comparison to dextran ( $Dext_m$ ) oligomers.....	31
3.2 Reducing end activation of $A_nM$ oligomers prepared by nitrous acid depolymerisation.....	32
3.2.1 Preparation of $A_nM$ oligomers .....	32
3.2.2 Activation of $A_nM$ oligomers by PDHA and ADH: the amination step .....	33
3.2.3 Activation of $A_nM$ oligomers by PDHA and ADH: the reduction step .....	34
3.2.4 Comparison to $D_nM$ oligomers .....	36
3.3 Reductive amination using $NaCNBH_3$ as the reductant: comparison to PB .....	37
3.4 Protocols for the preparation of activated oligosaccharides.....	38
3.4.1 Comparison of activation kinetics for different oligosaccharides.....	38
3.4.2 Two pot reductive amination protocols for $A_nM$ (and $D_nM$ ) oligomers .....	40
3.4.3 One pot reductive amination protocols for oligomers with pyranose reducing end residues ....	40
3.5 Chitin- and chitosan-based diblock polysaccharides .....	41
3.5.1 Chitin- <i>b</i> -chitin diblocks .....	41
3.5.2 Chitin- <i>b</i> -dextran diblocks .....	42

3.5.3 Chitosan-based diblocks .....	43
3.5.4 Diblocks with water-insoluble chitin oligomers .....	44
3.5.5 Purification of diblock polysaccharides .....	45
3.6 Non-reducing end functionalisation of chitin blocks for the preparation of complex block polysaccharides and soluble chitin polymers .....	46
3.6.1 Non-reducing end functionalisation of chitin blocks .....	46
3.6.2 Water-soluble chitin block polysaccharides.....	47
<b>4. Concluding remarks .....</b>	<b>49</b>
<b>5. References.....</b>	<b>53</b>
<b>Appendix I: Preparation and activation of D<sub>n</sub>M oligomers .....</b>	<b>62</b>
<b>Appendix II: Preparation and activation of β-1,3-glucan oligomers.....</b>	<b>67</b>
<b>Appendix III: De-<i>N</i>-acetylation of A<sub>n</sub>M conjugates.....</b>	<b>72</b>
<b>Appendix IV: Chitin-based diblocks from water-insoluble A<sub>n</sub>M oligomers.....</b>	<b>76</b>

**Paper I**

**Paper II**

**Paper III**

## 1. Introduction

### 1.1 General background

There is a general need for new approaches to utilise abundant biomass and to gradually shift the focus from synthetic polymers, often obtained from non-renewable and petroleum-based resources, to biocompatible and biodegradable biopolymers from renewable resources. In this context, polysaccharides are highly relevant due to the large variation in chemical composition and inherent properties ranging from water-soluble and flexible to polysaccharides with high viscosity and self-assembling properties.

Lateral modification of polysaccharides has traditionally been used to prepare polysaccharides with a range of new properties. However, such substitutions or modifications will suppress many of the original chain properties. Terminal linking of polysaccharides to other molecules will in contrast retain their intrinsic properties and provide new and well-defined architectures. This has been widely studied in the context of polysaccharide-containing block copolymers, where a range of different polysaccharides have been linked to synthetic polymers.

Here, we introduce the concept of *block polysaccharides*, where the block structures are exclusively composed of terminally linked polysaccharides. Such structures may have potential in e.g. the field of materials including biomaterials and for different biomedical applications. However, methods to prepare such structures are necessary to be able to study their properties and applications. As a first step, we have therefore developed a method for the preparation of block structures exclusively composed of polysaccharides by terminal coupling of the blocks using bivalent linkers. The coupling strategy was developed for chitin and chitosan due to their high abundance and relevant intrinsic properties such as biocompatibility, biodegradability, self-assembling properties (chitin) and tuneable charge (chitosan). However, we also show that the coupling strategy is versatile and can be used for other polysaccharides.




### 1.2 Block copolymers

#### 1.2.1 Synthetic block copolymers

Block copolymers, composed of two or more chemically dissimilar and terminally linked synthetic blocks, have been around for decades providing polymers with new properties<sup>1</sup>. Their structures can vary from simple AB-type (Figure 1.1a) to more complex ABA-, (AB)<sub>n</sub>- or ABC- type block copolymers<sup>2</sup>. Such block copolymers are generally prepared by bottom-up techniques, with sequential addition of monomers which enable fine tuning of properties and provide a good control over molecular weight and polydispersity<sup>3</sup>. Most synthetic block copolymers are amphiphilic, commonly composed of a hydrophilic and a hydrophobic block, which allow them to self-assemble under appropriate conditions<sup>4</sup>. The self-

## INTRODUCTION

assembly depends on the composition of the copolymer, the relative fraction of blocks and their solubility in relevant solvents. The self-assembly of AB- or ABC-type block copolymers has attracted considerable attention due to their potential to form ordered structures with a wide range of morphologies, including micelles, polymersomes, lamellae and, cylinders with applications in many fields<sup>5,6</sup>.

AB-type block structures	Petroleum based	Boimass derived
a) Synthetic block copolymers 	<input checked="" type="checkbox"/>	<input checked="" type="checkbox"/>
b) Polysaccharide containing block copolymers 	<input checked="" type="checkbox"/>	<input checked="" type="checkbox"/>
c) Block polysaccharides 	<input checked="" type="checkbox"/>	<input checked="" type="checkbox"/>

**Figure 1.1:** General structure of simple AB-type engineered block polymers and the origin of the blocks for **a)** synthetic block copolymers, **b)** polysaccharide containing block copolymers and **c)** block polysaccharides

### 1.2.2 Polysaccharide-containing block copolymers

Polysaccharide-containing block copolymers (Figure 1.1b) are attracting increasing interest since they represent more sustainable alternatives to copolymers exclusively composed of synthetic polymers<sup>3,7</sup>. An emerging number of block copolymers based on polysaccharides with different inherent properties combined with various synthetic blocks is described in the literature. Examples include polysaccharide-*b*-polyethylene glycol (PEG)-based copolymers prepared with either dextran, hyaluronic acid, or chitosan, hence utilising polysaccharides with different inherent properties<sup>8</sup> and dextran-based copolymers prepared with hydrophilic PEG, hydrophobic polystyrene (PS) and thermo responsive poly(*N*-isopropylacrylamide)<sup>9</sup>.

Three main routes for the preparation of polysaccharide-containing block copolymers are described in the literature: Enzymatic polymerisation of the polysaccharide block from a polymeric macroinitiator, polymerisation of a synthetic block from an end-functionalised polysaccharide block, and end-to-end coupling of polysaccharides with preformed synthetic blocks<sup>7</sup>. Even though methods for enzymatic polymerisation are available for some polysaccharides, such bottom-up techniques are not generally applicable<sup>3</sup>. Polymerisation of the synthetic block is also often limited by the conditions where the



polysaccharide is soluble. Most polysaccharide-containing block copolymers are therefore prepared by end-to-end coupling of polysaccharides obtained from natural resources with premade synthetic blocks.

Similar to synthetic block structures, polysaccharide-containing block copolymers have been used as compatibilizers in immiscible polymer blends<sup>10, 11</sup>, emulsifiers<sup>12</sup>, and surfactants<sup>13</sup>. There are also several examples of self-assembling block copolymers prepared with different polysaccharides in the literature<sup>7, 14-16</sup>. The assembly of such structures is, however, mostly governed by self-association of the synthetic (often hydrophobic) block, whereas the hydrophilic polysaccharide block stabilises the assembled polymer core by forming a stable interphase towards the aqueous phase. Such self-assembled nanostructures can be highly relevant for biomedical applications. E.g. micelles and polymersomes, prepared from polysaccharide-containing block copolymers with dextran and hyaluronan, respectively, have shown potential for delivery of the chemotherapeutic drug doxorubicin<sup>17, 18</sup>. Other polysaccharide-containing block copolymers for biomedical applications include chitosan-*b*-PEG block copolymers which formed a temperature-responsive and injectable hydrogel<sup>19</sup>. Polysaccharide-containing hydrogels can have potential as advanced biomaterials for cell encapsulation, tissue engineering, for localized drug delivery or as biodegradable competitors to superabsorbent materials<sup>3</sup>.

The synthetic polymer blocks are, however, not always fully biodegradable and can in some cases be recognised as foreign materials by the immune system and elicit immune responses<sup>20</sup>. Even PEG, which has market approval as a synthetic polymeric therapeutic, has shown drawbacks such as interactions with the immune system and bioaccumulation<sup>21</sup>. In addition, some synthetic blocks, such as PS<sup>3</sup> and poly(acrylamide)<sup>21</sup> can form toxic degradation products. Therefore, block copolymers exclusively composed of natural and non-toxic biopolymers are relevant for improving the current systems involving synthetic polymers for biomedical applications.

### 1.2.3 Block polysaccharides

*Block polysaccharides* represent a new class of engineered block copolymers, exclusively composed of biomass derived blocks (Figure 1.1c). The large variation in structural composition, functional groups and linkages between sugar residues among polysaccharides, can enable the preparation of complex block polysaccharides with tailor-made properties for e.g. biomedical and industrial applications. Polysaccharides with intrinsic self-assembling properties (e.g. chitin, cellulose and  $\beta$ -1,3-glucans) or pH-dependent properties (e.g. chitosan, alginate, hyaluronan) can be relevant for the preparation of self-assembling nanostructures exclusively based on polysaccharides. The end-to-end coupling of polysaccharides through their reducing ends provides block structures with *antiparallel* chains. Coupling of the reducing end of one polysaccharide to the non-reducing end of another block or enzymatic polymerisation of the blocks will in contrast provide structures with *parallel* chains.

## INTRODUCTION

There are, to the best of our knowledge, only a few examples of block structures exclusively composed of oligo- or polysaccharides described in the literature. The examples include a few amphiphilic AB-type block structures prepared by end-to-end coupling of an unmodified saccharide block and a hydrophobic block obtained by lateral modification of the same saccharide, either through acetylation or acetalation of the block backbone<sup>22-26</sup>. Even though a pH-responsive amphoteric block polysaccharide has been prepared using chemoenzymatic methods<sup>27</sup> this approach is less attractive than end-to-end coupling of blocks due to the lack of generality of the method and the need for new approaches to utilise already existing biomass.

### 1.3 End functionalisation of polysaccharides and block coupling strategies

#### 1.3.1 Reducing end functionalisation of polysaccharides

The naturally occurring aldehyde in the open ring form of the reducing end (RE) residue of polysaccharides enables reactions with different nucleophiles such as amines. Reductive amination is therefore the dominating method for RE functionalisation of polysaccharides and has widely been used to introduce reactive groups for further modification, e.g. amine functionalised “click” reagents, or for direct conjugation to amine bearing compounds<sup>7</sup>. Other reducing end functionalisation methods include the conversion to a 1-glycosyl bromide by reaction with HBr<sup>28, 29</sup> which has been used to prepare monohydroxy-terminated cellulose esters, and solvolysis used for the preparation of trimethyl cellulose functionalised with  $\omega$ -unsaturated alcohol<sup>30</sup>. Lactonization of the reducing end residue of dextrans has also been shown to increase their reactivity towards amines<sup>31, 32</sup>. Another reducing end functionalisation method, specific to chitosan, is the nitrous acid depolymerisation which forms chitooligosaccharides with a 2,5-anhydro-D-mannose (M) residue at the reducing end (introduced in detail in chapter 1.6.2.3)<sup>33</sup>. The pending aldehyde of the M residue is highly reactive towards amines as demonstrated by the preparation of self-branched chitosans<sup>34</sup>.

#### 1.3.2 Non-reducing end functionalisation of polysaccharides

Selective functionalisation of the non-reducing end (NRE) of oligo- and polysaccharides is less straight forward. However, some polysaccharide specific methods have been developed. Polysaccharides which only have one pair of vicinal diols (or closely related structures) in the NRE residue, can be selectively oxidised by periodate to obtain a dialdehyde. Such polysaccharides include unbranched 1,3-linked glucans and chitin. Recently, a selective functionalisation method for the NRE of unbranched dextrans was developed<sup>9</sup>, taking advantage of the C6 OH-group which is the only primary alcohol in the polysaccharide. *N*-bromosuccinimide bromination of this OH-group provides a reactive site which can react with amines in a selective displacement reaction with bromide as the leaving group<sup>9</sup>. In addition, lyase- or alkali degradation of 1,4-linked uronides (such as alginate, hyaluronan, heparin and pectin) can form a carbon-carbon double bond (C=C) between C4 and C5 in the NRE residue<sup>35-38</sup>. Thiols can react with such

unsaturated double bonds e.g. through thiol-Michael addition<sup>39</sup> which has been demonstrated for fluorescent labelling of the NRE of heparin<sup>37</sup>.

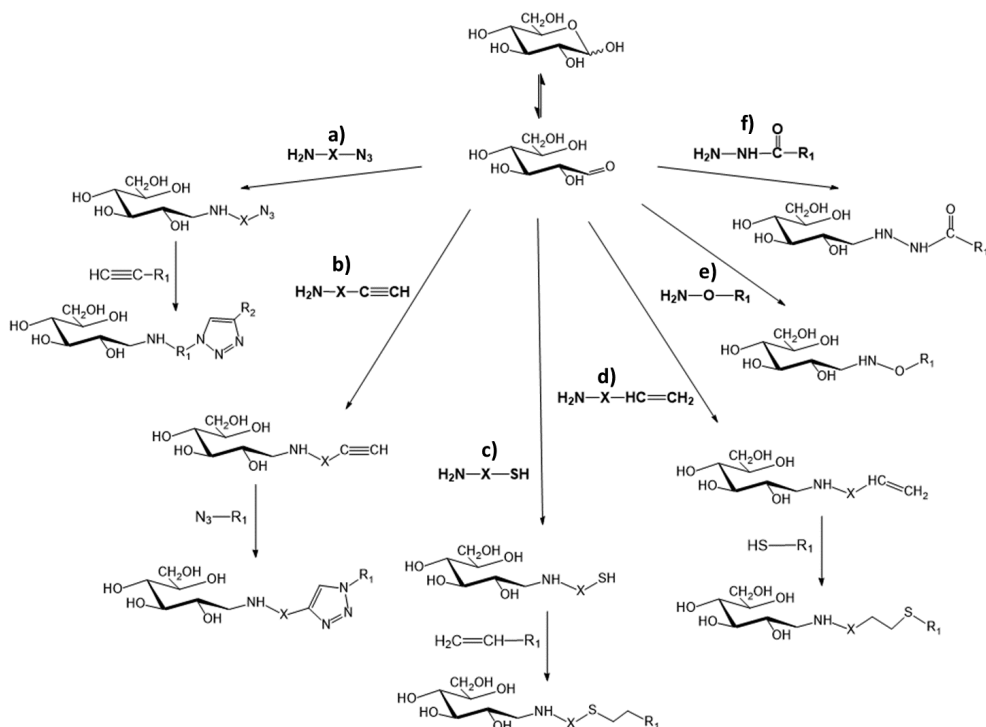
### 1.3.3 Block coupling strategies

“Click” reactions are widely used for various lateral and terminal polysaccharide modifications<sup>39</sup>. The concept of “click” chemistry was first introduced by Sharpless and his co-workers<sup>40</sup> and to qualify as “click”, reactions should be stereospecific, generate only inoffensive and easily removable by-products, give high yields under simple reaction conditions and be easy to perform<sup>39</sup>. This is obtained by orthogonal reactions i.e. direct conjugation of moieties with complementary reactivities without involving or being affected by other functional groups.

Various “clickable” chemical groups, such as azide, alkyne, thiol, or alkene (Figure 1.2a-d), can be introduced to the reducing end of polysaccharides by reductive amination. Hence, block polysaccharides can in theory be prepared by direct coupling of blocks functionalised with complementary “click” reactivities through e.g. copper (Cu)-catalysed azide-alkyne cycloaddition (shown in brief in Figure 1.2a and b) or radical-initiated thiol-ene reaction (shown in brief in Figure 1.2c and d).

Even though these “click” reactions are known to be highly specific and quantitative, the radical induced thiol-ene click reaction has shown limitations for longer (synthetic) blocks<sup>41</sup>, and the Cu-catalyst has been shown to induce oxidative chain cleavage of polysaccharides<sup>7, 39</sup>. Cu can also be difficult to fully remove and traces can remain in the purified product<sup>24</sup>. This is an issue for biological and biomedical applications since Cu can be toxic to cells and organisms in micromolar concentrations<sup>24</sup>. Amino-containing polysaccharides (e.g. chitosans) also have a tendency to chelate heavy metals, which makes the removal of Cu ions even more laborious<sup>42</sup>. Other “click” reactions such as strain promoted (Cu-free) azide-alkyne cycloaddition<sup>43</sup>, thiol-Michael addition, Diels-Alder reactions, or thiol exchange reactions may serve as alternative coupling strategies<sup>39</sup>. However, in the context of block polysaccharides, all these “click” reactions require terminal functionalisation of the blocks prior to coupling, and to our knowledge, only thiol exchange<sup>24</sup> and Cu-catalysed azide-alkyne cycloaddition<sup>22, 23, 25, 26</sup> have been used for the preparation of block oligo- or polysaccharides.

## INTRODUCTION



**Figure 1.2:** Reducing end functionalisation of carbohydrates with various “clickable” groups by reductive amination: **a)** azide, **b)** alkyne, **c)** thiol and **d)** alkene, and the subsequent attachment of a second block ( $R_1$ ) functionalised with a complementary reactivity (alkyne, azide, alkene and thiol, respectively). Direct coupling of a **e)** oxime or **f)** hydrazide functionalised block ( $R_1$ ) to the reducing end of carbohydrates by reductive amination. The general structure of the reducing end residue is illustrated by a D-glucopyranose monomer for all reactions.

Oxime “click” reactions were introduced by Novoa-Carballal and Müller for the preparation of polysaccharide-containing block copolymers<sup>8</sup>. In contrast to other “click” reactions, oxime functionalised PEG was reacted directly with the reducing end residues, without initial functionalisation of the polysaccharide blocks. The oxime click reaction was performed under mild conditions without the use of a metal catalyst or radicals and the oxime conjugates were sufficiently stable for pharmaceutical applications<sup>8</sup>. Subsequent reduction of the oxime provides stable secondary amine conjugates. Hence, reductive amination reactions with oximes can be highly relevant for covalent coupling of polysaccharides to form block structures.

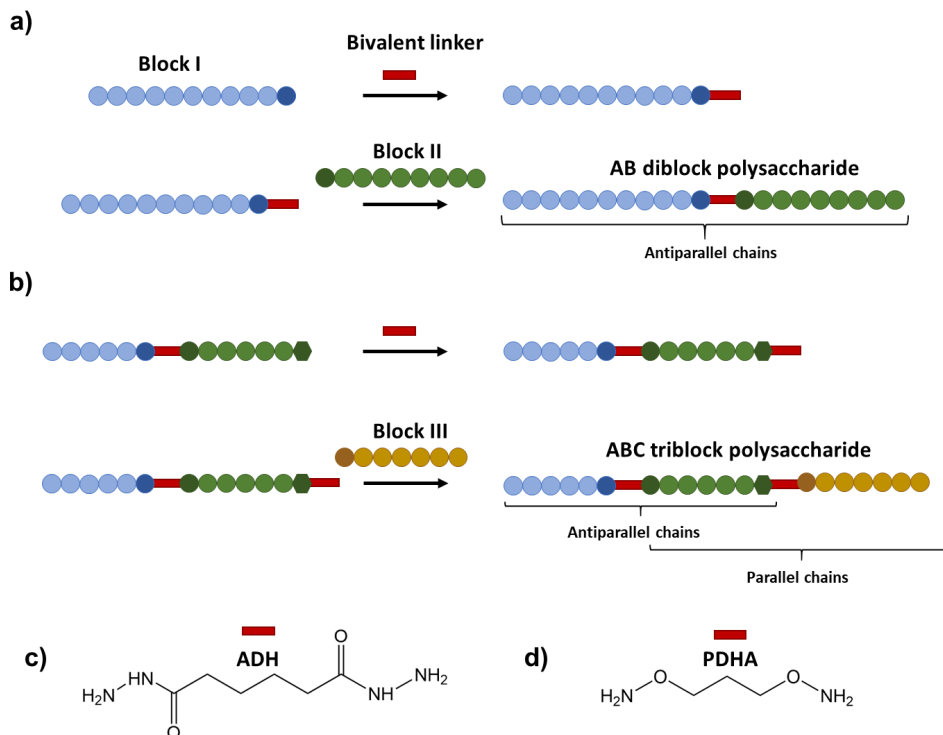
### 1.3.4 Our block coupling strategy

Both oxyamines ( $\text{NH}_2\text{-O-}$ , Figure 1.2e) and hydrazides ( $\text{NH}_2\text{-NH-(CO)-}$ , Figure 1.2f) have higher nucleophilicities than amines<sup>44</sup> and these amine derivatives have been shown to efficiently react with the reducing end aldehyde of carbohydrates<sup>8, 45-48</sup>. With this in mind, bivalent oxyamines or hydrazides (dioxyamines or dihydrazides) can serve as linkers between two polysaccharides for the preparation of antiparallel block structures. Activation of one polysaccharide block by such bivalent molecules and the subsequent attachment of a second polysaccharide block to the free end (Figure 1.3a) requires less steps than other “click” reactions where both ends need to be functionalised prior to coupling.

More complex block polysaccharides, such as ABA- or ABC-types, additionally require reactions at the NRE. As discussed above, only a few and highly polysaccharide specific non-reducing end functionalisation methods are described in the literature. However, by obtaining aldehydes in the non-reducing end residues of polysaccharides, e.g. by periodate oxidation of chitin or  $\beta$ -1,3-glucan, dioxyamine and dihydrazide linkers may also be relevant for the preparation of ABA or ABC triblock polysaccharides with both parallel and antiparallel blocks (Figure 1.3b).

In this study we introduce the use of adipic acid dihydrazide (ADH, Figure 1.3c) and *O,O'*-1,3-propanediylbishydroxylamine (PDHA, Figure 1.3d) as such bivalent linkers for the preparation of block polysaccharides. Both these linkers are commercially available. However, other bi- and multi-functional oxyamine and hydrazide linkers can be prepared with shorter or longer hydrocarbon ( $-(\text{CH}_2)_n-$ ) spacers between the functional groups.

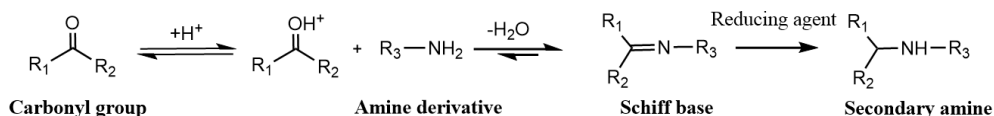
## INTRODUCTION



**Figure 1.3:** **a)** Preparation of antiparallel AB-type diblock polysaccharides by activation of the reducing end of Block I with a bivalent linker and subsequent attachment of Block II to the free end of the linker. **b)** Preparation of ABC-type triblock polysaccharides by non-reducing end (NRE) functionalisation of one of the blocks followed by activation, as in **a)**, and subsequent attachment of Block III to the free end of the linker resulting in structures composed of both antiparallel and parallel chains. Chemical structure of the bivalent linkers **c)** adipic acid dihydrazide (ADH) and **d)** 1,3-propanediylbishydroxylamine (PDHA).

### 1.4 Reductive amination

Reductive amination is a two-step condensation reaction between an amine derivative and a carbonyl group to form a Schiff base which is subsequently reduced to a stable secondary amine (Figure 1.4).



**Figure 1.4:** General mechanism for the reductive amination reaction.

### 1.4.1 Reductive amination of carbohydrates

Reductive amination is widely used for labelling and functionalisation of carbohydrates due to the native aldehyde of the reducing end residue<sup>49-51</sup>. However, due to the low amount of free aldehyde at equilibrium compared to the cyclic hemiacetal forms ( $\alpha$  and  $\beta$ )<sup>52, 53</sup>, reductive amination of carbohydrates is strictly dependent on acid catalysis<sup>54</sup>. Sun *et al.* have described a model for predicting optimal conditions for reactions between amine derivatives and carbohydrates by reductive amination based on the influence of temperature,  $pK_a$  of the amine derivative and pH on the reaction rate and yield<sup>54</sup>. Low pH promotes protonation of the carbonyl oxygen which makes the carbonyl carbon more susceptible towards nucleophilic attack and increases the reaction rate. The pH should, however, be above the  $pK_a$  of the amine derivative as the unshared electron pair makes the amine group reactive. Hence, low pH above the  $pK_a$  of the amine derivative will give the highest amination rates<sup>54</sup>.

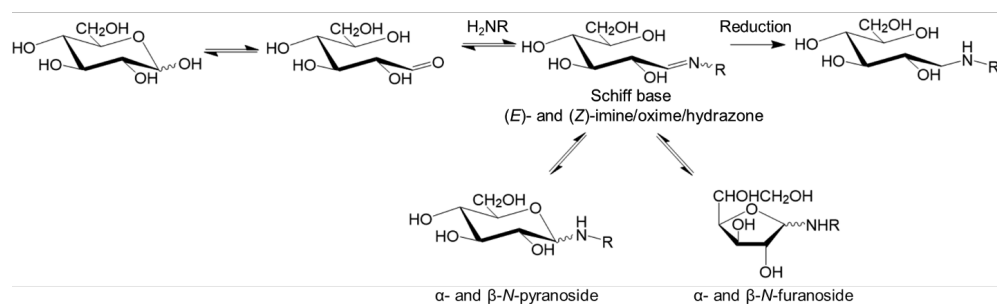
Conventional one-pot reductive amination reactions require reducing agents which selectively reduces Schiff bases over aldehydes and ketones. Sodium cyanoborohydride ( $NaCNBH_3$ ) is a commonly used reducing agent for such reactions, but selective Schiff base reduction is only obtained at neutral pH whereas reduction of aldehydes and ketones is favoured at low pH (3-4)<sup>55</sup>. Hence, the need for acid catalysis for reactions with carbohydrates limits the use of  $NaCNBH_3$  in one pot reductive amination protocols. Another major drawback with the use of  $NaCNBH_3$  is the formation of volatile and toxic hydrogen cyanide (HCN) upon hydrolysis which limits its applicability in the context of green chemistry, especially in industry. Alternative reducing agents such as sodium triacetoxyborohydride ( $NaBH(OAc)_3$ )<sup>56</sup> and pyridine borane ( $pyr-BH_3$ )<sup>57</sup> have shown similar Schiff base selectivity and reducing efficacy, but are limited by solvent specificity and low stability, respectively<sup>58</sup>.  $\alpha$ -picoline borane (PB) has in contrast been introduced as a cheap, a non-toxic and commercially available alternative to  $NaCNBH_3$  for the reductive amination of carbohydrates with equal or even better reducing efficacy<sup>50, 51, 59, 60</sup>. Reductive amination with PB has also been shown to be highly efficient in water, even though it is generally accepted that strict anhydrous conditions are favourable for reductive amination and other dehydration reactions<sup>58</sup>. This is advantageous for reactions with carbohydrates, most of which are highly water-soluble<sup>51</sup>.

Due to the low nucleophilicity of primary amines and the reduced reactivity of the masked aldehyde of the reducing end residue, aniline can be used as a catalyst for the reductive amination of carbohydrates<sup>61</sup>. Aniline can, however, give side products<sup>61, 62</sup> and its toxicity may raise HSE concerns.

Both acyclic (Schiff bases) and cyclic (*N*-glycosides i.e. *N*-pyranosides and *N*-furanosides) conjugates can be formed upon reaction of amine derivatives with the reducing end of carbohydrates (Figure 1.5). The relative distribution of conjugates depends on the nature of the reducing end and the chemistry of the amine derivative<sup>45</sup>.

## INTRODUCTION

Oxyamines and hydrazides have higher nucleophilicities as compared to amines<sup>44</sup> and have therefore been introduced for the functionalisation of the reducing end of carbohydrates. Their low basicity (low  $pK_a$ ) allows them to conjugate to carbohydrates under acidic conditions and the resulting Schiff bases (oximes and hydrazones) have shown increased hydrolytic stability as compared to Schiff bases formed with amines (imines)<sup>63</sup>. Oxyamines tend to form acyclic oximes with carbohydrates, both in the (*E*)- and (*Z*)-configuration, in equilibrium with cyclic *N*-glycosides<sup>47</sup>. Hydrazides, on the other hand, predominantly form *N*-glycosides when conjugated to carbohydrates under acidic conditions<sup>48, 64</sup>. The subsequent reduction of conjugates to form stable secondary amines depends on the distribution of conjugates due to the sluggish (i.e. rate limiting) conversion from cyclic to reducible acyclic Schiff bases<sup>49</sup>.



**Figure 1.5:** Reaction of the free aldehyde at the reducing end of carbohydrates with amine derivatives ( $H_2NR$ ) and the subsequent reduction of the Schiff bases to form stable secondary amines. D-glucopyranose is here shown as example. Based on Ramsay *et al.*<sup>49</sup>.

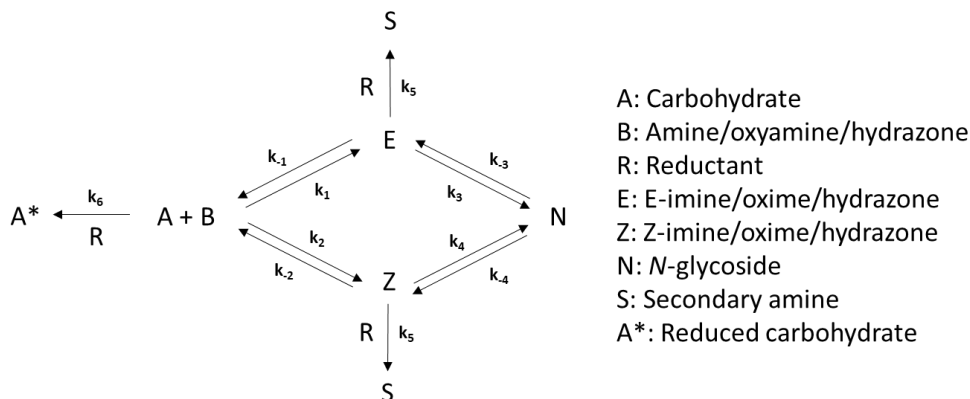
### 1.4.2 Kinetic modelling of reductive amination reactions with carbohydrates

Reaction modelling is a powerful tool to simulate reactions and to predict the effects of different conditions (e.g. concentrations of reactants). In the work of this thesis we introduce the use of reaction modelling to obtain kinetic data for the reductive amination reactions as a tool to develop preparative protocols and to compare the reactivity of different carbohydrates towards oxyamines and hydrazides under the same conditions or the reactivity of the same carbohydrates under different conditions (e.g. variations in pH).

Reductive amination reactions with carbohydrates are complex reactions comprised of several individual reaction steps with independent rates and rate constants (Figure 1.5). The overall reaction with amines, oxyamines or hydrazides involves amination of the carbohydrate, where *E*- and *Z*-imines, oximes, or hydrazones (Schiff bases) are formed, respectively. For carbohydrate reducing ends where the aldehyde is in equilibrium with a hemiacetal, the acyclic Schiff bases are in equilibrium with cyclic *N*-glycosides (*N*-pyranosides or *N*-furanosides). The Schiff bases are irreversibly reduced to stable secondary amine conjugates upon addition of reducing agent. Irreversible reduction of the carbohydrates by the reducing



agent will, however, prevent the reductive amination reaction from going to completion. The general reaction scheme for the reductive amination of carbohydrates is shown in Figure 1.6, however, simplified with only one cyclic *N*-glycoside conjugate in equilibrium with the acyclic E- and Z-conjugates.



**Figure 1.6:** General reaction scheme for the reductive amination of carbohydrates including assigned rate constants for each independent reaction step involved. Reversible reactions are described by two rate constants (forward and reverse), whereas irreversible reactions are described by one rate constant. For simplification, the reaction scheme assumes one cyclic product (*N*-glycoside) formed from both E- and Z- amines/oxyamines/hydrazones and the same rate constant for the reduction of E- and Z- to secondary amines ( $k_5$ ).

When considering such reactions to be *first order* with respect to each reactant (abbreviations from Figure 1.6), reaction rates can be determined by the following equations

$$\frac{d[A]}{dt} = -k_1[A][B] + k_{-1}[E] - k_2[A][B] + k_{-2}[Z] - k_6[A][R] \quad (\text{Eq. 1})$$

$$\frac{d[B]}{dt} = -k_1[A][B] + k_{-1}[E] - k_2[A][B] + k_{-2}[Z] \quad (\text{Eq. 2})$$

$$\frac{d[R]}{dt} = -k_5[E][R] - k_5[Z][R] - k_6[A][R] \quad (\text{Eq. 3})$$

$$\frac{d[E]}{dt} = k_1[A][B] - k_{-1}[E] - k_3[E] + k_{-3}[N] - k_5[E][R] \quad (\text{Eq. 4})$$

$$\frac{d[Z]}{dt} = k_2[A][B] - k_{-2}[Z] - k_4[Z] + k_{-4}[N] - k_5[Z][R] \quad (\text{Eq. 5})$$

$$\frac{d[N]}{dt} = k_3[E] - k_{-3}[N] + k_4[Z] - k_{-4}[N] \quad (\text{Eq. 6})$$

## INTRODUCTION

$$\frac{d[A^*]}{dt} = k_6[A][R] \quad (\text{Eq. 7})$$

$$\frac{d[S]}{dt} = k_5[Z][R] + k_5[E][R] \quad (\text{Eq. 8})$$

The concentration of each reactant or product at specific time points,  $[X]_t$ , can be obtained from the reaction rates by the following equation

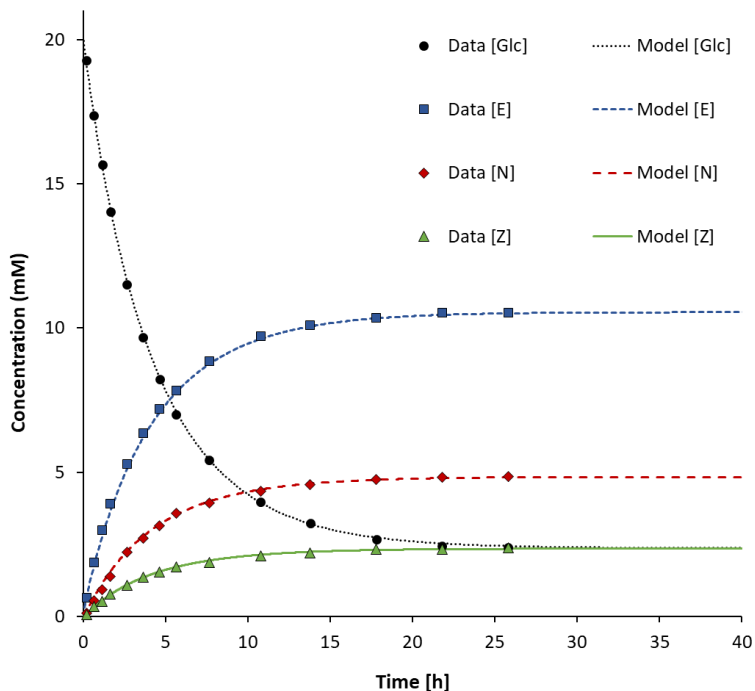
$$[X]_t = [X]_{t-\Delta t} + \frac{d[X]}{dt} \Delta t \quad (\text{Eq. 9})$$

where,  $t$  is the time, and  $\Delta t$  is the time difference from last modelled time point. Numeric modelling of such reactions can be performed by substituting differentials of the type  $d[X]/dt$  with  $\Delta[X]/\Delta t$ . From starting concentrations  $[A]_0$ ,  $[B]_0$  etc, the concentrations at successive time increments  $t_{i+1} = t_i + \Delta t$  can inductively be calculated as

$$[X]_{i+1} = [X]_i + \left( \frac{\Delta[X]_i}{\Delta t} \right) \Delta t \quad (\text{Eq. 10})$$

The *pseudo* first order kinetic model can be fitted to the experimental data by adjusting the rate constants ( $k_x$  and  $k_{-x}$ ). All reaction modelling presented in the work of this thesis was carried out using this numeric approach in Excel. The time interval ( $\Delta t$ ) was chosen sufficiently small to result in a simulation which did not further change when choosing an even smaller time interval. The model was fitted to experimental data by adjusting the rate constants to give the minimum sum of squares.

Modelling of reductive amination reactions with carbohydrates can be challenging due to the large number of individual reactions which need to be considered. To simplify the reaction modelling, amination products (E-/Z-amines/oximes/hydrazones and cyclic *N*-glycosides) can be treated as one product. The reduction can also be modelled separately by obtaining data for the reduction after the formation of amination products. An example of the *pseudo* first order kinetic model fitted to experimental data obtained for the reaction of glucose (Glc) with an oxyamine (PDHA) without reducing agent is given in Figure 1.7. Here, the formation of E-oximes (E), Z-oximes (Z) and *N*-glycosides (in this case  $\beta$ -*N*-pyranosides, N) was modelled separately.



**Figure 1.7:** Example of the *pseudo* first order model fitted to experimental data (concentrations in mM over time) obtained in the reaction of glucose (Glc) with an oxyamine (PDHA). E: E-oximes, Z: Z-oximes, N: N-glucosides (in this case  $\beta$ -N-pyranosides).

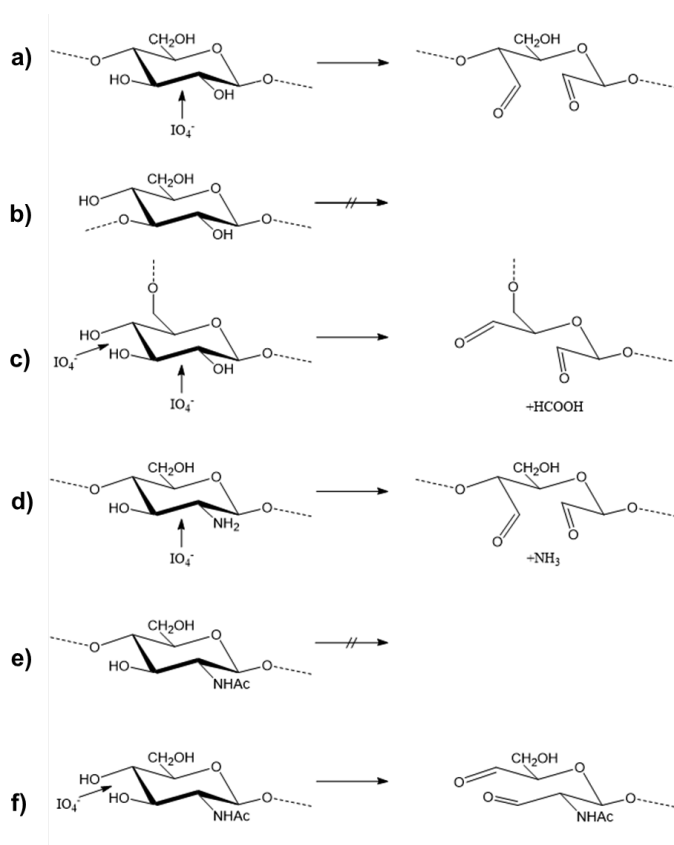
### 1.5 Periodate oxidation

Periodate oxidation was traditionally used for structure determination of complex carbohydrates by the well-known Smith degradation<sup>65</sup>. In more recent years, periodate oxidation has more commonly been used for physical modification of polysaccharides by providing e.g. chain extension, flexibility, and hydrolytic lability, or for chemical modification by functionalising of oxidised residues through aldehyde-based reactions<sup>66</sup>.

The periodate ion ( $\text{IO}_4^-$ ) oxidise vicinal diols or closely related structures such as 2-hydroxylaldehydes, 1,2-dicarbonyl compounds, and  $\alpha$ -hydroxy and  $\alpha$ -keto acids or  $\alpha$ -amino alcohols to dialdehydes<sup>66</sup>. The vicinal diols (or closely related structures) must be oriented in an equatorial-equatorial or axial-equatorial position for the oxidation to occur<sup>66</sup>. 1,4-linked glucans have one pair of vicinal diols prone to oxidation in every glucose residue along the polysaccharide backbone (Figure 1.8a). The ability to be oxidised for other polysaccharides is limited by modification of the OH groups and linkage geometry. E.g. 1,3-linkages will

## INTRODUCTION

render glucose residues along glucan chains resistant to periodate oxidation (Figure 1.8b). The residues of 1,6-linked glucans (Figure 1.8c) have three consecutive OH-groups which will result in a double oxidation of the residue and the release of formic acid. The dialdehydes formed after periodate oxidation can readily form inter- or intra-residue hemiacetals<sup>67</sup> which are acid stable and difficult to structurally elucidate<sup>65</sup>.



**Figure 1.8:** The impact of the periodate ion ( $\text{IO}_4^-$ ) on **a**) 1,4-linked glucose residues (oxidation), **b**) 1,3-linked glucose residues (no oxidation) **c**) 1,6-linked glucose residues (double oxidation with the release of formic acid) **d**) 1,4-linked glucosamine residues (oxidation with the release of ammonia) **e**) 1,4-linked *N*-acetylglucosamine residues (no oxidation) **f**) the non-reducing end residue of 1,4-linked *N*-acetylglucosamine residues (oxidation).

The  $\beta$ -1,4-linked glucosamine residues of chitosan are prone to oxidation by periodate due to the amino group of C2 ( $\alpha$ -amino alcohol). Nitrogen is released as ammonia upon oxidation (Figure 1.8d), which can be detected and quantified as a measure of the degree of oxidation<sup>66</sup>. Depolymerisation of chitosan has been shown to occur concomitantly with the oxidation which exposes new periodate consuming end residues.

The rate of both oxidation and depolymerisation and hence, the extent of overoxidation, is reduced with higher  $F_A$ <sup>68</sup>. Internal  $\beta$ -1,4-linked *N*-acetylglucosamine residues are, in contrast to glucosamine residues, resistant to periodate oxidation (Figure 1.8e), whereas non-reducing end residues are prone to oxidation by periodate due to the vicinal diol (Figure 1.8f). Periodate oxidation can therefore serve as a selective non-reducing end functionalisation method for fully *N*-acetylated chitin oligomers<sup>69</sup>.

## 1.6 Chitin and chitosan

Chitin is the second most abundant polysaccharide found in nature after cellulose. It occurs mainly as a structural component in the cell walls of yeast and fungi, and in the exoskeleton of crustaceans and insects<sup>70</sup>. Chitosan is less commonly found naturally in nature, but has been isolated from the mycelia of the fungus *Mucor rouxii*<sup>71, 72</sup>. Chitin is available in large quantities as a by-product from the seafood processing industry<sup>73</sup> and chitosan is commonly obtained from chitin by partial de-*N*-acetylation.

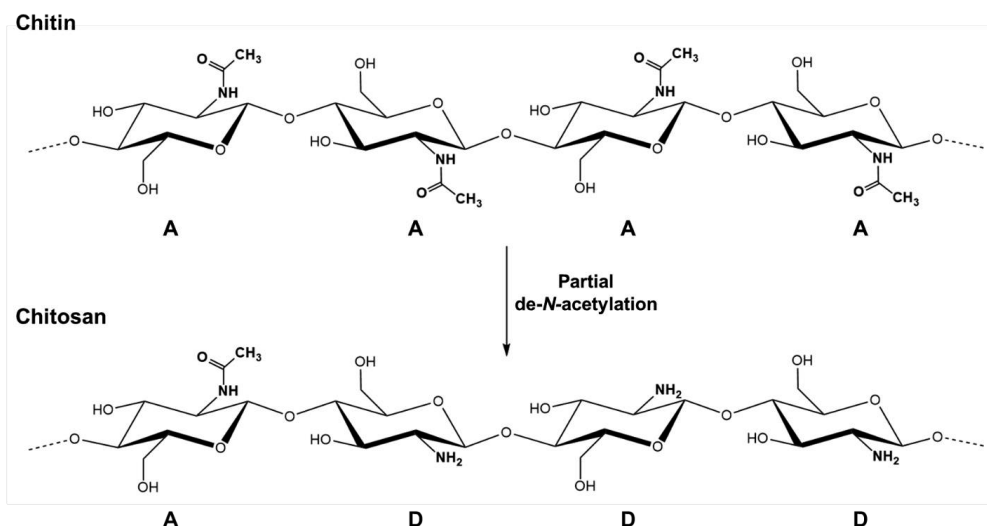
### 1.6.1 Structure and chemical properties

Chitin is a high molecular weight unbranched homopolysaccharide composed of  $\beta$ -1,4-linked *N*-acetylglucosamine (GlcNAc, A) residues (Figure 1.9). Chitin resembles cellulose both in its chemical structure, being a cellulose derivative with an acetamido group at C2, and in its biological function as a structural polysaccharide<sup>73</sup>. There are two main allomorphs of chitin:  $\alpha$  and  $\beta$ .  $\alpha$ -chitin, where the polymer chains are arranged in an antiparallel manner and packed densely by intra- and intermolecular hydrogen bonds, is the most abundant form.  $\beta$ -chitin is composed of less tightly packed parallel chains and is less abundant in nature but has been found in e.g. squid pens<sup>70</sup>. Due to its crystallinity and low water-solubility, chitin has few applications other than serving as a raw material for the preparation of chitosan, chitooligosaccharides and glucosamine<sup>73</sup>.

Partial de-*N*-acetylation of chitin provides chitosan with varying amounts of glucosamine (GlcN, D) residues, and chitosans are commonly described by the fraction of residual A residues ( $F_A$ ) following de-*N*-acetylation (Figure 1.9)<sup>74</sup>. The distribution of A and D residues after homogenous de-*N*-acetylation of chitin is random, whereas heterogenous de-*N*-acetylation, where chitin remains insoluble, leads to the formation of a chitin fraction with high  $F_A$  and a chitosan fraction with low  $F_A$ <sup>74, 75</sup>. Due to the free amino group of the D residues in chitosan, this polysaccharide has a polycationic character when  $\text{pH} < \text{pK}_a$  with an expanded structure due to the electrostatic repulsion between charged residues which gives chitosan a rather high intrinsic viscosity. Chitosan is in fact the only pseudo-natural polycationic polysaccharide which can be isolated from biomass. The  $\text{pK}_a$  of chitosans is approximately 6.5 and has been shown to be independent of their composition ( $F_A$ )<sup>76</sup>. The solubility of chitosans depends on their  $F_A$ , pH, ionic strength and molecular weight (chain length). High molecular weight chitosans with low  $F_A$  (between 0 and 0.2) are

## INTRODUCTION

only soluble in aqueous solutions at low pH, and precipitates when pH approaches  $pK_a^{77}$ . In contrast, chitosans with  $F_A$  between 0.4 and 0.6 are also soluble at neutral pH, due to the decreased possibility of aligning neutral polymer chains with higher amount of A residues<sup>75, 78</sup>.



**Figure 1.9:** The chemical structure of chitin, a homopolymer composed of  $\beta$ -1,4-linked *N*-acetylglucosamine (GlcNAc, A) residues, and its partially de-*N*-acetylated derivative, chitosan, a heteropolymer composed of  $\beta$ -1,4-linked *N*-acetylglucosamine and glucosamine (GlcN, D) residues.

### 1.6.2 Preparation of chitooligosaccharides (CHOS)

Chitooligosaccharides (CHOS) are homo or heterooligomers of glucosamine and/or *N*-acetylglucosamine residues prepared by either chemical or enzymatic depolymerisation of chitosan. Their composition ( $F_A$ ), degree of polymerisation (DP), and sequence (pattern of acetylation) depend on the degradation method, conditions, and the composition of the degraded chitosan.

#### 1.6.2.1 Acid hydrolysis

CHOS can be prepared by common acid hydrolysis, typically using dilute or concentrated hydrochloric acid (HCl). A-A and A-D glycosidic linkages are cleaved with an equal rate and three orders of magnitude faster than D-A and D-D linkages in concentrated HCl, and the hydrolysis rate therefore depends on the  $F_A$  of the degraded chitosan<sup>79</sup>. The low water content of concentrated HCl also prevents hydrolysis of the *N*-acetyl linkage, whereas the rate of de-*N*-acetylation is equal to the rate of hydrolysis of glycosidic linkages in dilute acid. This is assumingly due to the fact that the de-*N*-acetylation is a  $S_N2$  reaction where addition of water to the carbonium ion is the rate-limiting step, whereas hydrolysis of the glycosidic linkages is a

$S_N1$  reaction where the formation of the carbonium ion is the rate-limiting step<sup>79, 80</sup>. Hence, the degree of scission ( $\alpha$ ), the number average degree of polymerisation ( $DP_n$ ) and  $F_A$  of the resulting CHOS depend on the acid concentration. However, due to the random distribution of A and D residues in chitosans<sup>74</sup> the sequence of the oligomers cannot be predetermined by this degradation method.

### 1.6.2.2 Enzymatic hydrolysis

Enzymatic degradation using glycoside hydrolases such as e.g. chitinases or chitosanases is another common method for preparation of CHOS. The  $F_A$ , sequence and  $DP_n$  of the resulting CHOS mixture depend on the chitosan substrate and the specificity of the enzyme used<sup>81</sup>.

Subsites in the active site of glycoside hydrolases are labelled from  $-n$  to  $+n$ , where  $n$  is an integer depending on the number of subsites.  $-n$  represent subsites where sugar residues of the new reducing end formed after cleavage are attached, whereas  $+n$  represents subsites for binding of residues which will be at the non-reducing end of a new sugar chain after cleavage. The hydrolysis of the glycosidic linkage takes place between the  $-1$  and  $+1$  subsites<sup>82</sup>.

Chitinase B (ChiB, EC 3.2.1.14) from *Serratia marcescens* is a family 18 chitinase. This exoenzyme hydrolyse chitosan processively (without releasing the substrate) from the non-reducing end. The active site of ChiB has six sugar-binding subsites, labelled from  $-3$  to  $+3$ . The  $-1$  subsite has an absolute specificity for A residues<sup>83</sup> as the carbonyl oxygen from the *N*-acetyl group of the A residue catalyse the hydrolysis reaction by acting as a nucleophile in the formation of an oxazolinium ion intermediate<sup>81</sup>. The  $-2$  subsite also have a strong but less stringent specificity for A residues. Hence, the degradation is described by biphasic kinetics, where the fast phase is dominated by the cleavage on the reducing side of oligomers with A residues occupying both the  $-1$  and  $-2$  subsite of the active site, while the slower phase reflects the cleavage on the reducing side of oligomers with one A residue and one D residue occupying the  $-1$  and  $-2$  subsite, respectively<sup>83</sup>. CHOS prepared using ChiB will for this reason always have A reducing end residues. Depending on the  $F_A$  of the degraded chitosan and the time of action for the enzyme (extent of degradation), CHOS with predetermined  $F_A$  and sequence can be prepared. E.g. complete degradation (long degradation time) of a chitosan with low  $F_A$  using ChiB will only produce  $D_nXA$  oligomers, where  $D_n$  is a homogenous sequence of D residues and X is either a D or an A residue.

### 1.6.2.3 Nitrous acid depolymerisation of chitosan

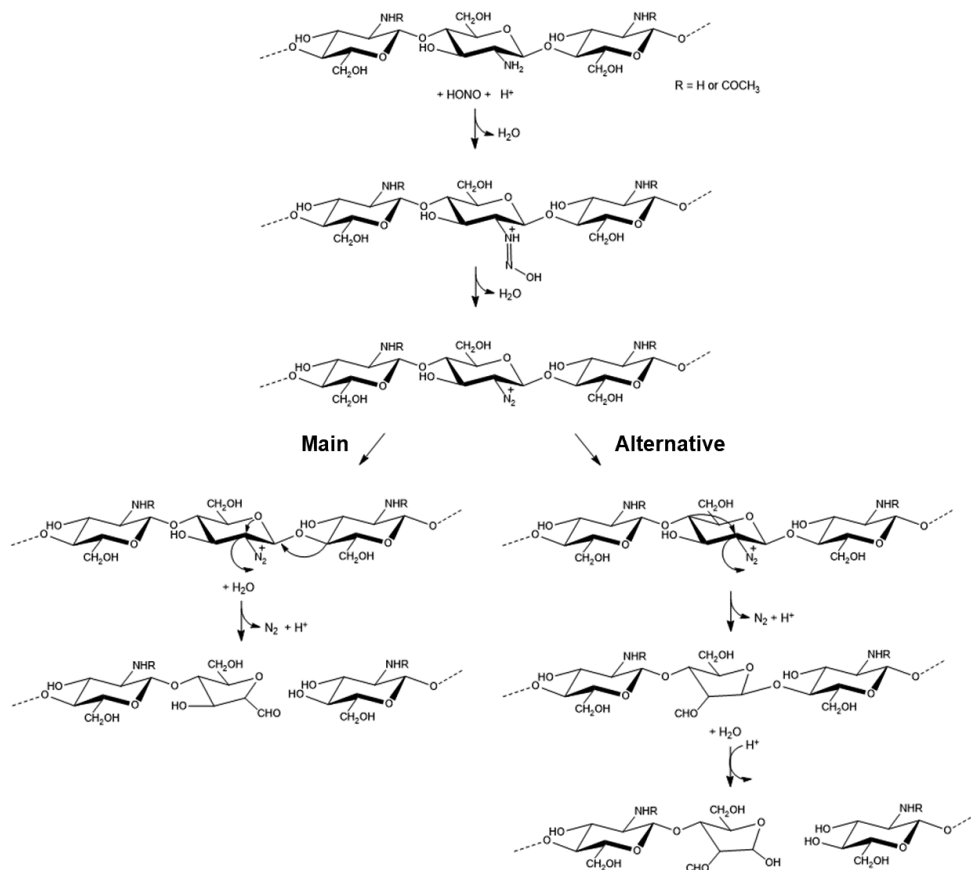
Nitrous acid (HONO) depolymerisation of chitosan is a commonly used method for the preparation of CHOS with a 2,5-anhydro-D-mannose (M) residue at the reducing end. The nitrous acid only affects the D residues of chitosan which are converted to M residues by deamination, whereas A residues remain unaffected. The reaction is first order with respect to concentration of HONO and D residues and one mole

## INTRODUCTION

of HONO is consumed per deamination subsequently followed by chain scission. The rate of depolymerisation is independent of the molecular weight of chitosan, and the degree of scission ( $\alpha$ ) is therefore only dependent of the fraction of D residues ( $F_D = 1 - F_A$ ) and the concentration of HONO<sup>84, 85</sup>. The nitrous acid depolymerisation is well known, cheap, fast, homogenous and easy to control and therefore offers several advantages over enzymatic degradation and hydrolysis by other acids<sup>86</sup>.

The mechanism for the nitrous acid depolymerisation was first proposed by Peat<sup>87</sup> and later reviewed by others<sup>88-90</sup>. The first step of the depolymerisation mechanism (Figure 1.10, *Main*) is protonation of the nitrous acid to form an acidium ion ( $\text{NH}_2\text{O}_2^+$ ) which attacks the amino group of a D residue and forms an unstable *N*-nitrosamine. Subsequent rearrangement of the *N*-nitrosamine and the release of water results in an unstable diazonium ion. The release of nitrogen by heterolysis results in the formation of a high-energy carbonium ion which is attacked by the ring oxygen. This leads to the formation of a furanose with a pending aldehyde at C1 of the ring, simultaneous as the glycosidic linkage is broken, resulting in a M residue at the new reducing end<sup>88-90</sup>. An alternative mechanism, where C4 of the ring attacks the carbonium ion, has also been suggested in the literature<sup>91, 92</sup>. This alternative deamination mechanism results in the formation of a furanose residue with the pending aldehyde at C2 of the ring but will not, in contrast to the main mechanism, result in cleavage of the glycosidic linkage (Figure 1.10, *Alternative*). The glycosidic linkage is, however, labile to acid hydrolysis after the rearrangement and can be cleaved under conditions which leave ordinary glycosidic linkages unaffected<sup>92</sup>. Hence, oligosaccharides with this alternative M reducing end residue can in theory be formed but have, to our knowledge, not been reported in the literature.





**Figure 1.10:** Mechanism for the nitrous acid (HONO) depolymerisation of chitosan (*main*) and the alternative deamination mechanism (*alternative*) leading to chain scission after subsequent acid hydrolysis.

According to Allan and Payron<sup>34</sup> there are no by-products of the nitrous acid depolymerisation, except the degradation of the M residue which leads to the formation of 5-hydroxymethyl-2-furfural (HMF). HMF is a common by-product of Millard browning and in the case of chitosan this product can be formed when the pending aldehyde of the M residue reacts with the unprotonated amino group of a D residue ( $\text{pH} > \text{pK}_a$ ) to form a Schiff base. The Schiff base-formation is followed by two acid catalysed eliminations of water and chain cleavage which results in the formation HMF and a chitooligomer with a normal (A or D) reducing end residue<sup>33</sup>. Hence, degradation of the M residue is highly pH dependent. The standard procedure to prevent the abovementioned degradation is to reduce the M residue to the corresponding 2,5-anhydro-D-

## INTRODUCTION

mannitol by e.g. sodium borohydride ( $\text{NaBH}_4$ )<sup>85</sup>. Reduction of the pending aldehyde will, however, remove the reactivity of the M residue for subsequent conjugation reactions.

Nitrous acid depolymerisation of chitosan has previously been used to prepare fully *N*-acetylated and fully de-*N*-acetylated CHOS with M reducing end residues by varying the concentration of nitrous acid and the  $F_A$  of the chitosan<sup>33</sup>. E.g. fully *N*-acetylated oligomers with M residues at the reducing end ( $A_nM$ ) can be prepared using an excess of HONO relative to the  $F_D$ . In contrast, fully de-*N*-acetylated oligomers ( $D_nM$ ) can be prepared by degrading a chitosan with a low  $F_A$  (e.g.  $F_A < 0.001$ ) using a sub-stoichiometric amount of HONO. The  $DP_n$  of the oligomers can be tuned by the choice of  $F_A$  in the first case, and the concentration of HONO in the latter.

Compared to pyranose reducing end residues of carbohydrates, where the aldehyde is in equilibrium with the hemiacetal, the pending aldehyde of the M residue is more available for reactions. The high reactivity of the M residue been exploited to prepare self-branched chitosans<sup>34</sup> and reducing end functionalised chitosans as precursors for chitosan-based block copolymers<sup>8, 93-95</sup>.

### 1.6.3 Applications

Chitin and chitosan are non-toxic, biocompatible, and biodegradable, and have numerous applications in the fields of agriculture, cosmetics, water treatment, biomedicine, pharmacy, and food and nutrition<sup>96</sup>. Applications of chitin are, however, often limited by its low water-solubility. Chitosan, on the other hand have unique and thoroughly explored properties such as film- and gel-forming ability, antimicrobial activity, biocompatibility, biodegradability and surface active properties<sup>70, 97</sup>. Chitosan applications are, however, also limited by its poor solubility under neutral and basic conditions or its high viscosity of high molecular weight chitosan in dilute acidic solutions<sup>93</sup>. The use of chitosan also suffers from the inability to reproduce the composition of the polymer. It is therefore a growing interest towards the use of more defined CHOS and their derivatives for various applications.

Compared to longer chitosans, CHOS have higher water-solubility and lower viscosity in aqueous solutions<sup>93</sup>. Shorter CHOS with low  $F_A$  also have higher solubility at neutral pH. COS are known to possess diverse biological activities such as antifungal, antibacterial, immunoregulatory and antioxidant effects<sup>98, 99</sup>. In the context of human health, various medical applications of CHOS have been reported, including inhibition of tumour growth, vectors for gene delivery, improvement of bone strength, haemostatic agents in wound-dressings and anti-malaria agents<sup>81, 100</sup>.

The biological activities of CHOS are significantly related to their  $F_A$  and  $DP$ <sup>101, 102</sup>. The preparation of well-defined CHOS mixtures or single CHOS with specific DP and composition has therefore attracted

more attention lately. There are several methods for isolation, purification and characterisation of defined CHOS<sup>81, 102</sup>. Some of these methods are described in chapter 1.9.

### 1.7 Dextran

Dextran is a highly flexible and neutral homopolymer composed of  $\alpha$ -1,6-linked glucose residues. The polysaccharide backbone may be branched with  $\alpha$ -linked glucose chains from the secondary hydroxyl groups in position 2, 3 or 4 of the glucose residues<sup>103</sup>. Dextran is synthesised from sucrose by the enzyme dextran sucrose in a number of bacteria from the *Lactobacillae* family (e.g. *Leuconostoc* and *Streptococcus*) and other microorganisms<sup>104</sup> and the nature and the degree of branching depends on the dextran-producing microorganism<sup>103</sup>. Dextran can also be synthesised from maltodextrins by the enzyme dextran dextrinase found in certain *Gluconobacter* strains<sup>105</sup>.

Industrial biosynthesis of dextran is commonly performed using *Leuconostoc mesenteroides* which produce high molecular dextran with low antigenicity and low degree of branching<sup>103, 105</sup>. The low degree of branching and hence, high percentage of  $\alpha$ -1,6-linkages (95%) is advantageous for clinical applications of dextrans since enzymes in the human body only can slowly hydrolyse such linkages in contrast to e.g.  $\alpha$ -1,4-linkages which are rapidly hydrolysed by human  $\alpha$ -amylases. The low antigenicity prevents dextran from being recognised by antibodies generated as a result of the immune response to a foreign substance<sup>105</sup>.

Initially, dextran was introduced for clinical use as a plasma volume expander<sup>105, 106</sup>. Lately, numerous other applications of dextrans and dextran derivatives are described in the literature e.g. as additives in food and cosmetics, and for various biomedical applications<sup>105</sup>. However, the most widely use of this polysaccharide is the cross-linked dextran commercialised as Sephadex®. Sephadex and Sephadex derivatives are used as filling in gel filtration chromatography columns and has revolutionised the purification of biomacromolecules such as proteins, nucleic acids, and oligo- and polysaccharides<sup>105</sup>.

Dextran has also been suggested as a natural analogue to the synthetic polymer polyethylene glycol (PEG) for biomedical applications, due to its high water-solubility, neutral character, biocompatibility, biodegradability and low immunogenicity<sup>18</sup>.

### 1.8 $\beta$ -1,3-glucan

$\beta$ -glucans are homopolysaccharides exclusively composed of glucose residues linked through  $\beta$ -glycosidic bonds. Such glucose-based polymers are often found in the cell walls of plants, bacteria, and fungi. The  $\beta$ -glucans from yeast and fungi share a common structure where the backbone is composed of  $\beta$ -1,3-glycosidic linkages with randomly distributed  $\beta$ -1,6-linked side chains of different length<sup>107</sup>. These glucans are usually highly branched and found in the inner cell wall layer, sometimes covalently associated with

## INTRODUCTION

other cell wall polymers<sup>108</sup>. In contrast to cellulose, which is a  $\beta$ -1,4-linked water-insoluble glucan, shorter  $\beta$ -1,3-linked glucans with a low number of branches are water-soluble. Such soluble  $\beta$ -glucans (SBGs) can be extracted from the cell wall of yeast in the *Saccharomyces* family, such as e.g. *Saccharomyces cerevisiae*, commonly known as Baker's yeast<sup>109</sup>. The 1,6-linkages of the branches are more acid labile than the 1,3-linkages of the backbone, and hence, branches can be removed by acid hydrolysis<sup>110</sup>.

SBGs are known to possess antitumor, antibacterial, antiviral, anticoagulant and wound healing activities due to their immune-enhancing effects<sup>111, 112</sup>. The SBGs activate the innate immune system by binding to  $\beta$ -glucan receptors (e.g. dectin-1) of immune cells such as macrophages and neutrophils<sup>113</sup>. SBG-loaded nanofibrous dressings have been shown to improve wound healing in diabetic mice<sup>114</sup> assumingly by reactivating immunosuppressed macrophages.

### 1.9 Purification and characterisation of oligosaccharides

#### 1.9.1 Gel filtration chromatography (GFC)

Gel filtration chromatography (GFC), also referred to as size exclusion chromatography (SEC) or gel permeation chromatography (GPC), is used to separate molecules depending on their size (hydrodynamic volume) or to remove impurities. The method is based on distribution of molecules between a stationary phase (the porous packing material of the columns) and the mobile phase (eluent). Molecules are separated depending on their ability to penetrate the pores and thereby be retained by the packing material. The time used to travel through the column(s) is therefore called the retention time. Larger molecules, that are not retained by the packing material, will be excluded in the void volume which equals the volume of the mobile phase in the columns (not including the volume inside the particles). Molecules travelling through the particles will be excluded at larger volumes (and hence, after longer times), depending on their size. By connecting an on-line refractive index (RI) detector to the column(s), the concentration of molecules eluting at different times can be detected and measured<sup>115</sup>. In the work of this thesis, GFC was used to fractionate oligosaccharides depending on their DP and/or composition and to isolate and purify reaction products.

#### 1.9.2 Nuclear magnetic resonance (NMR)

Nuclear magnetic resonance (NMR) spectroscopy is commonly used for characterisation of oligo- and polysaccharides. <sup>1</sup>H-NMR can be used to determine their chemical composition and DP<sub>n</sub>. Other NMR techniques such as <sup>13</sup>C-NMR and homo- and hetero-nuclear 2D NMR techniques can provide additional information about their structure and linkage geometry.

In the work of this thesis, different NMR techniques were used to characterise oligosaccharides and products formed after reducing end functionalisation and activation. Time course <sup>1</sup>H-NMR was also used to study the kinetics of the reductive amination reactions.

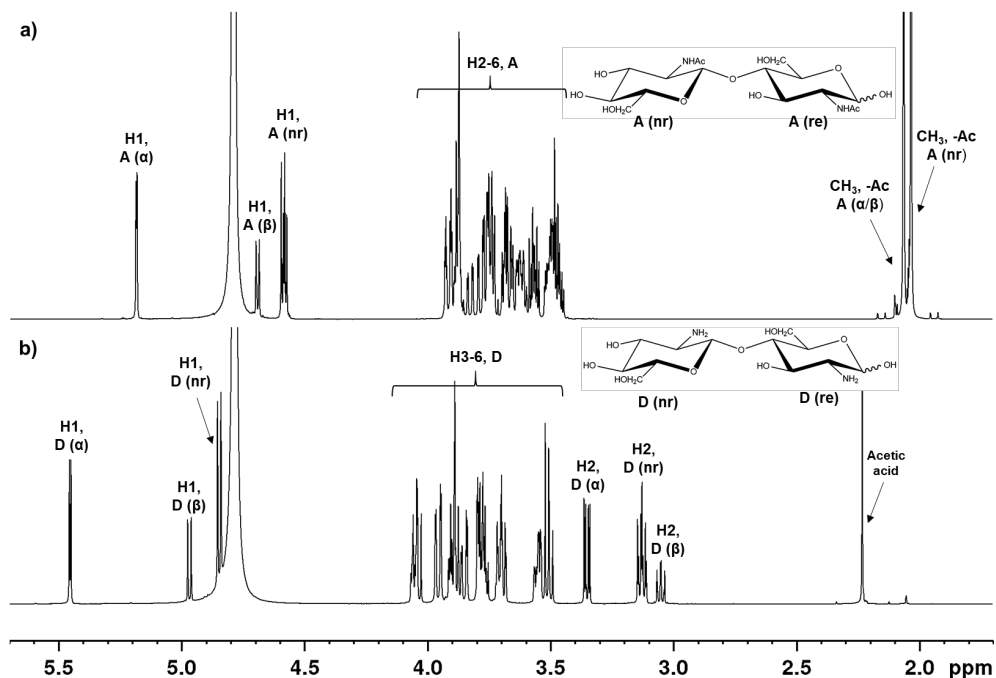
The general  $^1\text{H-NMR}$  spectrum for chitin and chitosan has been resolved and the proton resonances can be used to determine their  $F_A$ <sup>74</sup> and  $DP_n$ . The sequence of shorter CHOS from defined fractions can also, in some cases, be determined by a combination of  $^1\text{H-}$  and  $^{13}\text{C-NMR}$  spectroscopy since the resonances of the reducing and non-reducing end residues can be influenced by the nature of the neighbouring residues<sup>83, 116</sup>.

The M residue of CHOS prepared by nitrous acid depolymerisation of chitosan is most commonly found in the hydrated *gem-diol* form in aqueous solutions with H1 resonances in the anomeric region<sup>33</sup>. The chemical shifts for the proton resonances of the reducing end A, D ( $\alpha$  or  $\beta$ ) or M (*gem-diol*) residues and the internal/middle (m) and non-reducing (nr) A or D residues of the trisaccharides AAA, DDD, AAM and DDM are given in Table 1.1. The chemical shifts for the resonances of internal and non-reducing end residues are from oligomers with A or D residues at the reducing end. Annotated  $^1\text{H-NMR}$  spectra of the disaccharides DD and AA in  $\text{D}_2\text{O}$  are given in Figure 1.11.

**Table 1.1:** Chemical shifts for proton resonances of chitin (fully *N*-acetylated) and chitosan (fully de-*N*-acetylated) trisaccharides<sup>117</sup> and the reducing end M residue of chitin and chitosan trisaccharides prepared by nitrous acid depolymerisation<sup>33</sup> in  $\text{D}_2\text{O}$ , reported as ppm from TSP.

Residue	H1	H2	H3	H4	H5	H6a	H6b	CH <sub>3</sub> , -Ac
A ( $\alpha$ )	5.20	3.86	3.88	3.63	3.89	3.68	3.80	2.05
A ( $\beta$ )	4.72	3.69	3.66	3.62	3.52	3.67	3.84	2.05
A (m)	4.60	3.79	3.74	3.65	3.56	3.66	3.85	2.07
A (nr)	4.60	3.75	3.58	3.47	3.48	3.73	3.92	2.07
D ( $\alpha$ )	5.44	3.34	4.03	3.88	4.04	3.77	3.84	-
D ( $\beta$ )	4.96	3.03	3.86	3.71	3.88	3.75	3.94	-
D (m)	4.87	3.16	3.88	3.74	3.94	3.76	3.95	-
D (nr)	4.84	3.12	3.69	3.49	3.55	3.76	3.95	-
M ( <i>gem-diol</i> , AAM)	5.01	3.76	4.35	4.13	3.98	3.43	3.49	-
M ( <i>gem-diol</i> , DDM)	5.09	3.84	4.44	4.22	4.13	n.d.	n.d.	-

## INTRODUCTION



**Figure 1.11:** <sup>1</sup>H-NMR spectra of **a)** AA and **b)** DD in D<sub>2</sub>O. The spectra are annotated according to literature data<sup>117</sup>.

### 1.9.3 Mass spectrometry (MS)

Mass spectrometry (MS) is used for accurate mass determination of compounds in a sample from which chemical information can be obtained. MS has in the recent years become an important tool for the structural analysis of oligosaccharides and their derivatives<sup>118</sup>. The basic principles of MS are to convert molecules into ions, separate the ions and subsequently measure their mass-to-charge ( $m/z$ ) ratio. Various MS techniques are available, which rely on different ionisation methods, mass analysers and detectors<sup>119</sup>. Additional information regarding the chemical structure of oligosaccharides can be obtained through fragmentation of the ions using tandem MS (MS/MS) techniques. A common method for structure determination of oligosaccharides is through derivatisation of the reducing end which will promote specific fragmentation patterns<sup>118</sup>. In the present work, quadrupole time of flight (qTOF) MS was used to determine the mass of CHOS, and products formed after reducing and non-reducing end functionalisation and activation to determine their DP and structure, respectively.

## 2. Scope of the thesis

The work presented in this thesis has been motivated by the need for new approaches to utilise abundant biomass obtained from renewable resources. Polysaccharides are in this context highly relevant due to their large variation in chemical composition and properties. Terminal modification of polysaccharides will, in contrast to the traditional lateral substitution, retain their intrinsic properties as it does not perturbate the chain structure. Hence, end-coupling of different polysaccharides can enable the preparation of new and complex macromolecular architectures.

The main objective of this thesis is to investigate the terminal activation of chitin and chitosan oligosaccharides by a dioxyamine (PDHA) and a dihydrazide (ADH). Oxyamines and hydrazides can, in contrast to other “click” reagents, react directly with the reducing end of polysaccharides. They also have higher reactivities than amines and can be used in reductive amination reactions without the use of a catalyst. Reductive amination of polysaccharides is, however, known to be dependent of the nature of the reducing end residue and the chemistry of the amine derivative. In this work we therefore aim to perform a detailed kinetic and structural study of each step of the reductive amination reaction, and on this basis develop preparative protocols for the activation of chitin and chitosan oligosaccharides with PDHA or ADH, using  $\alpha$ -picoline borane as the reductant. These reactants allow for greener protocols with lower HSE concerns compared to reductive amination protocols with e.g. aniline and  $\text{NaCNBH}_3$ . The work also includes activation studies with oligosaccharides obtained from glucans (dextran and  $\beta$ -1,3-glucan) to investigate the versatility of the method.

Reducing end activation of polysaccharides by PDHA or ADH further enables preparation of AB-type diblock structures by attachment of a second polysaccharide to the free end of the bivalent linkers. In the work presented we therefore also aim to develop strategies for the preparation of chitin- and chitosan-based diblock polysaccharides.

Non-reducing end (NRE) functionalisation of polysaccharides can in principle enable the preparation of more complex block polysaccharides (e.g. ABC-type) but this has scarcely been studied in the literature. However, in contrast to most other polysaccharides, chitin oligomers can be selectively functionalised at the NRE by periodate oxidation, introducing a new dialdehyde. The work therefore also includes an initial study of the oxidation of the NRE of chitin oligomers and the subsequent activation by PDHA and ADH as a basis for the preparation of more complex block polysaccharides or block polymers with multiple chitin blocks.

### 3. Summary of results and discussion

The following sections provide a summary of the results and discussion of the two published papers in the thesis (**Paper I** and **Paper II**), one unpublished manuscript (**Paper III**), in addition to some relevant supplementing results from various side projects during the work with the thesis (**Appendix I-IV**). For experimental details, see the appended papers. Experimental details for the supplementing results are provided in brief in the appendices.

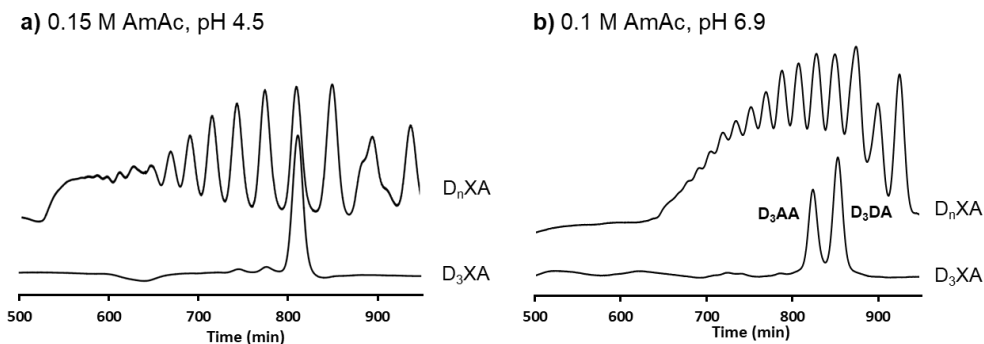
The study presented in chapter 3.1 was initiated during the late part of the work with the Doctoral thesis of Yiming Feng (2018). Some preliminary results were presented as an unpublished manuscript in her thesis. The  $D_nXA$  oligomers (described in chapter 3.1.1) were prepared and characterised by her and results are therefore only briefly repeated below. All other results, protocols, strategies, and interpretations presented are ascribed to the present author.

#### 3.1 Reducing end activation of $D_nXA$ oligomers prepared by enzymatic degradation

##### 3.1.1 Preparation of $D_nXA$ oligomers

Degradation of chitosan by Chitinase B (ChiB) from *Serratia marcescens* exclusively provides chitooligosaccharides (CHOS) with A (GlcNAc) residues at the reducing end<sup>83</sup>. In the present case,  $D_nXA$  ( $X = A$  or  $D$ ) oligomers were obtained by complete degradation of a chitosan with  $F_A = 0.25$  using ChiB (**Paper I**). Oligomers of specific DP ( $n = 2-8$ ) were isolated by GFC fractionation (0.15 M AmAc-buffer, pH 4.5, Figure 3.1a). We observed that subsequent fractionation of isolated oligomers at pH 6.9 (Figure 3.1b) enabled separation of  $D_nAA$  from  $D_nDA$ . Hence GFC fractionation at neutral pH can be used for sequence specific purification of shorter CHOS. This effect is ascribed to the change in hydrodynamic volume when the D (GlcN) residues become uncharged. Solubility at pH 6.9 was observed for oligomers up to DP = 10 ( $D_8XA$ ). The longer oligomers precipitated at neutral pH as expected for chitosan with low  $F_A$ <sup>77</sup>.





**Figure 3.1:** **a)** GFC fractionation of the mixture of  $D_nXA$  oligomers obtained by complete enzymatic degradation of chitosan ( $F_A = 0.25$ ) using ChiB in 0.15 M AmAc at pH 4.5. Fractionation of isolated  $D_3XA$  is included to show the DP distribution. **b)** GFC fractionation of the mixture of  $D_nXA$  oligomers in 0.1 M AmAc at pH 6.9. Fractionation of  $D_3XA$  is included to demonstrate the ability to separate oligomers with different chemical composition (Figure S1 from Supporting Information, **Paper I**).

### 3.1.2 Activation of $D_nXA$ oligomers by PDHA and ADH: the amination step

Activation of the reducing end of  $D_nXA$  oligomers by PDHA and ADH was studied in detail in **Paper I**. Reactions with AA (*N,N'*-diacetylchitobiose, Figure 3.2) were used as a model system for oligomers with A reducing end residues since short oligosaccharides give relatively simple NMR spectra (Figure 3.2b and f). Activation by PDHA resulted in mixtures of acyclic (*E*)- and (*Z*)-oxime (Schiff base) and  $\beta$ -*N*-pyranoside conjugates, whereas ADH almost exclusively yielded cyclic *N*-glycosides, in agreement with literature<sup>45, 47, 48, 64</sup> (Figure 3.2a and e).

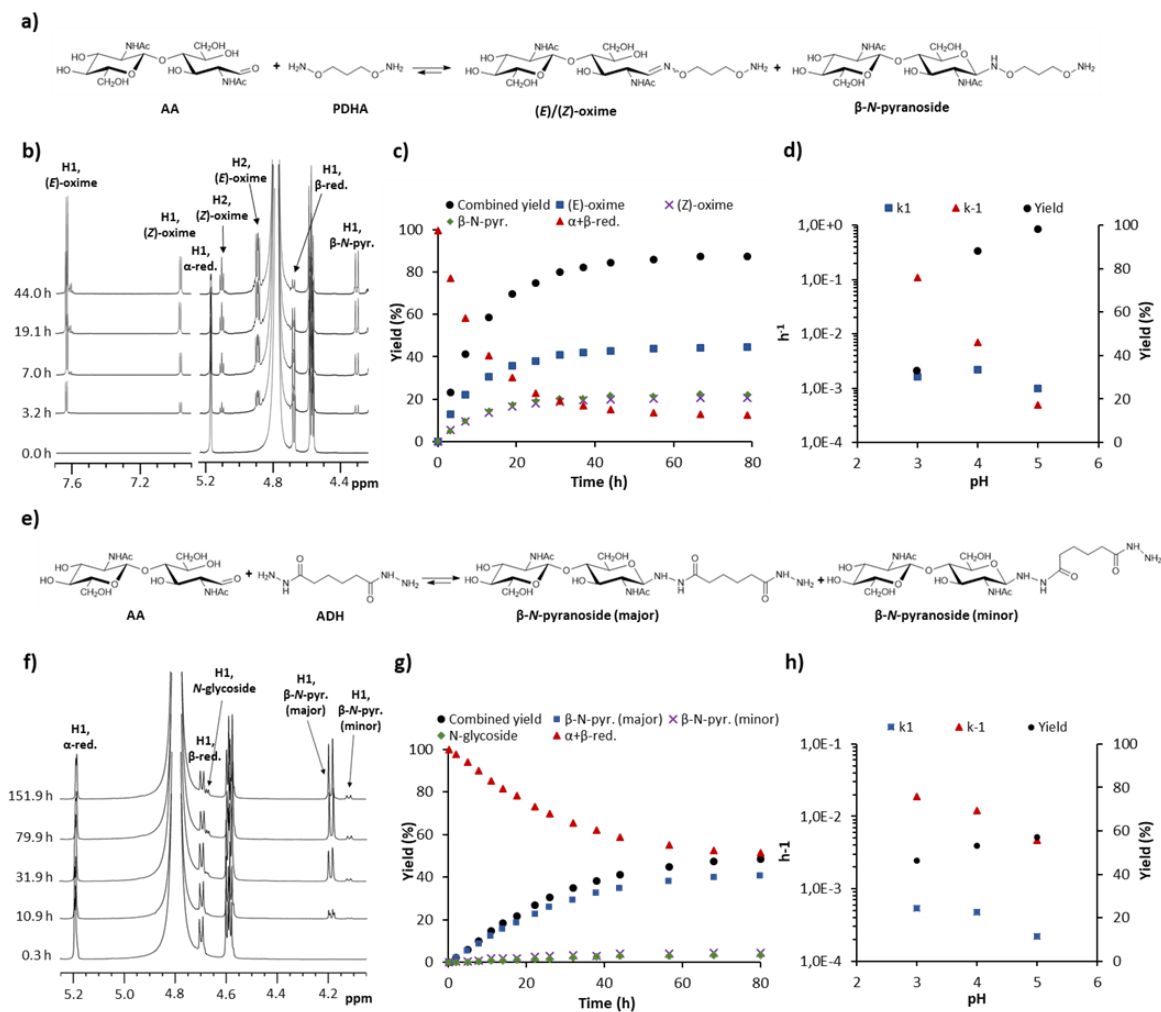
The conjugation reactions were assumed to follow first order kinetics, and a kinetics model was developed as described in **Paper I** (Supporting information, S4). The model was fitted to the experimental data obtained by real time <sup>1</sup>H-NMR (e.g. Figure 3.2c and g). Here, conjugates (oximes and/or *N*-pyranosides) were treated as a single (combined) product, providing rate constants for the forward ( $k_1$ ) and reverse ( $k_{-1}$ ) reactions. Generally, good fits were obtained, confirming first order kinetics for the reactions. Whereas the forward rate constants depended marginally on pH, the reverse rate constants were highly pH-dependent (Figure 3.2 d and h) which partly can be attributed to the acid lability of *N*-pyranosides<sup>64</sup>. The highest equilibrium yields were obtained at pH 5.0 in both cases. The larger pH-dependence for the yields obtained with PDHA can be explained by its higher  $pK_a$  (4.2) relative to the  $pK_a$  of ADH (3.1) which results in a reduced reactivity of the free amine groups at lower pH. Rates were highest at pH 3.0 for both linkers, attributed to the acid catalysed protonation of carboxyl group to make it more susceptible towards nucleophilic attack. High yields and short reaction times are desired for the preparation of conjugates. Rate constants can be used to simulate and predict reaction outcomes, particularly when using other

## SUMMARY OF RESULTS AND DISCUSSION

concentrations of reactants. We found that carrying out the reaction at pH 4.0 using a large excess of PDHA and ADH (10 equivalents or more) gave the best compromise between yield and reaction time for both linkers.

The kinetic study provided data for  $D_nXA$  oligomers ranging from DP 2 (AA) to DP 10 ( $D_8XA$ ). Importantly, the reaction kinetics was shown to be essentially independent of DP. Yields and distribution of conjugates were also marginally affected by DP. Hence, these results imply that optimised protocols can be applied for shorter oligomers as well as longer polysaccharides.

## SUMMARY OF RESULTS AND DISCUSSION



**Figure 3.2:** Reactions of AA with PDHA (a-d) and ADH (e-h). a) and e) Conjugation of PDHA/ADH to AA, b) and f)  $^1\text{H-NMR}$  spectra at defined time points for the conjugation reactions with 2 equivalents PDHA/ADH at pH 4.0, RT, c) and g) course of the reactions obtained from the integrals of spectra shown in b) and f), d) and h) influence of pH on combined yield and rate constants for the conjugation and the reverse reaction. Abbreviations:  $\alpha$ -red. and  $\beta$ -red.:  $\alpha$ - and  $\beta$ -configurations of the unreacted oligomer, respectively.  $\beta$ -N-pyr.:  $\beta$ -configuration of the N-pyranoside (Figure 3 from **Paper I**).

## SUMMARY OF RESULTS AND DISCUSSION

### 3.1.3 Comparison to CHOS with D residues at the reducing end

Enzymatic degradation of chitosan by other enzymes than ChiB or by other degradation methods (e.g. acid hydrolysis using HCl) can provide CHOS terminating in D residues. To study the reactivity of such oligomers, PDHA and ADH were reacted with the disaccharide chitobiose (DD) under same conditions as for AA. Indeed, DD showed poor reactivity compared to AA. For example, the combined equilibrium yields after 72 hours were as low as 2 and 10 % for ADH and PDHA, respectively, using the same conditions as for AA in Figure 3.2c and g. These observations are in agreement with literature data for reactions with other types of amines<sup>61, 120</sup>. Due to the low reactivity of the D residues, enzymatically produced CHOS with A reducing end residues are more favourable for conjugations of this type.

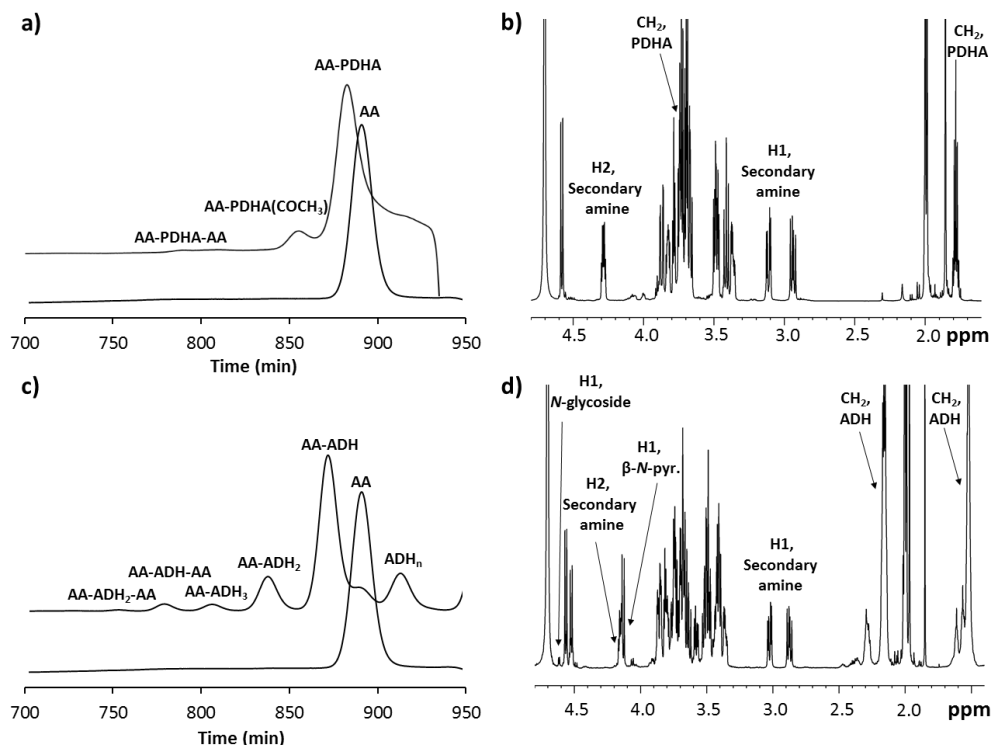
### 3.1.4 Activation of D<sub>n</sub>XA oligomers by PDHA and ADH: the reduction step

All steps in the reactions between carbohydrates and oxyamines or hydrazides are in principle reversible. Moreover, the stability of the conjugates (oximes/hydrazones and/or *N*-pyranosides) may vary considerably<sup>47</sup>. Reduction of the Schiff bases will in contrast yield stable secondary amines. Reduction of D<sub>n</sub>XA conjugates was therefore investigated using  $\alpha$ -picoline borane (PB) as the reductant (**Paper I**). Exceptionally slow reduction kinetics was observed for these conjugates at room temperature. Fully reduced PDHA conjugates could be obtained using a high concentration of PB (20 equivalents) after 40 days whereas the reduction of ADH conjugates was even slower and only approx. 50 % reduced conjugates were obtained under the same conditions (Figure 3.3b and c). The slower reduction of ADH conjugates can be attributed to the large fraction of non-reducible cyclic (*N*-pyranoside) conjugates which needs to be converted to reducible hydrazones (rate limiting step)<sup>49</sup>.

Subsequent GFC fractionation of the reaction mixtures revealed a fraction of doubly substituted linkers which suggested an enhanced reactivity of the free end after conjugation to the first oligomer (further discussed below). In the case of ADH, a complex mixture of conjugates was formed (Figure 3.3 c) resulting from a 'polymerisation' of the linker (ADH<sub>n</sub>). To the best of our knowledge, this side reaction has not been described in the literature (details in **Paper I**).

Unreacted oligomers (in the case of ADH) were unaffected after 40 days and hence, the reduction of CHOS with A reducing end is slow. Therefore, reductive amination reactions with D<sub>n</sub>XA can be performed as conventional one pot reductive amination.

Higher temperatures (40-60 °C) and high concentrations of PB (20-40 equivalents) improved the reduction significantly, resulting in acceptable yields after 24 hours, with rates comparable to aniline- and NaCNBH<sub>3</sub>-based reductive amination protocols (**Paper I**). However, the faster decomposition of PB at higher temperatures had to be compensated for by multiple additions of the reducing agent.



**Figure 3.3:** a) and c) GFC fractionation of the mixture of conjugates formed in the reaction of PDHA or ADH (10 equivalents) with AA after subsequent reduction for 40 days at RT using 20 equivalents PB at pH 4.0, respectively. Fractionation of AA is included as a reference.  $^1\text{H-NMR}$  spectra of b) the main fraction from the AA-PDHA reaction (completely reduced) and d) the main fraction from the AA-ADH reaction (approx. 50% reduced) (Figure 4 from **Paper I**).

### 3.1.5 Comparison to dextran ( $\text{Dext}_m$ ) oligomers

To study whether the results obtained for the CHOS were specific to their reducing end residues, dextran ( $\text{Dext}_m$ ) oligomers, obtained by acid hydrolysis of dextran ( $\alpha$ -1,6-linked glucan exclusively composed of glucose (Glc) residues), were activated by PDHA and ADH (**Paper I**). Both ADH and PDHA reacted faster with  $\text{Dext}_m$  compared to the  $\text{D}_n\text{XA}$  oligomers (2-3 times for PDHA and 7-10 times for ADH). This was in agreement with literature data for oxime ligation where Glc (monosaccharide) was shown to react 4 times faster than  $\text{GlcNac}^{45}$ . High yields and a mixture of oximes and *N*-pyranosides were obtained for reactions with PDHA whereas ADH resulted in lower yields and formed exclusively cyclic conjugates, as also observed for the  $\text{D}_n\text{XA}$  oligomers. Hence, the reaction kinetics is clearly dependent of the reducing end residue, whereas the yield and the type of conjugates formed are linker dependent (PDHA or ADH).

## SUMMARY OF RESULTS AND DISCUSSION

Dext<sub>m</sub> oligomers were also unaffected (not reduced) by PB. Reductive amination was therefore performed as a conventional one pot. The kinetics for the one pot reductive amination reactions of Dext<sub>m</sub> oligomers with PDHA and ADH was compared to corresponding reactions with AA, and reaction rates were much higher for the former (kinetics included in Figure 3.6). Hence, the slow reduction of CHOS-based conjugates can specifically be attributed to the nature of their reducing end residues (A or D). The reaction rates were, however, also linker dependent in the case of Dext<sub>m</sub> oligomers, with a higher rate of reduction for PDHA conjugates.

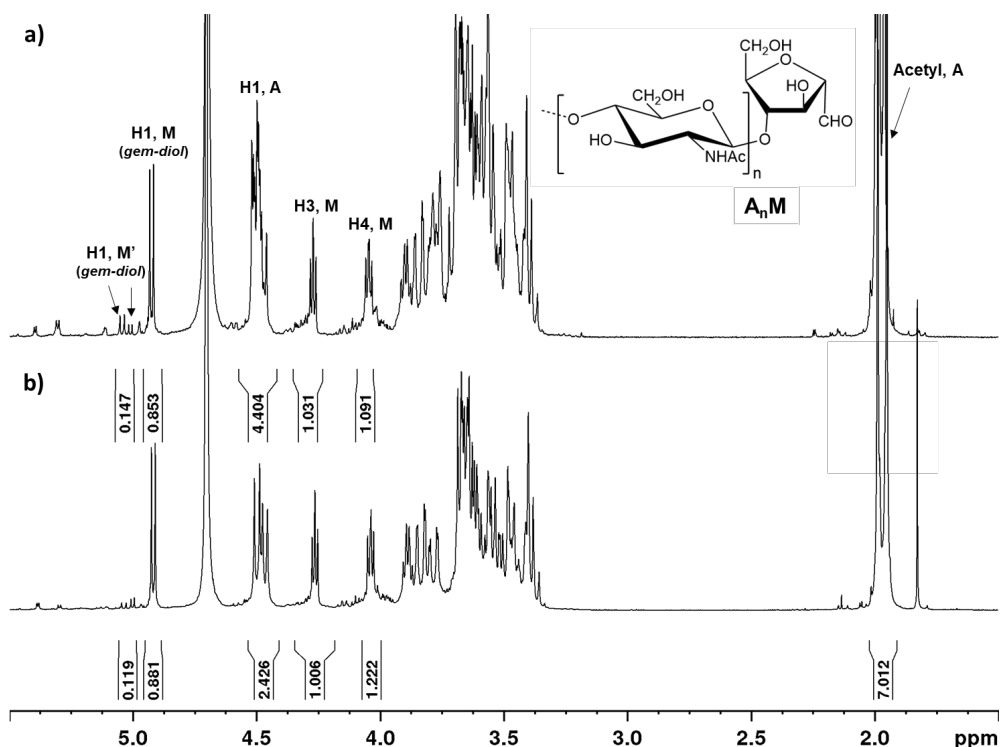
### 3.2 Reducing end activation of A<sub>n</sub>M oligomers prepared by nitrous acid depolymerisation

#### 3.2.1 Preparation of A<sub>n</sub>M oligomers

Nitrous acid depolymerisation of chitosan provides CHOS with a 2,5-anhydro-D-mannose (M) residue at the reducing end (Figure 3.4). The pending aldehyde of the M residue been shown to be highly reactive towards amines<sup>49</sup>, and hence, such oligomers may serve as attractive alternatives for the preparation of CHOS-based conjugates.

In the present case, chitin (A<sub>n</sub>M) oligomers were prepared by nitrous acid depolymerisation of a chitosan with F<sub>A</sub> = 0.48 using an excess nitrous acid (HONO) to the fraction of D residues (**Paper II**). Due to the low water-solubility of chitin, only A<sub>n</sub>M oligomers with DP up to 9 (n = 8) were isolated by GFC fractionation. Characterisation of the oligomers by <sup>1</sup>H-NMR (Figure 3.4) revealed that the reducing end aldehyde appeared in the hydrated *gem-diol* form (H1, M) as also observed by others<sup>33</sup>.

Two minor *gem-diol* resonances around 5 ppm (marked as M' in Figure 3.4) were also present in the spectra obtained of the A<sub>n</sub>M oligomers. These were assumed to be resulting from an alternative form of the M residue formed by the alternative deamination mechanism suggested in the literature<sup>91, 92</sup>. The mechanism in itself will not lead to cleavage of the glycosidic linkages, but the rearrangement of the D residue after deamination results in an acid labile glycosidic linkage<sup>92</sup>. Hence, our results suggest that the conditions for the preparation of the A<sub>n</sub>M oligomers resulted in a cleavage of these glycosidic linkages forming oligomers with the M' residue at the reducing end. The M' residue has the pending aldehyde located at C2 of the ring, and can, in contrast to the main M from, appear in the open ring form with two aldehydes. The two minor *gem-diol* resonances observed in the NMR spectra of A<sub>n</sub>M oligomers can therefore assumingly be assigned to the hydrated α- and β-configurations of this M' form. This is, to our knowledge, the first reported evidence of the alternative deamination mechanism leading to depolymerisation chitosan. The M' residue was structurally elucidated after activation of the A<sub>n</sub>M oligomers (see chapter 3.2.3).

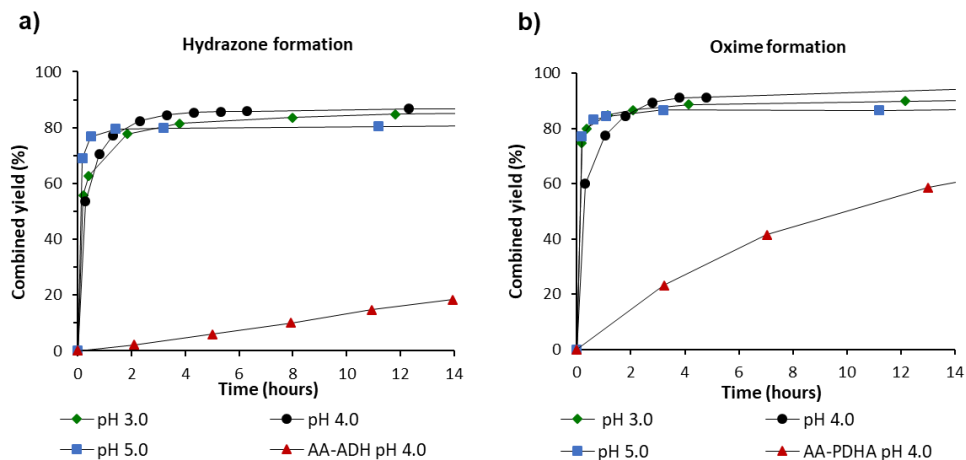


**Figure 3.4:**  $^1\text{H-NMR}$  spectra of purified **a)**  $\text{A}_4\text{M}$  and **b)**  $\text{A}_2\text{M}$  including annotations and integrals. M' refers to alternative (minor) forms of M (Figure 3 from **Paper II**).

### 3.2.2 Activation of $\text{A}_n\text{M}$ oligomers by PDHA and ADH: the amination step

Activation of  $\text{A}_n\text{M}$  oligomers by PDHA and ADH was studied in detail in **Paper II**. Due to the pending aldehyde of the M residue, only acyclic Schiff bases (oximes and hydrazones) can be formed in reactions with PDHA and ADH<sup>93</sup>. The reactivity of the  $\text{A}_n\text{M}$  oligomers was high compared to CHOS with A reducing end residues (Figure 3.5). The equilibrium yields were also high (> 75 %) for both PDHA and ADH even with a low excess of linkers (2 equivalents). Moreover, activation reactions with  $\text{A}_n\text{M}$  were only weakly dependent of pH in the range studied (pH 3.0-5.0) in contrast to  $\text{D}_n\text{XA}$  oligomers where the reverse rate constants and equilibrium yields were highly pH-dependent. Reaction kinetics also appeared to be essentially independent of DP in the range studied (DP 3-6) as observed for the  $\text{D}_n\text{XA}$  oligomers.

## SUMMARY OF RESULTS AND DISCUSSION



**Figure 3.5:** Kinetics for the reactions of  $A_2M$  oligomers (20.1 mM) with 2 equivalents a) ADH (hydrazone formation) and b) PDHA (oxime formation) at pH 3.0, 4.0 and 5.0. Kinetics for the corresponding reactions with AA at pH 4.0 (from **Paper I**) is included for comparison (Figure 5 from **Paper II**).

### 3.2.3 Activation of $A_nM$ oligomers by PDHA and ADH: the reduction step

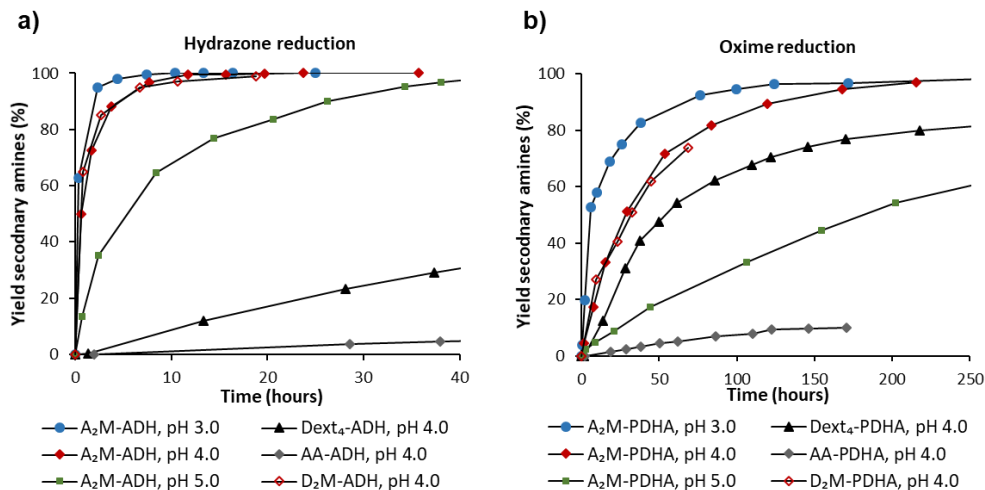
The high reactivity of the pending aldehyde of the M residue was also reflected in a high rate of reduction by PB (Figure 6 in **Paper II**). Hence, reductive amination of  $A_nM$  oligomers needs to be performed as two separate, consecutive reactions (see also 3.3). However, favourable kinetics in the first reaction facilitates this approach.

Reduction of  $A_nM$ -ADH conjugates (hydrazone reduction, Figure 3.6a) turned out to be very fast compared to reduction of  $Dext_m$ - and AA-ADH conjugates (included in Figure 3.6a). The difference corresponded roughly to 1 and 2 orders of magnitude at pH 4.0, respectively. The reduction of hydrazones was further strongly pH-dependent (in the range 3.0-5.0) and clearly fastest at pH 3.0. Protocols with 3 equivalents PB at pH 3.0 or 4.0 were sufficient to obtain fully reduced conjugates within 24 hours.

$A_nM$ -PDHA conjugates were on the other hand reduced with a much lower rate (oxime reduction, Figure 3.6b) and a higher concentration of reductant was therefore necessary to obtain acceptable reduction rates. 20 equivalents PB at pH 4.0, RT gave complete oxime reduction after 48 hours. The pH-dependence of the reduction was, however, qualitatively similar to that of hydrazones with higher reduction rate at lower pH. The pH-dependence can be attributed to the protonation of Schiff bases to form reducible iminium ions. Hence, the two step reductive amination reactions with  $A_nM$  oligomers can be performed at low pH since the activation (amination) step only is marginally dependent on pH. The higher reduction rates for  $A_nM$



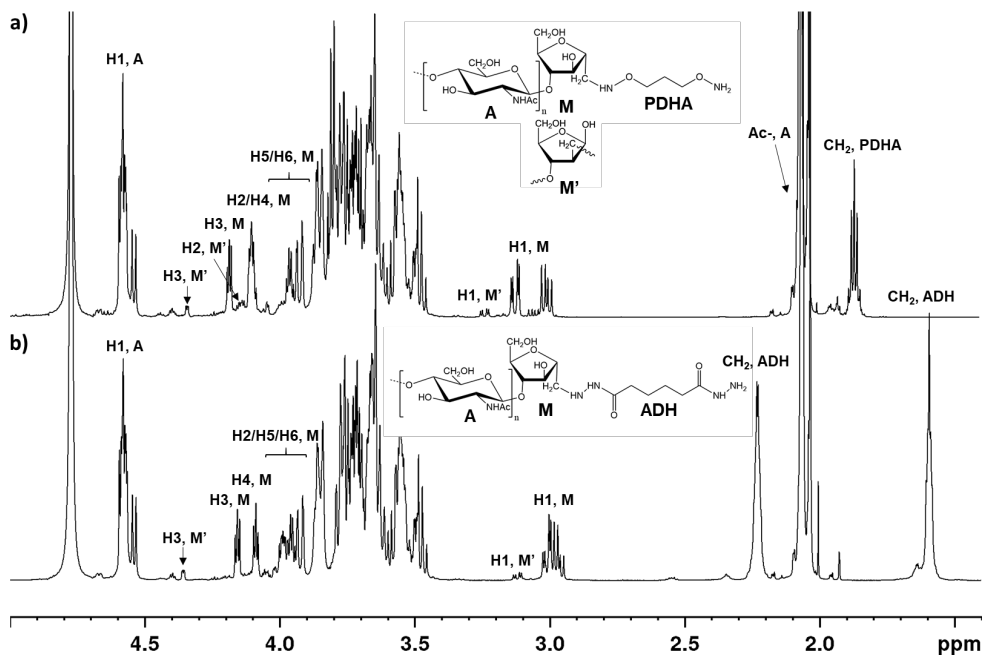
conjugates compared to Dext<sub>n</sub> and AA conjugates can presumably be attributed to the exclusive formation of reducible acyclic conjugates (oximes and hydrazones) for the former.



**Figure 3.6:** Kinetics for the reduction of **a)** A<sub>2</sub>M-ADH conjugates (hydrazone reduction) and **b)** A<sub>2</sub>M-PDHA conjugates (oxime reduction) at pH 3.0, 4.0, and 5.0 using 3 equivalents PB at RT. Kinetics for the reduction of D<sub>n</sub>M conjugates and the one pot reductive amination of AA and Dext<sub>4</sub> at pH 4.0 under otherwise identical conditions is included for comparison. Two equivalents ADH or PDHA were used in all reactions.

<sup>1</sup>H-NMR spectra of fully reduced and purified (by GFC) A<sub>5</sub>M-PDHA and A<sub>5</sub>M-ADH conjugates are given in Figure 3.7. The structure of the alternative form of the M residue (M') was confirmed by 2D NMR characterisation (S10 Supporting Information, **Paper II**). The structure and annotations are included in Figure 3.7. Conjugates corresponding to the open ring form of the M' residue were not detected, and it appeared that M' reacts with PDHA and ADH in the same way as the main M form. To the best of our knowledge, this is the first observation of the formation and subsequent reaction of oligomers with the M' reducing end residue. Conjugates formed the two different forms of the M residue were not separated during purification and without further investigation, we also assume that the two forms are indistinguishable when part of a block polysaccharide.

## SUMMARY OF RESULTS AND DISCUSSION



**Figure 3.7:**  $^1\text{H-NMR}$  spectra of reduced and purified a)  $\text{A}_5\text{M-PDHA}$  and b)  $\text{A}_5\text{M-ADH}$  conjugates. The structures of the conjugates with normal M residue and the alternative M' are included in the figure (Figure 8 from **Paper II**).

### 3.2.4 Comparison to $\text{D}_n\text{M}$ oligomers

The high reactivity of the M residue observed for the  $\text{A}_n\text{M}$  oligomers could possibly also be valid in the case of CHOS with lower  $F_A$  prepared by nitrous acid depolymerisation of chitosan. Such oligomers may serve as more reactive alternatives to the  $\text{D}_n\text{XA}$  oligomers for the preparation of chitosan conjugates. Fully de-*N*-acetylated ( $\text{D}_n\text{M}$ ) oligomers were therefore prepared by nitrous acid depolymerisation using a chitosan with low  $F_A$  and a sub-stoichiometric amount of HONO (unpublished results are given in **Appendix D**). The kinetics for the activation and subsequent reduction of  $\text{D}_n\text{M}$  oligomers (included in Figure 3.6) was indeed identical to the kinetics of the  $\text{A}_n\text{M}$  oligomers, indicating that the reactions with PDHA and ADH were reducing end specific (M residue) and independent of the  $F_A$  of the oligomers.

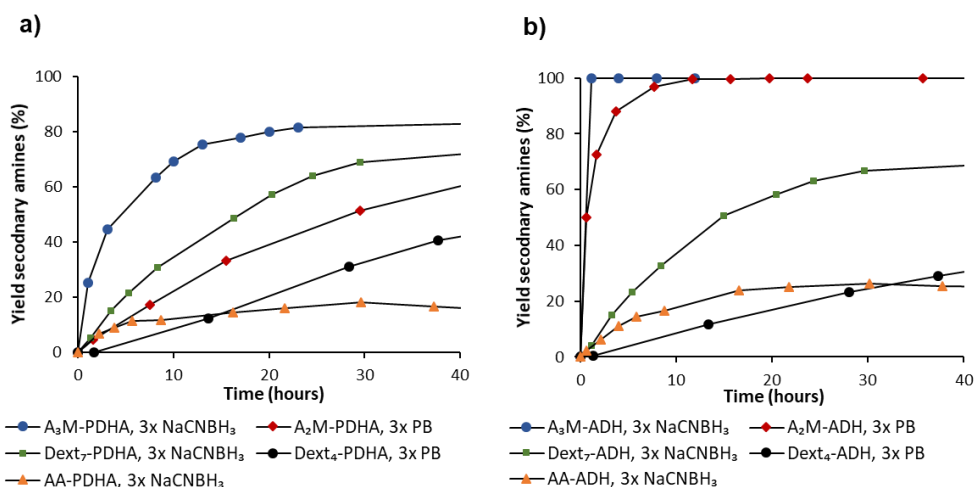
Interestingly, the formation of the alternative form of the M residue ( $\text{M}'$ ) observed for  $\text{A}_n\text{M}$  oligomers was not observed for  $\text{D}_n\text{M}$ , suggesting that the alternative deamination mechanism is triggered by the excess HONO used for the preparation of the former.

### 3.3 Reductive amination using NaCNBH<sub>3</sub> as the reductant: comparison to PB

The extremely slow reduction of D<sub>n</sub>XA conjugates by PB and the high rate of reduction of the A<sub>n</sub>M oligomers prompted us to investigate whether the results were reducing agent specific. Hence, reactions were performed with NaCNBH<sub>3</sub> for comparison.

As observed for PB, A<sub>n</sub>M oligomers were rapidly reduced by NaCNBH<sub>3</sub>. Reductive amination reactions with A<sub>n</sub>M oligomers should therefore be performed in two consecutive reactions (amination followed by reduction) with both reducing agents (and probably also with other reducing agents). D<sub>n</sub>XA and Dext<sub>m</sub> oligomers were in contrast unaffected by NaCNBH<sub>3</sub> and reductive amination can therefore be performed as one pot also with this reducing agent.

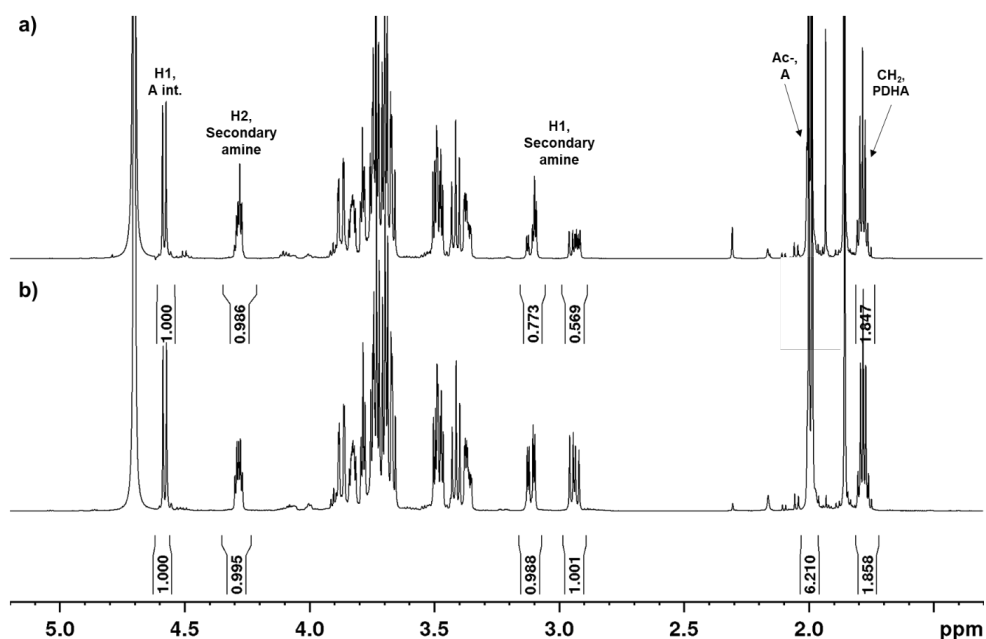
The reducing efficacy of NaCNBH<sub>3</sub> compared to that of PB was further studied for A<sub>n</sub>M and Dext<sub>m</sub> conjugates prepared with either PDHA or ADH (Figure 3.8). The reduction by NaCNBH<sub>3</sub> was in all cases faster than the corresponding reactions with PB. However, reactions with NaCNBH<sub>3</sub> (except the extremely fast A<sub>n</sub>M-ADH reduction) were limited by its rapid decomposition in the buffer (20 times faster than PB at RT, **Paper II**), resulting in incomplete reduction when 3 equivalents were used. Hence, these reactions need multiple additions of NaCNBH<sub>3</sub> or higher initial concentration of reducing agent to go to completion.



**Figure 3.8:** Comparison of the reaction kinetics for the reduction of **a)** PDHA conjugates and **b)** ADH conjugates formed with A<sub>n</sub>M, Dext<sub>m</sub> or AA with PB or NaCNBH<sub>3</sub> (3 equivalents, 3x) at pH 4.0, RT. Reactions with Dext<sub>m</sub> were performed as one pot, whereas reactions with A<sub>n</sub>M and AA were performed as two pot (sequential amination and reduction). Two equivalents ADH or PDHA were used in all reactions.

## SUMMARY OF RESULTS AND DISCUSSION

Interestingly, the reduction of AA-PDHA and AA-ADH conjugates by  $\text{NaCNBH}_3$  behaved very differently than the reduction of other conjugates. Instead of a steady increase in the yield of secondary amines, the yield started to diminish after an initial increase (observed for both PDHA and ADH, kinetics included in Figure 3.8).  $^1\text{H-NMR}$  characterisation of purified conjugates revealed a lower intensity of the H1, secondary amine resonances after complete reduction by  $\text{NaCNBH}_3$  compared to the conjugates reduced by PB (shown for AA-PDHA in Figure 3.9), suggesting that a different type of conjugates were formed. This observation has, to our knowledge, not been reported in the literature.  $\text{NaCNBH}_3$  is therefore not recommended as reducing agent for reactions with CHOS possessing A residues at the reducing end.



**Figure 3.9:**  $^1\text{H-NMR}$  spectra of the purified AA-PDHA conjugates after complete reduction by a)  $\text{NaCNBH}_3$  or b) PB.

### 3.4 Protocols for the preparation of activated oligosaccharides

The above-mentioned results show that reductive amination of carbohydrates is clearly not universal. Hence, protocols need to be adapted for individual oligo- or polysaccharide systems.

#### 3.4.1 Comparison of activation kinetics for different oligosaccharides

Our kinetic studies show that the activation of oligosaccharides by PDHA and ADH is highly dependent on the nature of the reducing end. Kinetic parameters obtained for the activation (amination) reactions with

## SUMMARY OF RESULTS AND DISCUSSION

different oligosaccharides under the same conditions are presented in Table 3.1. The times to reach 50 and 90 % of the combined equilibrium yields ( $t_{0.9}$  and  $t_{0.5}$ ) are included as a more empirical approach to describe reaction rates<sup>45</sup>. The rates demonstrate the high reactivity of the M reducing end residue of A<sub>n</sub>M (and D<sub>n</sub>M) oligomers compared to the reducing end residues of D<sub>n</sub>XA and Dext<sub>m</sub>. The high rates and yields obtained for A<sub>n</sub>M (with both PDHA and ADH) can be attributed to the availability of the pending aldehyde of the M residue and the inability to form cyclic conjugates (*N*-glycosides).

The low reactivity of CHOS with terminal A (and D) residues is reflected in slow activation rates (data for terminal D residues not included due to extremely slow kinetics). Even though the type of conjugates (Schiff bases and/or *N*-pyranosides) and yields for oligomers with terminal pyranose residues (GlcNAc (A), GlcN (D) and Glc) were shown to be linker dependent, kinetics was in contrast highly dependent on the chemistry of the reducing end residue. Terminal Glc residues of Dext<sub>m</sub> oligomers reacted faster with ADH than with PDHA, whereas the opposite was the case for the terminal A and D residues of CHOS.

The results of the Dext<sub>m</sub> oligomers were also compared to activation of oligomers obtained from β-1,3-linked glucan (SBG<sub>n</sub>). Interestingly, the SBG<sub>n</sub> oligomers reacted slightly faster with both PDHA and ADH compared to Dext<sub>m</sub> and provided also higher yields (results included in Table 3.1). Hence, the results suggest that even the geometry of internal linkages to some extent affects the kinetics of the reducing end activation of oligomers composed of the same residues (unpublished results are given in **Appendix II**).

**Table 3.1:** Kinetic parameters obtained for the activation (amination) of different oligosaccharides by PDHA or ADH (2 equivalents) at pH 4.0, RT. The rates ( $t_{0.9}$  and  $t_{0.5}$ ) and the rate constants ( $k_1$  and  $k_{-1}$ ) are based on the combined yield of conjugates (oximes/hydrazones and/or *N*-pyranosides).

Reaction	Ratio acycl.:cycl.	$t_{0.5}$ [h]	$t_{0.9}$ [h]	$k_1$ [h <sup>-1</sup> ]	$k_{-1}$ [h <sup>-1</sup> ]	Combined equilibrium yield [%]
A <sub>2</sub> M-PDHA	1:0	0.2	0.9	$7.7 \times 10^{-2}$	$1.6 \times 10^{-1}$	91
SBG <sub>5</sub> -PDHA	5.1:1	1.8	7.1	$1.1 \times 10^{-2}$	$1.5 \times 10^{-2}$	94
Dext <sub>5</sub> -PDHA	4.3:1	2.2	8.6	$8.0 \times 10^{-3}$	$2.0 \times 10^{-2}$	90
AA-PDHA	2.9:1	7.6	30.0	$2.2 \times 10^{-3}$	$7.0 \times 10^{-3}$	88
A <sub>2</sub> M-ADH	1:0	0.3	1.2	$5.5 \times 10^{-2}$	$1.9 \times 10^{-1}$	87
SBG <sub>5</sub> -ADH	1:44	1.2	4.2	$7.1 \times 10^{-3}$	$2.3 \times 10^{-1}$	49
Dext <sub>5</sub> -ADH	1:41	1.9	6.4	$3.5 \times 10^{-3}$	$1.9 \times 10^{-1}$	38
AA-ADH	1:47	20.4	71.4	$4.7 \times 10^{-4}$	$1.2 \times 10^{-2}$	53

## SUMMARY OF RESULTS AND DISCUSSION

### 3.4.2 Two pot reductive amination protocols for A<sub>n</sub>M (and D<sub>n</sub>M) oligomers

Reduction of unreacted A<sub>n</sub>M (and D<sub>n</sub>M) oligomers by both PB and NaCNBH<sub>3</sub> is fast and hence, reductive amination of these oligomers needs to be performed as consecutive reactions. The amination should further be performed using a large excess of ADH and PDHA (> 10 equivalents) to reduce the fraction of unreacted oligomers prior to the addition of reducing agent and to minimise the formation of doubly substituted linkers. ADH conjugates (hydrazones) were reduced with much higher rates than PDHA conjugates (oximes) with both reducing agents. However, the fast decomposition of NaCNBH<sub>3</sub> needs to be compensated for by several additions for the reduction of PDHA-conjugates. This, as well as other drawbacks associated with NaCNBH<sub>3</sub> (including HSE concerns), makes protocols with PB highly recommended for the reductive amination of A<sub>n</sub>M oligomers. For ADH conjugates, 3 equivalents of PB and a reaction time of 24 hours was enough to obtain fully reduced conjugates at RT, pH 3.0 and 4.0. For PDHA conjugates, a higher concentration of PB (20 equivalents) and 48 hours of reduction were necessary at RT, pH 4.0 but higher temperatures or lower pH would presumably improve the protocol further.

D<sub>n</sub>M oligomers were shown to have identical amination and reduction kinetics as the A<sub>n</sub>M oligomers. Hence, the protocols developed for A<sub>n</sub>M will also apply for D<sub>n</sub>M oligomers. A partial degradation of the M residues was, however, observed during the purification of isolated D<sub>n</sub>M oligomers (unpublished results in **Appendix I**). The degradation was attributed to a pH-dependent reaction of the M residues with unprotonated free amino groups of the D residues, resulting in the formation of 5-hydroxymethyl-2-furfural (HMF) and oligomers with the unreactive D residues at the reducing end (D<sub>n</sub>). Activation of the mixture of D<sub>n</sub>M oligomers prior to purification prevented the M degradation, and this protocol can therefore be used for oligomers prepared by nitrous acid depolymerisation with F<sub>A</sub> < 1. This protocol is also time saving, as the purification from excess linker and isolation of activated oligomers of specific DP can be performed in the same step. The protocol can therefore also be highly relevant for other oligomer mixtures.

### 3.4.3 One pot reductive amination protocols for oligomers with pyranose reducing end residues

The slow reduction of unreacted oligosaccharides with pyranose reducing ends (GlcNAc, GlcN and Glc) allows for conventional one pot reductive amination protocols. The slower activation and reduction kinetics for these oligomers compared to oligomers with M reducing ends, was compensated for by using a large excess of ADH and PDHA (10 equivalents), a high concentration of PB (>20 equivalents), and higher temperatures (40 or 60 °C).

For Dext<sub>m</sub>-PDHA, Dext<sub>m</sub>-ADH, and SBG<sub>n</sub>-PDHA/SBG<sub>n</sub>-ADH complete reduction of conjugates was obtained after 1, 2, and 3 days, respectively, using 20 equivalents PB at 40°C with oligomers of DP 9 or 10 (unpublished results are given in **Appendix II**). The slower kinetics for the SBG<sub>n</sub>-based conjugates

compared to Dext<sub>m</sub>-conjugates, suggest that the geometry of internal linkages also affects the rate of reduction for the conjugates.

The improved protocols with PB serve as good alternatives to corresponding protocols with NaCNBH<sub>3</sub>. The applicability of the protocols was demonstrated by the preparation of fully activated and reduced dextran-based conjugates with longer chains (DP<sub>n</sub> = 340, unpublished results in **Appendix IV**). The reaction time was however increased for the longer chains (e.g. from 2 to 4 days for Dext<sub>m</sub>-ADH conjugates) to ensure complete reaction.

The slow kinetics for both the amination and the reduction of CHOS with normal pyranose (A or D) reducing end residues makes the use of CHOS terminating in M residues more attractive. However, in cases where pyranose reducing end residues are preferred, enzymatically produced CHOS with A residues at the reducing end should be used as these are much more reactive than CHOS terminating in D residues. The reductive amination of D<sub>n</sub>XA oligomers needs harsher conditions compared to Dext<sub>m</sub> and SBG<sub>n</sub> and the one pot reductive amination protocol for D<sub>n</sub>XA oligomers with PB described in **Paper I** needs further improvements to give fully reduced conjugates. However, by increasing the reaction temperature to 60 °C and the concentration of PB to 40 equivalents we obtained 84 and 43 % reduced conjugates after 24 hours with PDHA and ADH, respectively. The faster decomposition of PB at 60 °C was compensated for by multiple additions (**Paper I**). Longer reaction times and higher concentration of PB will enable preparation of fully reduced conjugates. The formation of other (unidentified) conjugates prevents the use of NaCNBH<sub>3</sub> as the reducing agent for CHOS terminating in A residues. Therefore, PB also serves as the recommended reducing agent for D<sub>n</sub>XA oligomers even though the reduction is slow.

### 3.5 Chitin- and chitosan-based diblock polysaccharides

#### 3.5.1 Chitin-*b*-chitin diblocks

In the context of block polysaccharides, chitin-*b*-chitin prepared using A<sub>n</sub>M oligomers serve as simple model for diblocks with antiparallel chains. The preparation of A<sub>n</sub>M-*b*-MA<sub>n</sub> was studied using two different approaches: Either attaching a second block to A<sub>n</sub>M-ADH or A<sub>n</sub>M-PDHA (fully reduced) conjugates, or in a single step using 0.5 equivalents of linker, in both cases followed by a reduction step.

The kinetics for both these approaches was first studied and compared (**Paper II**). The kinetic data enabled (as before) simple simulations of the reactions when exploring the influence of e.g. different concentrations and relative proportions of reactants to optimise the reaction.

In both approaches it was found that reaction rates and equilibrium yields (prior to reduction) were higher than for the activation of oligomers (first step). The results were supported by the formation of higher

## SUMMARY OF RESULTS AND DISCUSSION

amounts of diblocks than those predicted using a simple statistical approach (equation derived and described in **Paper II**). In combination, these results demonstrated that the reactivity of the free amine end of the linkers (PDHA/ADH) was in fact increased after attachment of the first oligomer/block. This is an unexpected, but useful aspect in the preparation of diblocks from PDHA and ADH activated oligosaccharides.

The best strategy to prepare fully reduced chitin-*b*-chitin diblocks turned out to be the first approach, i.e. reacting  $A_nM$  to preformed  $A_nM$ -ADH or  $A_nM$ -PDHA conjugates. Close to 100 % yield of diblocks could be obtained after 24 or 48 hours of reduction using 3 or 20 equivalents PB for ADH- or PDHA-based diblocks, respectively, using 2 equivalents of the activated block. The activated block can be reused after purification, in contrast to an excess of  $A_nM$  which is rapidly reduced after addition of PB.

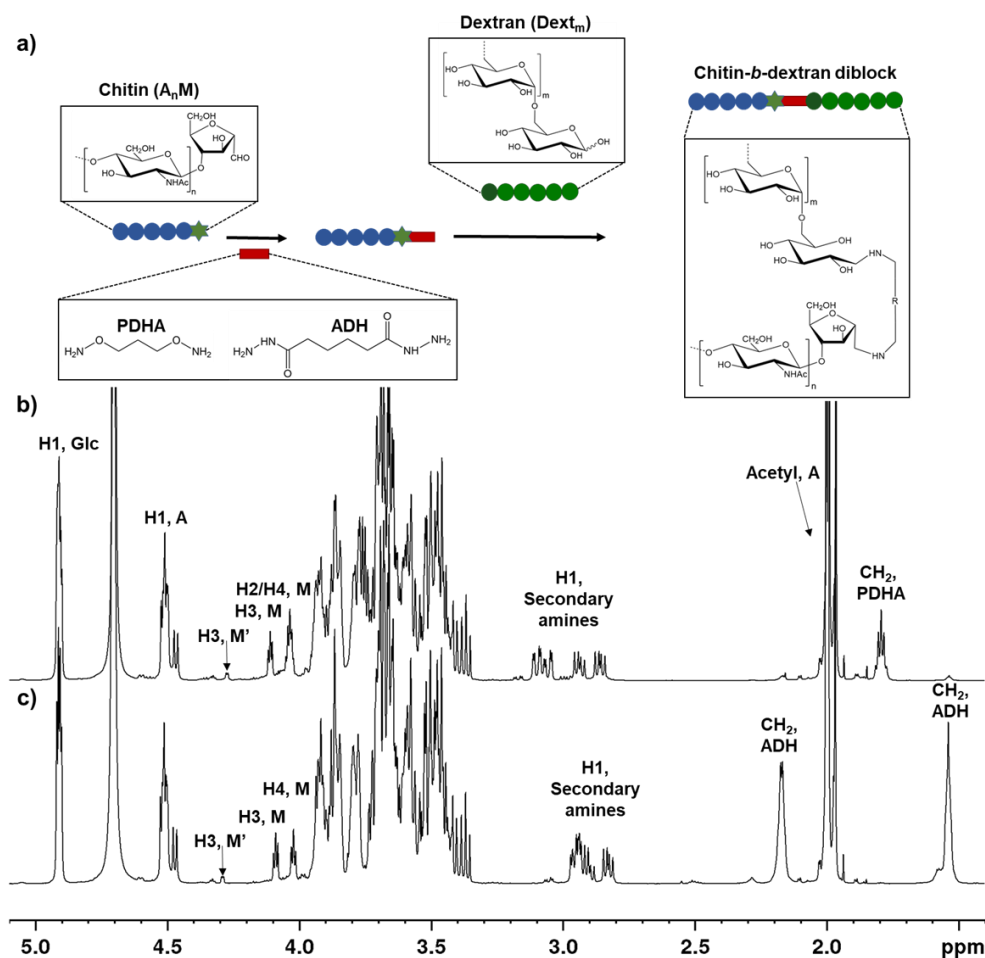
The second approach, using 0.5 equivalents of the linker, is experimentally simple, but results in a mixture of diblocks, activated blocks and unreacted oligomers at equilibrium. Due to the rapid reduction of unreacted  $A_nM$ , the addition of reductant did not improve the yield of diblocks much and hence, this approach was rejected.

### 3.5.2 Chitin-*b*-dextran diblocks

Chitin-*b*-dextran diblocks were prepared by attaching  $Dext_m$  oligomers to PDHA or ADH activated  $A_nM$  oligomers using equimolar concentrations of the blocks (**Paper II**). Higher equilibrium yields and rates for the second conjugation were observed compared to the reactions of  $Dext_m$  with free PDHA or ADH, confirming an increased reactivity of the free end of the linkers after attachment of the first block. The lower reactivity of  $Dext_m$  oligomers compared to  $A_nM$  resulted in low equilibrium yields of diblocks prior to reduction. However, due to the slow reduction of unreacted  $Dext_m$  oligomers we could obtain approximately 90 % yield of  $A_nM$ -*b*- $Dext_m$  diblocks after the reduction step. The structure of the  $A_nM$ -*b*- $Dext_m$  diblock was verified by  $^1H$ -NMR (Figure 3.10). These diblocks serve as a proof of principle for the preparation of diblock polysaccharides composed of two different oligo- or polysaccharides using ADH or PDHA as linkers between the blocks.

Since the attachment of  $Dext_m$  to activated  $A_nM$  is slow, particularly when equimolar concentrations are used, the protocol may be improved by reversing the reaction order. The ‘reverse’ strategy overcomes the slow kinetics for the reductive amination of dextran by first preparing activated  $Dext_m$  oligomers using a large excess of linkers, and subsequently react these conjugates with  $A_nM$  oligomers. The fast reduction of  $A_nM$  oligomers can be circumvented by using an excess of the activated dextran block (as discussed above). This strategy is generally applicable for the block with the lowest reactivity for the preparation of block structures.





**Figure 3.10:** a) Preparation of chitin-*b*-dextran diblocks with PDHA and ADH.  $^1H$ -NMR spectra of the fully reduced and purified b)  $A_5M$ -PDHA- $Dext_6$  diblock and c)  $A_5M$ -ADH- $Dext_6$  diblock (Figure adapted from **Paper II**).

### 3.5.3 Chitosan-based diblocks

Chitosan oligomers prepared by nitrous acid depolymerisation are preferred over enzymatically produced oligomers for the preparation of chitosan-based diblocks, due to the low reactivity of the A and, in particular, D reducing end residues. Depending on the conditions for the nitrous acid depolymerisation and the  $F_A$  of chitosan degraded, chitosan oligomers with various compositions ( $F_A$ ) can be prepared. However, as discussed in chapter 3.4.2, the preparation of defined oligomers with low  $F_A$  can be challenging due to the pH-dependent degradation of the M residues during purification. The degradation can, however, be

## SUMMARY OF RESULTS AND DISCUSSION

prevented by activating the mixture of oligomers prior to purification. Such activated oligomers will need to be used as the first block for the preparation of chitosan-based diblock polysaccharides. Hence, the high reactivity of the M residues will not be utilised.

De-*N*-acetylation of A<sub>n</sub>M blocks may serve as an alternative approach to prepare chitosan-based diblock polysaccharides. We therefore studied the de-*N*-acetylation of A<sub>n</sub>M-PDHA and A<sub>n</sub>M-ADH conjugates (unpublished results are given in **Appendix III**). Interestingly, the secondary amine linkage was shown to be stable throughout the de-*N*-acetylation, whereas the harsh conditions resulted in the loss of an -NH group from the free end of the linkers. We hypothesize that the attachment of a second block to the free end can protect the linkers from degradation. Hence, the high reactivity of the M residue can be utilised in e.g. the preparation of chitin-*b*-*x* diblocks, where *x* is a different polysaccharide, which subsequently can be de-*N*-acetylated to form chitosan-*b*-*x* block polysaccharides. This approach is however limited by the low solubility of A<sub>n</sub>M oligomers and is therefore only applicable for oligomers with DP < 10.

For the preparation of chitosan-based block polysaccharides with CHOS terminating in A (or D) reducing end residues, chitosan should be used as the first block (prepared using a large excess of the linker) due to the slow kinetics for the reductive amination of such oligomers.

### 3.5.4 Diblocks with water-insoluble chitin oligomers

The high reactivity observed for the M residues prompted us to attempt to form dextran-*b*-chitin diblocks with the water-insoluble fraction of A<sub>n</sub>M oligomers (DP > 9) obtained by the depolymerisation of chitosan using an excess nitrous acid. Dextran was chosen since this is a highly water-soluble polysaccharide and we therefore postulated that the dextran block could increase the water-solubility of the chitin block. ADH was chosen as the linker between the blocks since the reduction of hydrazones formed with A<sub>n</sub>M oligomers is much faster than the corresponding oximes formed with A<sub>n</sub>M and PDHA. Two different Dext<sub>m</sub>-ADH conjugate samples were prepared with DP<sub>n</sub> = 80 and 340 (m = DP<sub>n</sub>) to study the effect of the chain length of the dextran block. The activated dextran was reacted with 2 equivalents of the water-insoluble A<sub>n</sub>M (assuming DP<sub>n</sub> = 12) using conditions optimised for A<sub>n</sub>M-ADH reactions (unpublished results are given in **Appendix IV**).

<sup>1</sup>H-NMR characterisation of the water-soluble fractions obtained from the heterogenous reaction mixtures revealed weak resonances from A<sub>n</sub>M oligomers (H1, A internal and *N*-acetyl) suggesting the presence of A<sub>n</sub>M oligomers in the sample. The resonances from the H1, secondary amines were also of slightly higher complexity suggesting conjugation of A<sub>n</sub>M to the free end of ADH. Interestingly, the weight of the soluble fraction after freeze-drying was reduced compared to the weight of the Dext<sub>m</sub>-ADH samples prior to reaction (independent of DP<sub>n</sub>).

These preliminary results imply that the highly reactive M residue of the water-insoluble  $A_nM$  oligomers can react with the free end of ADH under heterogenous conditions, however, without the  $Dext_m$  fraction being able to increase the water-solubility of the chitin block (independent of  $DP_n$  of the  $Dext_m$  block). Water-insoluble dextran-*b*-chitin diblocks may, however, serve as precursors for the preparation of dextran-*b*-chitosan block polysaccharides by de-*N*-acetylation of the chitin block as suggested above.

Chitin is soluble in dimethyl acetamide (DMAc) containing a few percent LiCl<sup>121, 122</sup> and we therefore performed an initial experiment to form chitin-based diblocks in this solvent (unpublished results are given in **Appendix IV**). After establishing that all chitin fractions (including the water-insoluble fraction) were soluble in DMAc/LiCl (8 %),  $A_4M$ -PDHA conjugates (fully activated and reduced) were reacted with an equimolar amount of  $A_4M$  (without reducing agent). A high yield (> 95 %) of oximes was obtained. Hence, these preliminary results indicate that DMAc/LiCl is a viable solvent for the preparation of chitin-based diblock structures with longer chitin blocks. Further we propose that the solvent can be used for reactions of water-insoluble  $A_nM$  oligomers with other oligo- or polysaccharides activated with PDHA which are soluble in DMAc/LiCl, e.g. dextran and  $\beta$ -1,3-glucans, for the preparation of block polysaccharides.

### 3.5.5 Purification of diblock polysaccharides

The protocols for preparation of chitin- and chitosan-based diblock polysaccharides where an excess of the activated block is used, require subsequent purification to isolate the diblocks. For the shorter oligosaccharide blocks used here, GFC fractionation was proven useful. For the preparation of block structures with longer oligo- or polysaccharides, other purification methods are required. In some cases, block specific solvents may be relevant. E.g. for chitosan-based diblocks, unreacted chitosan blocks can be removed by precipitation under conditions where the diblock remain soluble, or in the opposite case, chitosan-based diblocks can be removed by precipitation under conditions where the unreacted block is soluble. However, this purification method requires specific solubility of the blocks which needs to be thoroughly studied.

Another possible method to remove the excess of the unreacted activated block could be through reactions with solid beads, surfaces or columns functionalised with aldehyde or ketone groups. If the reaction is performed without reducing agent, the Schiff base formation can be reversed under specific conditions and the activated block can be reused after detachment. This, and other purification methods clearly deserve future attention.

### 3.6 Non-reducing end functionalisation of chitin blocks for the preparation of complex block polysaccharides and soluble chitin polymers

#### 3.6.1 Non-reducing end functionalisation of chitin blocks

Most of the terminal functionalisation reactions of polysaccharides reported in the literature are performed at the reducing end (RE). There are only a few polysaccharide specific methods available for functionalisation of the non-reducing end (NRE) residue hence, limiting the possibilities for the preparation of e.g. ABC-type block polysaccharides, where B is an oligo- or polysaccharide.

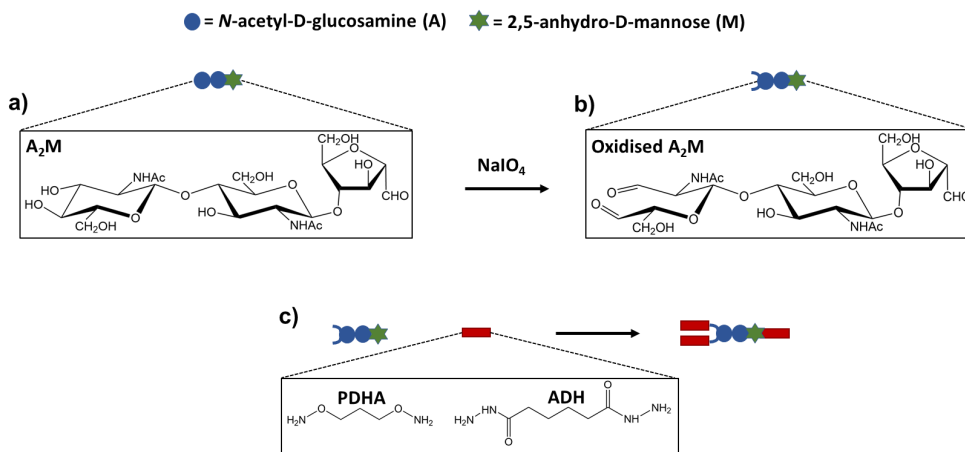
Chitin oligomers prepared by nitrous acid of chitosan ( $A_nM$ ) are however, special in this context as they only possess a single vicinal diol in their structure, located in the NRE residue (Figure 3.11a). Such oligosaccharides can, therefore, be selectively oxidised at the NRE by periodate to provide a dialdehyde (Figure 3.11b). Periodate oxidised  $A_nM$  activated by PDHA or ADH can further serve as precursors for more complex block polysaccharide structures such as e.g. ABC triblocks.

The preparation and activation of oxidised  $A_nM$  oligomers are described in **Paper III**. Activation was first studied using an excess of the bivalent linkers (10 equivalents ADH or PDHA). The results showed that both the aldehydes formed at the oxidised NRE (O-NRE) were reactive in contrast to lateral dialdehydes formed by periodate oxidation of alginates<sup>123, 124</sup>. The O-NRE aldehydes were also shown to be even more reactive than the pending aldehyde of the M reducing end residue. Due to reactivity of both aldehydes in the O-NRE, fully substituted oligomers could be obtained with an excess of the bivalent linkers (e.g. Figure 3.11 c). However, due to incomplete oxidation of the oligomers, a complex mixture of conjugates was formed. The incomplete oxidation was most probably a result of slow oxidation kinetics. The bivalency of the linkers (PDHA and ADH) also enabled the formation of several different chitin-based block structures and, perhaps surprisingly, cyclic structures. The presence of these structures suggested that the excess of the bivalent linkers was too low.

In the case of ADH, the reaction with periodate oxidised  $A_nM$  resulted in an excessive 'polymerisation' of ADH (also observed and discussed in **Paper I**) which limits the use of ADH in this context. However, we suggest that the polymerisation was enhanced by traces of periodate and that a more thorough purification of the oxidised oligomers (e.g. by GFC) will reduce the polymerisation rate. The slower reduction of oximes as compared to hydrazones (**Paper II**) was also observed for the Schiff bases formed with the aldehydes in the O-NRE residue. Therefore, longer reduction times were required for the PDHA activation of oxidised oligomers.

Further optimisation of oxidation and activation conditions is necessary for the applicability of this method. However, the preliminary results presented in **Paper III** shows that oxidised and fully substituted

(activated)  $A_nM$  oligomers can be prepared. Such activated oligomers can, in theory, enable the preparation of complex block polymers by attaching other oligo- or polysaccharides to the free end of the bivalent linkers.



**Figure 3.11:** a) chemical structure of an  $A_2M$  oligomer, b) chemical structure of a periodate oxidised  $A_2M$  oligomer, c) conjugation of PDHA or ADH to the RE and NRE of an oxidised  $A_2M$  oligomer (Figure 1 from **Paper III**).

### 3.6.2 Water-soluble chitin block polysaccharides

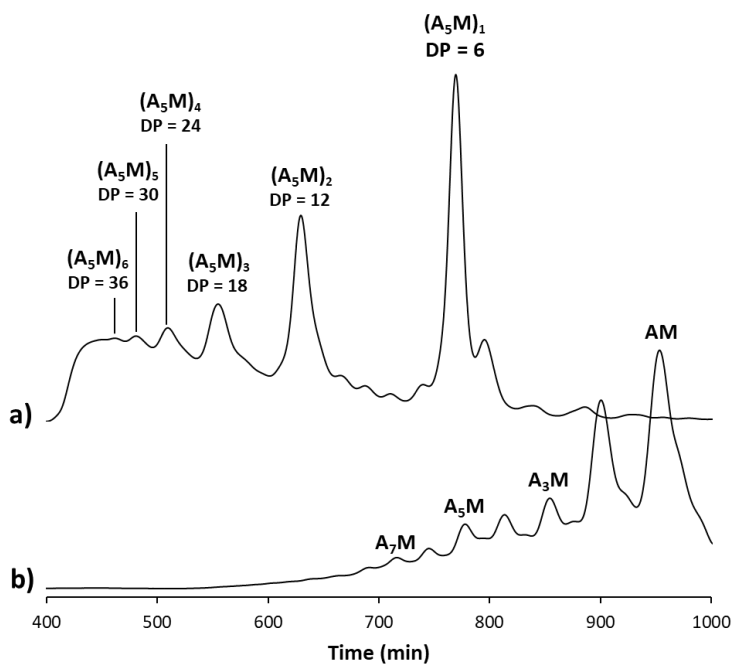
The low water-solubility of chitin limits its applicability and  $A_nM$  oligomers prepared by nitrous acid depolymerisation of chitosan are only water-soluble up to DP = 9. Even though water-soluble chitin derivatives are described in the literature (e.g. CM-chitin, DHP-chitin<sup>125</sup> and PEG-chitin<sup>126</sup>), these are, to the best of our knowledge, in all cases modified by lateral substitution which may suppress the intrinsic properties such as e.g. biochemical activities<sup>126, 127</sup>. Terminal modification of chitin is in contrast expected to retain much of the intrinsic properties.

When reacting periodate oxidised  $A_nM$  oligomers with sub-stoichiometric amounts of PDHA we observed not only the formation of the expected  $A_nM$ -PDHA- $MA_n$  diblocks, but also longer chitin block structures where the  $A_nM$  oligomers were linked through both the RE and O-NRE (**Paper III**). In the case of  $A_nM$  oligomers of DP 6 ( $n = 5$ ), which are close to the solubility limit of chitin, the ‘polymerisation’ of oxidised blocks resulted in water-soluble chitin polymers with a DP > 36 (based on the GFC calibration, Figure 3.12). Hence, a new type of modular and water-soluble chitin-based block polysaccharides had been prepared.

## SUMMARY OF RESULTS AND DISCUSSION

Due to the unoptimized oxidation conditions (discussed above), a large fraction of unreacted and unoxidized  $A_5M$  oligomers ( $(A_5M)_1$ , Figure 3.12) was present after reaction with PDHA. Their presence confirms the high reactivity of the O-NRE aldehydes since all the oxidised  $A_5M$  oligomers were part of longer ‘polymerised’ block structures. Hence, optimised oxidation protocols will enable formation of a larger fraction chitin block polymers and the length of the block structures can be adjusted by the concentration of bivalent linker.

The longest water-soluble  $A_nM$  oligomers may retain intrinsic chitin properties, such as biodegradability and self-assembling properties, as part of the chitin-block polymers. Hence, this new type of water-soluble chitin-based block polysaccharides can be relevant for pharmaceutical and biomaterial applications in the near future. These preliminary results are, however, in need for further investigation.



**Figure 3.12:** a) GFC fractionation following reaction of oxidised  $A_5M$  blocks ( $(A_5M)_n$ ) with 0.5 equivalents PDHA, b) fractionation of a standard mixture of  $A_nM$  oligomers for GFC calibration (Figure 7 from **Paper III**).

#### 4. Concluding remarks

The terminal activation of polysaccharides with bivalent oxyamines and hydrazides enables preparation of block polysaccharides. In contrast to other ‘click’ reactions, end coupling of polysaccharides by such linkers can be obtained by two simple reductive amination steps; activation of the first block and subsequent attachment of the second block to the free end of the bivalent linkers.

Chitin and chitosan are highly relevant in the context of block polysaccharides due to their high abundance, biocompatibility, biodegradability and, in the case of chitosan, its tuneable positive charge. In the work presented in this thesis, chitin and chitosan oligomers were terminally activated by PDHA (dioxyamine) and ADH (dihydrazide) using reductive amination with PB as the reductant. The kinetics of each step of the reductive amination reactions was studied in detail as a basis for developing activation protocols as the first step towards the preparation of chitin- and chitosan-based block polysaccharides.

Chitin and chitosan oligomers, prepared by nitrous acid depolymerisation of chitosan ( $A_nM$  and  $D_nM$  oligomers, respectively), were highly reactive towards activation by ADH and PDHA. The inability of such oligomers to form cyclic conjugates due to the pending aldehyde of the reducing end M residue, was reflected in high reaction rates and yields for the amination step (formation of oximes and hydrazones). Interestingly, the kinetics was independent of pH in the range studied (3.0 to 5.0). Reaction kinetics was also independent of the  $F_A$  of the oligomers, and hence, clearly reducing end specific.

The unreacted  $A_nM$  and  $D_nM$  oligomers were rapidly reduced due to the availability of the pending aldehyde. This was observed for both PB and for comparison  $NaCNBH_3$ . The reductive amination of such oligomers should therefore be performed in sequential reactions (e.g. amination followed by reduction). The reduction was, in contrast to the amination, highly pH-dependent and clearly fastest at low pH (3.0) for both linkers. Interestingly, conjugates formed with ADH (hydrazones) were reduced with a much higher rate than PDHA conjugates (oximes) and ADH is therefore the linker of choice for the preparation of conjugates composed of oligomers with M reducing end residues. The high rate of reduction for such conjugates by PB in combination with a fast decomposition of  $NaCNBH_3$  in addition to other drawbacks (including HSE concerns) makes protocols with PB recommended for these oligomers.

The high reactivity of the M residue is a complicating factor during the purification of oligomers with low  $F_A$  due to a pH-dependent degradation of the M residues following reactions with the free amino groups of the D residues. Such oligomers can, however, be activated by PDHA or ADH prior to purification to prevent the M degradation. This approach is also time saving as the purification from excess linker and isolation of activated oligomers of specific DP can be performed in the same step

## CONCLUDING REMARKS

Enzymatically produced CHOS with A residues at the reducing end ( $D_nXA$ ) were shown to have extremely low reactivity towards ADH and PDHA compared to the  $A_nM$  and  $D_nM$  oligomers, and also compared to glucan oligomers (dextran or  $\beta$ -1,3-glucans).  $D_nXA$  oligomers were, however, more reactive than CHOS terminating in D residues, encouraging us to recommend oligomers with terminal A residues as the best alternative for CHOS with pyranose reducing ends for reactions with PDHA and ADH.

The kinetics for the amination reactions with  $D_nXA$  oligomers and PDHA or ADH was, in contrast to the reactions with  $A_nM/D_nM$ , highly pH-dependent (in the range 3.0 to 5.0). For PDHA a drastic reduction in yield was observed at low pH, whereas the rates were reduced for both linkers at higher pH. pH 4.0 is therefore recommended to obtain high yields at acceptable rates for the activation of  $D_nXA$  oligomers. Yields and types of conjugates formed (acyclic Schiff bases or cyclic *N*-pyranosides) were highly linker dependent, and only cyclic conjugates (*N*-pyranosides) were formed with ADH whereas reaction with PDHA resulted in a mixture of acyclic and cyclic conjugates.

The reduction  $D_nXA$ -based conjugates was extremely slow compared to reduction of conjugates based on the other oligomers studied ( $A_nM/D_nM$ ,  $Dext_m$  and  $SBG_n$ ). Unreacted  $D_nXA$  oligomers were, however, not affected by PB and hence, reductive amination with these oligomers can be performed as conventional one pot.  $NaCNBH_3$  does not serve as an alternative reducing agent for these oligomers due to the formation of other (unidentified) types of conjugates. The reduction conjugates formed with ADH was slow compared to the reduction of PDHA conjugates and PDHA is therefore a better choice of linker for the preparation of  $D_nXA$ -based conjugates. The slow kinetics for the reductive amination of  $D_nXA$  oligomers was compensated for by using a high concentration of linkers, high concentration of PB and high temperatures.

The preparation of chitin- and chitosan-based diblock polysaccharides was demonstrated by attaching a second oligomer block to the free end of the linkers of ADH- and PDHA-activated oligomers. An increased reactivity was observed for the free end of both linkers after activation of the first block which facilitates the use of PDHA and ADH for the preparation of block polysaccharides.

Oligo- or polysaccharides with the lowest reactivity towards the linkers should be used as the first block in the preparation of block polysaccharides. This will most probably always apply to CHOS terminating in A or D residues, due to their extremely low reactivity towards PDHA and ADH compared to the other oligosaccharides studied.

To utilise the high reactivity of the M residue,  $A_nM$  oligomers prepared by nitrous acid depolymerisation should be used as the second block in the preparation of chitin-based diblock polysaccharides. However, due to the rapid reduction of unreacted oligomers, an excess of the activated block is required to obtain high amination yields prior to reduction. The activated block can be reused after purification, in contrast to



## CONCLUDING REMARKS

reduced and inactivated oligomers. In the case of oligomers with low  $F_A$  (e.g.  $D_nM$ ), degradation of the M residue was prevented by activation of the oligomers prior to purification, but this approach also prevents the use of chitosan oligomers ( $F_A < 1$ ) with M reducing end residues as the second block. De-*N*-acetylation of  $A_nM$  in premade block structures may therefore serve as an alternative for the preparation of chitosan-based block structures utilising the high reactivity of the M residue.

Even though  $D_nXA$ ,  $Dext_m$  and  $SBG_n$  oligomers can be reacted with the activated block in an equimolar ratio due to the slow reduction of unreacted oligomers, such protocols are limited by slow kinetics. An excess of the activated block is therefore also recommended for diblock protocols with these oligomers. However, protocols using an excess of the activated block will require purification of the diblocks. GFC fractionation was proven useful for shorter oligosaccharide blocks but block specific solvents and other purification methods deserve future attention.

The preparation of chitin-based block polysaccharides is limited by the low water-solubility of chitin, and  $A_nM$  oligomers are only water-soluble up to DP 9. Water-insoluble  $A_nM$  oligomers were, however, shown to react with PDHA in DMAc/LiCl and hence, this solvent can serve as an alternative for the preparation of chitin-based diblocks with longer water-insoluble chitin blocks.

The vicinal diol in the NRE residue of  $A_nM$  oligomers was selectively oxidised by periodate. Both aldehydes formed in the oxidised NRE residue were highly reactive towards PDHA and ADH and even more reactive than the aldehyde of the M residue. Oxidised  $A_nM$  oligomers activated by bivalent linkers at both termini can therefore serve as precursor for the preparation of more complex block polysaccharides (e.g. ABA- or ABC-type). However, limitations in the preceding oxidation step resulted in the presence of unoxidised oligomers and the protocols need to be optimised to increase the degree of oxidation. A large excess of linkers relative to aldehydes should also be used in optimised protocols to prevent the formation of cyclic conjugates and obtain fully activated oxidised oligomers

By reacting the periodate oxidised  $A_nM$  oligomers with a sub-stoichiometric amount of PDHA, a discrete distribution of 'polymerised' oligomers was formed. These chitin-based block polysaccharides were, in contrast to chitins of the same length, water-soluble. Hence, we have developed a relatively simple method for the preparation of a new type of water-soluble chitin polymers without lateral modification. Even though the method needs optimisation, the longest water-soluble  $A_nM$  oligomers may retain intrinsic chitin properties such as biodegradability and self-assembling properties and hence, such soluble chitin-based polymers may be relevant for pharmaceutical and biomaterial applications.

To summarise, we have developed  $NaCNBH_3$ - and aniline-free reductive amination protocols for the terminal activation of chitin and chitosan oligosaccharides by PDHA and ADH. Activation by PDHA and

## CONCLUDING REMARKS

ADH enables subsequent attachment of a second polysaccharide block to the free end of the bivalent linkers. Initial experiments with other polysaccharides (e.g., dextrans,  $\beta$ -1,3-glucans, and alginates) show that reactions with PDHA and ADH are versatile but conditions need to be adapted for each polysaccharide system. The block coupling strategy developed here can therefore be used for the preparation of a range of different chitin- and chitosan-based block polysaccharides where the intrinsic properties of the polysaccharide blocks (e.g. biodegradability, biocompatibility, charge, flexibility, crystallinity etc.) are retained.

## 5. References

1. Ruzette, A.-V.; Leibler, L. (2005) *Block copolymers in tomorrow's plastics*. *Nature Materials* 4 (1), 19-31.
2. Noshay, A.; McGrath, J. E. *Block copolymers: Overview and critical survey*. 1st ed., Academic (1977).
3. Volokhova, A. S.; Edgar, K. J.; Matson, J. B. (2020) *Polysaccharide-containing block copolymers: Synthesis and applications*. *Materials Chemistry Frontiers* 4 (1), 99-112.
4. Alexandridis, P.; Lindman, B. *Amphiphilic block copolymers: Self-assembly and applications*. 1st ed., Elsevier (2000).
5. Mai, Y.; Eisenberg, A. (2012) *Self-assembly of block copolymers*. *Chemical Society Reviews* 41 (18), 5969-5985.
6. Yu, G.-E.; Eisenberg, A. (1998) *Multiple morphologies formed from an amphiphilic ABC triblock copolymer in solution*. *Macromolecules* 31 (16), 5546-5549.
7. Schatz, C.; Lecommandoux, S. (2010) *Polysaccharide-containing block copolymers: synthesis, properties and applications of an emerging family of glycoconjugates*. *Macromolecular rapid communications* 31 (19), 1664-1684.
8. Novoa-Carballal, R.; Müller, A. H. E. (2012) *Synthesis of polysaccharide-b-PEG block copolymers by oxime click*. *Chemical Communications* 48 (31), 3781-3783.
9. Chen, J.; Spiering, G.; Mosquera-Giraldo, L.; Moore, R. B.; Edgar, K. J. (2020) *Regioselective bromination of the dextran nonreducing end creates a pathway to dextran-based block copolymers*. *Biomacromolecules* 21 (5), 1729-1738.
10. Yagi, S.; Kasuya, N.; Fukuda, K. (2010) *Synthesis and characterization of cellulose-b-polystyrene*. *Polymer Journal* 42 (4), 342-348.
11. Arrington, K. J.; Haag Iv, J. V.; French, E. V.; Murayama, M.; Edgar, K. J.; Matson, J. B. (2019) *Toughening cellulose: Compatibilizing polybutadiene and cellulose triacetate blends*. *ACS Macro Letters* 8 (4), 447-453.
12. Bernard, J.; Save, M.; Arathoon, B.; Charleux, B. (2008) *Preparation of a xanthate-terminated dextran by click chemistry: Application to the synthesis of polysaccharide-coated nanoparticles via surfactant-free ab initio emulsion polymerization of vinyl acetate*. *Journal of Polymer Science Part A: Polymer Chemistry* 46 (8), 2845-2857.
13. Halila, S.; Manguian, M.; Fort, S.; Cottaz, S.; Hamaide, T.; Fleury, E.; Driguez, H. (2008) *Syntheses of well-defined glyco-polyorganosiloxanes by "click" chemistry and their surfactant properties*. *Macromolecular Chemistry and Physics* 209 (12), 1282-1290.
14. Upadhyay, K. K.; Meins, J. F. L.; Misra, A.; Voisin, P.; Bouchaud, V.; Ibarboure, E.; Schatz, C.; Lecommandoux, S. (2009) *Biomimetic doxorubicin loaded polymersomes from hyaluronan-block-poly( $\gamma$ -benzyl glutamate) copolymers*. *Biomacromolecules* 10 (10), 2802-2808.

## REFERENCES

15. Otsuka, I.; Osaka, M.; Sakai, Y.; Travelet, C.; Putaux, J.-L.; Borsali, R. (2013) *Self-assembly of maltoheptaose-block-polystyrene into micellar nanoparticles and encapsulation of gold nanoparticles*. *Langmuir* 29 (49), 15224-15230.
16. Belbekhouche, S.; Ali, G.; Dulong, V.; Picton, L.; Le Cerf, D. (2011) *Synthesis and characterization of thermosensitive and pH-sensitive block copolymers based on polyetheramine and pullulan with different length*. *Carbohydrate Polymers* 86 (1), 304-312.
17. Upadhyay, K. K.; Bhatt, A. N.; Mishra, A. K.; Dwarakanath, B. S.; Jain, S.; Schatz, C.; Le Meins, J.-F.; Farooque, A.; Chandraiah, G.; Jain, A. K.; Misra, A.; Lecommandoux, S. (2010) *The intracellular drug delivery and anti tumor activity of doxorubicin loaded poly( $\gamma$ -benzyl l-glutamate)-b-hyaluronan polymersomes*. *Biomaterials* 31 (10), 2882-2892.
18. Sun, H.; Guo, B.; Li, X.; Cheng, R.; Meng, F.; Liu, H.; Zhong, Z. (2010) *Shell-sheddable micelles based on dextran-SS-poly( $\epsilon$ -caprolactone) diblock copolymer for efficient intracellular release of doxorubicin*. *Biomacromolecules* 11 (4), 848-854.
19. Ganji, F.; Abdekhodaie, M. J. (2008) *Synthesis and characterization of a new thermosensitive chitosan-PEG diblock copolymer*. *Carbohydrate Polymers* 74 (3), 435-441.
20. Yang, Q.; Lai, S. K. (2015) *Anti-PEG immunity: Emergence, characteristics, and unaddressed questions*. *WIREs Nanomedicine and Nanobiotechnology* 7 (5), 655-677.
21. Knop, K.; Hoogenboom, R.; Fischer, D.; Schubert, U. S. (2010) *Poly(ethylene glycol) in drug delivery: Pros and cons as well as potential alternatives*. *Angewandte Chemie International Edition* 49 (36), 6288-6308.
22. Breitenbach, B. B.; Schmid, I.; Wich, P. R. (2017) *Amphiphilic polysaccharide block copolymers for pH-responsive micellar nanoparticles*. *Biomacromolecules* 18 (9), 2839-2848.
23. de Medeiros Modolon, S.; Otsuka, I.; Fort, S. b.; Minatti, E.; Borsali, R.; Halila, S. (2012) *Sweet block copolymer nanoparticles: Preparation and self-assembly of fully oligosaccharide-based amphiphile*. *Biomacromolecules* 13 (4), 1129-1135.
24. Breitenbach, B. B.; Steiert, E.; Konhäuser, M.; Vogt, L.-M.; Wang, Y.; Parekh, S. H.; Wich, P. R. (2019) *Double stimuli-responsive polysaccharide block copolymers as green macrosurfactants for near-infrared photodynamic therapy*. *Soft Matter* 15 (6), 1423-1434.
25. Cheng, L.; Luan, T.; Liu, D.; Cheng, J.; Li, H.; Wei, H.; Zhang, L.; Lan, J.; Liu, Y.; Zhao, G. (2018) *Diblock copolymer glyco-nanomicelles constructed by a maltoheptaose-based amphiphile for reduction- and pH-mediated intracellular drug delivery*. *Polymer Chemistry* 9 (11), 1337-1347.
26. Gauche, C.; Soldi, V.; Fort, S.; Borsali, R.; Halila, S. (2013) *Xyloglucan-based diblock co-oligomer: Synthesis, self-assembly and steric stabilization of proteins*. *Carbohydrate Polymers* 98 (2), 1272-1280.
27. Nakauchida, T.; Takata, Y.; Yamamoto, K.; Kadokawa, J.-i. (2016) *Chemoenzymatic synthesis and pH-responsive properties of amphoteric block polysaccharides*. *Organic & Biomolecular Chemistry* 14 (27), 6449-6456.

## REFERENCES

28. De Oliveira, W.; Classer, W. G. (1994) *Novel cellulose derivatives. II. synthesis and characteristics of mono-functional cellulose propionate segments*. *Cellulose 1* (1), 77-86.
29. Mezger, T.; Cantow, H.-J. (1983) *Cellulose containing block copolymers. 4. Cellulose triester macroinitiators*. *Die Angewandte Makromolekulare Chemie 116* (1), 13-27.
30. Chen, J.; Kamitakahara, H.; Edgar, K. J. (2020) *Synthesis of polysaccharide-based block copolymers via olefin cross-metathesis*. *Carbohydrate Polymers 229*, 115530.
31. Hashimoto, K.; Imanishi, S.-I.; Okada, M.; Sumitomo, H. (1991) *Chemical modification of the reducing chain end in dextrans and trimethylsilylation of its hydroxyl groups*. *Journal of Polymer Science Part A: Polymer Chemistry 29* (9), 1271-1279.
32. Zhang, T.; Marchant, R. E. (1994) *Novel polysaccharide surfactants: Synthesis of model compounds and dextran-based surfactants*. *Macromolecules 27* (25), 7302-7308.
33. Tømmeraa, K.; Vårum, K. M.; Christensen, B. E.; Smidsrød, O. (2001) *Preparation and characterisation of oligosaccharides produced by nitrous acid depolymerisation of chitosans*. *Carbohydrate Research 333* (2), 137-144.
34. Tømmeraa, K.; Strand, S. P.; Christensen, B. E.; Smidsrød, O.; Vårum, K. M. (2011) *Preparation and characterization of branched chitosans*. *Carbohydrate Polymers 83* (4), 1558-1564.
35. Albersheim, P.; Neukom, H.; Deuel, H. (1960) *Splitting of pectin chain molecules in neutral solutions*. *Archives of Biochemistry and Biophysics 90* (1), 46-51.
36. Haug, A.; Larsen, B.; Smidsrød, O. (1967) *Alkaline degradation of alginate*. *Acta Chemica Scandinavia 21*, 2859-2870.
37. Wang, Z.; Shi, C.; Wu, X.; Chen, Y. (2014) *Efficient access to the non-reducing end of low molecular weight heparin for fluorescent labeling*. *Chemical Communications 50* (53), 7004-7006.
38. Linhardt, R. J.; Galliher, P. M.; Cooney, C. L. (1987) *Polysaccharide lyases*. *Applied Biochemistry and Biotechnology 12* (2), 135-176.
39. Meng, X.; Edgar, K. J. (2016) *“Click” reactions in polysaccharide modification*. *Progress in Polymer Science 53*, 52-85.
40. Kolb, H. C.; Finn, M. G.; Sharpless, K. B. (2001) *Click chemistry: diverse chemical function from a few good reactions*. *Angewandte Chemie International Edition 40* (11), 2004-2021.
41. Koo, S. P. S.; Stamenović, M. M.; Prasath, R. A.; Inglis, A. J.; Du Prez, F. E.; Barner-Kowollik, C.; Van Camp, W.; Junkers, T. (2010) *Limitations of radical thiol-ene reactions for polymer-polymer conjugation*. *Journal of Polymer Science Part A: Polymer Chemistry 48* (8), 1699-1713.
42. Mi, F.-L. (2005) *Synthesis and characterization of a novel chitosan-gelatin bioconjugate with fluorescence emission*. *Biomacromolecules 6* (2), 975-987.

## REFERENCES

43. Lallana, E.; Fernandez-Megia, E.; Riguera, R. (2009) *Surpassing the use of copper in the click functionalization of polymeric nanostructures: A strain-promoted approach*. Journal of the American Chemical Society *131* (16), 5748-5750.
44. Fina, N. J.; Edwards, J. O. (1973) *The alpha effect. A review*. International Journal of Chemical Kinetics *5* (1), 1-26.
45. Baudendistel, O. R.; Wieland, D. E.; Schmidt, M. S.; Wittmann, V. (2016) *Real-time NMR studies of oxamine ligations of reducing carbohydrates under equilibrium conditions*. Chemistry - A European Journal *22* (48), 17359-17365.
46. Hermanson, G. T. *Bioconjugate Techniques*. 2nd ed., Academic Press (2008).
47. Kwase, Y. A.; Cochran, M.; Nitz, M. (2014) *Protecting-group-free glycoconjugate synthesis: Hydrazide and oxamine derivatives in N-glycoside formation*. Modern Synthetic Methods in Carbohydrate Chemistry.
48. Lee, M.-R.; Shin, I. (2005) *Facile preparation of carbohydrate microarrays by site-specific, covalent immobilization of unmodified carbohydrates on hydrazide-coated glass slides*. Organic Letters *7* (19), 4269-4272.
49. Ramsay, S. L.; Freeman, C.; Grace, P. B.; Redmond, J. W.; MacLeod, J. K. (2001) *Mild tagging procedures for the structural analysis of glycans*. Carbohydrate Research *333* (1), 59-71.
50. Unterieser, I.; Mischnick, P. (2011) *Labeling of oligosaccharides for quantitative mass spectrometry*. Carbohydrate Research *346* (1), 68-75.
51. Ruhaak, L. R.; Steenvoorden, E.; Koeleman, C. A. M.; Deelder, A. M.; Wuhrer, M. (2010) *2-Picoline-borane: A non-toxic reducing agent for oligosaccharide labeling by reductive amination*. PROTEOMICS *10* (12), 2330-2336.
52. Dworkin, J. P.; Miller, S. L. (2000) *A kinetic estimate of the free aldehyde content of aldoses*. Carbohydrate Research *329* (2), 359-365.
53. Los, J.; Simpson, L.; Wiesner, K. (1956) *The kinetics of mutarotation of D-glucose with consideration of an intermediate free-aldehyde form*. Journal of the American Chemical Society *78* (8), 1564-1568.
54. Sun, Z.; Wei, Z.; Wei, K. (2009) *A model for predicting the optimal conditions for labeling the carbohydrates with the amine derivatives by reductive amination* Letters in Organic Chemistry *6* (7), 549-551.
55. Borch, R. F.; Bernstein, M. D.; Durst, H. D. (1971) *Cyanohydridoborate anion as a selective reducing agent*. Journal of the American Chemical Society *93* (12), 2897-2904.
56. Abdel-Magid, A. F.; Carson, K. G.; Harris, B. D.; Maryanoff, C. A.; Shah, R. D. (1996) *Reductive amination of aldehydes and ketones with sodium triacetoxymethylborohydride. Studies on direct and indirect reductive amination procedures*. The Journal of Organic Chemistry *61* (11), 3849-3862.

## REFERENCES

57. Pelter, A.; Rosser, R. M.; Mills, S. (1984) *Reductive aminations of ketones and aldehydes using borane-pyridine*. Journal of the Chemical Society, Perkin Transactions 1, 717-720.
58. Sato, S.; Sakamoto, T.; Miyazawa, E.; Kikugawa, Y. (2004) *One-pot reductive amination of aldehydes and ketones with  $\alpha$ -picoline-borane in methanol, in water, and in neat conditions*. Tetrahedron 60 (36), 7899-7906.
59. Fang, J.; Qin, G.; Ma, J.; She, Y.-M. (2015) *Quantification of plant cell wall monosaccharides by reversed-phase liquid chromatography with 2-aminobenzamide pre-column derivatization and a non-toxic reducing reagent 2-picoline borane*. Journal of Chromatography A 1414, 122-128.
60. Cosenza, V. A.; Navarro, D. A.; Stortz, C. A. (2011) *Usage of  $\alpha$ -picoline borane for the reductive amination of carbohydrates*. ARKIVOC: Online Journal of Organic Chemistry 7, 182-194.
61. Guerry, A.; Bernard, J.; Samain, E.; Fleury, E.; Cottaz, S.; Halila, S. (2013) *Aniline-catalyzed reductive amination as a powerful method for the preparation of reducing end-“clickable” chitooligosaccharides*. Bioconjugate Chemistry 24 (4), 544-549.
62. Thygesen, M. B.; Munch, H.; Sauer, J.; Cló, E.; Jørgensen, M. R.; Hindsgaul, O.; Jensen, K. J. (2010) *Nucleophilic catalysis of carbohydrate oxime formation by anilines*. The Journal of Organic Chemistry 75 (5), 1752-1755.
63. Kalia, J.; Raines, R. T. (2008) *Hydrolytic stability of hydrazones and oximes*. Angewandte Chemie International Edition 47 (39), 7523-7526.
64. Shinohara, Y.; Sota, H.; Gotoh, M.; Hasebe, M.; Tosu, M.; Nakao, J.; Hasegawa, Y.; Shiga, M. (1996) *Bifunctional labeling reagent for oligosaccharides to incorporate both chromophore and biotin groups*. Analytical Chemistry 68 (15), 2573-2579.
65. Sharon, N. *Complex carbohydrates: Their Chemistry, Biosynthesis, and Functions*. 1st ed., Addison-Wesley Publishing Company (1975).
66. Kristiansen, K. A.; Potthast, A.; Christensen, B. E. (2010) *Periodate oxidation of polysaccharides for modification of chemical and physical properties*. Carbohydrate Research 345 (10), 1264-1271.
67. Ishak, M. F.; Painter, T.; Andersen, V.; Enzell, C.; Lousberg, R.; Weiss, U. (1971) *Formation of inter-residue hemiacetals during the oxidation of polysaccharides by periodate ion*. Acta Chemica Scandinavia 25 (10), 3875-3877.
68. Vold, I. M. N.; Christensen, B. E. (2005) *Periodate oxidation of chitosans with different chemical compositions*. Carbohydrate Research 340 (4), 679-684.
69. Hirano, S.; Yagi, Y. (1981) *Periodate oxidation of the non-reducing end-groups of substrates increases the rates of enzymic hydrolyses by chitinase and by lysozyme*. Carbohydrate Research 92 (2), 319-322.
70. Rinaudo, M. (2006) *Chitin and chitosan: Properties and applications*. Progress in Polymer Science 31 (7), 603-632.

## REFERENCES

71. Bartnicki-Garcia, S.; Nickerson, W. J. (1962) *Isolation, composition, and structure of cell walls of filamentous and yeast-like forms of Mucor rouxii*. *Biochimica et Biophysica Acta* 58 (1), 102-119.
72. Synowiecki, J.; Al-Khateeb, N. A. A. Q. (1997) *Mycelia of Mucor rouxii as a source of chitin and chitosan*. *Food Chemistry* 60 (4), 605-610.
73. Kurita, K. (2006) *Chitin and chitosan: Functional biopolymers from marine crustaceans*. *Marine Biotechnology* 8 (3), 203-226.
74. Vårum, K. M.; Antohonsen, M. W.; Grasdalen, H.; Smidsrød, O. (1991) *Determination of the degree of N-acetylation and the distribution of N-acetyl groups in partially N-deacetylated chitins (chitosans) by high-field n.m.r. spectroscopy*. *Carbohydrate Research* 211 (1), 17-23.
75. Vårum, K. M.; Anthonsen, M. W.; Grasdalen, H.; Smidsrød, O. (1991) *<sup>13</sup>C-N.m.r. studies of the acetylation sequences in partially N-deacetylated chitins (chitosans)*. *Carbohydrate Research* 217, 19-27.
76. Strand, S. P.; Tømmeraas, K.; Vårum, K. M.; Østgaard, K. (2001) *Electrophoretic light scattering studies of chitosans with different degrees of N-acetylation*. *Biomacromolecules* 2 (4), 1310-1314.
77. Vårum, K. M.; Ottøy, M. H.; Smidsrød, O. (1994) *Water-solubility of partially N-acetylated chitosans as a function of pH: Effect of chemical composition and depolymerisation*. *Carbohydrate Polymers* 25 (2), 65-70.
78. Sannan, T.; Kurita, K.; Iwakura, Y. (1976) *Studies on chitin, 2. Effect of deacetylation on solubility*. *Die Makromolekulare Chemie* 177 (12), 3589-3600.
79. Vårum, K. M.; Ottøy, M. H.; Smidsrød, O. (2001) *Acid hydrolysis of chitosans*. *Carbohydrate Polymers* 46 (1), 89-98.
80. Einbu, A.; Vårum, K. M. (2007) *Depolymerization and de-N-acetylation of chitin oligomers in hydrochloric acid*. *Biomacromolecules* 8 (1), 309-314.
81. Aam, B. B.; Heggset, E. B.; Norberg, A. L.; Sørli, M.; Vårum, K. M.; Eijsink, V. G. H. (2010) *Production of chitooligosaccharides and their potential applications in medicine*. *Marine Drugs* 8 (5), 1482-1517.
82. Davies, G. J.; Wilson, K. S.; Henrissat, B. (1997) *Nomenclature for sugar-binding subsites in glycosyl hydrolases*. *Biochemical Journal* 321 (2), 557-559.
83. Sørbotten, A.; Horn, S. J.; Eijsink, V. G. H.; Vårum, K. M. (2005) *Degradation of chitosans with chitinase B from Serratia marcescens*. *The FEBS Journal* 272 (2), 538-549.
84. Allan, G. G.; Peyron, M. (1995) *Molecular weight manipulation of chitosan I: Kinetics of depolymerization by nitrous acid*. *Carbohydrate Research* 277 (2), 257-272.
85. Allan, G. G.; Peyron, M. (1995) *Molecular weight manipulation of chitosan II: Prediction and control of extent of depolymerization by nitrous acid*. *Carbohydrate Research* 277 (2), 273-282.



## REFERENCES

86. Allan, G. G.; Peyron, M. *The kinetics of depolymerization of chitosan by nitrous acid*. In *Chitin and chitosan*, Elsevier Applied Science (1989), pp 443-466.
87. Peat, S. *The chemistry of anhydro sugars*. In *Advances in Carbohydrate Chemistry*, Elsevier (1946), pp 37-77.
88. Williams, J. M. *Deamination of carbohydrate amines and related compounds*. In *Advances in Carbohydrate Chemistry and Biochemistry*, Elsevier (1975), pp 9-79.
89. Defaye, J. *2,5-Anhydrides of sugars and related compounds*. In *Advances in Carbohydrate Chemistry and Biochemistry*, Elsevier (1970), pp 181-228.
90. Shafizadeh, F. *Formation and cleavage of the oxygen ring in sugars*. In *Advances in carbohydrate chemistry*, Elsevier (1958), pp 9-61.
91. Lindberg, B.; Lönnngren, J.; Svensson, S. *Specific degradation of polysaccharides*. In *Advances in Carbohydrate Chemistry and Biochemistry*, Academic Press (1975), pp 185-240.
92. Erbing, C.; Lindberg, B.; Svensson, S. (1973) *Deamination of methyl 2-amino-2-deoxy- $\alpha$ - and  $\beta$ -D-glucopyranosides* Acta Chemica Scandinavia 27 (10), 3699-3704.
93. Moussa, A.; Crépet, A.; Ladavière, C.; Trombotto, S. (2019) *Reducing-end "clickable" functionalizations of chitosan oligomers for the synthesis of chitosan-based diblock copolymers*. Carbohydrate Polymers 219, 387-394.
94. Pickenhahn, V. D.; Darras, V.; Dziopa, F.; Biniecki, K.; De Crescenzo, G.; Lavertu, M.; Buschmann, M. D. (2015) *Regioselective thioacetylation of chitosan end-groups for nanoparticle gene delivery systems*. Chemical Science 6 (8), 4650-4664.
95. Coudurier, M.; Faivre, J.; Crepet, A.; Ladaviere, C.; Delair, T.; Schatz, C.; Trombotto, S. (2020) *Reducing-end functionalization of 2,5-Anhydro-D-mannofuranose-linked chitoooligosaccharides by dioxamine: Synthesis and characterization*. Molecules 25 (5), 1143.
96. Zargar, V.; Asghari, M.; Dashti, A. (2015) *A review on chitin and chitosan polymers: Structure, chemistry, solubility, derivatives, and applications*. ChemBioEng Reviews 2 (3), 204-226.
97. Ravi Kumar, M. N. V. (2000) *A review of chitin and chitosan applications*. Reactive and Functional Polymers 46 (1), 1-27.
98. Kim, S.-K.; Rajapakse, N. (2005) *Enzymatic production and biological activities of chitosan oligosaccharides (COS): A review*. Carbohydrate Polymers 62 (4), 357-368.
99. Zou, P.; Yang, X.; Wang, J.; Li, Y.; Yu, H.; Zhang, Y.; Liu, G. (2016) *Advances in characterisation and biological activities of chitosan and chitosan oligosaccharides*. Food Chemistry 190, 1174-1181.
100. Liaqat, F.; Eltem, R. (2018) *Chitoooligosaccharides and their biological activities: A comprehensive review*. Carbohydrate Polymers 184, 243-259.

## REFERENCES

101. Bahrke, S.; Einarsson, J. M.; Gislason, J.; Haebel, S.; Letzel, M. C.; Peter-Katalinić, J.; Peter, M. G. (2002) *Sequence analysis of chitoooligosaccharides by matrix-assisted laser desorption ionization postsources decay mass spectrometry*. *Biomacromolecules* 3 (4), 696-704.
102. Li, K.; Xing, R.; Liu, S.; Li, P. (2016) *Advances in preparation, analysis and biological activities of single chitoooligosaccharides*. *Carbohydrate Polymers* 139, 178-190.
103. Heinze, T.; Liebert, T.; Heublein, B.; Hornig, S. *Functional polymers based on dextran*. In *Polysaccharides II*, Springer Berlin Heidelberg (2006), pp 199-291.
104. Kasai, M. R. (2012) *Dilute solution properties and degree of chain branching for dextran*. *Carbohydrate Polymers* 88 (1), 373-381.
105. Naessens, M.; Cerdobbel, A.; Soetaert, W.; Vandamme, E. J. (2005) *Leuconostoc dextranucrase and dextran: Production, properties and applications*. *Journal of Chemical Technology & Biotechnology* 80 (8), 845-860.
106. Couch, N. P. (1965) *The clinical status of low molecular weight dextran: A critical review*. *Clinical Pharmacology & Therapeutics* 6 (5), 656-665.
107. Zlatković, D.; Jakovljević, D.; Zeković, Đ.; Vrvic, M. (2003) *A glucan from active dry baker's yeast (Saccharomyces cerevisiae): A chemical and enzymatic investigation of the structure*. *Journal of the Serbian Chemical Society* 68 (11), 805-809.
108. Zhu, F.; Du, B.; Xu, B. (2016) *A critical review on production and industrial applications of beta-glucans*. *Food Hydrocolloids* 52, 275-288.
109. Qin, F.; Kes, M.; Christensen, B. E. (2013) *A study of bioactive, branched (1→3)-β-D-glucans in dimethylacetamide/LiCl and dimethyl sulphoxide/LiCl using size-exclusion chromatography with multi-angle light scattering detection*. *Journal of Chromatography A* 1305, 109-113.
110. Stier, H.; Ebbeskotte, V.; Gruenwald, J. (2014) *Immune-modulatory effects of dietary Yeast Beta-1,3/1,6-D-glucan*. *Nutrition Journal* 13 (1), 38.
111. Bohn, J. A.; BeMiller, J. N. (1995) *(1→3)-β-d-Glucans as biological response modifiers: a review of structure-functional activity relationships*. *Carbohydrate Polymers* 28 (1), 3-14.
112. Lee, J.-N.; Lee, D.-Y.; Ji, I.-H.; Kim, G.-E.; Kim, H. N.; Sohn, J.; Kim, S.; Kim, C.-W. (2001) *Purification of soluble β-glucan with immune-enhancing activity from the cell wall of yeast*. *Bioscience, Biotechnology, and Biochemistry* 65 (4), 837-841.
113. Ma, J.; Underhill, D. M. (2013) *β-Glucan signaling connects phagocytosis to autophagy*. *Glycobiology* 23 (9), 1047-1051.
114. Grip, J.; Engstad, R. E.; Skjæveland, I.; Škalko-Basnet, N.; Isaksson, J.; Basnet, P.; Holsæter, A. M. (2018) *Beta-glucan-loaded nanofiber dressing improves wound healing in diabetic mice*. *European Journal of Pharmaceutical Sciences* 121, 269-280.
115. Smidsrød, O.; Moe, S. T. *Biopolymer chemistry*. Tapir Academic Press (2008).

## REFERENCES

116. Vårum, K. M.; Kristiansen Holme, H.; Izume, M.; Torger Stokke, B.; Smidsrød, O. (1996) *Determination of enzymatic hydrolysis specificity of partially N-acetylated chitosans*. *Biochimica et Biophysica Acta (BBA) - General Subjects* 1291 (1), 5-15.
117. Sugiyama, H.; Hisamichi, K.; Sakai, K.; Usui, T.; Ishiyama, J.-I.; Kudo, H.; Ito, H.; Senda, Y. (2001) *The conformational study of chitin and chitosan oligomers in solution*. *Bioorganic & Medicinal Chemistry* 9 (2), 211-216.
118. Zaia, J. (2004) *Mass spectrometry of oligosaccharides*. *Mass Spectrometry Reviews* 23 (3), 161-227.
119. Ho, C. S.; Lam, C. W. K.; Chan, M. H. M.; Cheung, R. C. K.; Law, L. K.; Lit, L. C. W.; Ng, K. F.; Suen, M. W. M.; Tai, H. L. (2003) *Electrospray ionisation mass spectrometry: Principles and clinical applications*. *The Clinical Biochemist Reviews* 24 (1), 3-12.
120. Beaudoin, M.-E.; Gauthier, J.; Boucher, I.; Waldron, K. C. (2005) *Capillary electrophoresis separation of a mixture of chitin and chitosan oligosaccharides derivatized using a modified fluorophore conjugation procedure*. *Journal of Separation Science* 28 (12), 1390-1398.
121. Poirier, M.; Charlet, G. (2002) *Chitin fractionation and characterization in N,N-dimethylacetamide/lithium chloride solvent system*. *Carbohydrate Polymers* 50 (4), 363-370.
122. Terbojevich, M.; Carraro, C.; Cosani, A.; Marsano, E. (1988) *Solution studies of the chitin-lithium chloride-N,N-di-methylacetamide system*. *Carbohydrate Research* 180 (1), 73-86.
123. Kristiansen, K. A.; Ballance, S.; Potthast, A.; Christensen, B. E. (2009) *An evaluation of tritium and fluorescence labelling combined with multi-detector SEC for the detection of carbonyl groups in polysaccharides*. *Carbohydrate Polymers* 76 (2), 196-205.
124. Dalheim, M. Ø.; Vanacker, J.; Najmi, M. A.; Aachmann, F. L.; Strand, B. L.; Christensen, B. E. (2016) *Efficient functionalization of alginate biomaterials*. *Biomaterials* 80, 146-156.
125. Tokura, S.; Nishi, N.; Tsutsumi, A.; Somorin, O. (1983) *Studies on chitin VIII. Some properties of water soluble chitin derivatives*. *Polymer Journal* 15 (6), 485-489.
126. Sugimoto, M.; Morimoto, M.; Sashiwa, H.; Saimoto, H.; Shigemasa, Y. (1998) *Preparation and characterization of water-soluble chitin and chitosan derivatives*. *Carbohydrate Polymers* 36 (1), 49-59.
127. Maeda, R.; Matsumoto, M.; Kondo, K. (1997) *Enzymatic hydrolysis reaction of water-soluble chitin derivatives with egg white lysozyme*. *Journal of Fermentation and Bioengineering* 84 (5), 478-479.

## Appendix I: Preparation and activation of D<sub>n</sub>M oligomers

### Background

Fully de-*N*-acetylated oligomers with the highly reactive M residue (D<sub>n</sub>M) can be prepared by degradation of chitosans with low F<sub>A</sub> using a sub-stoichiometric amount nitrous acid (HONO). Such oligomers have previously been used for the preparation of branched chitosans<sup>1</sup>. However, the purification of isolated D<sub>n</sub>M oligomers can be troublesome due to reactions of the highly reactive M residues with the free amino groups of the D residues, which can lead to self-branching through Schiff base formation and subsequent degradation of the M residue (pH-dependent)<sup>2</sup>. Here, we attempted to prepare isolated D<sub>n</sub>M oligomers and subsequently activate the oligomers by PDHA and ADH to compare their reactivity to the reactivity of fully *N*-acetylated (A<sub>n</sub>M) oligomers (**Paper II**).

### Materials and methods

Chitosan with low F<sub>A</sub> was an in-house sample prepared by extensive de-*N*-acetylation of chitin (F<sub>A</sub> = 0.01). The chitosan (20 mg/mL) was dissolved in acetic acid (AcOH, 2.5 vol%) by stirring overnight. Dissolved oxygen was removed by bubbling the solution with N<sub>2</sub> gas for 15 minutes. After cooling the solution to approx. 4 °C, solid NaNO<sub>2</sub> (0.22 moles HONO: mole D residues) was added directly to the chitosan solution. The reaction mixture was agitated in the dark at 4 °C for 72 hours. The mixture of oligomers was dialysed (MWCO = 100-500 Da) against MQ-water until the measured conductivity was < 2 μS/cm and freeze-dried.

D<sub>n</sub>M oligomers were fractionated according to degree of polymerization (DP) using the analytical gel filtration chromatography (GFC) system described in **Paper I** and **II**. Oligomer fractions were purified by direct freeze-drying, to remove the volatile GFC-buffer (0.15 M AmAc-buffer, pH 4.5), or by dialysis (as describe above) and characterized by <sup>1</sup>H-NMR as described for A<sub>n</sub>M oligomers in **Paper II**. The activation of D<sub>n</sub>M oligomers with PDHA and ADH was studied by course <sup>1</sup>H-NMR at pH 4.0, RT as described for A<sub>n</sub>M oligomers in **Paper II**.

The unfractionated mixture of D<sub>n</sub>M oligomers formed after depolymerisation was activated by PDHA and ADH using the preparative protocol developed for A<sub>n</sub>M oligomers in **Paper II**. The activated oligomers were fractionated according to DP by GFC and purified by direct freeze-drying.

Dextran (Dext<sub>m</sub>) oligomers were obtained by acid hydrolysis and fractionated according to DP by GFC as described in **Paper II**. The activated D<sub>n</sub>M conjugates were reacted with Dext<sub>m</sub> oligomers using the protocol described in **Paper II**.

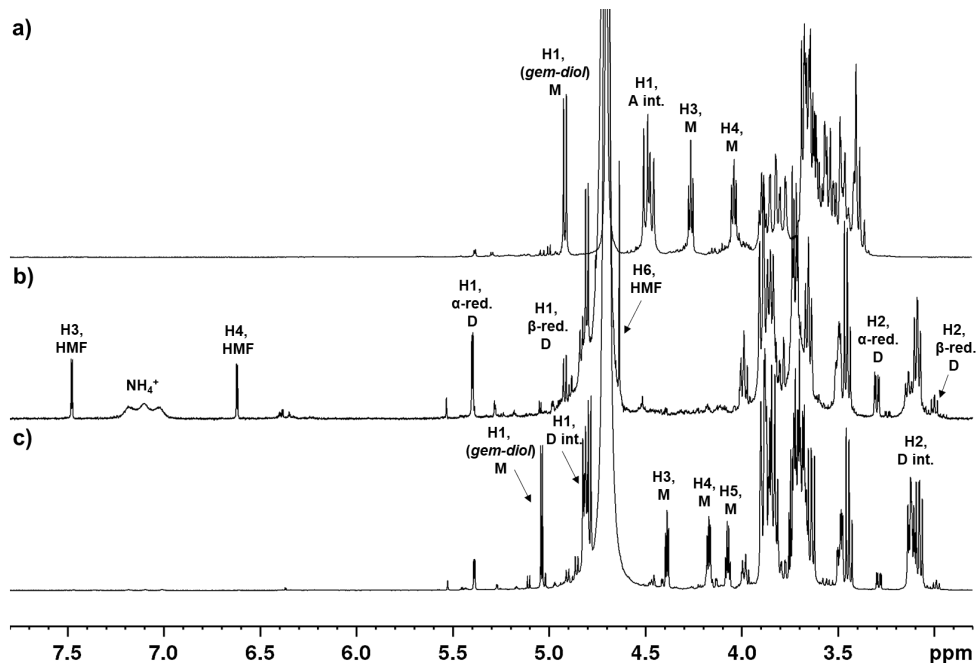
## Results

### Preparation of defined D<sub>n</sub>M oligomers

D<sub>n</sub>M were prepared by degradation of chitosan using a sub-stoichiometric amount of HONO and oligomers of specific DP were obtained by subsequent GFC fractionation. Initially, direct freeze-drying was used to purify the fractionated D<sub>n</sub>M oligomers from the volatile GFC buffer (0.15 M AmAc-buffer, pH 4.5). However, a close to complete loss of the M residues was observed by <sup>1</sup>H-NMR characterisation of the oligomers after purification, and 5-hydroxymethyl-2-furfural (HMF) and chitosan oligomers with normal reducing end (D<sub>n</sub>) were formed (Figure AI.1b). The degradation of the M residue was attributed to the increase in pH during the freeze-drying process as a result of water and acetic acid from the buffer evaporating first, leaving ammonia<sup>2</sup>. The deprotonation of primary amine groups of the D residues at higher pH enables reactions with the aldehydes of the M residues to form Schiff bases and a subsequent decrease in pH resulted in the degradation of the M residues and formation of HMF.

To prevent the degradation of M residues, oligomer fractions were purified by extensive dialysis (approximately 4 days) to remove buffer components, and the pH was adjusted to < 4.0 prior to freeze-drying. This purification method resulted in a higher preservation of the M residues (Figure AI.1c), but still 30-50 % were degraded. Interestingly, the preservation of the M residues was higher for shorter oligomers than for longer. Approximately 30, 40 and 50 % of the M residues were degraded in the D<sub>3</sub>M, D<sub>8</sub>M, and D<sub>11</sub>M fractions, respectively. Hence, the purification of D<sub>n</sub>M oligomers require an even longer dialysis step to prevent the degradation of the M residue.

## APPENDIX I



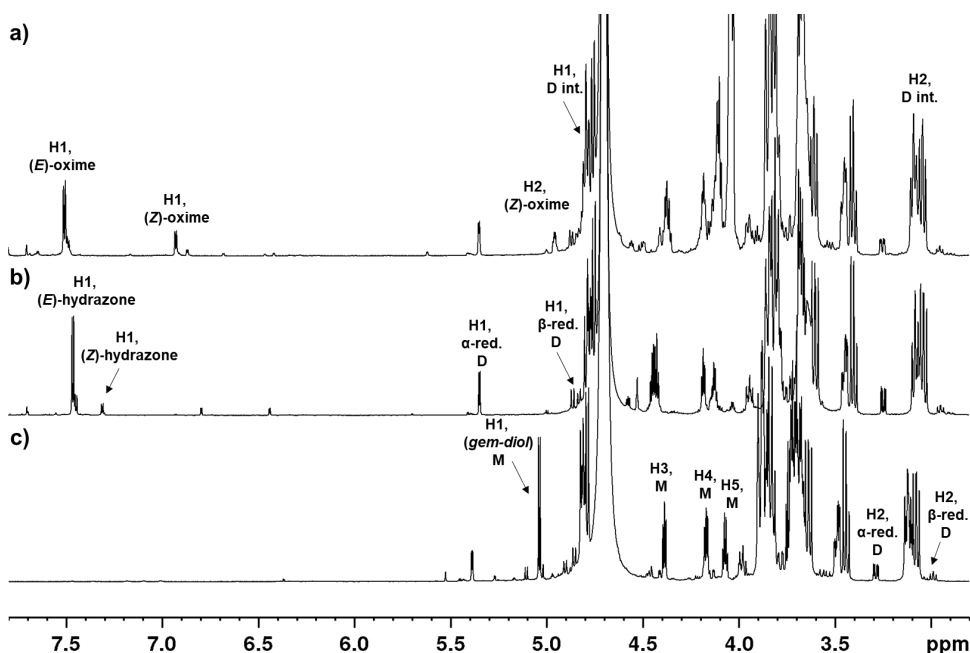
**Figure AI.1:**  $^1\text{H-NMR}$  spectra of **a)** purified  $\text{A}_2\text{M}$  oligomers with intact M residues, **b)** the  $\text{D}_3\text{M}$  fraction after purification by direct freeze-drying resulting in complete loss of the M residues, and **c)** the  $\text{D}_3\text{M}$  fraction after purification by extensive dialysis and subsequent freeze-drying with approx. 70 % intact M residues.

### Activation of $\text{D}_n\text{M}$ oligomers by PDHA and ADH

Purified  $\text{D}_3\text{M}$  oligomers (70 % intact M residues) were activated by PDHA and ADH using the protocol described for  $\text{A}_n\text{M}$  oligomers in **Paper II** (pH 4.0, 2 equivalents linker relative to oligomer, RT) and the amination and reduction were studied separately by time course  $^1\text{H-NMR}$ . The high reactivity observed for the M residue of  $\text{A}_n\text{M}$  oligomers was confirmed for the  $\text{D}_n\text{M}$  oligomers and Schiff base equilibria (> 90 % yield of conjugates) were obtained in < 4 hours. The H1, M *gem-diol* resonance was completely disappeared from the  $^1\text{H-NMR}$  spectrum at equilibrium (Figure AI.2). The H1 ( $\alpha$ - and  $\beta$ -red.) resonances from the reducing end D residues formed upon M degradation were, however, unaffected, confirming the low reactivity of D residues described in **Paper I**. The relative ratio of (*E*)-:(*Z*)- oximes/hydrazones was approx. 3:1 and 8:1 for the reaction with PDHA and ADH, respectively, in good compliance with the reactions with  $\text{A}_n\text{M}$  oligomers (described in **Paper II**).

Subsequent reduction of the Schiff bases formed with  $\text{D}_n\text{M}$  oligomers by PB was studied and compared to the equivalent reactions with  $\text{A}_n\text{M}$  oligomers (3 equivalents PB, pH 4.0, RT) revealing identical reduction

kinetics. The kinetics for the reduction of the unreacted  $D_nM$  oligomers was also close to equal to the reduction of  $A_nM$  oligomers under the same conditions.



**Figure A1.2:**  $^1\text{H-NMR}$  spectra of **a)** the equilibrium mixture obtained for reaction of the  $D_3M$  fraction with 2 equivalents PDHA, **b)** the equilibrium mixture obtained for reaction of the  $D_3M$  fraction with 2 equivalents ADH **c)** the  $D_3M$  fraction prior to activation.

### Alternative activation strategy for $D_nM$ oligomers

We proposed that protection of the highly reactive aldehyde of the M residue could prevent its degradation during purification. As an alternative approach, the mixture of  $D_nM$  oligomers was therefore activated by PDHA and ADH using an excess of the linkers prior to fractionation by GFC. This method preserved the M residues and provided fully activated  $D_nM$  oligomers, however, with a broad DP distribution. Due to the masking of the M aldehyde, purification after subsequent GFC fractionation was performed by direct freeze-drying. In addition to protect the M residue from degradation, this alternative approach is time saving as it combines the purification of conjugates from excess PDHA or ADH and the isolation of conjugates with specific DP and can therefore also be applicable for other oligomers.

## APPENDIX I

### **D<sub>n</sub>M-based block polysaccharides**

Due to the high reactivity of the M residue, defined A<sub>n</sub>M oligomers can be used as the second block for the preparation of block polysaccharides, however, using an excess of the first block to prevent reduction of unreacted oligomers (discussed in **Paper II**). A similar strategy can be relevant for D<sub>n</sub>M oligomers. However, this is only applicable if an unfractionated mixture of oligomers is used (due to the current purification issues) and the pH of the reaction is below pK<sub>a</sub> of the amino groups (to prevent self-branching and subsequent degradation of the M residues). If D<sub>n</sub>M oligomers of defined DP are desired, the alternative approach should be applied to form activated (protected) D<sub>n</sub>M oligomers. In this case, the defined D<sub>n</sub>M conjugates need to serve as the first block for the preparation of block polysaccharides. D<sub>n</sub>M-*b*-Dext<sub>m</sub> block polysaccharides were successfully prepared using this approach and the protocols developed for the preparation of A<sub>n</sub>M-*b*-Dext<sub>m</sub> described in **Paper II**.

### **Conclusions**

D<sub>n</sub>M oligomers were shown to have the same high reactivity as observed for A<sub>n</sub>M oligomers when activated by PDHA and ADH (amination). The kinetics of the subsequent reduction of the conjugates formed with D<sub>n</sub>M was also identical to the reduction of A<sub>n</sub>M conjugates. Hence, both the amination and reduction are clearly dependent on the chemistry of the M residue, but independent of the composition (F<sub>A</sub>) of the oligomers. Due to the degradation of the M residue during purification of isolated D<sub>n</sub>M oligomers, an alternative approach was applied for these oligomers where the activation of oligomers by PDHA and ADH was performed prior to isolation and purification. This approach is time saving and provides activated oligomers of specific DP with only one purification step. However, it prevents the use of D<sub>n</sub>M oligomers as the second block for the preparation of block polysaccharides.

### **References**

1. Tømmerraas, K.; Strand, S. P.; Christensen, B. E.; Smidsrød, O.; Vårum, K. M. (2011) *Preparation and characterization of branched chitosans*. Carbohydrate Polymers 83 (4), 1558-1564.
2. Tømmerraas, K.; Vårum, K. M.; Christensen, B. E.; Smidsrød, O. (2001) *Preparation and characterisation of oligosaccharides produced by nitrous acid depolymerisation of chitosans*. Carbohydrate Research 333 (2), 137-144.



## Appendix II: Preparation and activation of $\beta$ -1,3-glucan oligomers

### Background

$\beta$ -1,3-linked glucans with a low number of  $\beta$ -1,6-linked branches can be extracted from the cell wall *Saccharomyces cerevisiae*. Such  $\beta$ -glucans are water-soluble and are conveniently called soluble  $\beta$ -glucans (SBGs)<sup>1</sup>. In collaboration with the company Biotech BetaGlucans®, we prepared SBG oligomers of defined DP (SBG<sub>n</sub>, n = DP). The SBG<sub>n</sub> oligomers were activated by ADH and PDHA and results were compared to the activation of the  $\alpha$ -1,6-linked dextran (Dext<sub>m</sub>) oligomers (**Paper II**) to study if the geometry of the internal linkages would affect the reactivity of oligomers exclusively composed of glucose (Glc) residues. Preparative protocols for activation of SBG<sub>n</sub> and Dext<sub>m</sub> were also developed.

### Materials and methods

#### Materials

A heterogenous sample of very low molecular weight (VLM)-SBG (M<sub>n</sub> = 9.1 kDa, DP<sub>n</sub> = 56, M<sub>w</sub>/M<sub>n</sub> = 3.8), obtained by acid hydrolysis of  $\beta$ -1,3-linked glucans isolated from the cell wall of *Saccharomyces cerevisiae*, was provided by Biotech BetaGlucans®.

#### Methods

VLM-SBG (5 mg/mL) was dissolved in sulfuric acid (H<sub>2</sub>SO<sub>4</sub>, 0.1 M) and hydrolysed in a water bath (99°C) for 75 minutes to obtain a mixture of shorter SBG<sub>n</sub> oligomers. The hydrolysate was neutralised and freeze-dried and SBG<sub>n</sub> oligomers were fractionated according to degree of polymerization (DP) using the analytical gel filtration chromatography (GFC) system described in **Paper I** and **II**. Oligomer fractions were purified by direct freeze-drying to remove the volatile GFC-buffer (0.1 M AmAc-buffer, pH 6.9) and purified oligomers were characterized by <sup>1</sup>H-NMR as described in **Paper II**. The activation of SBG<sub>n</sub> oligomers with PDHA and ADH, and kinetic studies of the amination and the one pot reductive amination by time course <sup>1</sup>H-NMR was performed as described in **Paper I** and **II**.

Preparative protocols for the activation of SBG<sub>n</sub> and Dext<sub>m</sub> oligomers by PDHA and ADH were developed based on the methods described in **Paper II**.

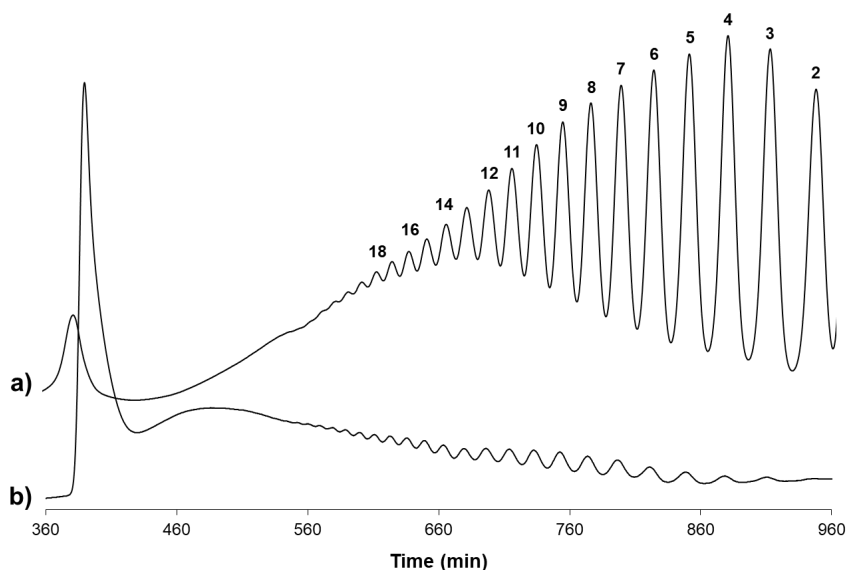
### Results

#### Preparation of defined SBG<sub>n</sub> oligomers

The mixture of SBG<sub>n</sub> oligomers obtained by acid hydrolysis of VLM-SBG sample was fractionated according to DP using GFC. The chromatograms obtained for fractionation of hydrolysate and the VLM-

## APPENDIX II

SBG prior to degradation sample are given in Figure AII.1a and b, respectively. The DP (represented by # in Figure AII.1a) and the degree of branching of the isolated SBG<sub>n</sub> oligomers was determined by <sup>1</sup>H-NMR characterisation. The oligomers were shown to have low degree of branching (e.g. 0.020 for SBG<sub>5</sub>), due to the repeated acid hydrolysis steps during the oligomer preparation.



**Figure AII.1:** GFC fractionation of **a)** the hydrolysate with shorter SBG<sub>n</sub> (# = DP) oligomers and **b)** the SBG-VLM sample prior to hydrolysis.

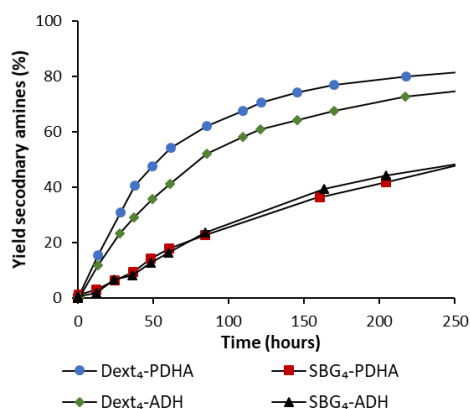
### Activation of SBG<sub>n</sub> oligomers by PDHA and ADH

Activation (amination) of SBG<sub>5</sub> oligomers by PDHA or ADH (2 equivalents, pH 4.0, RT) was studied by time course <sup>1</sup>H- NMR as described earlier for A<sub>n</sub>M, D<sub>n</sub>XA and Dext<sub>m</sub> oligomers (**Paper I** and **Paper II**). Kinetic data obtained for the reactions are presented in Table AII.1. The reactions were compared to the equivalent reactions performed with Dext<sub>5</sub> oligomers (data from **Paper I** included in Table AII.1). Interestingly, SBG<sub>5</sub> oligomers reacted slightly faster with both PDHA and ADH and gave also slightly higher combined equilibrium yields.

**Table AII.1:** Kinetic data obtained for the amination reactions of SBG<sub>5</sub> or Dext<sub>5</sub> oligomers with PDHA or ADH (2 equivalents) studied by time course <sup>1</sup>H-NMR.

Reaction	pH	T [°C]	Ratio acycl.:cycl.	t <sub>0.5</sub> [h]	t <sub>0.9</sub> [h]	k <sub>1</sub> [h <sup>-1</sup> ]	k <sub>-1</sub> [h <sup>-1</sup> ]	Combined equilibrium yield [%]
SBG <sub>5</sub> -PDHA	4.0	RT	5.1:1	1.8	7.1	1.1x10 <sup>-2</sup>	1.5x10 <sup>-2</sup>	94
Dext <sub>5</sub> -PDHA	4.0	RT	4.3:1	2.2	8.6	8.0x10 <sup>-3</sup>	2.0x10 <sup>-2</sup>	90
SBG <sub>5</sub> -ADH	4.0	RT	1:44	1.2	4.2	7.1x10 <sup>-3</sup>	2.3x10 <sup>-1</sup>	49
Dext <sub>5</sub> -ADH	4.0	RT	1:41	1.9	6.4	3.5x10 <sup>-3</sup>	1.9x10 <sup>-1</sup>	38

Reductive amination of SBG<sub>n</sub> oligomers with PDHA and ADH was performed as conventional one pot due to the slow reduction of Dext<sub>m</sub> oligomers. Reactions with SBG<sub>4</sub>, and for comparison Dext<sub>4</sub>, were studied by time course <sup>1</sup>H-NMR as described earlier for D<sub>n</sub>XA oligomers (**Paper I**) using 2 equivalents of the linkers and PB (3 equivalents) as the reductant. In contrast to the amination reactions, the one pot reductive amination reactions were evidently slower for SBG<sub>n</sub> oligomers than for Dext<sub>m</sub> oligomers with both PDHA and ADH (Figure AII.2). Interestingly, the rates for the reductive amination reactions of SBG<sub>n</sub> with PDHA and ADH were almost the same, whereas the rate for the reductive amination of Dext<sub>m</sub> with ADH was slower than for the reaction with PDHA (Figure AII.2).

**Figure AII.2:** Comparison of the reaction kinetics for the one pot reductive amination of Dext<sub>4</sub> and SBG<sub>4</sub> with 2 equivalents ADH or PDHA using 3 equivalents PB at pH 4.0, RT.

## APPENDIX II

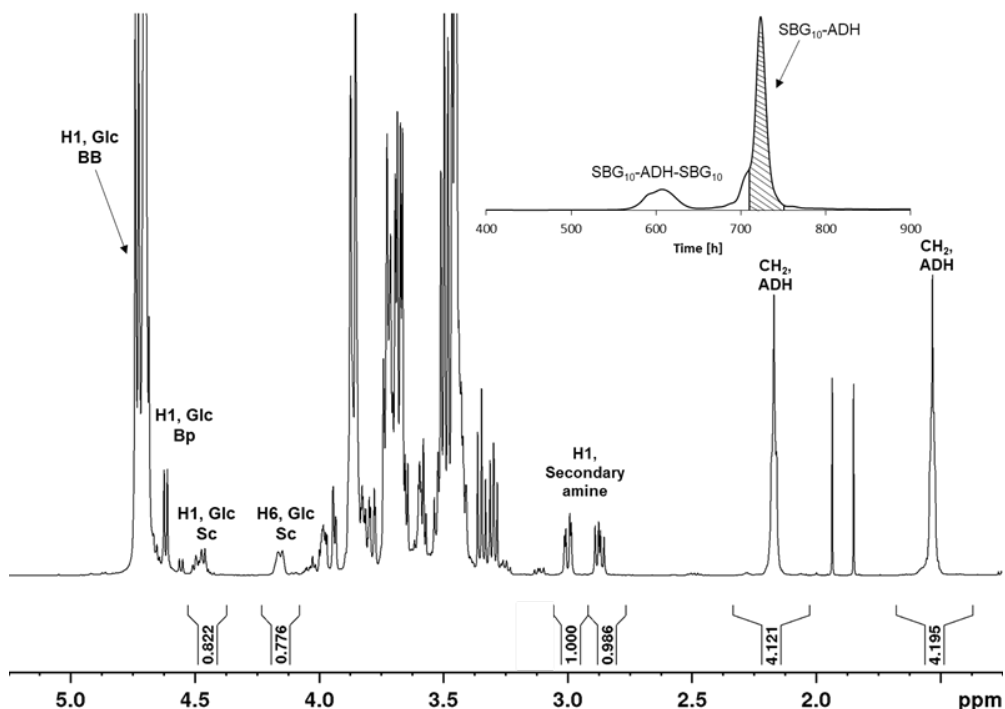
### **Preparative protocols for the activation of SBG<sub>n</sub> and Dext<sub>m</sub> oligomers by PDHA and ADH**

Preparative protocols for the one pot reductive amination of SBG<sub>n</sub> and Dext<sub>m</sub> with PDHA and ADH were developed using oligomers of higher DP. SBG<sub>n</sub> and Dext<sub>m</sub> oligomers of DP 9 and 10 ( $n/m = 9$  or  $10$ ) were reacted with PDHA and ADH, respectively, however, using a lower concentration of oligomers (10.05 mM) compared to the time course <sup>1</sup>H-NMR experiments due to the reduced solubility of longer polysaccharides.

The rates were improved using a higher temperature (40 °C), a large excess of linkers (10 equivalents) and 20 equivalents of PB. The reactions were performed in deuterated NaAc-buffer and the reaction mixtures were characterised by <sup>1</sup>H-NMR after 24, 48 and 72 hours.

Dext<sub>9</sub>-PDHA conjugates were completely reduced after 24 hours, and the reduction of the Dext<sub>10</sub>-ADH conjugates was complete after 48 hours. SBG<sub>n</sub> conjugates were in contrast completely reduced after 72 hours with both linkers. Subsequent GFC fractionation of the reaction mixtures provided fully reduced and purified SBG<sub>n</sub> and Dext<sub>m</sub> conjugates (confirmed by <sup>1</sup>H-NMR characterisation). The <sup>1</sup>H-NMR spectrum of purified SBG<sub>10</sub>-ADH conjugates is given in Figure AII.3.

Even though a large excess (10 equivalents) of PDHA or ADH was used in the reactions, a significant fraction of di-substituted linkers was formed in all reactions (e.g. chromatogram included in Figure AII.3). The results support the previous findings of a higher rate for the second attachment of oligomers to the bivalent linkers (PDHA and ADH) and hence, a higher amount of diblocks formed than statistically expected (discussed in **Paper II**).



**Figure AII.3:** <sup>1</sup>H-NMR spectrum of the SBG<sub>10</sub>-ADH conjugate after GFC fractionation and purification. BB = Back bone, Bp = branching point, Sc = side chain.

## Conclusions

Compared to Dext<sub>m</sub> oligomers, SBG<sub>n</sub> oligomers of the same DP reacted slightly faster with both PDHA and ADH (amination). The one pot reductive amination using PB was in contrast slower SBG<sub>n</sub> oligomers with both linkers compared to the Dext<sub>m</sub> oligomers. Hence, even though dextran and SBG both are glucans exclusively composed of glucose residues, the results show that the geometry of the internal linkages of the glucan backbones ( $\alpha$ -1,6- for Dext<sub>m</sub> and  $\beta$ -1,3- for SBG<sub>n</sub>) affects the reactivity of the reducing end residue. Preparative one pot reductive amination protocols were developed for longer Dext<sub>m</sub> and SBG<sub>n</sub> oligomers with both linkers, only differing in the time needed to obtain fully reduced conjugates.

## References

1. Qin, F.; Kes, M.; Christensen, B. E. (2013) *A study of bioactive, branched (1→3)- $\beta$ -D-glucans in dimethylacetamide/LiCl and dimethyl sulphoxide/LiCl using size-exclusion chromatography with multi-angle light scattering detection.* Journal of Chromatography A 1305, 109-113.

## Appendix III: De-*N*-acetylation of A<sub>n</sub>M conjugates

### Background

The tuneable positive charge makes chitosan highly relevant for the preparation of block polysaccharides. Unfortunately, we have shown that the D residues at the reducing end of CHOS have low reactivity towards PDHA and ADH compared to A residues, which in turn have much lower reactivity than M residues at the reducing end of CHOS prepared by nitrous acid depolymerisation (**Paper I** and **Paper II**). Hence, chitosan oligomers with the highly reactive M residue is preferred for the preparation of block polysaccharides. However, as discussed in **Appendix I**, the preparation of defined D<sub>n</sub>M oligomers can be troublesome due degradation of the M residue. As an alternative approach, we therefore attempted to prepare PDHA and ADH activated chitosan conjugates by de-*N*-acetylation of premade A<sub>n</sub>M conjugates, hence, taking advantage of the high reactivity of the M residue for the preparation of conjugates without the limitations of slow kinetics (for the A and D residues) and M degradation.

### Methods

PDHA and ADH activated A<sub>n</sub>M conjugates (A<sub>n</sub>M-PDHA/ADH) were prepared and purified by the methods described in **Paper II**. Purified A<sub>n</sub>M conjugates or unreacted A<sub>n</sub>M oligomers (5 mg/mL) were subjected to de-*N*-acetylation in 2.77 M NaOH for 48 h at room temperature (RT) or at 40°C. The de-*N*-acetylation was terminated by neutralisation and the reaction mixtures were subsequently dialysed (MWCO = 100-500 Da) against MQ-water until the measured conductivity was < 2 μS/cm and freeze-dried. Fractionation of the reaction mixtures by gel filtration chromatography (GFC) and characterisation of the reaction mixture or isolated conjugates by <sup>1</sup>H-NMR and MS were performed as described in **Paper I** and **II**.

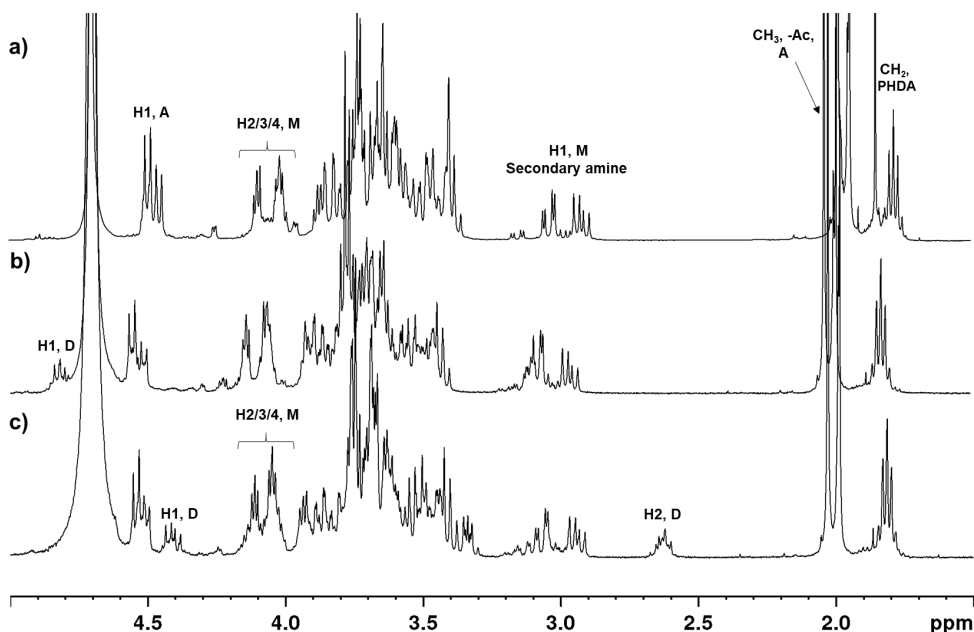
### Results

#### De-*N*-acetylation of A<sub>n</sub>M oligomers

De-*N*-acetylation of unreacted A<sub>n</sub>M oligomers at RT was first attempted, but the reaction resulted in degradation of the M residue, evident by the disappearance of M resonances in the <sup>1</sup>H-NMR spectrum. This may have been caused by reaction of the pending M aldehyde with the unprotonated free amine groups of the D residues formed upon de-*N*-acetylation leading to degradation of the M residue and the formation of HMF when pH was reduced under neutralisation (discussed in **Appendix I**). However, new reducing end resonances were absent from the spectrum, suggesting a more destructing degradation mechanism. De-*N*-acetylation of unreacted A<sub>n</sub>M oligomers was therefore excluded as a method to prepare chitosan oligomers.

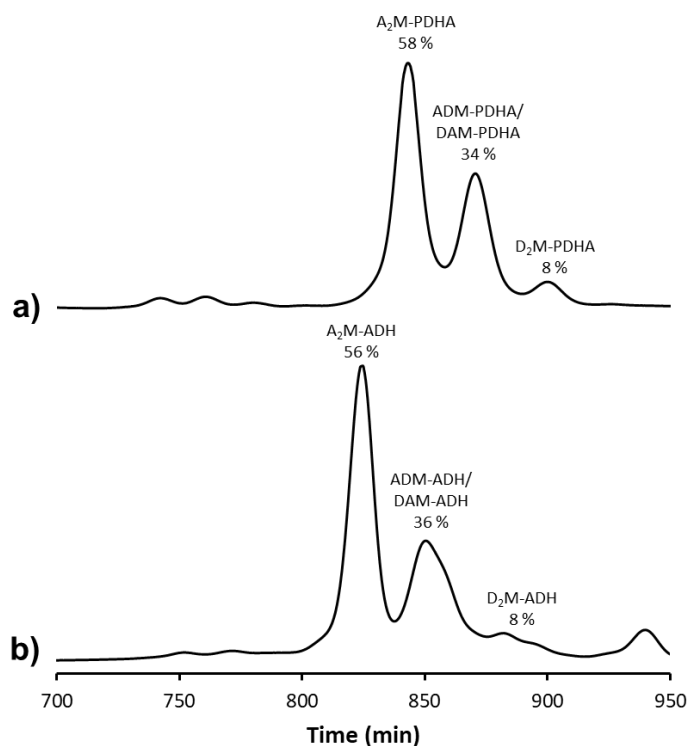
### De-*N*-acetylation of A<sub>n</sub>M conjugates at RT

We proposed that protection of the highly reactive aldehyde of the M residue could prevent its degradation during de-*N*-acetylation, as observed for the D<sub>n</sub>M oligomers in **Appendix I**. De-*N*-acetylation of A<sub>2</sub>M-PDHA and A<sub>2</sub>M-ADH conjugates was therefore first attempted at RT. Characterisation of the reaction mixtures by <sup>1</sup>H-NMR revealed the presence of characteristic conjugate resonances after treatment with NaOH (shown for A<sub>2</sub>M-PDHA in Figure AIII.1). However, the H1, M secondary amine resonances were of higher complexity after the de-*N*-acetylation and new resonances from D residues were present in the spectra. The characteristic resonance resulting from H2, D was separated from the H1, M secondary amine resonances at higher pH (Figure AIII.1 c).



**Figure AIII.3:** <sup>1</sup>H-NMR spectra of **a)** the A<sub>2</sub>M-PDHA conjugate prior to de-*N*-acetylation, **b)** and **c)** the mixture of conjugates formed after de-*N*-acetylation of A<sub>2</sub>M-PDHA (2.77 M NaOH, 48 hours, RT) at pH 5.8 and 13.5, respectively.

Subsequent GFC fractionation of the reaction mixtures and characterisation of the fractions by <sup>1</sup>H-NMR revealed three major products; unaffected A<sub>2</sub>M-PDHA or -ADH conjugates, chitosan conjugates with one D residue and fully de-*N*-acetylated conjugates (Figure AIII.2). The yield of each conjugate was obtained by integration of the chromatograms. The relative yields (%) of conjugates were close to identical for the two reactions suggesting that the rate of de-*N*-acetylation of the oligomers was independent on the linker attached to the reducing end.



**Figure AIII.2:** GFC fractionation of the mixture of products formed in the de-*N*-acetylation of **a)** A<sub>2</sub>M-PDHA and **b)** A<sub>2</sub>M-ADH in 2.77 M NaOH for 48 hours at RT.

#### De-*N*-acetylation of A<sub>n</sub>M conjugates at higher temperature

De-*N*-acetylation of A<sub>2</sub>M-PDHA was further studied at higher temperature (40°C) to improve the protocol. After 48 hours, only a small fraction of unreacted chitin conjugates (A<sub>2</sub>M-PDHA, <6 %) was present in the reaction mixture. Chitosan conjugates with one D residue (DAM-PDHA/ADM-PDHA) and fully de-*N*-acetylated conjugates (D<sub>2</sub>M-PDHA) accounted for 24 and 47 % of the fractions, respectively. The remaining 23 % was a mixture shorter de-*N*-acetylated conjugates, suggesting a concurrent depolymerisation of the oligomers as a result of too harsh conditions.

#### Stability of the free end of the linkers during the de-*N*-acetylation of conjugates

The unaffected A<sub>2</sub>M-ADH from the de-*N*-acetylation at RT was reacted with A<sub>3</sub>M to study the stability of the free end of the linker. The formation of diblocks suggested that the linker was intact. However, MS



characterisation of all the purified conjugates obtained after de-*N*-acetylation revealed loss of a -NH group. The loss of a -NH group could in theory be caused detachment of the free amino group after de-*N*-acetylation. This theory was, however, rejected since the loss also was observed for the unaffected chitin conjugates ( $A_2M$ -PDHA or -ADH). Without further investigation, we postulate that the -NH group is detached from the free end of the linkers (PDHA or ADH) during the reaction. The reactivity of the  $A_2M$ -ADH conjugate after the de-*N*-acetylation can be explained by the loss of the outermost free amine group resulting in an amide group at the free end of the linker which still can react with the pending aldehyde of the M residue. The loss of a -NH group at the free end of PDHA will, in contrast, result in an inactive -OH end group which prevents subsequent reactions of the de-*N*-acetylated conjugates.

#### **Alternative protocol for the preparation of chitosan-based diblocks**

Based on the abovementioned results we postulate that the structure of  $A_nM$  based-diblocks, where oligomers are attached to both ends PDHA and ADH, can prevent linker degradation during de-*N*-acetylation since the secondary amine linkages were shown to be stable. Hence, chitosan diblocks or chitosan-based diblocks can be prepared by de-*N*-acetylation of chitin diblocks ( $A_nM$ -*b*- $MA_n$ ) or chitin-based diblocks ( $A_nM$ -*b*-X, where X is another oligo- or polysaccharide), respectively. However, due to time limitations, this approach was not studied.

#### **Conclusions**

De-*N*-acetylation of premade chitin ( $A_nM$ ) conjugates resulted in chitosan conjugates. PDHA and ADH efficiently protected the M residue from degradation during de-*N*-acetylation, but the harsh conditions resulted in the loss of a -NH group from the free end of the linkers. The secondary amine linkages of the conjugates were, however, stable throughout the de-*N*-acetylation. We therefore postulate that chitosan-based diblocks can be prepared by de-*N*-acetylation of premade chitin-based diblock structures, which protects the M residue and the free end of the linkers during the reaction. The conditions (temperature, time) for the de-*N*-acetylation also need to be optimised to prevent concurrent depolymerisation of the oligomers.

## Appendix IV: Chitin-based diblocks from water-insoluble $A_nM$ oligomers

### Background

Chitin has low water-solubility, and chitin oligomers prepared by nitrous acid depolymerisation of chitosan ( $A_nM$ ) are only water-soluble up to DP 9 ( $n = 8$ ). The water-solubility of chitin may, however, be improved by conjugation to a highly water-soluble polysaccharide. We therefore attempted to prepare dextran-*b*-chitin block polysaccharides by conjugating the insoluble fraction of chitin oligomers ( $A_nM$ ,  $n > 8$ ), obtained in the degradation of chitosan using an excess nitrous acid (**Paper II**), to highly water-soluble dextran chains activated by ADH, assuming the high reactivity of the M residue would promote conjugation of the insoluble chitin oligomers to the free end of the linker. ADH was chosen as linker between the blocks since the reduction of hydrazones formed with  $A_nM$  oligomers is much faster than the corresponding oximes formed with  $A_nM$  and PDHA (**Paper II**).

Chitin is soluble in dimethyl acetamide (DMAc) containing a few percent  $LiCl^{1,2}$  and an oxyamine linked fluorescent probe has been coupled to intra-chain carbonyls of oxidised cellulose in DMAc/ $LiCl^3$ . Based on these results we suggested that reactions with PDHA and water-insoluble  $A_nM$  oligomers could possibly be performed in this solvent. We therefore performed an initial experiment with  $A_nM$  oligomers and PDHA in DMAc/ $LiCl$  as an alternative approach to form chitin-based block structures.

### Methods

#### Preparation of dextran-*b*-chitin diblocks with water-insoluble $A_nM$ oligomers

Dextran samples were prepared by acid hydrolysis as described in **Paper II**, however, with a shorter degradation time to obtain samples of higher  $DP_n$ . The unfractionated hydrolysates were subjected to activation by ADH (one pot reductive amination, 10 equivalents ADH, 20 equivalents PB, pH 4.0, 40°C, 4 days). The reaction mixtures were fractionated by GFC to remove unreacted ADH and obtain Dext<sub>m</sub>-ADH samples with a narrower chain length distribution and the conjugate samples were characterised by  $^1H$ -NMR to determine the  $DP_n$  by the methods described in **Paper I and II**.

Dext<sub>m</sub>-ADH conjugates were reacted with the water-insoluble fraction of  $A_nM$  oligomers ( $A_nM$ ,  $n > 9$ ). Due to the inability to characterise this fraction, we assumed a  $DP_n$  of 12. The heterogeneous reaction mixture of Dext<sub>m</sub>-ADH and insoluble  $A_nM$  (2 equivalents) was reacted for 24 hours prior to addition of PB (20 equivalents) and reduced for 24 hours (a total reaction time of 48 hours) at pH 4.0, RT using the methods described in **Paper II**. The insoluble fraction was removed by centrifugation and the soluble fraction was purified by dialysis, freeze-dried, and subsequently characterised by  $^1H$ -NMR.

### Preparation of chitin-based diblocks in DMAc/LiCl

A<sub>4</sub>M-PDHA conjugates (fully reduced) were prepared using the methods described in **Paper II**. The A<sub>4</sub>M-PDHA conjugates were reacted with an equimolar amount of A<sub>4</sub>M in in DMAc/LiCl (8%) for 48 hours at 40°C. The reaction mixture was subsequently diluted with an equal amount of H<sub>2</sub>O and dialysed against water, keeping the pH above 6 to avoid oxime hydrolysis<sup>4</sup>. The freeze-dried reaction mixture was dissolved in D<sub>2</sub>O and characterised by <sup>1</sup>H-NMR.

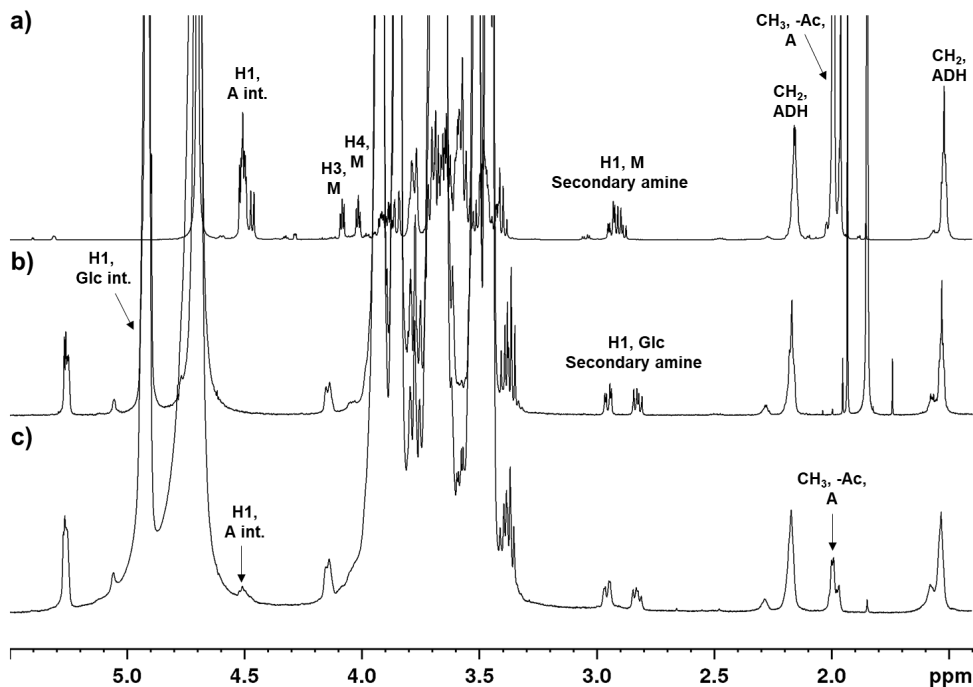
## Results

### Preparation of dextran-*b*-chitin diblocks with water-insoluble A<sub>n</sub>M oligomers

Two different Dext<sub>m</sub>-ADH conjugate samples ( $m = 80$  or  $340$ ), where  $m$  represents the DP<sub>n</sub> determined by <sup>1</sup>H-NMR characterisation, were reacted with the insoluble fraction of A<sub>n</sub>M oligomers to study the potential effect of the chain length of the Dext<sub>m</sub> block. The Dext<sub>m</sub>-ADH samples were fully reduced as shown for Dext<sub>80</sub>-ADH in Figure AIV.1b.

<sup>1</sup>H-NMR characterisation of the soluble fractions obtained after the homogenous reaction of the Dext<sub>m</sub>-ADH with the insoluble A<sub>n</sub>M oligomers, revealed weak resonances from H1, A internal and resonances from the *N*-acetyl protons (CH<sub>3</sub>, -Ac, A) suggesting the presence of A<sub>n</sub>M oligomers in the sample (Figure AIV.1c for the reaction with Dext<sub>80</sub>-ADH). A slight increase in the complexity of the resonances resulting from the H1, secondary amine protons also indicated formation of new secondary amine linkages, suggesting conjugation of A<sub>n</sub>M to the free end of ADH. However, integration of the spectra was limited by low resolution and we were therefore not able to draw conclusions from these results.

Interestingly, the weight of the soluble fractions after freeze-drying was reduced compared to the weight of the Dext<sub>m</sub>-ADH samples before reaction. The results therefore indicate that the insoluble A<sub>n</sub>M oligomers have reacted with Dext<sub>m</sub>-ADH, but without the Dext<sub>m</sub> fraction being able to solubilise the chitin blocks (observed for both samples independent of DP<sub>n</sub> of the Dext<sub>m</sub> block).



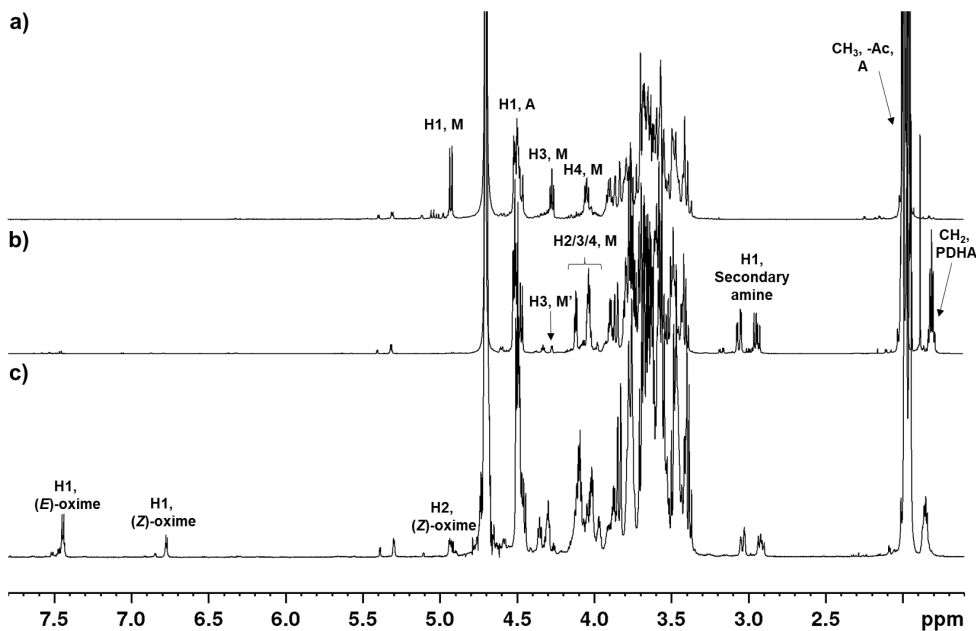
**Figure AIV.1:** <sup>1</sup>H-NMR spectra of **a)** a purified A<sub>5</sub>M-ADH conjugate, **b)** the Dext<sub>80</sub>-ADH sample prior to conjugation and **c)** the soluble fraction from the reaction of Dext<sub>80</sub>-ADH with insoluble A<sub>n</sub>M oligomers (2 equivalents).

### Preparation of chitin-based diblocks in DMAc/LiCl

All A<sub>n</sub>M fractions, including the water-insoluble fraction, were soluble in DMAc/LiCl. The reaction mixture obtained after reacting A<sub>4</sub>M-PDHA (fully reduced) with an equimolar amount of A<sub>4</sub>M (without reducing agent) in DMAc/LiCl was dissolved in D<sub>2</sub>O and characterised by <sup>1</sup>H-NMR (Figure AIV.2). The conjugation of A<sub>4</sub>M to the free end of PDHA was confirmed by the presence of resonances resulting from H1, *E*- and *Z*-oximes at approx. 7.5 and 6.8 ppm, respectively, from which an equilibrium yield of > 95 % was estimated. The yield of oximes is higher than the yield obtained in aqueous solvent under the same conditions (equimolar amount of the A<sub>n</sub>M blocks) suggesting that DMAc/LiCl serve as a better solvent for these reactions. The oximes can subsequently be reduced by PB or another reducing agent (e.g. NaBH<sub>3</sub>) to prepare stable secondary amine linkages.

These preliminary results indicate that DMAc/LiCl is a viable solvent for reactions with water-insoluble A<sub>n</sub>M oligomers and PDHA. Further we propose that the solvent can be used for reactions of water-insoluble A<sub>n</sub>M oligomers with other oligo- or polysaccharides activated with PDHA which are soluble in

DMAC/LiCl, e.g. dextran and  $\beta$ -1,3-glucans, for the preparation of diblock structures. Forthcoming studies will include a more detailed kinetic analysis by time course  $^1\text{H-NMR}$  (using deuterated DMAC) and systematic studies of conjugates with longer (water-insoluble)  $A_nM$  oligomers. This work will be carried out in a master project (T. Muren, NTNU) after the submission of this thesis (spring 2021).



**Figure AIV.2:**  $^1\text{H-NMR}$  spectrum of **a)** unreacted  $A_4M$ , **b)**  $A_4M$ -PDHA conjugate prior to reaction, **c)**  $A_4M$ -PDHA=MA<sub>4</sub> diblock **a** after reaction in DMAC/LiCl where the = indicates unreduced E/Z oximes.

## Conclusions

Our preliminary results suggest that the highly reactive M residue of the water-insoluble  $A_nM$  oligomers can react with the free end of ADH under heterogeneous conditions. However, the results also indicate that the conjugation of the  $A_nM$  oligomers to the free end of ADH reduce the solubility of the Dext<sub>m</sub>-ADH blocks, instead of increasing the solubility of the water-insoluble  $A_nM$  oligomers. These results need to be verified by characterisation of the water-insoluble fraction. However, if water-insoluble dextran-*b*-chitin diblocks are formed, these may serve as precursors for the preparation of dextran-*b*-chitosan block polysaccharides by de-*N*-acetylation of the chitin block as suggested in **Appendix III**.

Based on the preliminary study, DMAC/LiCl seems to be a very promising solvent for the preparation of diblock structures with water-insoluble  $A_nM$  oligomers and PDHA as the linker between the blocks. The

## APPENDIX IV

approach produces oximes in high yields, even with equimolar amounts of the blocks. Reactions with water-insoluble A<sub>n</sub>M oligomers in DMAc/LiCl will be studied in detail in the near future.

### References

1. Poirier, M.; Charlet, G. (2002) *Chitin fractionation and characterization in N,N-dimethylacetamide/lithium chloride solvent system*. Carbohydrate Polymers 50 (4), 363-370.
2. Terbojevich, M.; Carraro, C.; Cosani, A.; Marsano, E. (1988) *Solution studies of the chitin-lithium chloride-N,N-di-methylacetamide system*. Carbohydrate Research 180 (1), 73-86.
3. Röhring, J.; Potthast, A.; Rosenau, T.; Lange, T.; Ebner, G.; Sixta, H.; Kosma, P. (2002) *A novel method for the determination of carbonyl groups in celluloses by fluorescence labeling. 1. Method development*. Biomacromolecules 3 (5), 959-968.
4. Novoa-Carballal, R.; Müller, A. H. E. (2012) *Synthesis of polysaccharide-b-PEG block copolymers by oxime click*. Chemical Communications 48 (31), 3781-3783.

# Paper I







## Activation of enzymatically produced chitoooligosaccharides by dioxyamines and dihydrazides

Ingrid Vikøren Mo<sup>a</sup>, Yiming Feng<sup>a</sup>, Marianne Øksnes Dalheim<sup>a</sup>, Amalie Solberg<sup>a</sup>, Finn L. Aachmann<sup>a</sup>, Christophe Schatz<sup>b,\*</sup>, Bjørn E. Christensen<sup>a,\*</sup>

<sup>a</sup> NOBIPOL, Department of Biotechnology and Food Science, NTNU Norwegian University of Science and Technology, Sem Sælands vei 6/8, NO-7491 Trondheim, Norway

<sup>b</sup> LCPO, Université de Bordeaux, UMR5629, ENSCBP, 16, Avenue Pey Berland, 33607 Pessac Cedex, France

### ARTICLE INFO

This manuscript is dedicated to memory of Professor Kjell M. Vårum.

**Keywords:**  
Carbohydrates  
Chitosan  
Conjugation  
Hydrazides  
Oxyamines

### ABSTRACT

Reducing end activation of poly- and oligosaccharides by bifunctional dioxyamines and dihydrazides enables aniline-free and cyanoborohydride-free conjugation to aldehyde-containing molecules, particles and surfaces without compromising the chain structure. Chitosans are due to their polycationic character, biodegradability, and bioactivity important candidates for conjugation. Here, we present a kinetic and structural study of the conjugation of a dioxyamine and a dihydrazide to enzymatically produced chitoooligosaccharides ranging from *N,N'*-diacetylchitobiose to a decamer, all having *N*-acetyl *D*-glucosamine at the reducing end. Conjugation of the dioxyamine resulted in mixtures of (*E*)- and (*Z*)-oximes and  $\beta$ -*N*-pyranoside, whereas the dihydrazide yielded cyclic *N*-glycosides. Reaction kinetics was essentially independent of DP. Stable secondary amines were in both cases obtained by reduction with  $\alpha$ -picoline borane, but higher temperatures were needed to obtain acceptable reduction rate. Comparison to dextran oligomers shows that the nature of the reducing end strongly influences the kinetics of both the conjugation and reduction.

### 1. Introduction

Chemical modification of carbohydrates is commonly performed to change their properties for various applications. However, optimal retention of their intrinsic properties requires reactions at the chain termini (terminal conjugation) rather than traditional lateral substitution. Reaction at the reducing end is the dominating method for terminal modification (Novoa-Carballal & Müller, 2012; Schatz & Lecommandoux, 2010), where the hemiacetal-aldehyde equilibrium enables aldehyde-based reactions for the conjugation to other molecules, particles and surfaces. Among chemical modification methods, alkyne/azide click chemistry (Breitenbach, Schmid, & Wich, 2017; Rosselgong et al., 2019), thioacetylation (Pickenhahn et al., 2015), and reductive amination using oximes (Novoa-Carballal & Müller, 2012) or hydrazones (Kölmel & Kool, 2017) are the most common. It may be noted that the alkyne/azide click chemistry approach also depends on an initial reductive amination step with alkyne- or azide-bearing amines.

Amines, oxyamines and hydrazides can react with aldehydes to form Schiff bases (imines, oximes and hydrazones), normally combined with

subsequent reduction to form stable secondary amines (Fig. 1). Oxyamines and hydrazides have higher nucleophilicities compared to amines (Fina & Edwards, 1973), and can efficiently conjugate to the reducing end of carbohydrates (Baudendistel, Wieland, Schmidt, & Wittmann, 2016; Hermanson, 2008; Kwase, Cochran, & Nitz, 2013; Lee & Shin, 2005; Novoa-Carballal & Müller, 2012). They also increase the hydrolytic stability of the formed Schiff bases (oximes and hydrazones), and their low basicity allows them to form under acidic conditions (Kalia & Raines, 2008). Oxyamines tend to form acyclic oximes with carbohydrates, both in the (*E*)- and (*Z*)-configuration, in equilibrium with cyclic *N*-glycosides (Fig. 1) (Kwase et al., 2013). The relative distribution of conjugates depends on the chemistry of the reducing end residue (Baudendistel et al., 2016). Hydrazides, on the other hand, predominantly form *N*-glycosides when conjugated under acidic conditions (Lee & Shin, 2005; Shinohara et al., 1996). Hence, oxyamines and hydrazides can be used to form pH-sensitive carbohydrate-based conjugates or fully stable conjugates by reduction to secondary amines.

Aniline may be an effective catalyst in reactions with both amines (Guerry et al., 2013), oxyamines (Dirksen, Hackeng, & Dawson, 2006; Thygesen et al., 2010) and hydrazides (Dirksen & Dawson, 2008). It

\* Corresponding authors.

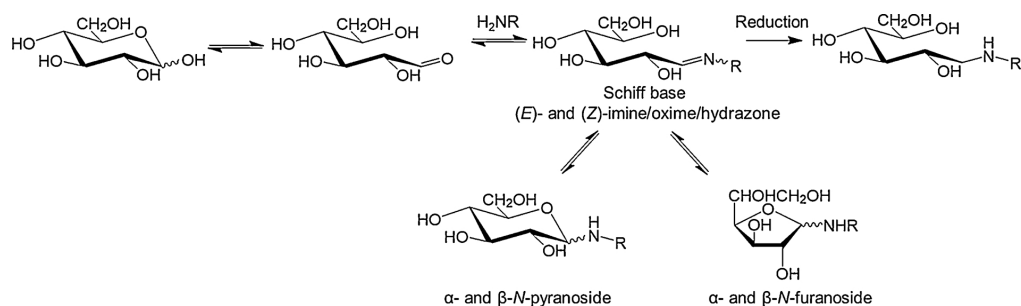
E-mail addresses: [ingrid.v.mo@ntnu.no](mailto:ingrid.v.mo@ntnu.no) (I. Vikøren Mo), [fengym@shanghaitech.edu.cn](mailto:fengym@shanghaitech.edu.cn) (Y. Feng), [marianne.dalheim@rise-pfi.no](mailto:marianne.dalheim@rise-pfi.no) (M. Øksnes Dalheim), [amalie.solberg@ntnu.no](mailto:amalie.solberg@ntnu.no) (A. Solberg), [finn.l.aachmann@ntnu.no](mailto:finn.l.aachmann@ntnu.no) (F.L. Aachmann), [schatz@enscbp.fr](mailto:schatz@enscbp.fr) (C. Schatz), [bjorn.e.christensen@ntnu.no](mailto:bjorn.e.christensen@ntnu.no) (B.E. Christensen).

<https://doi.org/10.1016/j.carbpol.2019.115748>

Received 4 October 2019; Received in revised form 19 November 2019; Accepted 16 December 2019

Available online 23 December 2019

0144-8617/© 2019 Elsevier Ltd. All rights reserved.



**Fig. 1.** Reaction of the free aldehyde at the reducing end of carbohydrates with amines and the subsequent reduction of the Schiff bases to form stable secondary amines. D-glucopyranose is here shown as example.

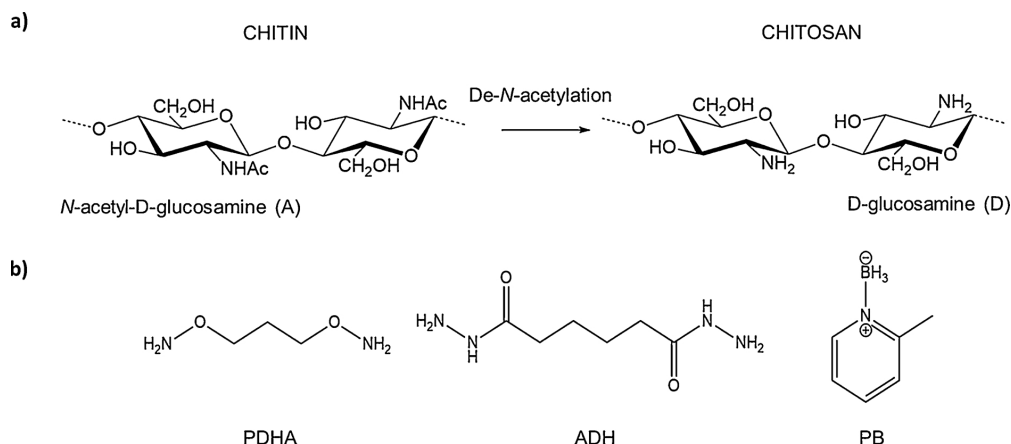
can, however, give side products (Guerry et al., 2013; Thygesen et al., 2010) and its toxicity may raise HSE and environmental concerns. Hence, aniline-free protocols are sometimes preferred.

Chitin is a highly abundant polysaccharide, found in e.g. the exoskeleton of crustaceans, insects, squid pens, and in the cell wall of some bacteria and fungi. It is a high molecular weight, crystalline, water-insoluble polymer consisting exclusively of 1,4-linked N-acetyl-D-glucosamine (GlcNAc, A) residues. Partial de-N-acetylation of chitin provides chitosan with varying amounts of D-glucosamine (GlcN, D) (Fig. 2a). Chitosans are commonly described by the fraction of residual A residues ( $F_A$ ) (Vårum, Antohonsen, Grasdalen, & Smidsrød, 1991) following de-N-acetylation (Supporting information, S1). Chitosans are the only polycationic polysaccharides which can be isolated from biomass and they are widely studied because of their (pH dependent) cationic properties, which can be utilised in polyelectrolyte complexes with e.g. DNA for transfection (Strand, Danielsen, Christensen, & Vårum, 2005), antimicrobial activity (Mellegård, Strand, Christensen, Granum, & Hardy, 2011), bioadhesive properties biocompatibility, and biodegradability.

Nitrous acid degradation of chitosan is a standard route to prepare chitooligosaccharides with a reactive 2,5-anhydro D-mannose (M) residue at the reducing end (Allan & Peyron, 1995; Moussa, Crepet, Ladaviere, & Trombotto, 2019; Tømmeraaas, Vårum, Christensen, & Smidsrød, 2001). However, oligomers of the type  $D_nM$  (where n is the number of contiguous uninterrupted D-units) can only be obtained from 100 % de-N-acetylated chitosans, which require extensive de-N-

acetylation. In contrast, chitooligosaccharides of the type  $D_nXA$  (where X is either D or A) may be more relevant from a biorefinery point of view because they can be obtained by enzymatic degradation of chitosans using specific chitinases such as chitinase B (ChiB) from *Serratia marcescens* (Sørbotten, Horn, Eijssink, & Vårum, 2005). The uninterrupted  $D_n$  sequences allow for cooperative, preferentially electrostatic, interactions with other molecules, in contrast to sequences with randomly positioned A residues. Residues of A at the reducing end are also preferred over D residues because of the poorer reactivity of the latter (Beaudoin, Gauthier, Boucher, & Waldron, 2005; Guerry et al., 2013). Further, the N-acetyl group of the terminal A residue provide a particularly useful marker in chemical analyses, besides allowing direct comparison to previous work based on monomeric A and the AA dimer (Baudendistel et al., 2016).

In the present work, we study in detail the conjugation of a dioxamine, O,O'-1,3-propanediylbishydroxylamine (PDHA, Fig. 2b) and a dihydrazide, adipic acid dihydrazide (ADH, Fig. 2b) to  $D_nXA$  chitooligosaccharides. All steps in the conjugation (amination) reactions with oxyamines and hydrazides are reversible, and the stability of the conjugates may vary considerably (Kwase et al., 2013). We have therefore further studied the oxime/hydrazone reduction using  $\alpha$ -picoline borane (PB, Fig. 2b). PB is a relatively new and so far little described reducing agent, introduced as a green and less hazardous alternative to sodium cyanoborohydride ( $NaCNBH_3$ ) (Cosenza, Navarro, & Stortz, 2011; Dalheim et al., 2016). PB has been applied for labelling of oligosaccharides and glycans by reductive amination, leading to



**Fig. 2.** a) Conversion of chitin to chitosan by partial or complete de-N-acetylation. Residues are conveniently abbreviated A (N-acetyl-D-glucosamine) and D (D-glucosamine). The fraction of unmodified A residues ( $F_A$ ) is used for characterization of the chitosan, and complete de-N-acetylation, as shown, gives  $F_A = 0$ . b) Structures of O,O'-1,3-propanediylbishydroxylamine (PDHA), adipic acid dihydrazide (ADH) and  $\alpha$ -picoline borane (PB).

equal or even better reducing efficacies compared to  $\text{NaCNBH}_3$  (Cosenza et al., 2011; Fang, Qin, Ma, & She, 2015; Ruhaak, Steenvoorden, Koelman, Deelder, & Wuhrer, 2010, 2010b; Unterrieser & Mischnick, 2011). Moreover, PB can be employed under both aqueous and non-aqueous conditions, which is advantageous for reactions with carbohydrates (Ruhaak, Zauner et al., 2010). Reduction is also a means to tailor the properties of the conjugates, as charge/ $\text{pK}_a$  and local flexibility are generally different for the reduced and unreduced forms.

Here, we show that chitoooligosaccharides react in rather different ways with PDHA and ADH, both in terms of kinetics, yields and selectivity. The same applies to the reduction by PB. We also show that the rate of conjugation and reduction depend significantly on the nature of the reducing end residue by comparing the chitoooligosaccharides to dextran oligomers. Taken together the findings provide a solid basis for selecting optimal aniline-free and cyanoborohydride-free protocols for the preparation of dioxyamine and dihydrazide activated chitoooligosaccharides (with and without reduction).

## 2. Experimental section

### 2.1. Materials

The chitosan ( $F_A = 0.25$ ,  $[\eta] = 420$  g/mL) was an in-house sample prepared by de-*N*-acetylation of chitin. Chitinase B (ChiB, *Serratia marcescens*) was kindly provided by Prof. Vincent G. H. Eijssink, NMBU, Norway. *N,N*-diacetyl chitobiose (AA), adipic acid dihydrazide (ADH), *O,O'*-1,3-propanediylbishydroxylamine dihydrochloride (PDHA) and 2-methylpyridine borane complex ( $\alpha$ -picoline borane, PB) were obtained from Sigma-Aldrich. All other chemicals were obtained from commercial sources and were of analytical grade.

### 2.2. Preparative gel filtration chromatography (GFC)

The preparative gel filtration system was composed of two Superdex 30 (prep. grade) columns (BPG 140/950, 140 mm x95 cm, GE Healthcare Life Sciences) connected in series, continuously eluting ammonium acetate (AmAc) buffer (0.15 M, pH 4.5) with a flow rate of 30 mL/min. Samples (0.5–3 g) were dissolved in buffer and injected into the system. The fractionation was monitored by an on-line refractive index (RI) detector (SHODEX R1-102). Fractions (160 mL/flask) were collected (Super Frac, Amersham Biosciences) and pooled according to elution times. The pooled fractions were reduced to appropriate volumes, dialyzed (MWCO = 100–500) against MQ-water until the measured conductivity of the water was  $< 2$   $\mu\text{S}/\text{cm}$  and freeze-dried.

### 2.3. Analytical gel filtration chromatography (GFC)

The analytical gel filtration system was composed of three Superdex 30 (prep. grade) columns (HiLoad 26/60, 26 mm x60 cm, GE Healthcare Life Sciences) connected in series, continuously eluting AmAc buffer (0.15 M, pH 4.5 or 0.1 M, pH 6.9) with a flow rate of 0.8 mL/min. Samples (5–100 mg) were dissolved in buffer and injected into the system. The fractionation was monitored by an on-line RI-detector (SHODEX R1-101). Fractions (3.2 mL/tube) were collected (LKB 2111 Multitrack KS1) and pooled according to elution times. The pooled fractions were reduced to appropriate volumes, dialyzed (MWCO = 100–500) against MQ-water until the measured conductivity of the water was  $< 2$   $\mu\text{S}/\text{cm}$  and freeze-dried.

### 2.4. NMR spectroscopy

Samples were dissolved in  $\text{D}_2\text{O}$  (450–600  $\mu\text{L}$ , approx. 10 mg/mL) and adjusted to target pD with  $\text{DCl}/\text{NaOD}$ . For some samples, 1 % sodium 3-(trimethylsilyl)-propionate- $d_4$  (TSP, 3  $\mu\text{L}$ ) was added as an internal standard. Samples for the time course NMR experiments were

prepared in deuterated NaAc-buffer (500 mM, pH = 3.0, 4.0 or 5.0, 2 mM TSP).

All homo and heteronuclear NMR experiments were carried out on a Bruker Ascend 400 MHz, ultra-shielded 600 MHz or Ascend 800 MHz spectrometer (Bruker BioSpin AG, Fällanden, Switzerland) equipped with Avance III HD electronics and a 5 mm SmartProbe with z-gradients, a 5 mm cryogenic CP-QCI z-gradient probe or a 5 mm z-gradient CP-CI cryogenic probe, respectively.

Characterisation of oligomers, purified conjugates or reaction mixtures were performed by obtaining 1D  $^1\text{H}$  NMR spectra at 300 K on the 600 MHz spectrometer. pH titration was performed by obtaining 1D  $^1\text{H}$ -NMR spectra at different pH values at 298 K on the 400 MHz spectrometer. Time course experiments were performed by obtaining 1D  $^1\text{H}$ -NMR spectra at specific time points at 300 K on the 600 MHz spectrometer. Chemical shift assignments were performed at 298–310 K on the 800 MHz spectrometer by obtaining the following homo and heteronuclear NMR spectra: 1D  $^1\text{H}$ , 2D double quantum filtered correlation spectroscopy (DQF-COSY), 2D total correlation spectroscopy (TOCSY) with 70 ms mixing time, 2D  $^{13}\text{C}$  heteronuclear single quantum coherence (HSQC) with multiplicity editing, 2D  $^{13}\text{C}$  Heteronuclear 2 Bond Correlation (H2BC), 2D  $^{13}\text{C}$  HSQC- $[\text{H}, \text{H}]$ TOCSY with 70 ms mixing time on protons and 2D heteronuclear multiple bond correlation (HMBC) with BIRD filter to suppress first order correlations.

All spectra were recorded, processed and analysed using TopSpin 3.5 software (Bruker BioSpin).

### 2.5. Flow injection analysis (FIA) coupled with quadrupole time of flight (qTOF) MS

The analyses were performed with an ACQUITY I-class UPLC system coupled to a Synapt G2Si HDMS mass spectrometer (Waters, Milford, MA, USA) equipped with an ESI source operating in negative or positive mode.

FIA analysis was performed by operating the UHPLC in bypass mode, directing the flow past the compartment directly to the mass spectrometer. A mobile phase consisting of 100 % methanol and a programmed linear flow gradient was used. The flow rate was constant at 0.150 mL/min for 0.10 min, then reduced to 0.030 min until 1.50 min, then increased to 0.200 mL/min until 1.60 min, and kept constant to 2.50 min. Finally, the system was equilibrated for additionally 0.50 min at 0.150 mL/min before the next injection. Total run time was 3.0 min. The injection volume was set to 2  $\mu\text{L}$ .

MS analysis was performed under constant ESI conditions. The capillary voltage, cone voltage and source offset voltage in negative and positive mode were set at  $-2.0$  kV/3.0 kV,  $-30$  V/30 V and  $-40$  V/40 V, respectively. The source temperature was maintained at 120 °C and the desolvation gas temperature and desolvation gas flow was set to 500 °C and 800 L/h, respectively. The cone gas flow rate was fixed at 50 L/h and the nebulizer gas flow was maintained at 6 bar. The instrument was operated in high-resolution mode with a cycle time of 1.015 s, consisting of a scan time of 1 s, and an inter-scan delay of 15 ms. The mass range was set to 50–2000 Da, the same range as the valid calibration performed with Na-formate immediately before analysis.

A reference mass/lock mass consisting of leucine enkephalin (1 ng/mL) in 50 % (v/v) acetonitrile in water was infused into the ion source through a separate capillary at a flow rate of 10  $\mu\text{L}/\text{min}$  to correct the mass axis on the fly. The capillary voltage of the lock mass was set to 2.5 kV (negative or positive depending on the operation mode).

Data was acquired and processed using MassLynx software (v4.1).

### 2.6. Preparation of chitoooligosaccharides ( $D_n\text{XA}$ , $X = D/A$ )

Chitosan ( $F_A = 0.25$ ) was dissolved in MQ water (deionized water purified with the MilliQ system from Millipore, Bedford, MA, USA) by stirring overnight and added an equal volume of NaAc-buffer (0.2 M,

pH = 5.5) to a final chitosan concentration of 10 mg/mL. The chitosan solution was incubated for 1 h in a shaking water bath (60 rpm, 37 °C). ChiB was added to the chitosan solution (4.3 µg/mg chitosan) and reacted in the shaking water bath for 7 days. The degradation was terminated by adjusting the pH to 2.5 using HCl (0.1 M) and boiling the solution for 5 min. Subsequently, pH was adjusted to pH 4.5 using NaOH (0.1 M). The degradation mixture was filtrated (0.22 µm) and freeze-dried. Chitosan oligomers were separated according to degree of polymerization (DP) using the preparative GFC system (0.15 M AmAc, pH 4.5). Pooled fractions from the GFC separation were dialyzed (MWCO = 100–500) against MQ-water to remove salt from the buffer until the measured conductivity was < 2 µS/cm and finally freeze-dried. Selected chitosan oligomers (D<sub>n</sub>XA, n = 2 and 3) were subsequently re-chromatographed using the analytical GFC system (0.1 M AmAc, pH 6.9). The oligomers were separated according to chemical composition (D<sub>n</sub>AA or D<sub>n</sub>DA) and purified by dialysis as described above. Purified oligomers were characterised by 1D <sup>1</sup>H-NMR (600 MHz spectrometer).

### 2.7. <sup>1</sup>H-NMR pH titration of PDHA and ADH

ADH or PDHA was dissolved in 1:10 v/v D<sub>2</sub>O in H<sub>2</sub>O (500 µL, 10 mg/mL). 1 % TSP (3 µL) was added as an internal standard. The pH was adjusted with HCl (0.1 and 1.0 M) or NaOH (0.1 and 1.0 M). <sup>1</sup>H-NMR spectra were obtained every 0.1 to 0.8 pH unit in the pH range 6.1 to 0.5 (400 MHz spectrometer). The system was locked on the internal D<sub>2</sub>O and the spectra were recorded using water suppression.

### 2.8. Conjugation and reduction studied by time course NMR

Deuterated NaAc-buffer (500 mM, pH = 3.0, 4.0 or 5.0) containing 2 mM TSP was prepared by dissolving the required volumes of deuterated acetic acid (CD<sub>3</sub>COOD, 99.5 % D<sub>4</sub>) and TSP (from a 20 mM stock solution prepared using D<sub>2</sub>O) in D<sub>2</sub>O (3/4 of total volume). The pH was adjusted with NaOD to the desired value and diluted with D<sub>2</sub>O to the final volume. As the pH-meter used was calibrated with non-deuterated buffers, the pH reading, pH\*, was converted to the real pH using the formula  $\text{pH} = 0.9291 \times \text{pH}^* + 0.421$  (Baudendistel et al., 2016; Krężel & Bal, 2004).

N,N'-diacetyl chitobiose (AA), chitobiose (DD), chito oligosaccharides (D<sub>n</sub>XA) or dextran oligomers (Dext<sub>n</sub>) (20.1 mM) and 2 or 10 equivalents ADH/PDHA (40.2 or 201 mM) were dissolved separately in deuterated NaAc-buffer (500 mM, pH = 3, 4 or 5) containing 2 mM TSP and transferred to a 5 mm NMR tube. The mixing of the reagents in the NMR tube served as time zero (t = 0). The concentrations given in parenthesis represents final concentrations after mixing, which also apply in all the following sections. For the reduction experiments, 3 equivalents (60.3 mM) of PB (solid) was added directly to the NMR tube with the equilibrium mixture of conjugates and the addition served as t = 0 for the reduction. The one pot reductive amination experiments were performed by adding all reactants to the NMR tube at the same time, serving as t = 0. 1D <sup>1</sup>H-NMR spectra were recorded at desired time-points (600 MHz spectrometer) and the extent of conjugation/reduction was quantified by integration. The samples were held at room temperature (RT) between the measurements.

Chemical shift assignment for the equilibrium mixture obtained for the conjugation of PDHA to AA (2 equivalents PDHA, pH 4.0) was achieved using homo and heteronuclear NMR experiments recorded at the 800 MHz spectrometer.

### 2.9. Reduction of AA-ADH/PDHA conjugates, semi preparative scale

AA (20.1 mM) and 10 equivalents of PDHA/ADH (201 mM) were dissolved in NaAc-buffer (500 mM, pH 4.0) to which 20 equivalents of PB (420 mM) were added after 24 h. The reactions were performed at room temperature for approx. 40 days. The reactions were terminated

by dialysis (MWCO = 100–500 Da) against 0.05 M NaCl until the insoluble PB was dissolved, followed by several shifts of MQ-water until the measured conductivity was < 2 µS/cm and subsequently freeze-dried. The mixture of products formed was separated by GFC (analytical scale), purified by dialysis and characterised by FIA-qTOF-MS. Selected products were additionally characterised by NMR spectroscopy (600 MHz spectrometer). Chemical shift assignment for the AA-PDHA secondary amine product was achieved using homo and heteronuclear NMR experiments recorded at the 800 MHz spectrometer.

### 2.10. Reduction at higher temperatures

AA (20.1 mM) and 10 equivalents of PDHA/ADH (201 mM) were dissolved in NaAc-buffer (500 mM, pH 4.0) to which 20 or 40 equivalents (402 mM or 804 mM) of PB were added in 1 portion at t = 0 h, or in portions after t = 0, 2, 4, 6 and 8 h. The reactions were performed in a water bath at 40 or 60 °C for 8 or 24 h, terminated by dialysis as described above and freeze-dried. The mixture of products formed was characterised by NMR spectroscopy (600 MHz spectrometer).

## 3. Results and discussion

### 3.1. Preparation of chito oligosaccharides

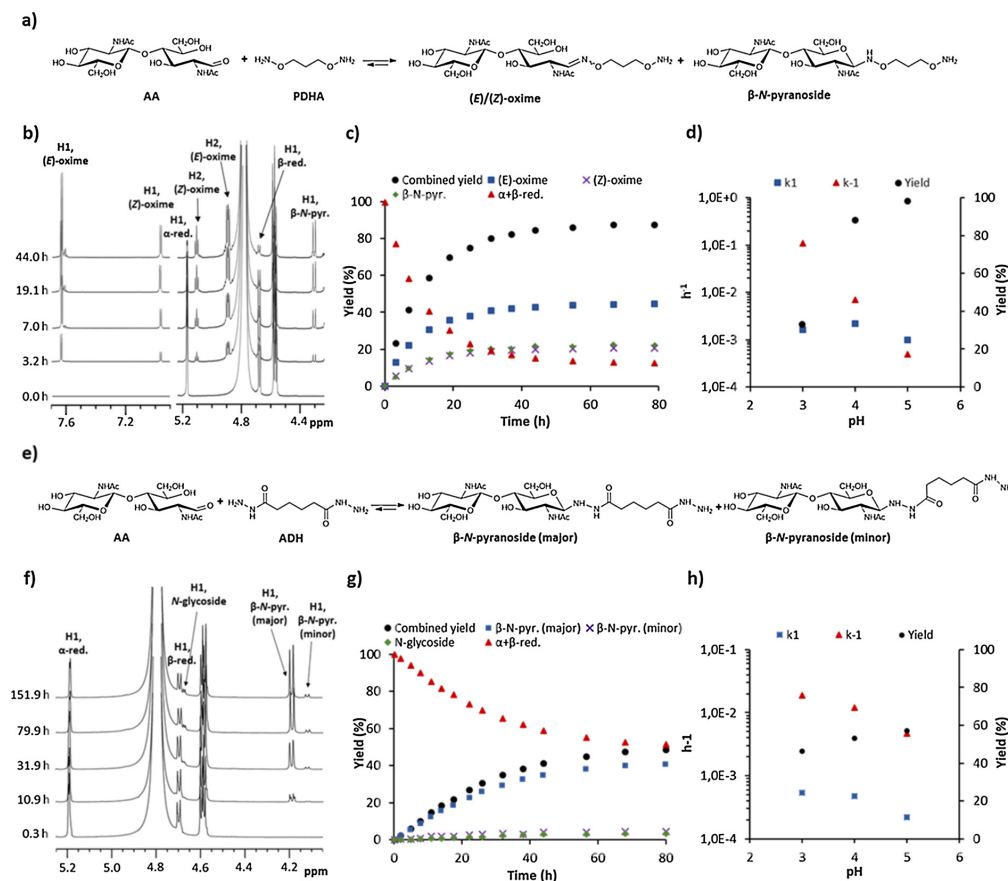
Chito oligosaccharides of the type D<sub>n</sub>XA (X = A or D) were obtained by enzymatic degradation of chitosan (F<sub>A</sub> = 0.25) using chitinase B (ChiB) (Sørbotten et al., 2005). Oligomers of specific degree of polymerization (DP) were isolated using gel filtration chromatography (GFC) at pH 4.5. The oligomers were mixtures of D<sub>n</sub>DA (51–66 %) and D<sub>n</sub>AA (34–49 %). Subsequent GFC of oligomers with specific DP at pH 6.9 separated D<sub>n</sub>DA from D<sub>n</sub>AA (e.g. D<sub>3</sub>DA from D<sub>3</sub>AA, Supporting information, S2). However, complete baseline separation of the oligomers was not obtained e.g. resulting in residual D<sub>2</sub>DA (< 15 %) in the purified D<sub>2</sub>AA oligomer fraction.

### 3.2. Conjugation of PDHA to AA

The conjugation of PDHA to the disaccharide AA (N,N'-diacetylchitobiose, Fig. 3a) was initially chosen as model system, since short oligosaccharides give relatively simple NMR spectra. Further, it allows for direct comparison to recently published data on conjugation of an ethoxyamine to mono- and disaccharides (Baudendistel et al., 2016). Compared to the protocol of Baudendistel et al. (2016) lower oligomer concentrations were used due to solubility limitations for oligomers of higher DPs. The concentration of diethylamine was, on the other hand, increased to obtain higher reaction rates and to keep the formation of doubly substituted PDHA to a minimum.

The reaction with 2 equivalents of PDHA at pH 4.0, was monitored by recording <sup>1</sup>H-NMR spectra at regular intervals until equilibrium was reached (Fig. 3b). The equilibrium mixture was studied in more detail by homo- and heteronuclear NMR correlation experiments (Supporting information, S3) to assign key resonances. The course of the reaction was obtained by integration of the recorded spectra. The corresponding yields were calculated relative to the total intensity of H1 protons resulting from the reducing end A-unit (sum of unreacted oligomers and conjugates (oximes and N-pyranosides), Fig. 3c). The ratio of acyclic ((E)- and (Z)-oximes) to cyclic (β-N-pyranosides) conjugates was 3:1 at equilibrium (Table 1), which is in good agreement with the conjugation of ethoxyamine to AA (Baudendistel et al., 2016), as was the absence of detectable amounts of furanosides and α-N-pyranoside.

Two equivalents of PDHA resulted in a combined equilibrium yield of 88 % conjugates and 12 % unreacted oligomers. By treating the combined yield as a single product, the reaction was fitted to a *pseudo* first order kinetics model (Supporting information, S4). The rate constants for the conjugation (k<sub>1</sub>) and the reverse reaction (k<sub>-1</sub>) are included in Table 1. The times to reach 50 and 90 % of the combined



**Fig. 3.** Reactions of AA with PDHA (a-d) and ADH (e-h). a) and e) Conjugation of PDHA/ADH to AA, b) and f)  $^1\text{H-NMR}$  spectra at defined time points for the conjugation reactions with 2 equivalents PDHA/ADH at pH 4.0, c) and g) course of the reactions obtained from the integrals of spectra shown in b) and f), d) and h) influence of pH on combined yield and rate constants for the conjugation and the reverse reaction. Abbreviations:  $\alpha$ -red. and  $\beta$ -red.:  $\alpha$ - and  $\beta$ -configurations of the unreacted oligomer, respectively.  $\beta$ -N-pyr.:  $\beta$ -configuration of the *N*-pyranoside (For interpretation of the references to colour in this figure legend, the reader is referred to the web version of this article).

yield at equilibrium ( $t_{0.5}$  and  $t_{0.9}$  values) are further included as a more empirical approach to describe the reaction rates (Baudendistel et al., 2016). Increasing the PDHA concentration to 10 equivalents resulted in correspondingly higher reaction rates, but practically the same rate constants. It also resulted in almost full conversion (combined yield of 96 %) but did not significantly influence the ratio of acyclic to cyclic conjugates (Table 1).

The influence of pH on the combined yield and reaction kinetics

with 2 equivalents of PDHA is shown in Fig. 3d. Whereas the forward reaction rate ( $k_1$ ) depended marginally on pH, the reverse reaction rate ( $k_{-1}$ ) was essentially proportional to  $[\text{H}^+]$ , resulting in a decreasing yield with decreasing pH as also observed for other oxyamine conjugation reactions (Baudendistel et al., 2016). We partly attribute this to the contribution from acid lability of *N*-pyranosides (Shinohara et al., 1996), which is consistent with the reduced fraction of cyclic conjugates at pH 3.0 (Table 1). It may be noted that the  $\text{pK}_a$  of PDHA was

**Table 1**

Reactions of AA with PDHA and ADH studied by time course NMR.  $^1\text{H-NMR}$  spectra of the equilibrium mixtures obtained for all the reactions are given in Supporting information, S6.

Reaction	PDHA/ADH [equivalents]	pH	T [°C]	Ratio acyl.:cycl.	$t_{0.5}$ [h]	$t_{0.9}$ [h]	$k_1$ [ $\text{h}^{-1}$ ]	$k_{-1}$ [ $\text{h}^{-1}$ ]	Combined equilibrium yield [%]
AA-PDHA	2	3.0	RT	4.6:1	3.4	12.0	$1.6 \times 10^{-3}$	$1.1 \times 10^{-1}$	33
	2	4.0	RT	2.9:1	7.6	30.0	$2.2 \times 10^{-3}$	$7.0 \times 10^{-3}$	88
	2	5.0	RT	3.6:1	20.4	84.6	$1.0 \times 10^{-3}$	$5.0 \times 10^{-4}$	98
	10	4.0	RT	3.1:1	2.8	9.7	$1.3 \times 10^{-3}$	$9.0 \times 10^{-3}$	96
AA-ADH	2	3.0	RT	1:47.2	15.1	52.8	$5.4 \times 10^{-4}$	$1.9 \times 10^{-2}$	46
	2	4.0	RT	1:47.2	20.4	71.4	$4.7 \times 10^{-4}$	$1.2 \times 10^{-2}$	53
	2	5.0	RT	1:42.5	46.6	116.0	$2.2 \times 10^{-4}$	$4.7 \times 10^{-3}$	57
	10	4.0	RT	1:45.2	7.6	25.8	$4.0 \times 10^{-4}$	$1.1 \times 10^{-2}$	89

found to be 4.2 (Supporting information, S5). Hence, the weak pH dependency of  $k_1$  in the range investigated may be attributed to the opposing effects of the decrease in reactive (deprotonated) PDHA below  $pK_a$ , and the increasing rate of acid catalysis at lower pH.

### 3.3. Conjugation of ADH to AA

Conjugation of the dihydrazide, ADH was studied using the same methods and conditions as described for the PDHA. The conjugation of ADH to AA deviated considerably from the reactions with PDHA (Fig. 3e-h, Table 1). Firstly, only cyclic conjugates ( $\beta$ -*N*-pyranoside and a minor unidentified *N*-glycoside product) were formed and no (*E*- and (*Z*)-hydrazones were detected. Secondly, two conformers of the  $\beta$ -*N*-pyranoside, one major and one minor, were observed (Fig. 3e and f), which is attributed to the partial double bond character of the hydrazide (Bendiak, 1997). Thirdly, the reaction rate was two to five times lower than for the PDHA reactions. However, as also observed for PDHA,  $k_1$  was weakly dependent on pH (in the pH range 3.0–5.0), whereas the reverse rate constant ( $k_{-1}$ ) increased with decreasing pH, although not as pronounced as for PDHA (Fig. 3h). As in the former case this may be partly attributed to acid hydrolysis of the *N*-pyranosides (Shinohara et al., 1996). Overall, the combined yield increased with increasing pH, but less pronounced than for PDHA. The differences are primarily attributed to the lower  $pK_a$  of ADH, which was found to be 3.1 (Supporting information, S5).

High yields and short reaction times are desired for the preparation of conjugates. Hence, carrying out the reaction at pH 4.0 and using a large excess of PDHA or ADH (10 equivalents or more) give the best compromise between yield and reaction time. Accordingly, all subsequent conjugation reactions were performed at pH 4.0.

### 3.4. Comparison to D at the reducing end

As a control experiment, 2 equivalents of PDHA or ADH were reacted with the disaccharide DD (chitobiose) under the same conditions as for AA (pH 4.0, RT). DD showed poor reactivity compared to AA (Supporting information, S7), as demonstrated by very low yields (in the range 2–10 % after 72 h), which is in agreement with the literature on other types of amines (Beaudoin et al., 2005; Guerry et al., 2013). Hence, D residues at the reducing end of chitoooligosaccharides are very unfavourable for conjugations of this type.

### 3.5. Conjugation of PDHA and ADH to longer chitoooligosaccharides (DP 4–10)

PDHA and ADH were subsequently conjugated to  $D_nXA$  oligomers (DP = 4–10,  $n = 2–8$ ). The  $^1H$ -NMR spectra and the course of the reaction with  $D_2XA$  ( $X = \text{either A or D}$ ) and 2 equivalents of ADH or PDHA, are shown in Supporting information, S8. For conjugation reactions with oligomers of DP > 4, a mixture of  $D_nXA$  ( $X = \text{D or A}$ ) oligomers was used. Results from the conjugation reactions with  $D_nXA$  oligomers are summarised in Table 2.

The reactions with longer chitoooligosaccharides followed the same trends as observed for AA in terms of kinetics, yields and selectivity. Surprisingly, reactions with  $D_nXA$  (Table 2) turned out to be slightly

faster than with AA (Table 1). A similar dependency on DP has also reported for ethoxyamine, which conjugates faster to AA than A (monomer) (Baudendistel et al., 2016). For PDHA, the combined yield increased with higher DP of the chitoooligosaccharides, whereas for ADH a slight decrease was observed.

The ratio of acyclic to cyclic conjugates increased for all reactions with the  $D_nXA$  oligomers compared to AA (Table 1) suggesting a higher stability of the oximes and hydrazones with increasing DP. This has also been observed when increasing the DP from one (A) to two (AA) shifting the ratio of acyclic to cyclic conjugates from 3.1:1 to 3.7:1 (Baudendistel et al., 2016)

### 3.6. Reduction of conjugates using $\alpha$ -picoline borane (PB)

Reduction of  $D_2AA$ -conjugates, prepared using 10 equivalents PDHA or ADH (pH 4.0), was studied by NMR, by adding solid  $\alpha$ -picoline borane (PB) directly to the NMR tube containing the oligosaccharide-PDHA/ADH equilibrium mixtures. PB has limited solubility under these conditions, and therefore, only 3 equivalents were used. The methylene protons of the secondary amines formed after reduction, gave proton resonances in the area 2.80–3.40 ppm, in agreement with literature data (Ridley et al., 1997), however partially overlapping with the H2 resonances of the D-units between 3.10 to 3.25 ppm (Supporting information, S10). Results obtained after 2 and 14 days of reduction are given in Table 3. For both reactions the reduction was exceptionally slow, and a large fraction of unidentified products was detected. PB, both in its reduced (r) and oxidized (o) form, has well defined proton resonances in the area 7.3–8.7 ppm, sufficiently separated from conjugate resonances in the same area, enabling the oxidation of the reducing agent to be monitored (Supporting information, S10). For the  $D_2AA$ -PDHA system 97 % of the dissolved PB was oxidised after 14 days, whereas 33 % of the dissolved PB was still in the reduced form in the  $D_2AA$ -ADH system, indicating the slower reduction of the latter.

### 3.7. Improvement of the reduction protocol

Reduction was further explored using higher concentrations of PB and higher temperatures. As PB has limited solubility in aqueous buffer at room temperature, continuous monitoring of the reactions by NMR was impractical. Therefore, only the products obtained at the end of the reactions were studied. Poor mixing during the time course NMR experiments may have lowered the reduction rate and hence, regular mixing was applied, except at higher temperatures which increase the solubility of PB (see below). Optimisation of the reduction protocol was performed using the dimer, AA, primarily to avoid the overlapping resonances from H2 of the D-units in the NMR-spectra.

First, AA-PDHA and AA-ADH conjugates, prepared using optimised conjugation conditions (10 equivalents PDHA/ADH, pH 4.0), were reduced using 20 equivalents PB. The reduction was performed for 40 days at room temperature, and the reaction mixtures were purified and fractionated by GFC. All fractions were characterised by mass spectroscopy and the main fractions were further analysed by  $^1H$ -NMR (Supporting information, S11). Annotated chromatograms based on the MS and NMR characterisation are given in Fig. 4a and c.

Reduction of AA-PDHA conjugates resulted in three fractions

**Table 2**

Reactions of  $D_nXA$  oligomers with PDHA and ADH studied by time course NMR.  $^1H$ -NMR spectra of the equilibrium mixtures obtained for all the reactions are given in Supporting information, S9.

Reaction	PDHA/ADH [equivalents]	pH	T [°C]	Ratio acycl:cycl.	$t_{0.5}$ [h]	$t_{0.9}$ [h]	$k_1$ [ $h^{-1}$ ]	$k_{-1}$ [ $h^{-1}$ ]	Combined equilibrium yield [%]
$D_2DA$ -PDHA	2	4.0	RT	7.6:1	5.8	24.2	$3.3 \times 10^{-3}$	$1.5 \times 10^{-3}$	98
$D_8XA$ -PDHA	10	4.0	RT	5.4:1	1.6	5.4	$2.2 \times 10^{-3}$	$6.0 \times 10^{-3}$	98
$D_2AA$ -ADH	2	4.0	RT	1:27.5	19.9	69.2	$4.3 \times 10^{-4}$	$1.4 \times 10^{-2}$	48
$D_8XA$ -ADH	10	4.0	RT	1:20.5	5.8	19.7	$5.2 \times 10^{-4}$	$1.5 \times 10^{-2}$	86

**Table 3**

Yields obtained at different time points during the reduction of conjugates, monitored by NMR.  $^1\text{H-NMR}$  spectra of the mixtures after 2 and 14 days are given in Supporting information, S10.

Reaction	PDHA/ADH [equivalents]	PB [equivalents]	Time [days]	Reduced conjugates [%]	Non-reduced conjugates [%]	Unreacted oligomers [%]	Unidentified products <sup>[a]</sup> [%]
D <sub>2</sub> AA-PDHA	10	3	2	7	66	1	26
			14	35	18	0	47
D <sub>2</sub> AA-ADH	10	3	2	7	75	11	7
			14	9	50	5	36

[a] The yield of unidentified products was calculated as the difference between the formation of reduced (secondary amine) conjugates and the decrease in non-reduced conjugates and unreacted oligomers. Hence, yield of unidentified products (%) = theoretical yield (100 %) – yield of reduced conjugates (%) – yield of non-reduced conjugates (%) – yield of unreacted oligomers (%).

(Fig. 4a) which based on MS and NMR were confirmed to be AA-PDHA (reduced to secondary amine), AA-PDHA-AA (doubly substituted and reduced), and a minor component with mass corresponding to acetylated AA-PDHA (reduced). The main fraction (reduced AA-PDHA), was further studied by homo- and heteronuclear NMR correlation experiments (Supporting information, S12). Assignment of the main resonances are given in the  $^1\text{H-NMR}$  spectrum in Fig. 4b. Integration confirmed an equimolar ratio of PDHA to AA. Resonances from (*E*)- and (*Z*)-oximes and  $\beta$ -*N*-pyranoside were absent and no unreacted AA was detected. A small fraction of doubly substituted PDHA (AA-PDHA-AA) was formed despite the large excess (10 equivalents) of dioxamine, suggesting an enhanced reactivity of the free oxyamine group following conjugation of PDHA to the first oligomer.

Reduction of AA-ADH conjugates resulted in a more complex mixture compared to PDHA (Fig. 4c).  $^1\text{H-NMR}$  characterisation of the main fraction (Fig. 4d), revealed a mixture of secondary amines (48 %) and non-reduced *N*-glycosides (52 %). The apparent resistance to reduction of the latter is attributed to the slow (i.e. rate limiting) conversion to reducible hydrazones (Ramsay, Freeman, Grace, Redmond, & MacLeod, 2001). In fact, *N*-glycosides were observed in all characterized fractions of the AA-ADH reaction. Detection of non-reduced, unreacted AA (Fig. 4c) confirm that PB selectively reduces Schiff bases under the given conditions, in addition to the slower conjugation of ADH compared to PDHA.

As for PDHA, a fraction of doubly substituted ADH (AA-ADH-AA) was observed. Additionally, fractions containing conjugates with multiple dihydrazides (ADH<sub>n</sub>) were detected (Supporting information, S11). To the best of our knowledge, this side reaction has not been described in the literature. These ‘polymerised’ dihydrazides also formed doubly substituted conjugates (AA-ADH<sub>n</sub>-AA). Conjugates containing ADH<sub>n</sub> showed reduced solubility when re-dissolved in D<sub>2</sub>O for NMR characterisation. Hence, a purification step is required to obtain reduced conjugates without multiple dihydrazides.

Reduction was subsequently studied at 40 and 60 °C. Higher temperatures improves the solubility of PB, although at the expense of faster decomposition. AA was reacted with 10 equivalents of PDHA or ADH, and 20 equivalents of PB for 8 h at pH 4.0. PB was added in one or several portions. Results and reaction conditions are given in Table 4. For AA-PDHA, the highest yield of reduced conjugates (49 %) could be obtained by combining 20 equivalents of PB, added in four portions (0, 2, 4 and 6 h), with reaction at 60 °C. For ADH, the same protocol gave 26 % reduced conjugates. By adding an additional portion of 20 equivalents PB after 8 h and leaving the reaction mixture for a total of 24 h at 60 °C, the yields were improved to 84 % reduced AA-PDHA and 43 % AA-ADH. The relative proportion of unidentified products decreased at higher temperatures, providing more optimised conditions for the reduction.

Overall, the yield of reduced chito oligosaccharide conjugates could

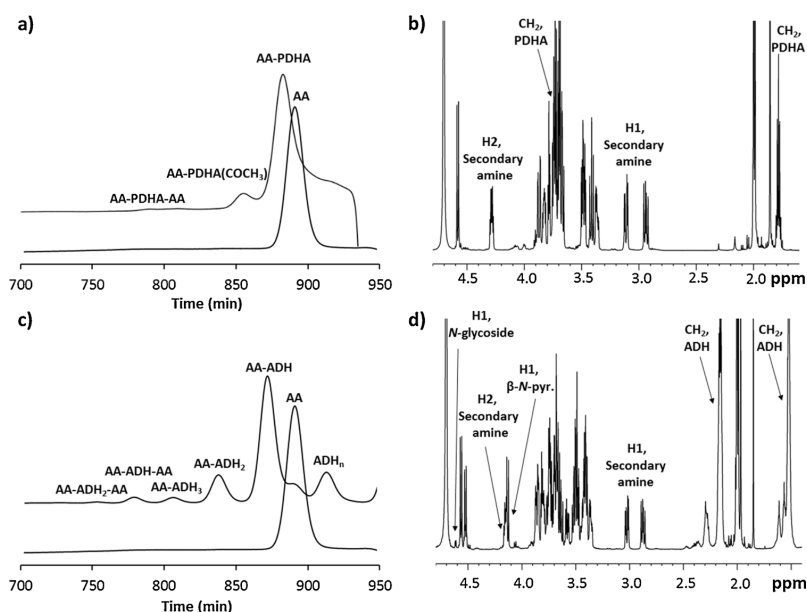


Fig. 4. a) and c) GFC fractionation of the mixture of products formed in the conjugation of PDHA and ADH (10 equivalents) to AA with subsequent reduction for 40 days at RT using 20 equivalents PB at pH 4.0, respectively. Fractionation of AA is included as a reference, b)  $^1\text{H-NMR}$  spectrum of the main fraction from the AA-PDHA reaction, d)  $^1\text{H-NMR}$  spectrum of the main fraction from the AA-ADH reaction.

**Table 4**

Reaction conditions and yields obtained for one pot reductive amination at higher temperatures. <sup>1</sup>H-NMR spectra of the reaction mixtures are given in Supporting information, S13.

Reaction	PB [equivalents]	Portions	Portions added [h]	Total rx. Time [h]	T [°C]	Reduced conjugates [%]	Non-reduced conjugates [%]	Unreacted oligomers [%]	Unidentified products <sup>[a]</sup> [%]
AA-PDHA	20	1	0	8	RT	11	87	1	1
	20	1	0	8	40	24	54	2	20
	20	1	0	8	60	40	37	1	22
	20	4	0, 2, 4, 6	8	60	49	27	1	23
	40	5	0, 2, 4, 6, 8	24	60	84	13	0	3
AA-ADH	20	1	0	8	RT	3	73	23	1
	20	1	0	8	40	12	63	13	12
	20	1	0	8	60	22	48	9	21
	20	4	0, 2, 4, 6	8	60	26	39	7	28
	40	5	0, 2, 4, 6, 8	24	60	43	23	4	30

[a] The yield of unidentified products was calculated as the difference between the formation of reduced conjugates and the decrease in non-reduced conjugates and unreacted oligomers. Hence, yield of unidentified products (%) = theoretical yield (100 %) – yield of reduced conjugates (%) – yield of non-reduced conjugates (%) – yield of unreacted oligomers (%).

be improved by increasing the temperature and the concentration of PB (added in several portions to compensate for the fast decomposition at higher temperatures). Higher temperatures have also been shown to increase the fraction of reducible acyclic conjugates for oligo-saccharide-oxyamine reactions (Baudendistel et al., 2016).

The slower reduction of ADH-conjugates compared to conjugates prepared with PDHA, both at room temperature and at higher temperatures, is attributed to the slow conversion of cyclic *N*-glycosides to reducible acyclic conjugates combined with the large fraction of cyclic conjugates formed with ADH.

### 3.8. Comparison to dextran oligomers

To investigate whether the results obtained for the chito-oligosaccharides were specific to the reducing end residue (GlcNAc), conjugation to a dextran oligomer (Dext<sub>5</sub>, DP 5) and the monomer (Glc, DP 1) was studied. Glc and Dext<sub>5</sub> were reacted with PDHA or ADH (2 equivalents, pH 4.0) and monitored by time course NMR as described above (Table 5). PDHA reacted two to three times faster than with the chito-oligosaccharides, in excellent agreement with the Glc- and GlcNAc-ethoxyamine systems (Baudendistel et al., 2016). Moreover, the ratio of acyclic to cyclic conjugates was 2.6:1 for the monomer (Glc), which corresponds well to the results obtained with ethoxyamine under similar conditions (Baudendistel et al., 2016). As observed for the chito-oligosaccharides, the ratio increased with increasing DP. Likewise, reaction rates increased slightly with increasing DP, whereas the yields slightly decreased.

In the case of ADH, only *N*-glycosides were formed when conjugated to Glc and Dext<sub>5</sub>, as also found for chito-oligosaccharides. In contrast, ADH reacted 7–10 times faster than with the chito-oligosaccharides. Hence, the nature of the residue at the reducing end (Glc versus GlcNAc) largely influences the conjugation rate, in agreement with other conjugation reactions (Baudendistel et al., 2016; Ramsay et al., 2001; Thygesen et al., 2010).

We further monitored the one pot reductive amination of Dext<sub>4</sub> with 2 equivalents of PDHA or ADH in the presence of PB (3 equivalents) and compared the results with the reaction of AA with PDHA or ADH under

the same conditions (RT, pH 4.0). The spectra obtained after 2 and 5 days for all reactions are given in Supporting information, S16. After 5 days, 70 % reduced Dext<sub>4</sub>-PDHA and 61 % Dext<sub>4</sub>-ADH were formed, as opposed to only 9 % and 6 % reduced AA-PDHA and AA-ADH, respectively. In contrast to the AA reactions, where a large fraction of unidentified products was formed, all products could be accounted for in the Dext<sub>4</sub> reactions (Supporting information, S16). We therefore attribute the slow and complex reduction of the chito-oligosaccharide-based conjugates to the nature of the reducing end, i.e. the GlcNAc residue.

## 4. Conclusions

In this study we have presented a systematic investigation of aqueous, aniline-free conjugation of the bifunctional linkers PDHA and ADH to the reducing end of chito-oligosaccharides ranging from DP 2 to DP 10, both without and with reduction using  $\alpha$ -picoline borane. The oligomers were of the type D<sub>n</sub>XA obtained by enzymatic degradation of chitosan and are therefore relevant in a biorefinery context. As expected from literature, reactions with PDHA resulted in a mixture of acyclic (*E*- and *Z*-) oximes and cyclic  $\beta$ -*N*-pyranosides, whereas ADH yielded only cyclic *N*-glycosides. The acyclic/cyclic ratio of conjugates, combined yield, and reaction kinetics depended in both cases on pH. In total, highest reaction rates were obtained at pH 3.0, whereas highest yields were obtained at pH 5.0. Carrying out the reaction at pH 4.0 therefore gives a good compromise between reaction time and yield. The influence of chain length is of utmost importance for general use of the methodology. We found that the rate of conjugation was essentially independent of DP within the range investigated.

The conjugation of PDHA and ADH to dextran oligomers was included for comparison. In general, both PDHA and ADH conjugated faster to dextran than to the chito-oligosaccharides and hence, the nature of the reducing end residue plays an important role for the outcome of the conjugation. In this perspective, it may be noted that oligomers terminating in D residues were confirmed to be less reactive than those having A at the reducing ends. Hence, the D<sub>n</sub>XA oligomers have an additional advantage over pure D<sub>n</sub> oligomers.

**Table 5**

Reactions of Dext<sub>n</sub> oligomers with 2 equivalents PDHA or ADH studied by time course NMR. The course of the reaction for Dext<sub>1</sub>-PDHA/ADH is given in Supporting information, S14. <sup>1</sup>H-NMR spectra of the equilibrium mixtures obtained for all the reactions are given in Supporting information, S15.

Reaction	DP [n]	pH	T [°C]	Ratio acycl.:cycl.	t <sub>0.5</sub> [h]	t <sub>0.9</sub> [h]	k <sub>1</sub> [h <sup>-1</sup> ]	k <sub>-1</sub> [h <sup>-1</sup> ]	Combined equilibrium yield [%]
Dext <sub>n</sub> -PDHA	1	4.0	RT	2.6:1	3.2	13.0	5.5 × 10 <sup>-3</sup>	1.2 × 10 <sup>-2</sup>	92
	5	4.0	RT	4.3:1	2.2	8.6	8.0 × 10 <sup>-3</sup>	2.0 × 10 <sup>-2</sup>	90
Dext <sub>n</sub> -ADH	1	4.0	RT	1:64	3.0	10.4	2.9 × 10 <sup>-3</sup>	9.0 × 10 <sup>-2</sup>	49
	5	4.0	RT	1:41	1.9	6.4	3.5 × 10 <sup>-3</sup>	1.9 × 10 <sup>-1</sup>	38



All protocols seem to give a small amount of disubstituted species, e.g. AA-PDHA-AA (Fig. 4a). This can in principle be tolerated in the subsequent coupling because they will be unreactive. They may alternatively be removed by chromatography as shown in the same figure. Further, detectable (but small) amounts of oligomers with multiple ADH, i.e. AA-ADH<sub>2</sub> were detected (Fig. 4c). They may, as shown here, still react to form e.g. AA-ADH<sub>2</sub>-AA, indicating the terminal ADH remains reactive. If undesired, they may also be removed after the activation step, at least for short oligosaccharides.

Although  $\alpha$ -picoline borane has proven useful in reductive amination with carbohydrates, we found that chito oligosaccharide-based PDHA- and ADH-conjugates were very slowly reduced at room temperature. However, a protocol using higher temperatures improved the reduction significantly with acceptable yields after 24 h, comparable to aniline- and cyanoborohydride-based protocols (Guerry et al., 2013). We attribute the slow reduction to the nature of the reducing end residue, as dextran-based conjugates were reduced with a much higher rate under the same conditions. The slower reduction of ADH conjugates for both types of oligomers is attributed to the large fraction of non-reducible cyclic conjugates. In general, the slow reduction of the chito oligosaccharide conjugates is considered unsuitable for typical labelling applications in biochemistry but may still be more acceptable in biomaterials preparation.

In summary, the reaction of enzymatically produced chito oligosaccharides with PDHA and ADH, without or with reduction using  $\alpha$ -picoline borane has been studied in detail. The outcome is protocols and kinetic constants for preparing both PDHA- and ADH-chito oligosaccharide conjugates. The protocols avoid toxic reagents such as sodium cyanoborohydride and aniline, and retains the inherent properties of the oligosaccharides. The PDHA- or ADH-activated D<sub>n</sub>XA chito oligosaccharide conjugates may be effectively linked to aldehyde-containing particles, surfaces or macromolecules e.g. other oligosaccharides for the preparation of block polysaccharides.

#### Author contributions

**Ingrid Vikøren Mo:** Investigation, Methodology, Writing

**Yiming Feng.:** Investigation.

**Marianne Øksnes Dalheim:** Investigation.

**Amalie Solberg:** Investigation.

**Finn L. Aachmann:** Investigation, Validation.

**Christophe Schatz:** Conceptualization, Writing- Reviewing and Editing.

**Bjørn E. Christensen:** Supervision, Conceptualization, Writing- Reviewing and Editing, Project administration.

#### Acknowledgements

This work was supported by a grant from the Norwegian University of Science and Technology to I.V. Mo. It was further partially supported by grant 6167 from VISTA (a basic research program in collaboration between The Norwegian Academy of Science and Letters, and Statoil), and grants 268490, 226244 and 221576 from the Research Council of Norway. Vincent G. H. Eijnsink is thanked for kindly providing ChiB. Odin Weberg Haarberg is thanked for running the conjugation experiments with dextran during his master work. Bård Helge Hoff and Hallvard Svendsen are thanked for useful discussions. Kåre Kristiansen is thanked for running the MS analysis and Ann-Sissel T. Ulset is thanked for technical assistance.

#### Appendix A. Supplementary data

Supplementary material related to this article can be found, in the online version, at doi:<https://doi.org/10.1016/j.carbpol.2019.115748>.

#### References

- Allan, G. G., & Peyron, M. (1995). Molecular-weight manipulation of chitosan .1. Kinetics of depolymerization by nitrous-acid. *Carbohydrate Research*, 277(2), 257–272.
- Baudendistel, O. R., Wieland, D. E., Schmidt, M. S., & Wittmann, V. (2016). Real-time NMR studies of oxamine ligations of reducing carbohydrates under equilibrium conditions. *Chemistry — A European Journal*, 22(48), 17359–17365.
- Beaudoin, M.-E., Gauthier, J., Boucher, I., & Waldron, K. C. (2005). Capillary electrophoresis separation of a mixture of chitin and chitosan oligosaccharides derivatized using a modified fluorophore conjugation procedure. *Journal of Separation Science*, 28(12), 1390–1398.
- Bendiak, B. (1997). Preparation, conformation, and mild hydrolysis of 1-glycosyl-2-acetylhydrazines of the hexoses, pentoses, 2-acetamido-2-deoxyhexoses, and fucose. *Carbohydrate Research*, 304(1), 85–90.
- Breitenbach, B. B., Schmid, I., & Wich, P. R. (2017). Amphiphilic polysaccharide block copolymers for pH-responsive micellar nanoparticles. *Biomacromolecules*, 18(11), 3844–3845.
- Cosenza, V. A., Navarro, D. A., & Stortz, C. A. (2011). Usage of  $\alpha$ -picoline borane for the reductive amination of carbohydrates. *Arkioc, 12*, 182–194.
- Dalheim, M.Ø., Vanacker, J., Najmi, M. A., Aachmann, F. L., Strand, B. L., & Christensen, B. E. (2016). Efficient functionalization of alginate biomaterials. *Biomaterials*, 80, 146–156.
- Dirksen, A., & Dawson, P. E. (2008). Rapid oxime and hydrazone ligations with aromatic aldehydes for biomolecular labeling. *Bioconjugate Chemistry*, 19(12), 2543–2548.
- Dirksen, A., Hackeng, T. M., & Dawson, P. E. (2006). Nucleophilic catalysis of oxime ligation. *Angewandte Chemie-International Edition*, 45(45), 7581–7584.
- Fang, J., Qin, G., Ma, J., & She, Y.-M. (2015). Quantification of plant cell wall monosaccharides by reversed-phase liquid chromatography with 2-aminobenzamide pre-column derivatization and a non-toxic reducing reagent 2-picoline borane. *Journal of Chromatography A*, 1414, 122–128.
- Finá, N. J., & Edwards, J. O. (1973). The alpha effect. A review. *International Journal of Chemical Kinetics*, 5(1), 1–26.
- Guerry, A., Bernard, J., Samain, E., Fleury, E., Cottaz, S., & Halila, S. (2013). Aniline-catalyzed reductive amination as a powerful method for the preparation of reducing end-“clickable” chito oligosaccharides. *Bioconjugate Chemistry*, 24(4), 544–549.
- Hermanson, G. T. (2008). *Bioconjugate techniques* (2nd ed.). Boston: Academic Press.
- Kalia, J., & Raines, R. T. (2008). Hydrolytic stability of hydrazones and oximes. *Angewandte Chemie*, 120(39), 7633–7636.
- Kržel, A., & Bal, W. (2004). A formula for correlating pKa values determined in D2O and H2O. *Journal of Inorganic Biochemistry*, 98(1), 161–166.
- Kwase, Y. A., Cochran, M., & Nitz, M. (2013). Protecting-group-free glycoconjugate synthesis: Hydrazide and oxamine derivatives in N-glycoside formation. In D. B. Werz, & S. Vidal (Eds.), *Modern synthetic methods in carbohydrate chemistry: From monosaccharides to complex glycoconjugates* (pp. 67–96). Wiley.
- Kölmel, D. K., & Kool, E. T. (2017). Oximes and hydrazones in bioconjugation: Mechanism and catalysis. *Chemical Reviews*, 117(15), 10358–10376.
- Lee, M.-r., & Shin, I. (2005). Facile preparation of carbohydrate microarrays by site-specific, covalent immobilization of unmodified carbohydrates on hydrazide-coated glass slides. *Organic Letters*, 7(19), 4269–4272.
- Mellegård, H., Strand, S. P., Christensen, B. E., Granum, P. E., & Hardy, S. P. (2011). Antibacterial activity of chemically defined chitosans: Influence of molecular weight, degree of acetylation and test organism. *International Journal of Food Microbiology*, 148(1), 48–54.
- Moussa, A., Crepet, A., Ladaviere, C., & Trombotto, S. (2019). Reducing-end “clickable” functionalizations of chitosan oligomers for the synthesis of chitosan-based diblock copolymers. *Carbohydrate Polymers*, 219, 387–394.
- Novoa-Carballal, R., & Müller, A. H. E. (2012). Synthesis of polysaccharide-b-PEG block copolymers by oxime click. *Chemical Communications*, 48(31), 3781–3783.
- Pickenhahn, V. D., Darras, V., Dziopa, F., Biniecki, K., De Crescenzo, G., Lavertu, M., ... Buschmann, M. D. (2015). Regioselective thioacetylation of chitosan end-groups for nanoparticle gene delivery systems. *Chemical Science*, 6(8), 4650–4664.
- Ramsay, S. L., Freeman, C., Grace, P. B., Redmond, J. W., & MacLeod, J. K. (2001). Mild tagging procedures for the structural analysis of glycans. *Carbohydrate Research*, 333(1), 59–71.
- Ridley, B. L., Spiro, M. D., Glushka, J., Albersheim, P., Darvill, A., & Mohnen, D. (1997). A method for biotin labeling of biologically active oligogalacturonides using a chemically stable hydrazide linkage. *Analytical Biochemistry*, 249(1), 10–19.
- Rossegong, J., Chemin, M., Almada, C. C., Hemery, G., Guigner, J.-M., Chollet, G., ... Cramail, H. (2019). Synthesis and self-assembly of xylan-based amphiphiles: From bio-based vesicles to antifungal properties. *Biomacromolecules*, 20(1), 118–129.
- Ruhaak, L. R., Steenvoorden, E., Koelman, C. A. M., Deelder, A. M., & Wuhrer, M. (2010). 2-Picoline-borane: A non-toxic reducing agent for oligosaccharide labeling by reductive amination. *Proteomics*, 10(12), 2330–2336.
- Ruhaak, L. R., Zauner, G., Huhn, C., Bruggink, C., Deelder, A. M., & Wuhrer, M. (2010). Glycan labeling strategies and their use in identification and quantification. *Analytical and Bioanalytical Chemistry*, 397(8), 3457–3481.
- Schatz, C., & Lecommandoux, S. (2010). Polysaccharide-containing block copolymers: Synthesis, properties and applications of an emerging family of glycoconjugates. *Macromolecular Rapid Communications*, 31(19), 1664–1684.
- Shinohara, Y., Sota, H., Gotoh, M., Hasebe, M., Tosu, M., Nakao, J., ... Shiga, M. (1996). Bifunctional labeling reagent for oligosaccharides to incorporate both chromophore and biotin groups. *Analytical Chemistry*, 68(15), 2573–2579.
- Strand, S. P., Danielsen, S., Christensen, B. E., & Vårum, K. M. (2005). Influence of chitosan structure on the formation and stability of DNA–Chitosan polyelectrolyte complexes. *Biomacromolecules*, 6(6), 3357–3366.

- Sorbotten, A., Horn, S. J., Eijsink, V. G. H., & Vårum, K. M. (2005). Degradation of chitosans with chitinase B from *Serratia marcescens*. *The FEBS Journal*, *272*(2), 538–549.
- Thygesen, M. B., Munch, H., Sauer, J., Cló, E., Jørgensen, M. R., Hindsgaul, O., ... Jensen, K. J. (2010). Nucleophilic catalysis of carbohydrate oxime formation by anilines. *The Journal of Organic Chemistry*, *75*(5), 1752–1755.
- Tømmeraas, K., Vårum, K. M., Christensen, B. E., & Smidsrød, O. (2001). Preparation and characterisation of oligosaccharides produced by nitrous acid depolymerisation of chitosans. *Carbohydrate Research*, *333*(2), 137–144.
- Unterieser, I., & Mischnick, P. (2011). Labeling of oligosaccharides for quantitative mass spectrometry. *Carbohydrate Research*, *346*(1), 68–75.
- Vårum, K. M., Antohonsen, M. W., Grasdalen, H., & Smidsrød, O. (1991). Determination of the degree of *N*-acetylation and the distribution of *N*-acetyl groups in partially *N*-deacetylated chitins (chitosans) by high-field n.m.r. Spectroscopy. *Carbohydrate Research*, *211*(1), 17–23.

# Supporting Information

## Activation of enzymatically produced chitooligosaccharides by dioxyamines and dihydrazides

Ingrid Vikøren Mo, Yiming Feng, Marianne Øksnes Dalheim, Amalie Solberg, Finn L. Aachmann, Christophe Schatz, and Bjørn E. Christensen

### Contents

<b>S1 Chitin and chitosan - nomenclature</b> .....	<b>1</b>
<b>S2 Preparation of chitosan oligomers (<math>D_nXA</math>, X = A or D)</b> .....	<b>1</b>
<b>S3 2D Characterisation of the equilibrium mixture for the conjugation of PDHA to AA</b> .....	<b>2</b>
<b>S4 Pseudo first order kinetics modelling of the conjugation reactions</b> .....	<b>4</b>
<b>S5 pH titration by <math>^1H</math>-NMR to determine the <math>pK_a</math> of PDHA and ADH</b> .....	<b>5</b>
<b>S6 <math>^1H</math>-NMR characterisation of the equilibrium mixtures for the conjugation reactions with AA</b> .....	<b>6</b>
<b>S7 Comparison to D at the reducing end</b> .....	<b>11</b>
<b>S8 Conjugation of PDHA and ADH to <math>D_2XA</math> studied by time course NMR</b> .....	<b>11</b>
<b>S9 <math>^1H</math>-NMR characterisation of the equilibrium mixtures for the conjugation reactions with <math>D_nXA</math> oligomers</b> .....	<b>12</b>
<b>S10 <math>^1H</math>-NMR characterisation of the reaction mixtures for the <math>D_nXA</math>-PDHA/ADH conjugates after 2 and 14 days of reduction</b> .....	<b>15</b>
<b>S11 <math>^1H</math>-NMR and MS characterisation of products formed in the reduction of AA-PDHA and AA-ADH conjugates using PB</b> .....	<b>16</b>
<b>S12 2D NMR characterisation of the reduced AA-PDHA conjugate</b> .....	<b>20</b>
<b>S13 <math>^1H</math>-NMR characterisation of the reaction mixtures for the reduction of conjugates at higher temperatures</b> .....	<b>21</b>
<b>S14 Conjugation of PDHA and ADH to <math>Dext_1</math> (Glc) studied by time course NMR</b> .....	<b>27</b>
<b>S15 <math>^1H</math>-NMR characterisation of the equilibrium mixtures for the conjugation reactions with <math>Dext_n</math> oligomers</b> .....	<b>28</b>
<b>S16 <math>^1H</math>-NMR characterisation of the reaction mixtures for the one pot reductive amination reaction of AA and <math>Dext_4</math> with PDHA or ADH after 2 and 5 days</b> .....	<b>30</b>
<b>S16 References</b> .....	<b>33</b>

## S1 Chitin and chitosan - nomenclature

In order to obtain unique but simple representations of monomer sequences, the chitin monomer, *N*-acetyl-D-glucosamine (GlcNAc), and its de-*N*-acetylated counterpart, D-glucosamine (GlcN) are abbreviated with the single letters A and D, respectively. Accordingly, the dimer *N,N'*-diacetyl chitobiose is abbreviated AA and chitobiose is abbreviated DD. The monomers are linked by  $\beta$ -1,4-linkages in both chitin and chitosan. The composition of chitosans is commonly described by the fraction of acetylated units ( $F_A$ ), hence, the fraction of A residues in the polysaccharide.  $F_A$  is defined as

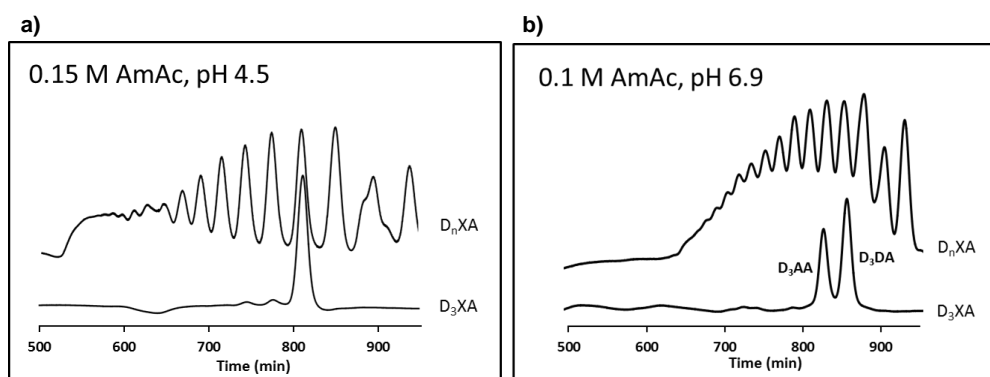
$$F_A = n_A / (n_A + n_D) \quad (\text{eq. 1})$$

where  $n_A$  is the number of A-units and  $n_D$  is the number of D-units in the chitosan. Another commonly used parameter for describing chitosan is the degree of de-*N*-acetylation, describing the fraction of A units in the chitosan related to  $F_A$  by the equation

$$\text{Degree of de-}N\text{-acetylation} = (1 - F_A) \times 100 \% \quad (\text{eq. 2})$$

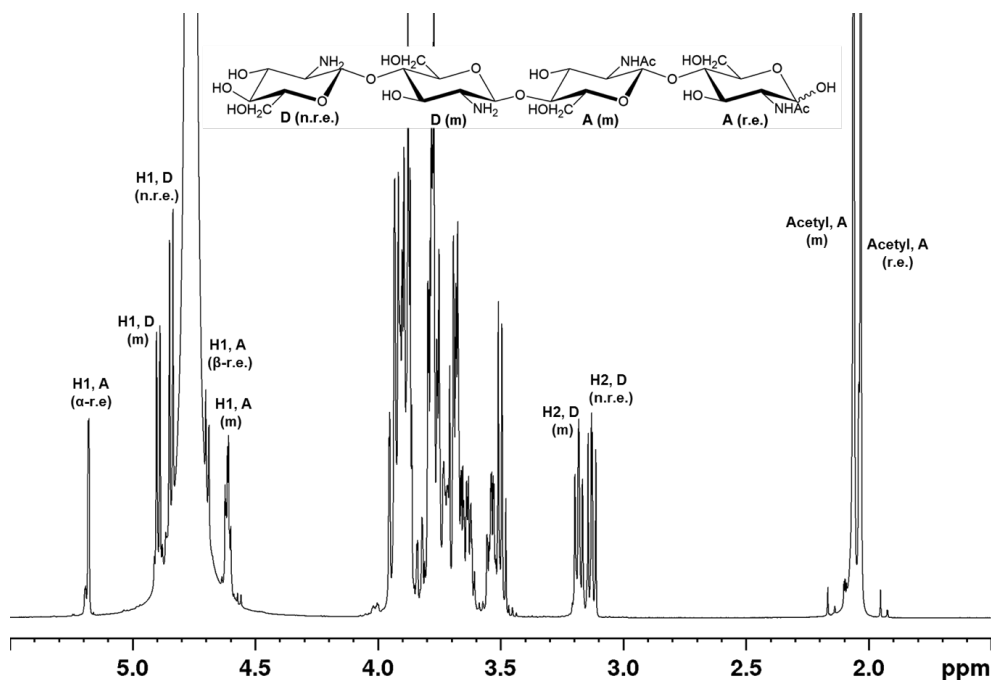
## S2 Preparation of chitosan oligomers ( $D_nXA$ , X = A or D)

Water soluble chitosan with  $F_A = 0.25$  was prepared by partial de-*N*-acetylation of chitin. The chitosan was further subjected to enzymatic degradation with chitinase B (ChiB) from *Serratia marcescens*. ChiB belongs to the GH18 family and has a specified cleavage site for *N*-acetyl glucosamine linkages (van Aalten et al., 2001). The enzyme works from the non-reducing end and cleaves the polymer after one or two A-units (preferably two A units in the -1 and -2 subsites, but will also cleave the polymer when a D-unit is present in the -2 subsite, however with a slower rate). Hence, depending on the  $F_A$  of the chitosan and the conditions, the enzymatic degradation can exclusively provide chitoooligosaccharides terminating in one or two A residues at the reducing end, but which otherwise contain uninterrupted (homogenous) sequences of D residues ( $D_n$ ) (Sørbotten, Horn, Eijsink, & Vårum, 2005). Oligomers with specific DP ( $D_nXA$ ,  $n = 2-8$ ) were fractionated by gel filtration chromatography (GFC) using 0.15 M ammonium acetate (AmAc) buffer, pH 4.5 (**Figure S1a**). Fractions were purified by dialysis and freeze-dried and the DP of the oligomers was determined by  $^1\text{H-NMR}$  spectroscopy. Individual fractions were subsequently re-chromatographed using 0.1 M AmAc buffer adjusted to pH 6.9. This step separated  $D_nAA$  from  $D_nDA$  (verified by NMR), although baseline separation only was obtained for  $n = 2-3$  (**Figure S1b**).



**Figure S1: a)** GFC fractionation of the mixture of  $D_nXA$  oligomers obtained by enzymatic degradation of chitosan ( $F_A = 0.25$ ) using ChiB in 0.15 M AmAc at pH 4.5. Fractionation of isolated  $D_3XA$  is included to show the DP distribution. **b)** GFC fractionation of the mixture of  $D_nXA$  oligomers in 0.1 M AmAc at pH 6.9. Fractionation of  $D_3XA$  is included to demonstrate the ability to separate oligomers with different chemical composition.

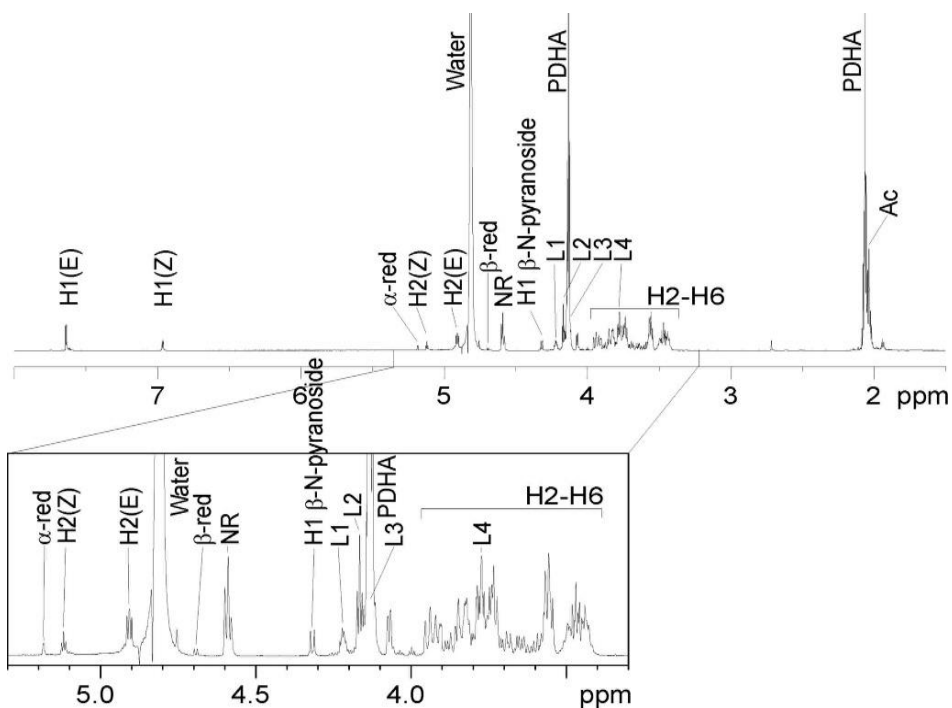
Isolated chitooligosaccharides were characterized by  $^1\text{H-NMR}$ . The spectrum obtained for the isolated  $\text{D}_2\text{AA}$  oligomers were assigned according to literature (**Figure S2**) (Sugiyama et al., 2001). Isolated  $\text{D}_2\text{AA}$  contained approximately 15 %  $\text{D}_2\text{DA}$ , evident in the  $^1\text{H NMR}$ -spectrum by side peaks for the reducing end (r.e.) resonances (H1, A r.e. in  $\alpha$ - and  $\beta$ -configuration). The middle D- and A-units are assigned m, whereas the non-reducing end D-unit is assigned n.r.e. The chemical shifts of the resonances resulting from the H2 of the D-units (m and n.r.e.) are very pH sensitive and increasing the pH above the  $\text{pK}_a$  of the amino group (approx. 6.5) shifts the resonances upfield to 2.5-2.7 ppm.



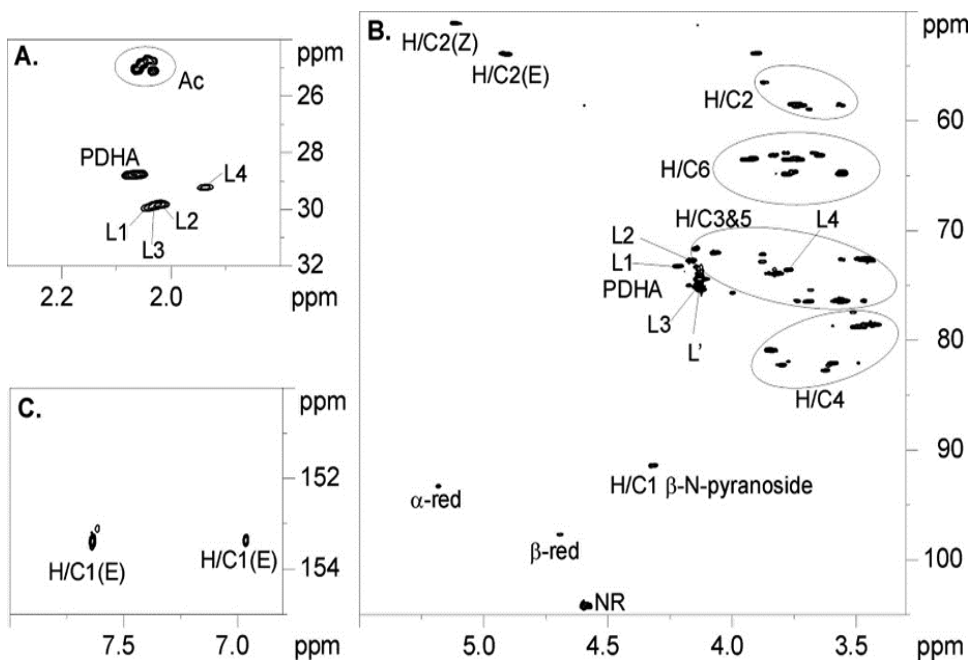
**Figure S2:**  $^1\text{H-NMR}$  spectrum of isolated  $\text{D}_2\text{AA}$  at pH 4.0, 298 K.

### S3 2D Characterisation of the equilibrium mixture for the conjugation of PDHA to AA

The dimer AA ( $N,N'$ -diacetyl chitobiose, 20.1 mM) was reacted with 2 equivalents of PDHA under standard reaction conditions (500 mM deuterated NaAc-buffer pH 4.0, room temperature). Resonances from conjugates and reactants at equilibrium (>48 h) were assigned by homo and hetero nuclear NMR correlation experiments. The NMR analysis was carried out at the 800 MHz spectrometer in a 3 mm NMR tube. Resonances were assigned by starting at the anomeric proton resonance and then following the proton-proton connectivity using TOCSY, DQF-COSY, and  $^{13}\text{C}$  HSQC- $[\text{H}, \text{H}]$  TOCSY spectra. The carbon chemical shifts were obtained from  $^{13}\text{C}$  HSQC.  $^{13}\text{C}$  HMBC was used for connecting the spin systems via long range connections. The following designations are used in the spectra displayed in **Figure S3** and **S4**: (E) and (Z) ((E)/(Z)-configuration of the oxime),  $\beta$ - $N$ -pyranoside ( $\beta$ -configuration of the  $N$ -pyranoside),  $\alpha$ - and  $\beta$ -red. (anomeric protons of the reducing A-unit), NR (anomeric proton of the non-reducing A-unit), L# (methylene protons from conjugated dioxamine (PDHA)), L' (methylene protons from unreacted PDHA), Ac ( $N$ -acetyl groups of the A-units). H# refers to the proton attached to the ring carbon number (C#) for the sugar units.



**Figure S3:** 1D proton spectrum of the mixture of products and reactants obtained for the conjugation of PDHA to AA after equilibrium was reached (>48 h) recorded at 298 K.



**Figure S4:**  $^{13}\text{C}$  HSQC spectrum of the mixture of products and reactants obtained for the conjugation of PDHA to AA after equilibrium was reached (>48 h) recorded at 298 K. **A.** shows the acetyl/methylene region, **B.** display the spectral region for anomeric and sugar resonances and **C.** shows the amino region.

**Table S1:** Assignment of the chemical shifts for the mixture of products and reactants obtained for the conjugation of PDHA to AA after equilibrium was reached (>48 h)

Structural unit	Assignment						
	H1; C1	H2; C2	H3; C3	H4; C4	H5; C5	H6; C6	Ac-H; C
(E)-oxime	7.63; 153.4	4.91; 53.7	4.07; 72.0	3.85; 80.8	3.83; 73.9	3.78, 3.56; 64.9	2.05; 24.7
(Z)-oxime	6.97; 153.2	5.13; 50.9	4.15; 71.4	3.80; 82.3	3.82; 73.9	3.76, 3.55; 64.6	2.04; 25.1
$\alpha$ -red.	5.18; 93.4	3.88; 56.6	3.88; 72.2	n.d	n.d	n.d	n.d
$\beta$ -red.	4.69; 97.7	3.69; 59.0	3.52; 77.5	3.62; 82.3	n.d	n.d	n.d
NR	4.60; 104.2	3.74; 58.6	3.56; 76.4	3.44; 78.6	3.46; 72.6	3.93, 3.74; 63.5	2.06; 25.1
$\beta$ -N-pyranoside	4.32; 91.5	3.90; 53.9	3.69; 76.6	3.59; 82.0	3.50; 78.8	3.83, 3.65; 63.1	2.05; 24.8
	<b>Methylene in PDHA closest to conjugation</b>	<b>Middle methylene in PDHA</b>	<b>Methylene in PDHA closest to free oxyamine end</b>				
L1	4.22; 73.1	2.04; 29.9	4.14; 75.1				
L2	4.16; 72.7	2.03; 29.8	4.14; 75.1				
L3	4.12; 75.4	2.04; 30.0	4.14; 75.1				
L4	3.77; 73.6	1.94; 29.3	4.14; 75.1				

n.d: not determined

#### S4 Pseudo first order kinetics modelling of the conjugation reactions

All conjugation reactions were assumed to follow *pseudo* first order kinetics. By treating the conjugates as one reaction product, the experimental data were fitted to a first order kinetics model (**Figure S5**) using the following rate equations



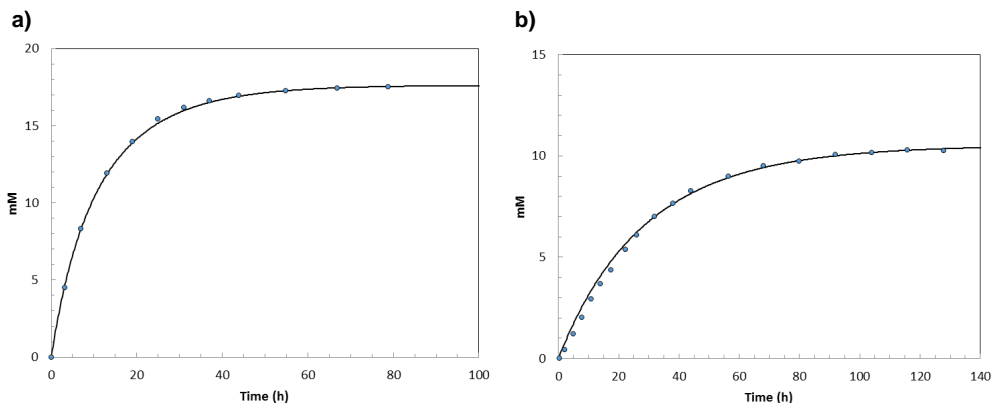
where [O] is the concentration of oligomers, [X] is the concentration of PDHA or ADH, [X=O] is the concentration of conjugates,  $k_1$  is the rate constant for the conjugation and  $k_{-1}$  is the rate constant for the reverse reaction. Hence, the rate of conjugation was determined from

$$\frac{d[X=O]}{dt} = k_1[O][X] - k_{-1}[X=O] \quad (\text{Eq. 4})$$

The concentration of conjugates at specific time points,  $[X=O]_t$  was calculated from the rate by the following equation

$$[X=O]_t = \frac{d[X=O]}{dt} \Delta t + [X=O]_{t-\Delta t} \quad (\text{Eq. 5})$$

where,  $t$  is the time, and  $\Delta t$  is the time difference from last modelled time point. All the conjugation reactions were modelled using this approach.



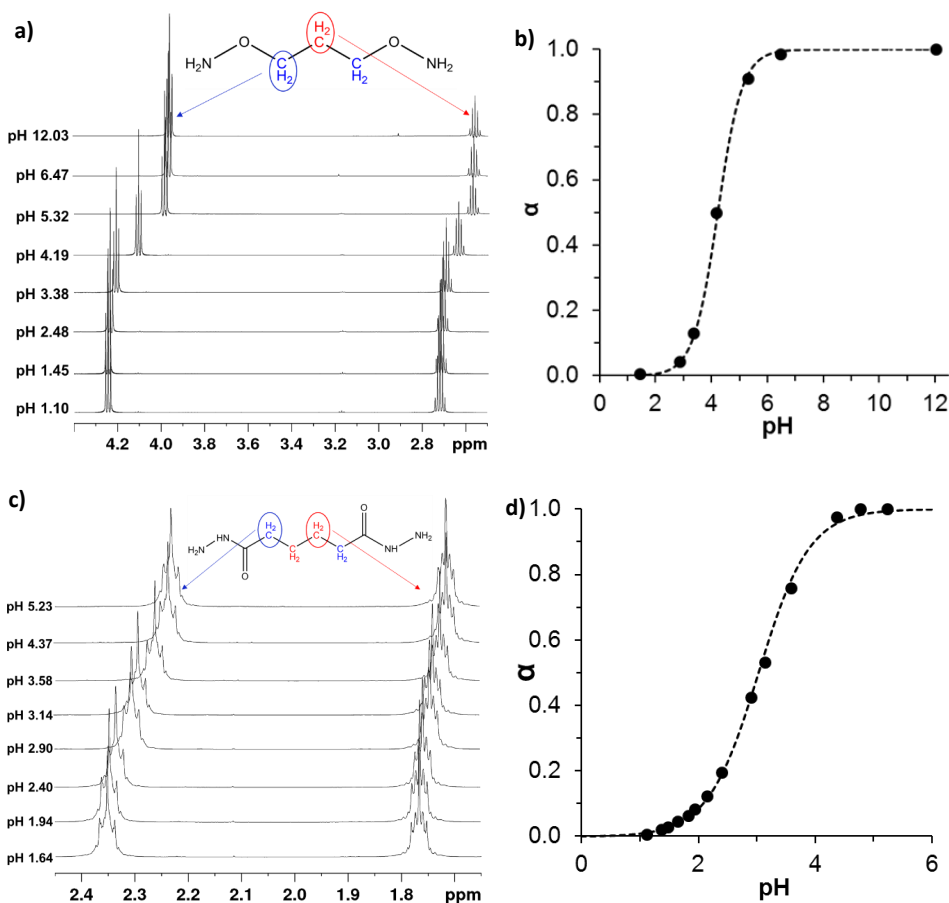
**Figure S5:** **a)** Model (solid line) fitted to the experimental data (blue dots, combined yield of conjugates in mM) obtained for the conjugation of PDHA (2 equivalents) to AA at pH 4.0 **b)** Model (solid line) fitted to the experimental data (blue dots combined yield of conjugates in mM) obtained for the conjugation of ADH (2 equivalents) at pH 4.0.

### S5 pH titration by $^1\text{H-NMR}$ to determine the $pK_a$ of PDHA and ADH

The  $pK_a$  of the terminal amino groups of PDHA and ADH was determined by monitoring the change in chemical shifts for the methylene protons over a range of different pH values (**Figure S6a** and **c**, respectively). The degree of dissociation ( $\alpha$ ) was calculated from the relative change in shifts going from fully protonated to deprotonated. The change in  $\alpha$  as a function of pH was fitted to the Henderson-Hasselbalch equation (Eq. 6) providing a  $pK_a$  of 4.2 and 3.1 for the free amine group of PDHA and ADH, respectively (**Figure S6b** and **d**).

$$pH = pK_a + \log \frac{[A^-]}{[HA]} \longleftrightarrow pH = pK_a + \log \left( \frac{\alpha}{1 - \alpha} \right) \quad (\text{Eq. 6})$$

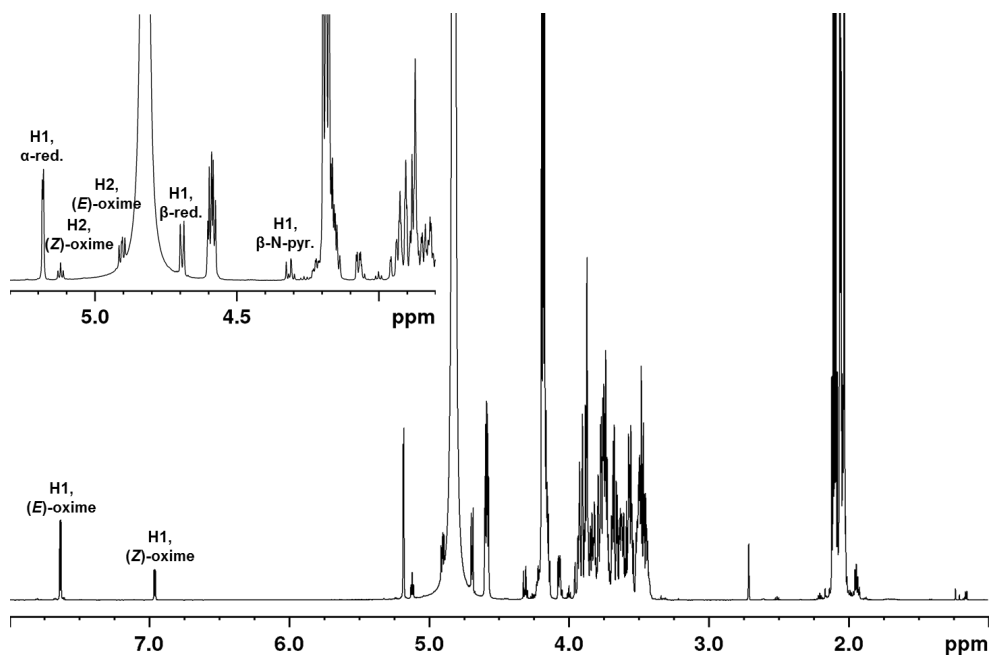




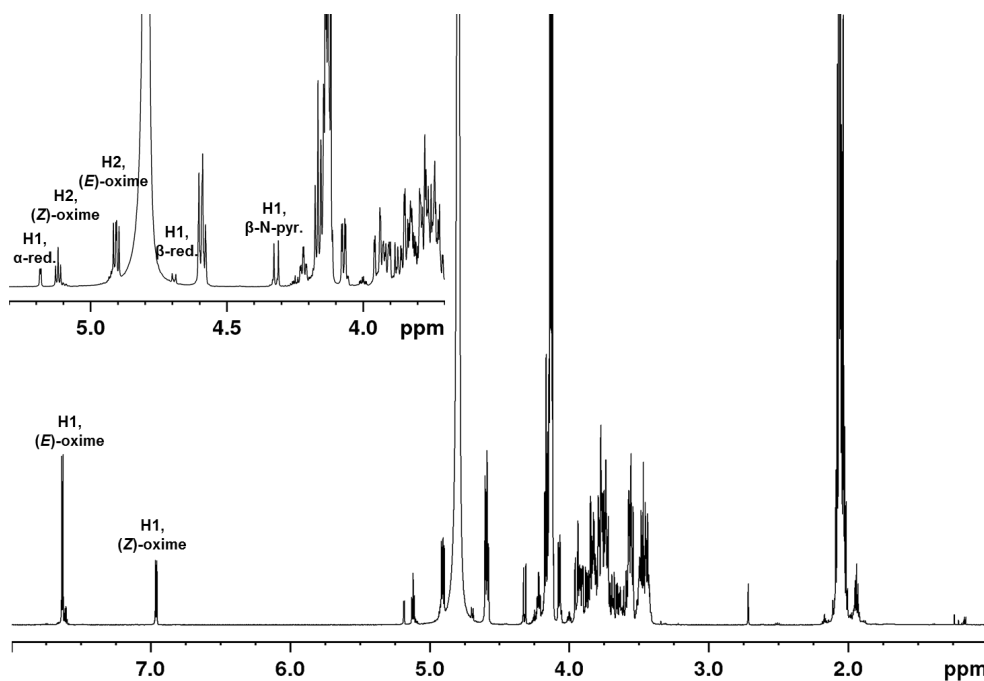
**Figure S6:** a)  $^1\text{H-NMR}$  spectra obtained for PDHA at different pH values b) pH dependence of the chemical shifts for the PDHA methylene protons, represented by the degree of dissociation calculated from the experimental data and fitted to the Henderson-Hasselbalch equation to obtain a  $\text{pK}_a$  of 4.2. c)  $^1\text{H-NMR}$  spectra obtained for ADH at different pH values d) pH dependence of the chemical shifts for the ADH methylene protons, represented by the degree of dissociation calculated from the experimental data and fitted to the Henderson-Hasselbalch equation to obtain a  $\text{pK}_a$  of 3.1.

### S6 $^1\text{H-NMR}$ characterisation of the equilibrium mixtures for the conjugation reactions with AA

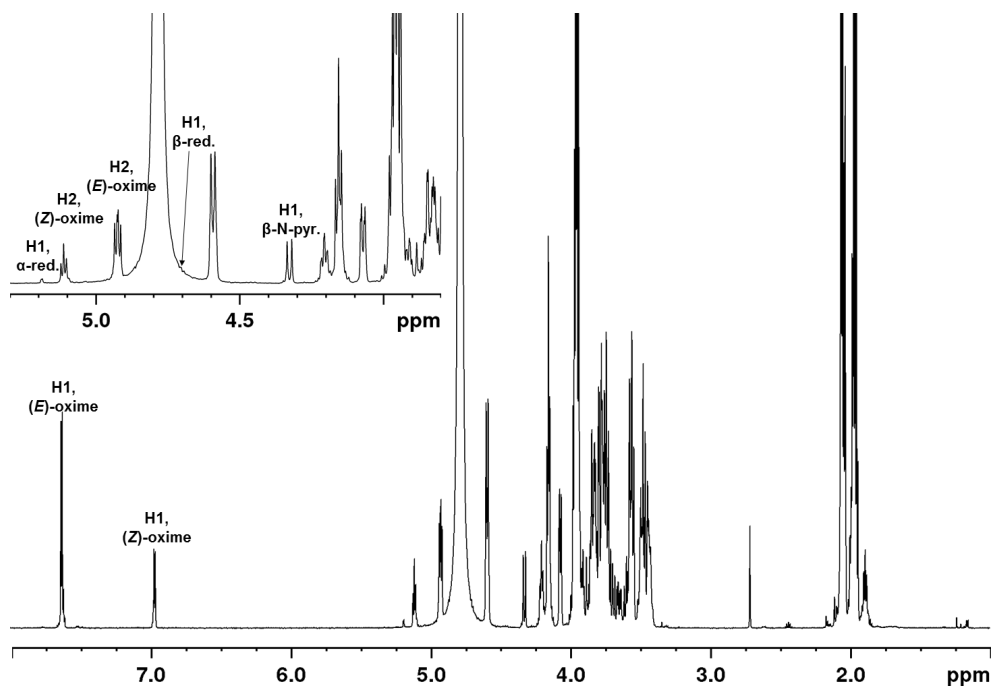
The mixture of conjugates and unreacted oligomers at equilibrium for the reactions of AA with 2 or 10 equivalents of PDHA or ADH at pH 3.0, 4.0 or 5.0 were characterized by  $^1\text{H-NMR}$ . The spectra are given in **Figure S7-S14**. Yields (%) were calculated by relating the integrals (not included) of the resonances resulting from H1 reducing end unit for the conjugates and unreacted oligomers at specific time points to the sum of these integrals (100 %, theoretical yield). The following designations are used in the  $^1\text{H-NMR}$  spectra: (*E*)- and (*Z*)-oxime ((*E*)/(*Z*)-configuration of the oxime),  $\beta$ -*N*-pyr. ( $\beta$ -configuration of the *N*-pyranoside), *N*-glycoside (unidentified *N*-glycoside conjugate) and  $\alpha$ - and  $\beta$ -red. ( $\alpha$ / $\beta$ -configuration of the anomeric proton in the reducing end A-unit).



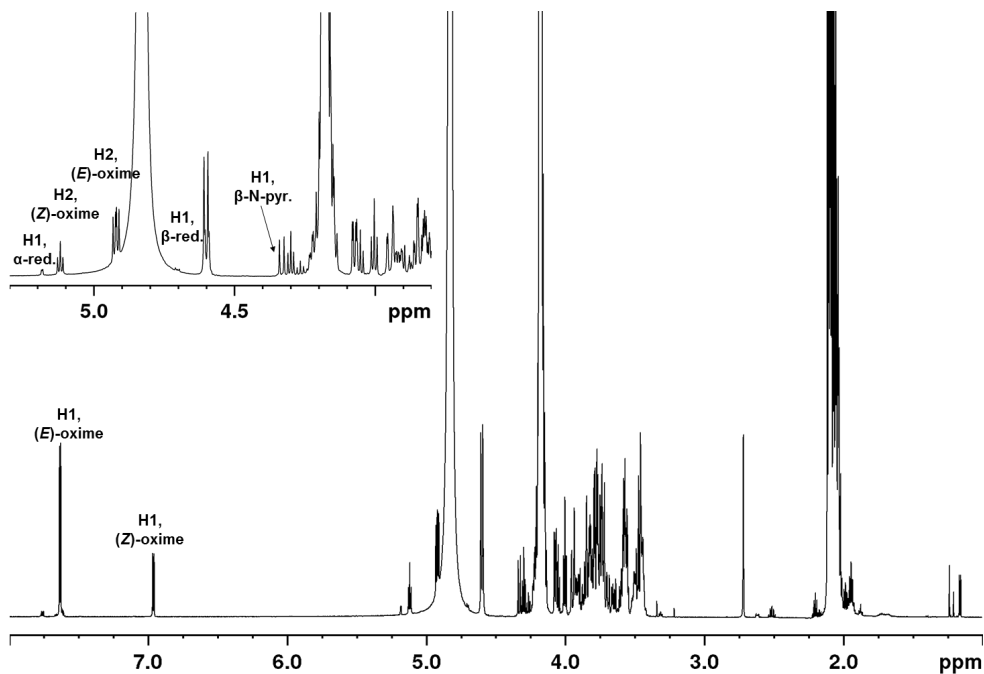
**Figure S7:**  $^1\text{H-NMR}$  characterisation of the mixture of conjugates and unreacted oligomers at equilibrium for the reaction of AA with 2 equivalents of PDHA in deuterated NaAc-buffer, pH 3.0. The yield of conjugates at equilibrium was 33 %.



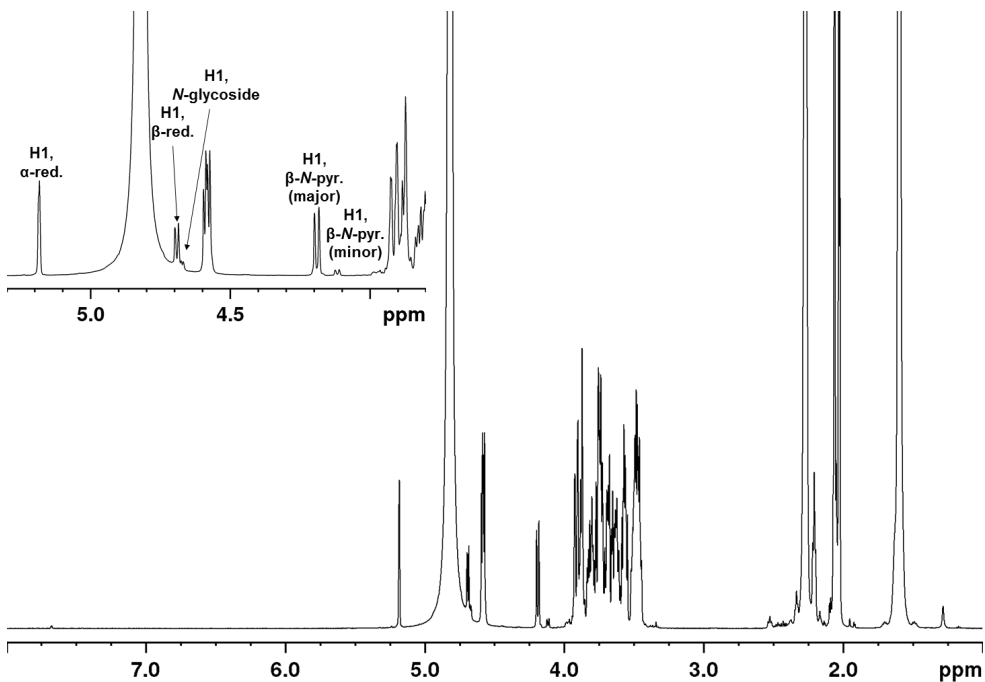
**Figure S8:**  $^1\text{H-NMR}$  characterisation of the mixture of conjugates and unreacted oligomers at equilibrium for the reaction of AA with 2 equivalents of PDHA in deuterated NaAc-buffer, pH 4.0. The yield of conjugates at equilibrium was 88 %.



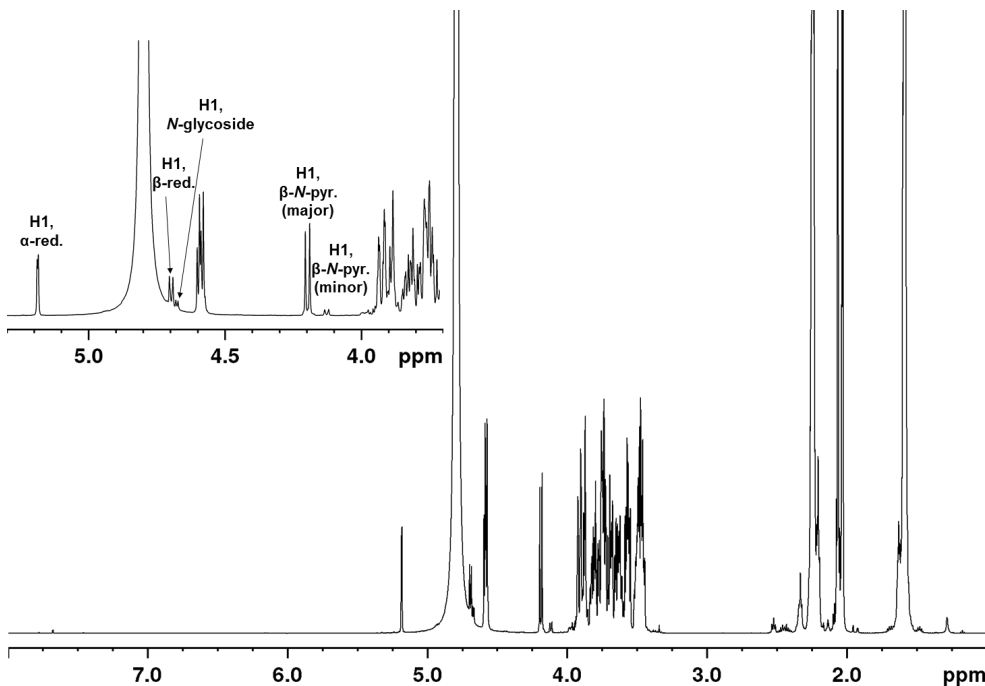
**Figure S9:**  $^1\text{H-NMR}$  characterisation of the mixture of conjugates and unreacted oligomers at equilibrium for the reaction of AA with 2 equivalents of PDHA in deuterated NaAc-buffer, pH 5.0. The yield of conjugates at equilibrium was 98 %.



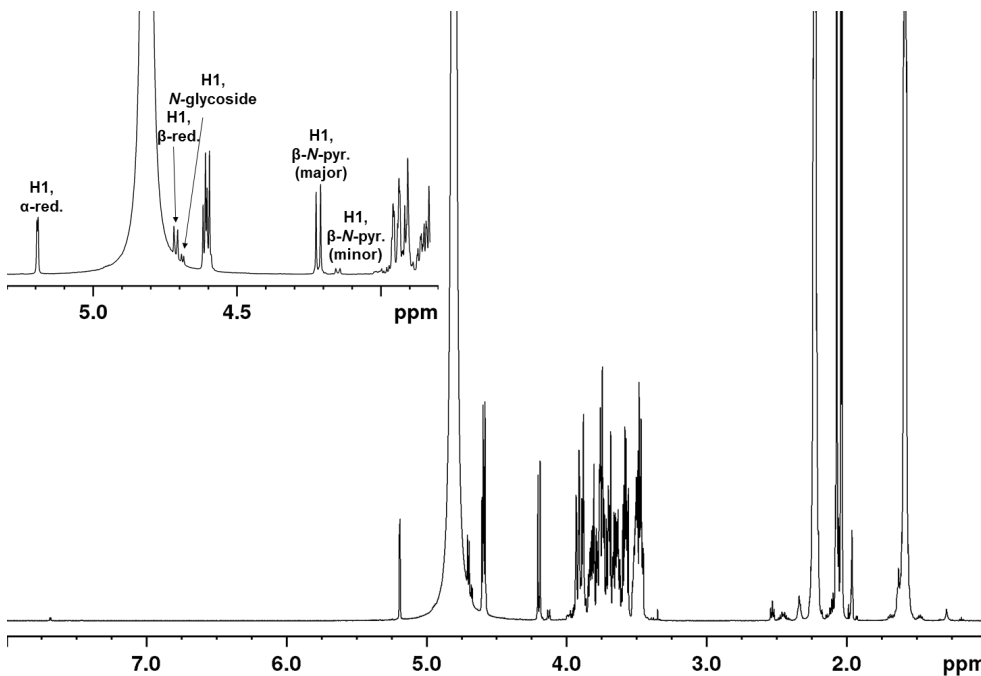
**Figure S10:**  $^1\text{H-NMR}$  characterisation of the mixture of conjugates and unreacted oligomers at equilibrium for the reaction of AA with 10 equivalents of PDHA in deuterated NaAc-buffer, pH 4.0. The yield of conjugates at equilibrium was 96 %.



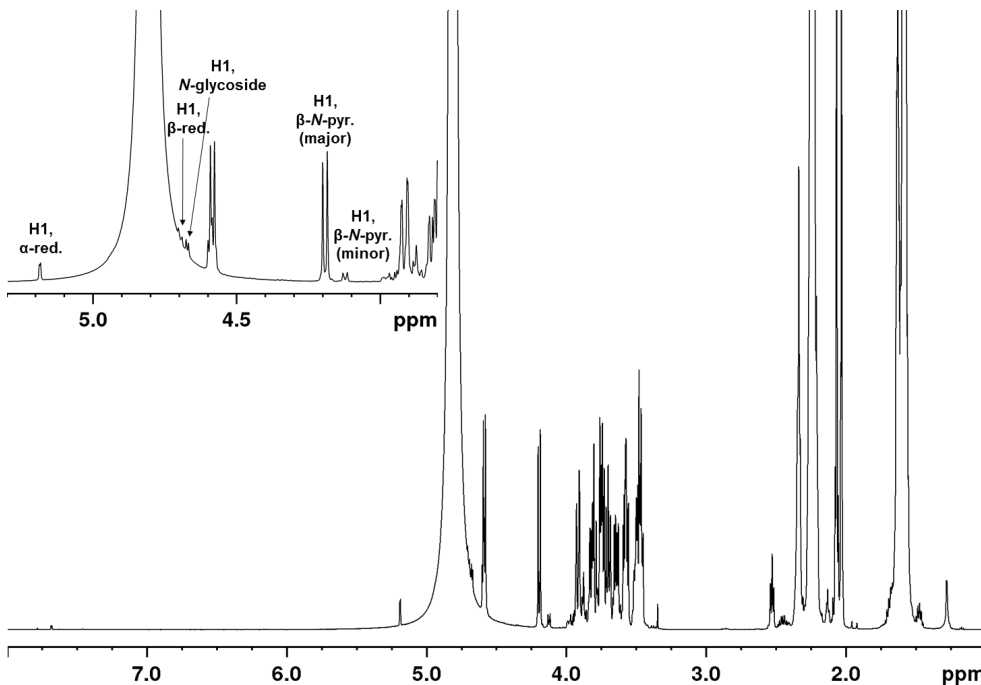
**Figure S11:**  $^1\text{H-NMR}$  characterisation of the mixture of conjugates and unreacted oligomers at equilibrium for the reaction of AA with 2 equivalents of ADH in deuterated NaAc-buffer, pH 3.0. The yield of conjugates at equilibrium was 46 %.



**Figure S12:**  $^1\text{H-NMR}$  characterisation of the mixture of conjugates and unreacted oligomers at equilibrium for the reaction of AA with 2 equivalents of ADH in deuterated NaAc-buffer, pH 4.0. The yield of conjugates at equilibrium was 53 %.



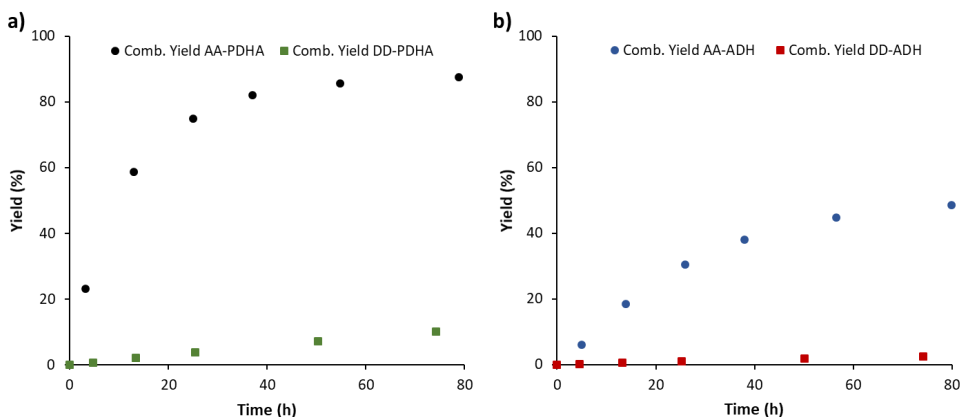
**Figure S13:** <sup>1</sup>H-NMR characterisation of the mixture of conjugates and unreacted oligomers at equilibrium for the reaction of AA with 2 equivalents of ADH in deuterated NaAc-buffer, pH 5.0. The yield of conjugates at equilibrium was 57 %.



**Figure S14:** <sup>1</sup>H-NMR characterisation of the mixture of conjugates and unreacted oligomers at equilibrium for the reaction of AA with 10 equivalents of ADH in deuterated NaAc-buffer, pH 4.0. The yield of conjugates at equilibrium was 89 %.

## S7 Comparison to D at the reducing end

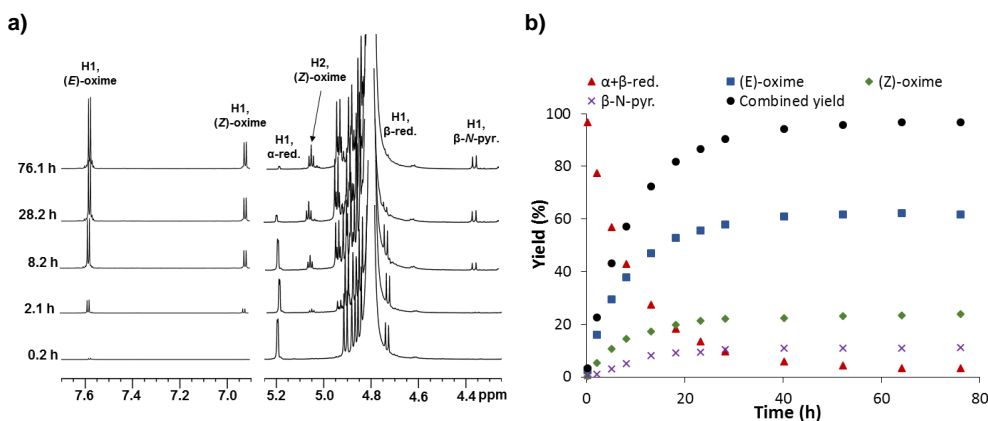
The conjugation of PDHA and ADH (2 equivalents) to DD (chitobiose) was studied by time course NMR and compared to the conjugation to AA under the same conditions (pH 4.0, RT). The course of the reactions, presented by the combined yield of conjugates (%) at defined time points, are given in **Figure S15**.



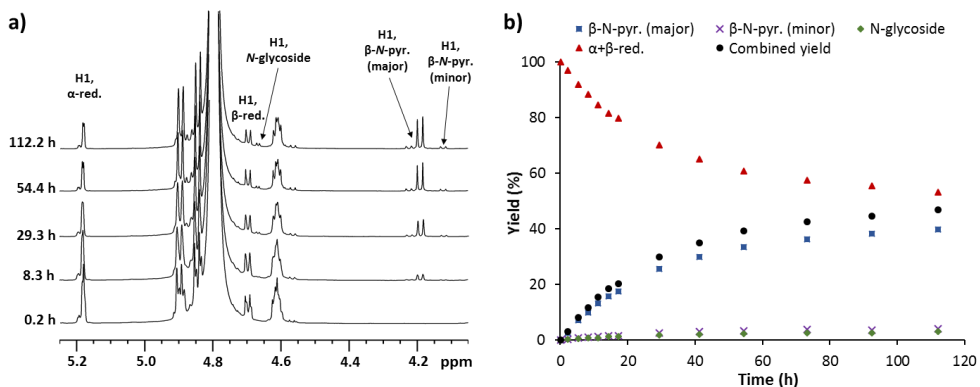
**Figure S15:** **a)** Course of the reaction for the conjugation of PDHA (2 equivalents) to AA and DD at pH 4.0, RT **b)** course of the reaction for the conjugation of ADH (2 equivalents) to AA and DD at pH 4.0, RT.

## S8 Conjugation of PDHA and ADH to D<sub>2</sub>XA studied by time course NMR

Conjugation of PDHA and ADH to D<sub>2</sub>XA (X = either A or D) was studied by time course NMR. <sup>1</sup>H-NMR spectra and the course of the reaction using 2 equivalents of PDHA and ADH, are given in **Figure S16** and **S17**, respectively. Key resonances established for AA were detected in the spectra. The D<sub>2</sub>AA oligomers contained small amounts (<15%) of D<sub>2</sub>DA (and opposite for the D<sub>2</sub>DA oligomers), appearing in the <sup>1</sup>H-NMR spectra by side peaks for the reducing end resonances (e.g. H1, α-red. and H1, β-red). Yields (%) were calculated by relating the integrals (not included) of the resonance resulting from the H1 reducing end unit for the conjugates and unreacted oligomers at specific time points to the sum of these integrals (100 %, theoretical yield). Yields, distribution of products and kinetics were in good agreement with the results obtained for the conjugation of PDHA and ADH to AA.



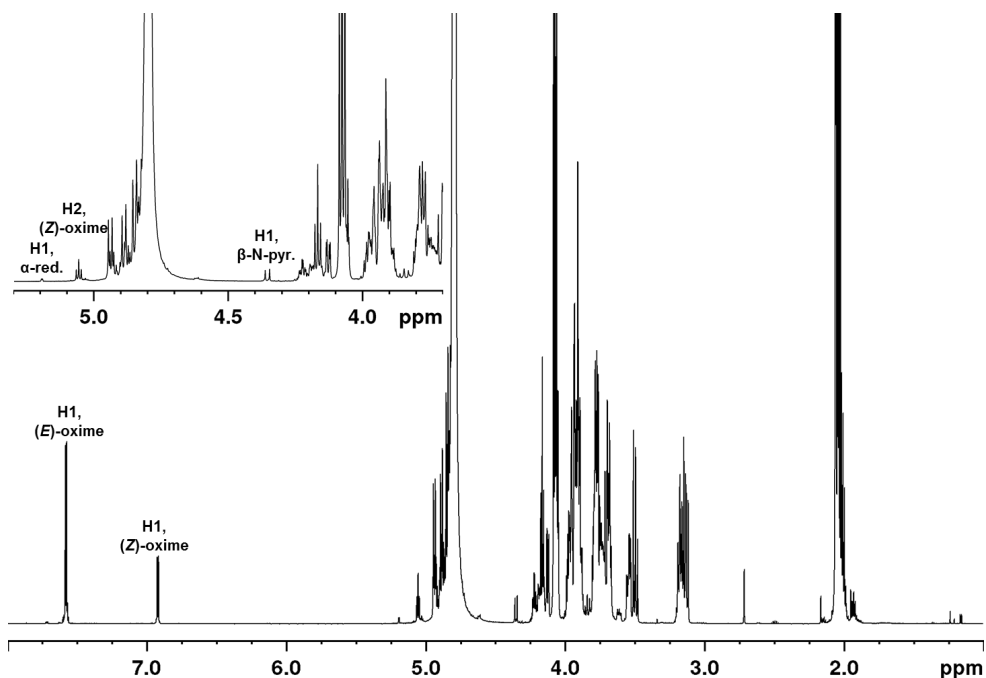
**Figure S16:** **a)** <sup>1</sup>H-NMR spectra at defined time points for the conjugation of PDHA (2 equivalents) to D<sub>2</sub>DA, pH 4.0 **b)** course of the reaction obtained from the integration of the spectra shown in a).



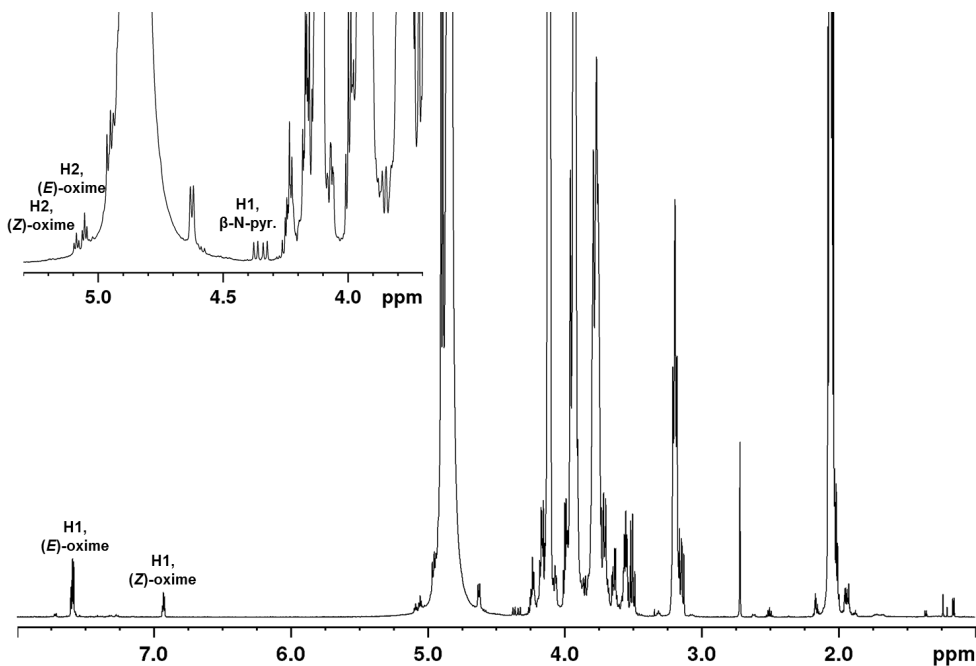
**Figure S17: a)** <sup>1</sup>H-NMR spectra at defined time points for the reaction of D<sub>2</sub>AA with 2 equivalents of ADH, at pH 4.0 **b)** Course of the reaction obtained from the integration of the spectra shown in a).

### S9 <sup>1</sup>H-NMR characterisation of the equilibrium mixtures for the conjugation reactions with D<sub>n</sub>XA oligomers

The mixture of conjugates and unreacted oligomers at equilibrium for the reactions of D<sub>n</sub>XA with 2 or 10 equivalents of PDHA or ADH at pH 4.0 were characterized by <sup>1</sup>H-NMR. The spectra are given in **Figure S18-S21**. Yields (%) were calculated by relating the integrals (not included) of the resonances resulting from H1 reducing end unit of the conjugates and unreacted oligomers at specific time points to the sum of these integrals (100 %, theoretical yield). The following designations are used in the <sup>1</sup>H-NMR spectra: (*E*)- and (*Z*)-oxime ((*E*)/(*Z*)-configuration of the oxime), β-*N*-pyr. (β-configuration of the *N*-pyranoside), *N*-glycoside (unidentified *N*-glycoside conjugate) and α- and β- red. (α-/β-configuration of the anomeric proton in the reducing end A-unit). The double peaks observed for the H1 reducing end resonances (oligomers and conjugates) result from the different chemistries of oligomers having one or two A-units at the reducing end (D<sub>n</sub>DA and D<sub>n</sub>AA, respectively).

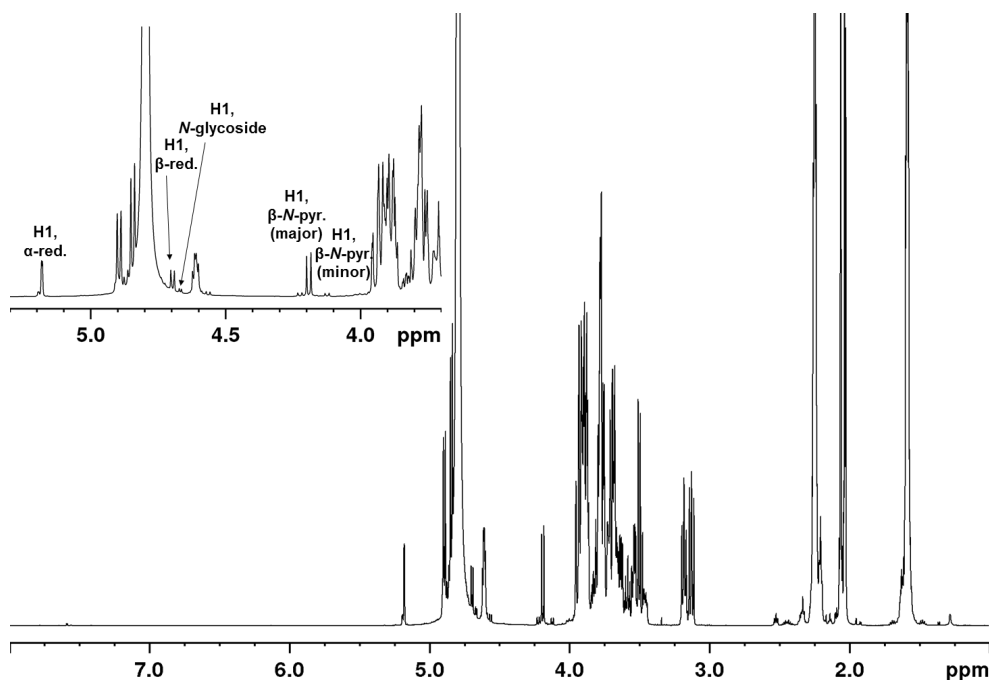


**Figure S18:**  $^1\text{H-NMR}$  characterisation of the mixture of conjugates and unreacted oligomers at equilibrium for the reaction of  $\text{D}_2\text{DA}$  with 2 equivalents of PDHA in deuterated NaAc-buffer, pH 4.0. The yield of conjugates at equilibrium was 98 %.

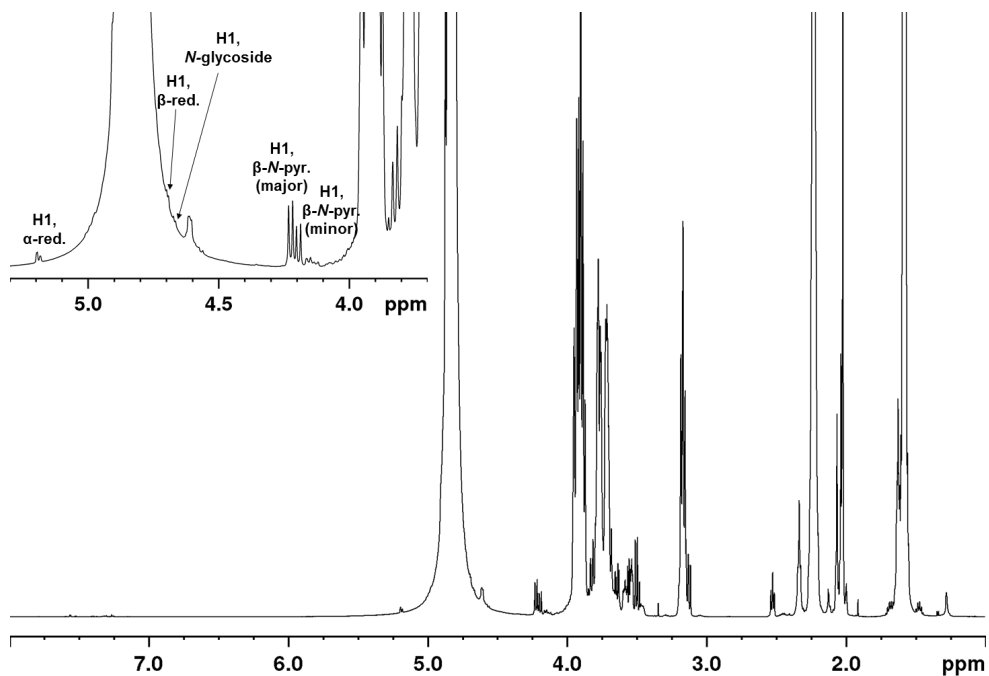


**Figure S19:**  $^1\text{H-NMR}$  characterisation of the mixture of conjugates and unreacted oligomers at equilibrium for the reaction of  $\text{D}_8\text{XA}$  with 10 equivalents of PDHA in deuterated NaAc-buffer, pH 4.0. The yield of conjugates at equilibrium was 98 %.





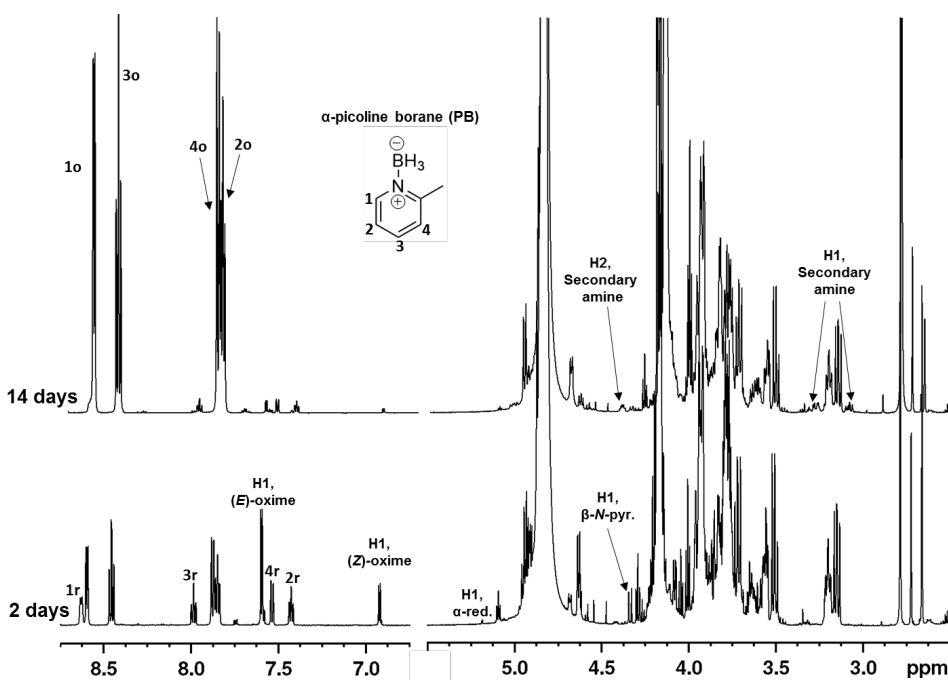
**Figure S20:**  $^1\text{H-NMR}$  characterisation of the mixture of conjugates and unreacted oligomers at equilibrium for the reaction of  $\text{D}_2\text{AA}$  with 2 equivalents of ADH in deuterated NaAc-buffer, pH 4.0. The yield of conjugates at equilibrium was 47 %.



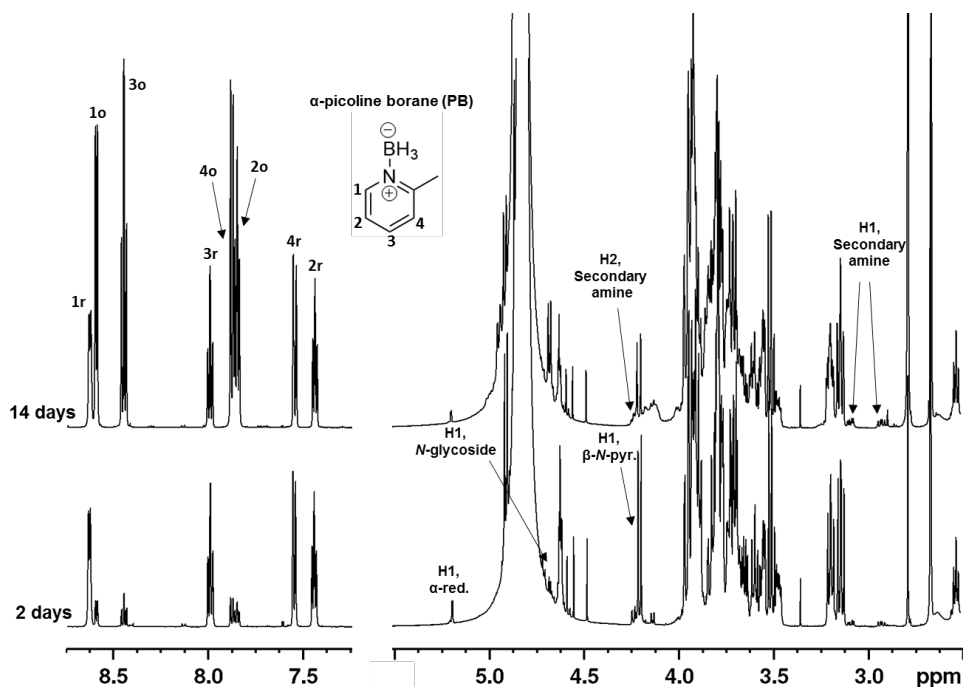
**Figure S21:**  $^1\text{H-NMR}$  characterisation of the mixture of conjugates and unreacted oligomers at equilibrium for the reaction of  $\text{D}_8\text{XA}$  with 10 equivalents of ADH in deuterated NaAc-buffer, pH 4.0. The yield of conjugates at equilibrium was 86 %.

### S10 <sup>1</sup>H-NMR characterisation of the reaction mixtures for the D<sub>n</sub>XA-PDHA/ADH conjugates after 2 and 14 days of reduction

Conjugates prepared with D<sub>2</sub>AA and 10 equivalents of PDHA or ADH at pH 4.0 were subjected to reduction using 3 equivalents of PB. The mixture of reduced secondary amine conjugates, non-reduced conjugates (oximes/hydrazones and *N*-glycosides) and unreacted oligomers after 2 and 14 days of reduction were characterized by <sup>1</sup>H-NMR. The spectra are given in **Figure S22 and S23**. The following designations are used for the assignment in the obtained <sup>1</sup>H-NMR spectra: (*E*)- and (*Z*)-oxime ((*E*)/(*Z*)-configurations of the oxime), β-*N*-pyr. (β-configuration of the *N*-pyranoside), *N*-glycoside (unidentified *N*-glycoside conjugate), α- and β- red. (α/β-configuration of the anomeric proton in the reducing end A-unit of the unreacted oligomer) and secondary amine (reduced secondary amine conjugates). Yields (%) were calculated by relating the integrals (not included) of the resonances resulting from the H1 reducing end unit of the secondary amines, conjugates and unreacted oligomers at specific time points to the sum of these integrals at the start of the reduction (100 %, theoretical yield). The yield of unidentified products was calculated as the difference between the obtained and theoretical yield. In addition, resonances resulting from PB both in its reduced (r) and oxidized form (in the area 7.3 to 8.7 ppm) are assigned in the spectra.



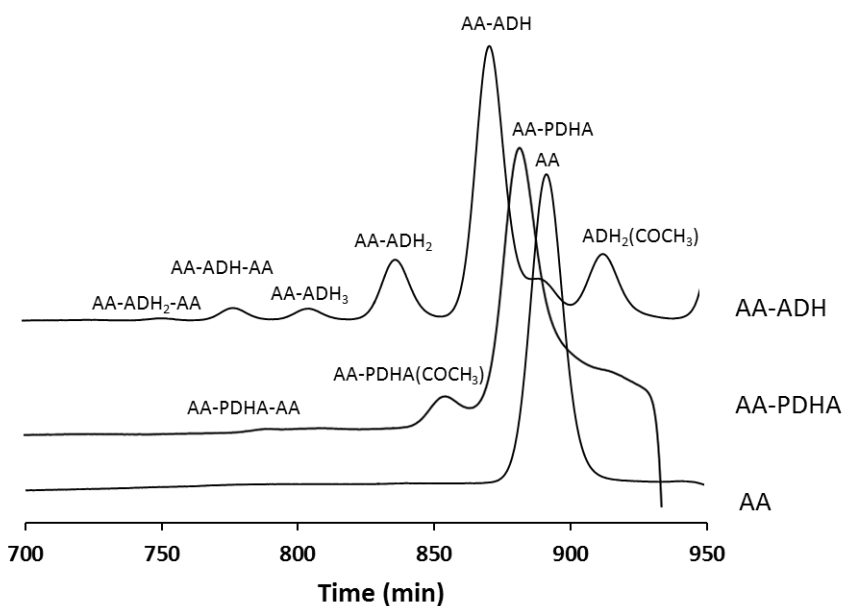
**Figure S22:** <sup>1</sup>H-NMR characterisation of the mixture of secondary amines, conjugates and unreacted oligomers obtained after 2 and 14 days for the reduction of DDAA-PDHA conjugates (prepared using 2 equivalents PDHA) at pH 4.0 using 3 equivalents PB.



**Figure S23:**  $^1\text{H-NMR}$  characterisation of the mixture of secondary amines, conjugates and unreacted oligomers obtained after 2 and 14 days for the reduction of DDAA-ADH conjugates (prepared using 2 equivalents ADH) at pH 4.0 using 3 equivalents PB.

### S11 $^1\text{H-NMR}$ and MS characterisation of products formed in the reduction of AA-PDHA and AA-ADH conjugates using PB

The products formed in the reduction of AA-PDHA and AA-ADH conjugates using PB (semi-preparative scale) were fractionated by gel filtration chromatography (**Figure S24**). All fractions (products) were characterized by MS (**Table S2**) and the main products were characterized by  $^1\text{H-NMR}$  (**Figure S25-S28**).



**Figure S24:** Fractionation of the mixture of products formed following conjugation and reduction of AA-PDHA and AA-ADH by gel filtration at pH 6.9. Fractionation of AA is included as a reference.

**Table S2:** Characterisation of the fractions from **Figure S24** by MS.

Reaction	Fraction	Ions ( $m/z$ )					
		$[M]^+$	$[M]H^-$	$[M]H^+$	$[M]Na^+$	$[M]Cl^-$	$[M]K^+$
AA-PDHA	AA-PDHA	514.25	513.24	515.26	537.24	549.22	553.21
	AA-PDHA(COCH <sub>3</sub> )	556.26	555.25	557.27	579.25	591.23	595.22
	AA-PDHA-AA	922.42	921.41	923.43	945.41	957.39	961.38
AA-ADH	ADH <sub>2</sub> (COCH <sub>3</sub> )	358.20	357.19	359.20	381.19	-	397.16
	AA	426.18	425.18	427.19	449.17	461.15	465.14
	AA-ADH	582.28	581.28	583.29	605.27	-	621.24
	AA-ADH <sub>2</sub>	724.36	723.35	725.37	747.35	759.33	763.32
	AA-ADH <sub>3</sub>	866.43	865.43	867.44	889.42	-	905.39
	AA-ADH-AA	988.44	987.43	989.45	1011.44	1023.41	-
	AA-ADH <sub>2</sub> -AA	1130.52	1129.51	1131.53	1153.51	1165.49	1169.48

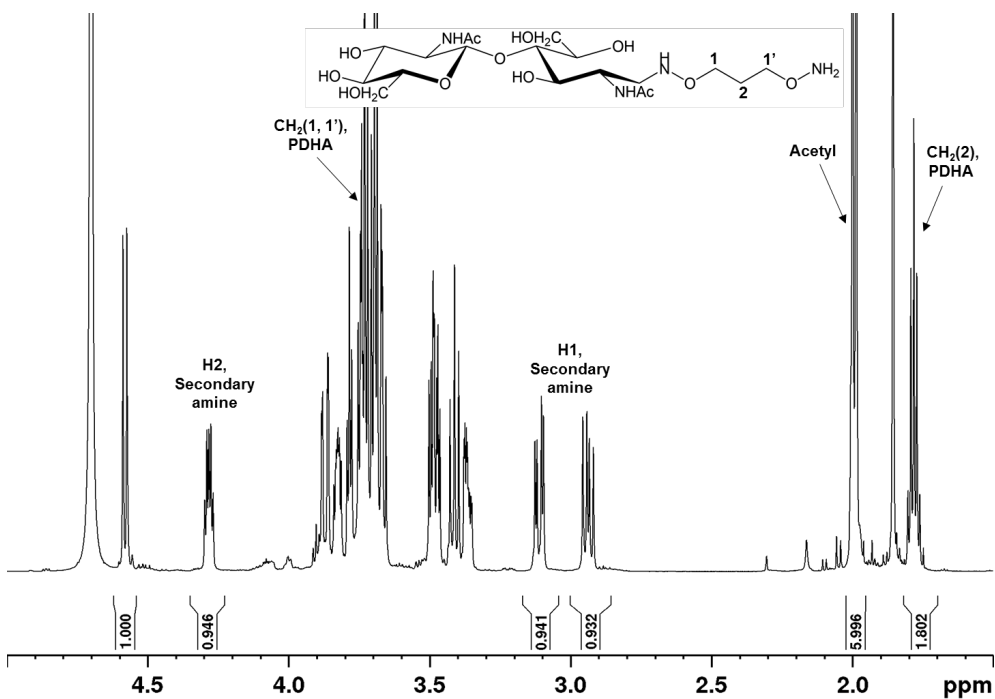


Figure S25:  $^1\text{H-NMR}$  characterisation of the AA-PDHA fraction from figure S23.

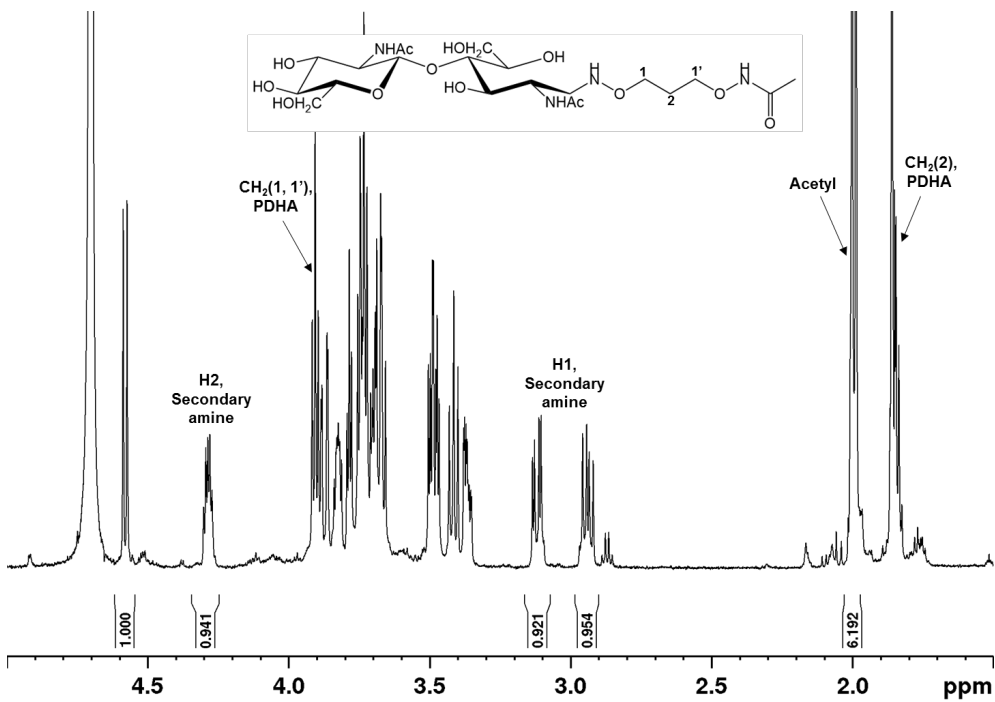


Figure S26:  $^1\text{H-NMR}$  characterisation of the AA-PDHA(COCH<sub>3</sub>) fraction from figure S23.

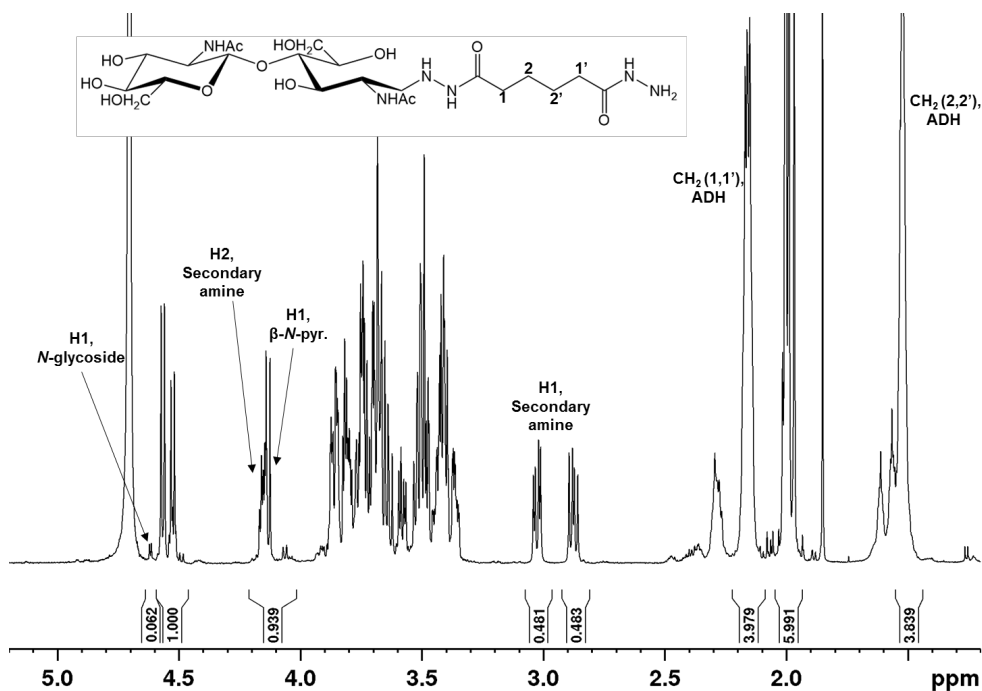


Figure S27: <sup>1</sup>H-NMR characterisation of the AA-ADH fraction from figure S23.

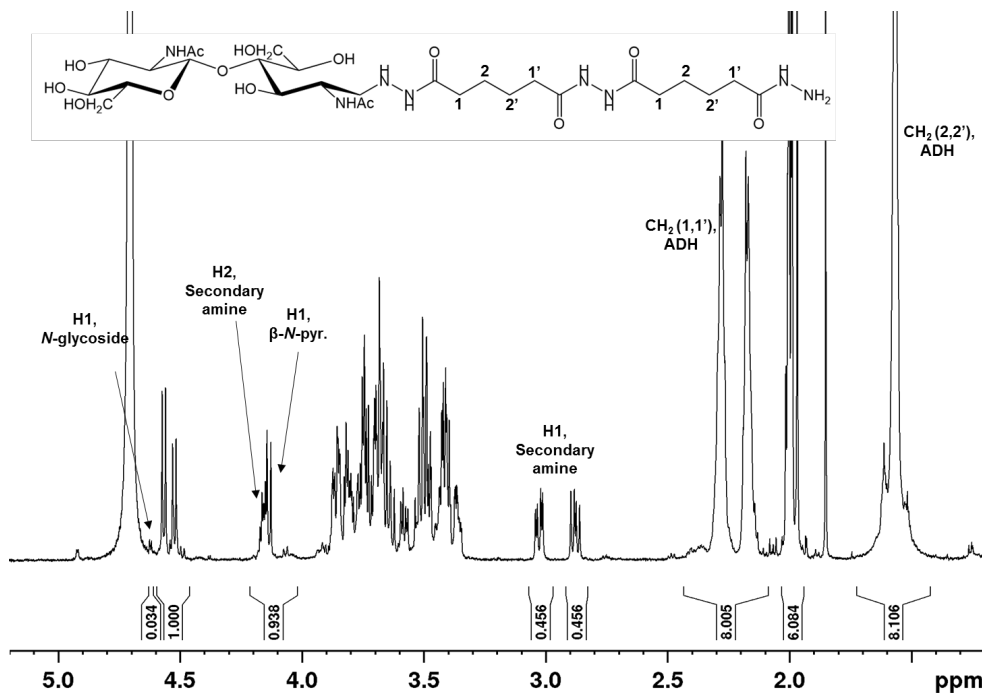
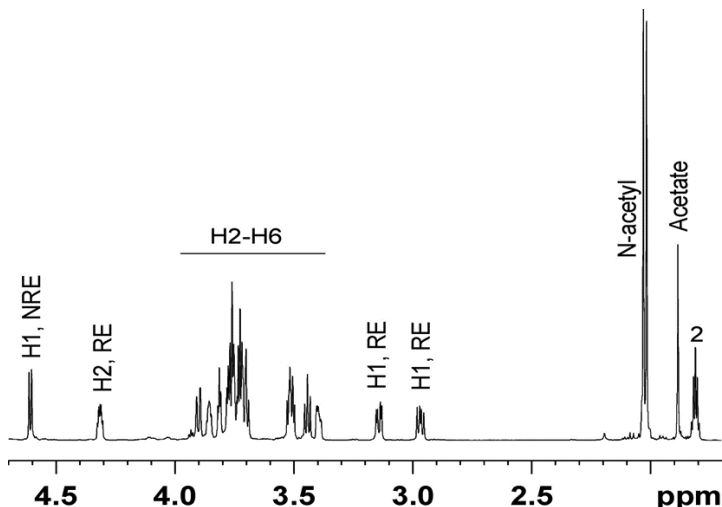


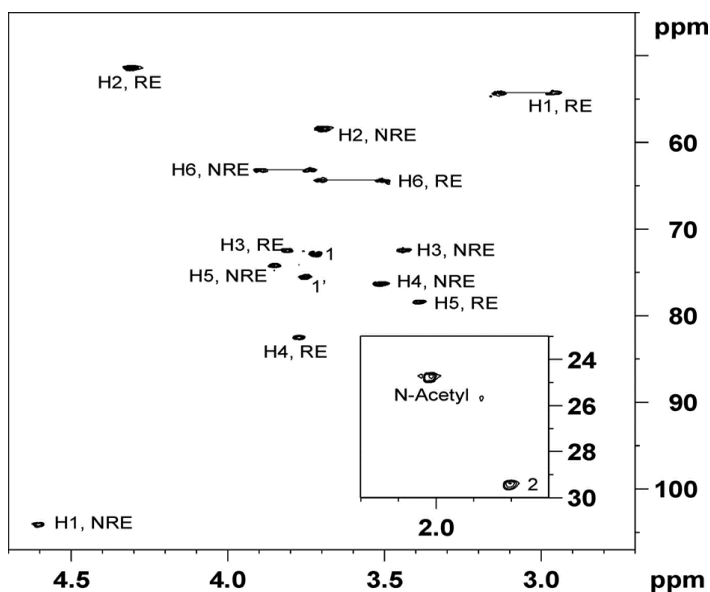
Figure S28: <sup>1</sup>H-NMR characterisation of the AA-ADH<sub>2</sub> fraction from figure S23. The 'polymerization' of ADH is observed by the splitting of the left methylene resonance resulting from the dihydrazide. The right methylene resonance is slightly shifted downfield compared to the AA-ADH conjugate.

### S12 2D NMR characterisation of the reduced AA-PDHA conjugate

The main fraction from the reduction of AA-PDHA conjugates (AA-PDHA, **Figure S24**) was studied in detail by homo- and heteronuclear NMR correlation experiments. The NMR analysis was carried out at the 800 MHz spectrometer in a 3 mm NMR tube. Resonances were assigned by starting at the anomeric proton resonance and then following the proton-proton connectivity using DQF-COSY in combination with  $^{13}\text{C}$  HSQC and  $^{13}\text{C}$  H2BC spectra. The following designations are used in the spectra displayed in **Figure S29** and **S30**: NRE (the non-reducing end A-unit in the conjugate), RE (the reducing end A-unit in the conjugate), # (unique identified methylene protons from the dioxyamine (PDHA) in the conjugate), *N*-acetyl (*N*-acetyl groups of the A-units in the conjugate). H# refers to the proton attached to the ring carbon number (C#) for the sugar units. The water resonance (4.75 ppm) was used as chemical shift reference for protons.



**Figure S29:** 1D proton spectrum for the reduced form of the AA-PDHA conjugate.



**Figure S30:**  $^{13}\text{C}$  HSQC spectrum for the reduced form of the AA-PDHA conjugate.

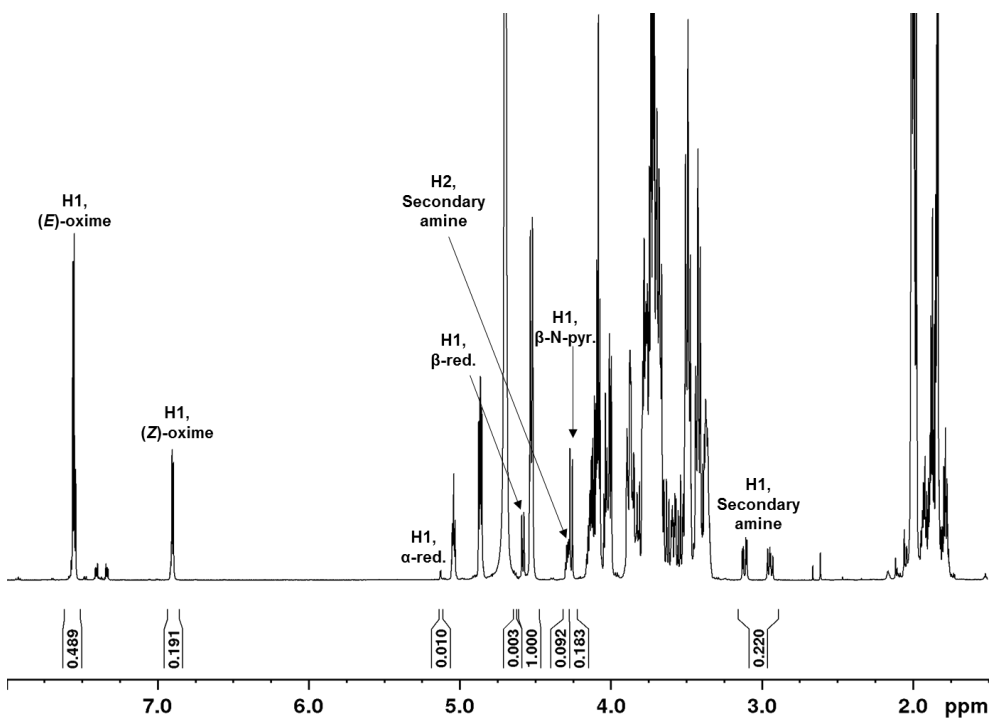
**Table S3:** Assignment of the chemical shifts for the reduced form of the AA-PDHA conjugate.

Structural unit	Assignment						
	H-1; C-1	H-2; C-2	H-3; C-3	H-4; C-4	H-5; C-5	H-6; C-6	Ac-H; C
NRE	4.61; 104.0	3.71; 58.5	3.44; 72.0	3.51; 76.3	3.85; 74.1	3.75,3.90; 63.2	2.01; 24.6
RE	2.97;3.14; 54.2	4.31; 51.4	3.81; 72.6	3.76; 82.2	3.39; 78.2	3.50, 3.72; 64.3	2.01; 24.6
	<b>Methylene in PDHA closest to conjugation</b>		<b>Middle methylene in PDHA</b>		<b>Methylene in PDHA closest to free oxyamine end</b>		
PDHA	4.22; 73.1		2.04; 29.9		4.14; 75.1		

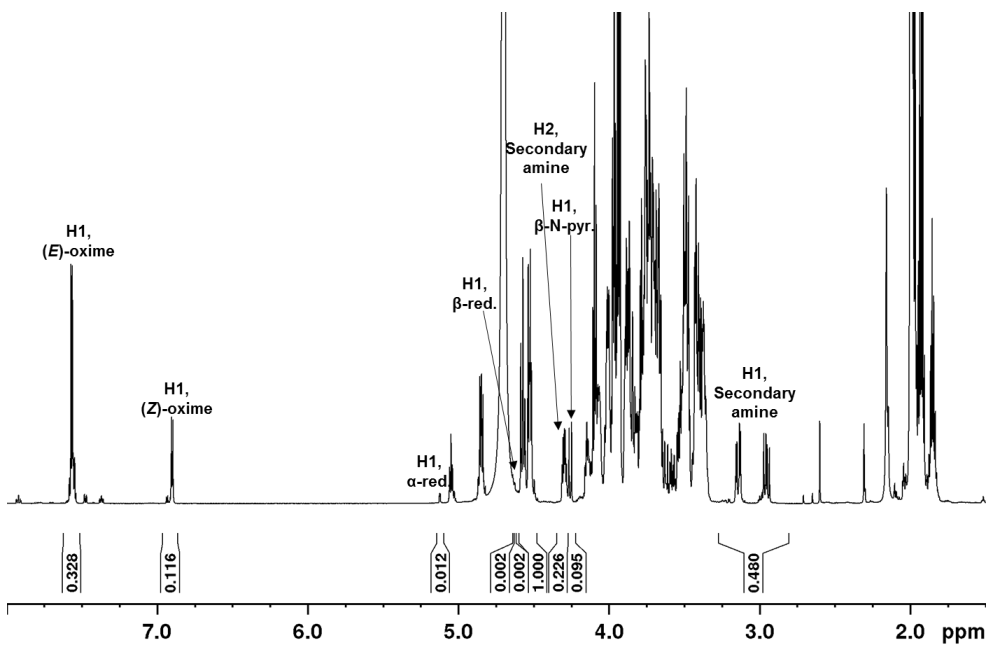
### S13 <sup>1</sup>H-NMR characterisation of the reaction mixtures for the reduction of conjugates at higher temperatures

The mixture of reduced secondary amine conjugates, non-reduced conjugates and unreacted oligomers obtained by one pot reductive amination at higher temperatures was characterised by <sup>1</sup>H-NMR. The spectra are given in **Figure S31-S40**. The dimer, AA, was used for the reduction experiments and the yields (%) were calculated by relating the integrals of the resonances from the various products to the integral of the resonance resulting from the H1 of the non-reducing A-unit set to 1 (100 %) in all spectra. The yield of unidentified products was calculated as the difference between the sum of reduced conjugates, non-reduced conjugates and unreacted oligomers and the theoretical yield (100 %). As the resonance from H2 secondary amine completely overlapped the resonance resulting from the β-*N*-pyranoside for the AA-ADH conjugates, the remaining non-reduced conjugates was calculated by subtracting the integral resulting from one of the secondary amine protons from the total integral for the overlapping resonances. The following designations are used in the <sup>1</sup>H-NMR spectra: (*E*)- and (*Z*)-oxime ((*E*)/(*Z*)-configuration of the oxime), β-*N*-pyr. (β-configuration of the *N*-pyranoside), *N*-glycoside (unidentified *N*-glycoside conjugate), α- and β- red. (α-/β-configuration of the anomeric proton in the reducing end A-unit) and secondary amine (reduced secondary amine conjugates).

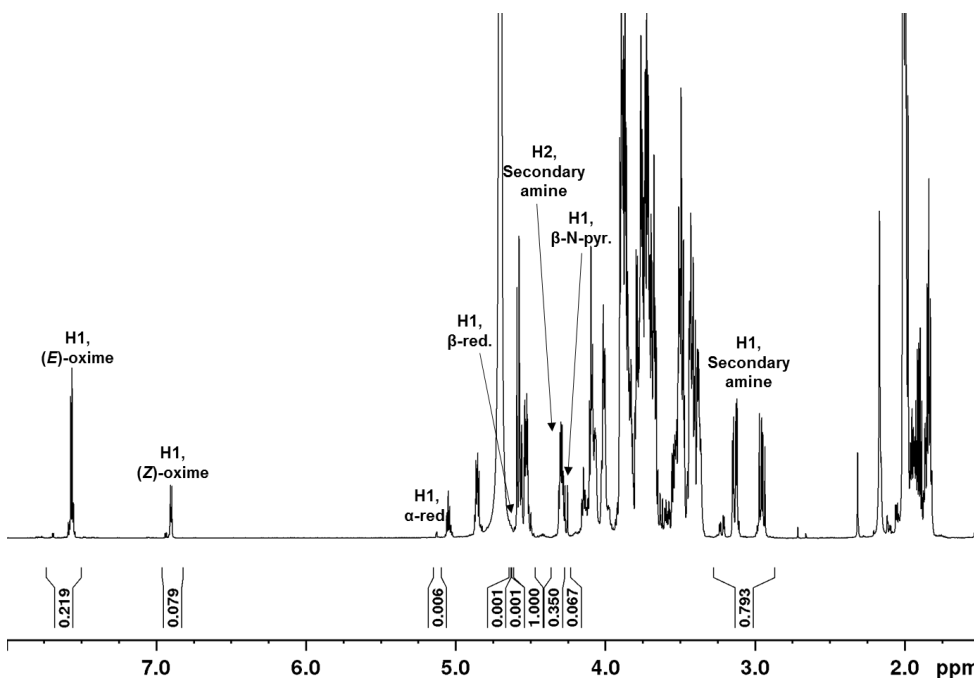




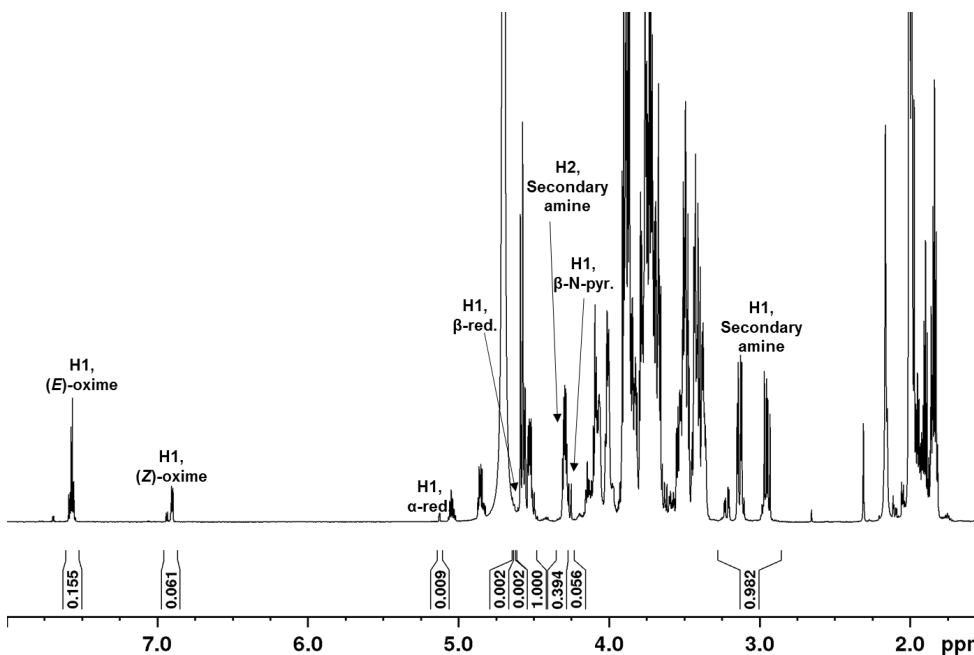
**Figure S31:**  $^1\text{H-NMR}$  characterisation of the mixture of secondary amines, conjugates and unreacted oligomers obtained for the one pot reductive amination with AA, 10 equivalents of PDHA and 20 equivalents of PB at RT for 8 hours.



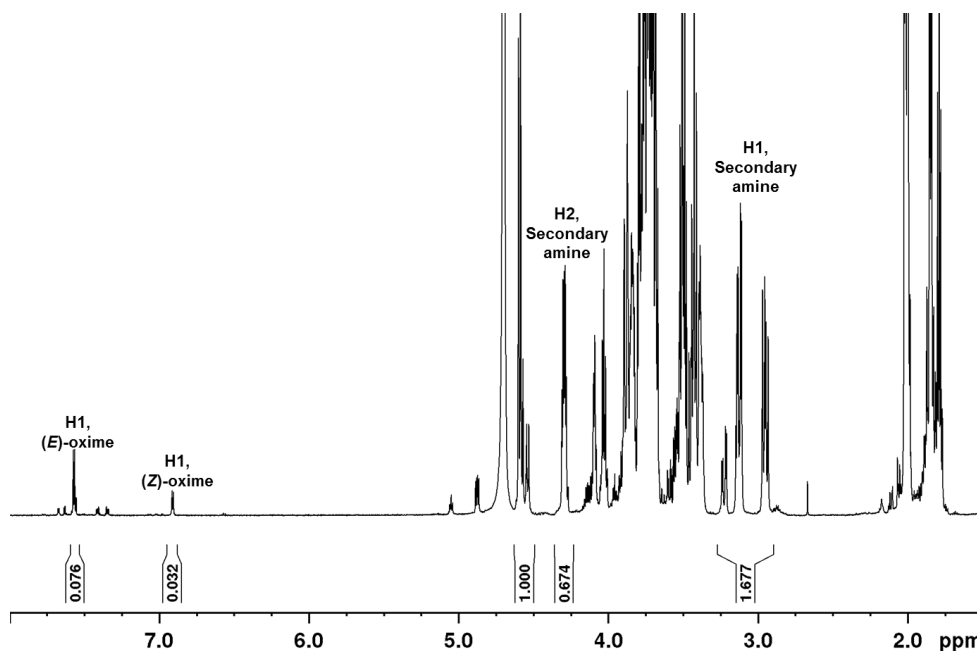
**Figure S32:**  $^1\text{H-NMR}$  characterisation of the mixture of secondary amines, conjugates and unreacted oligomers obtained for the one pot reductive amination with AA, 10 equivalents of PDHA and 20 equivalents of PB at 40 °C for 8 hours.



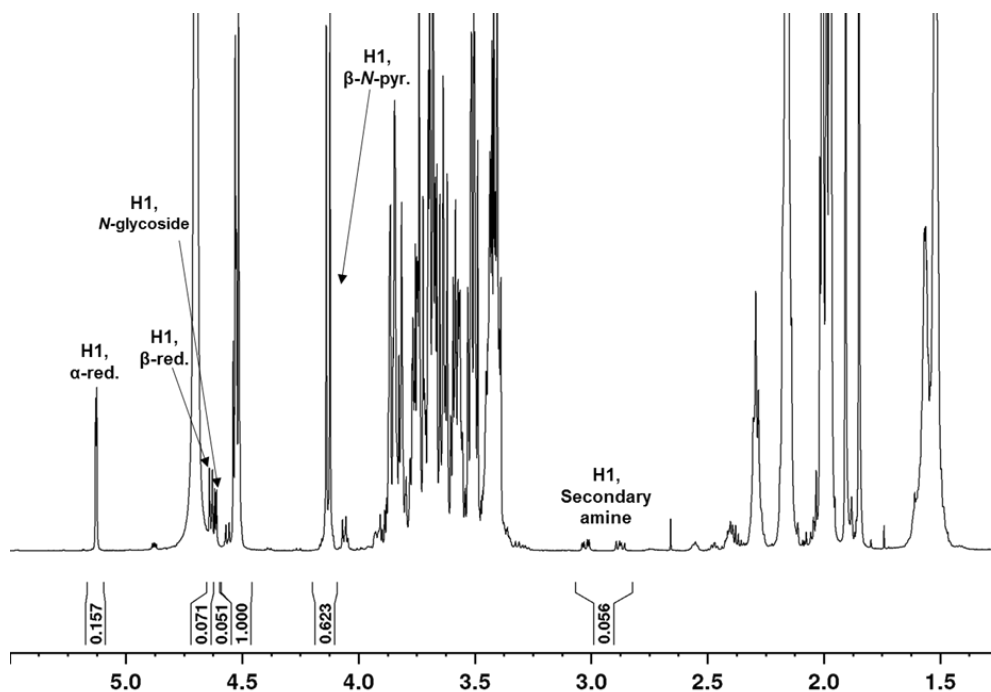
**Figure S33:**  $^1\text{H-NMR}$  characterisation of the mixture of secondary amines, conjugates and unreacted oligomers obtained for the one pot reductive amination with AA, 10 equivalents of PDHA and 20 equivalents of PB at 60 °C for 8 hours.



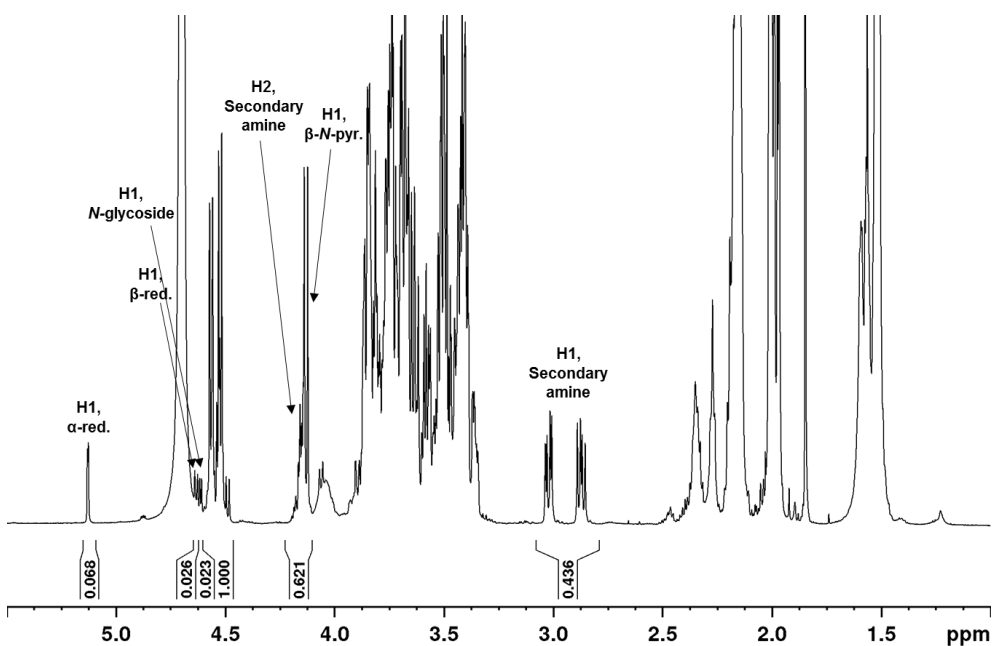
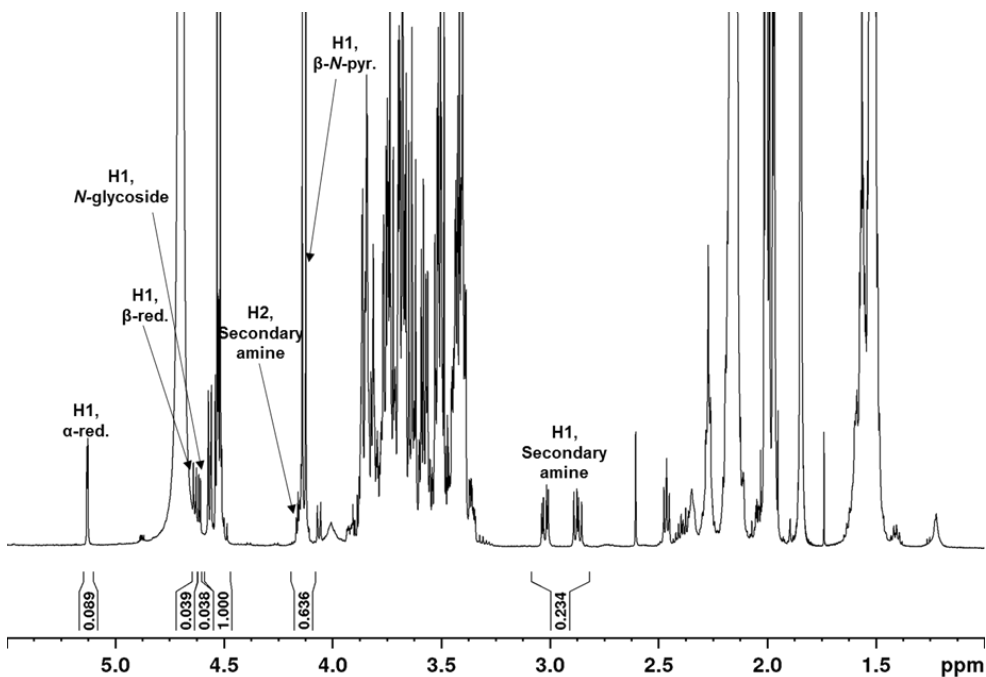
**Figure S34:**  $^1\text{H-NMR}$  characterisation of the mixture of secondary amines, conjugates and unreacted oligomers obtained for the one pot reductive amination with AA, 10 equivalents of PDHA and 20 equivalents of PB added in four portions (5 equivalents added at 0, 2, 4 and 6 hours) at 60 °C for 8 hours.

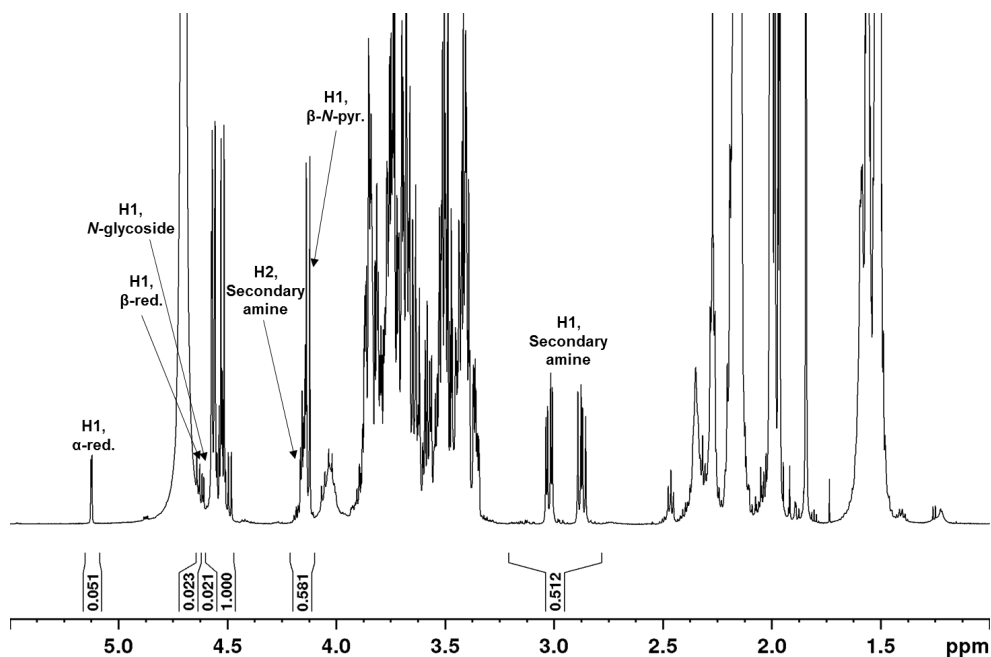


**Figure S35:** <sup>1</sup>H-NMR characterisation of the mixture of secondary amines, conjugates and unreacted oligomers obtained for the one pot reductive amination with AA, 10 equivalents of PDHA and 40 equivalents of PB added in five portions (5 equivalents added at 0, 2, 4 and 6 hours and 20 equivalents added after 8 hours) at 60 °C for 24 hours.

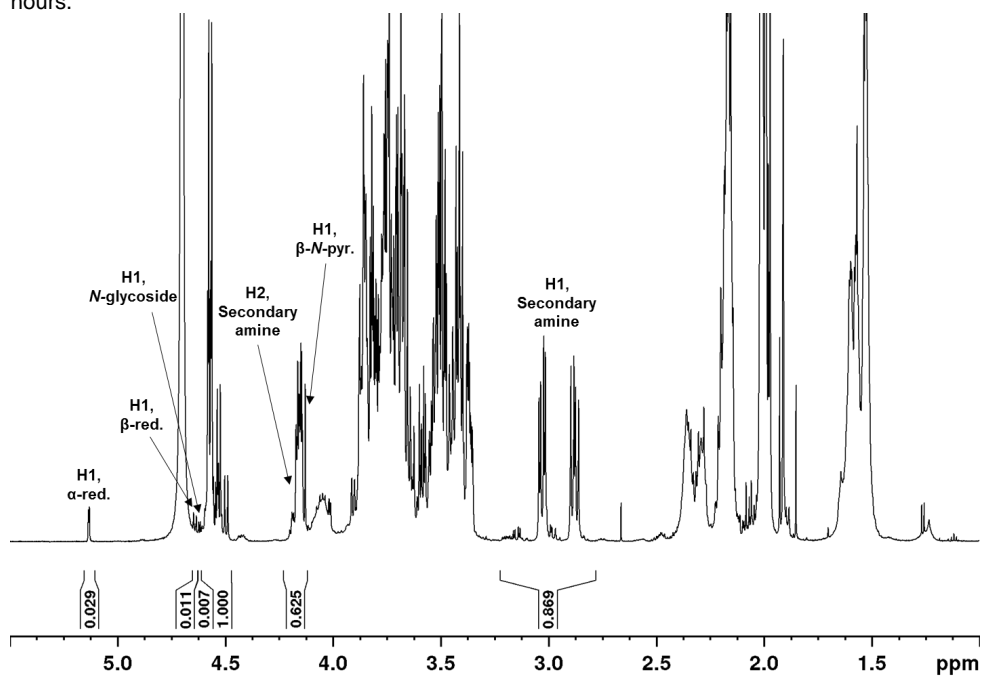


**Figure S36:** <sup>1</sup>H-NMR characterisation of the mixture of secondary amines, conjugates and unreacted oligomers obtained for the one pot reductive amination with AA, 10 equivalents of ADH and 20 equivalents of PB at RT for 8 hours.





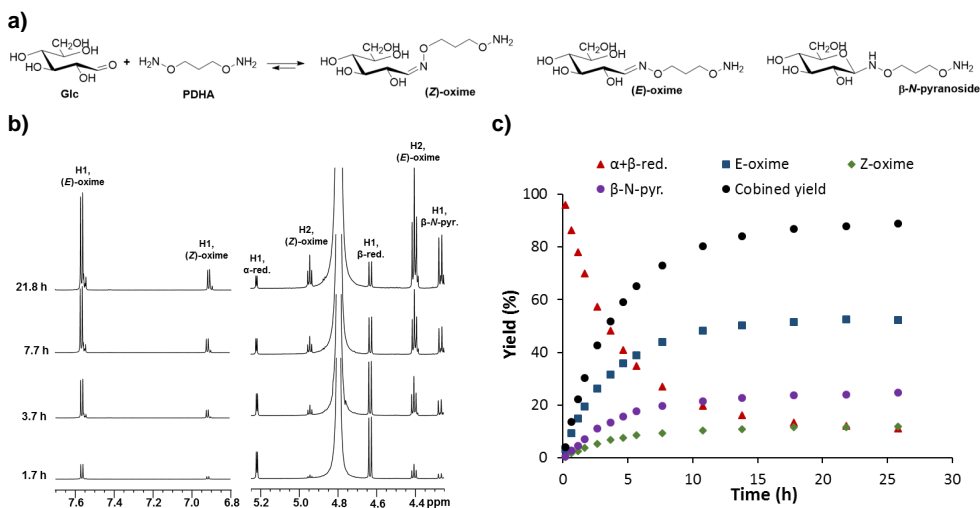
**Figure S39:**  $^1\text{H-NMR}$  characterisation of the mixture of secondary amines, conjugates and unreacted oligomers obtained for the one pot reductive amination with AA, 10 equivalents of ADH and 20 equivalents of PB added in four portions (5 equivalents added at 0, 2, 4 and 6 hours) at 60 °C for 8 hours.



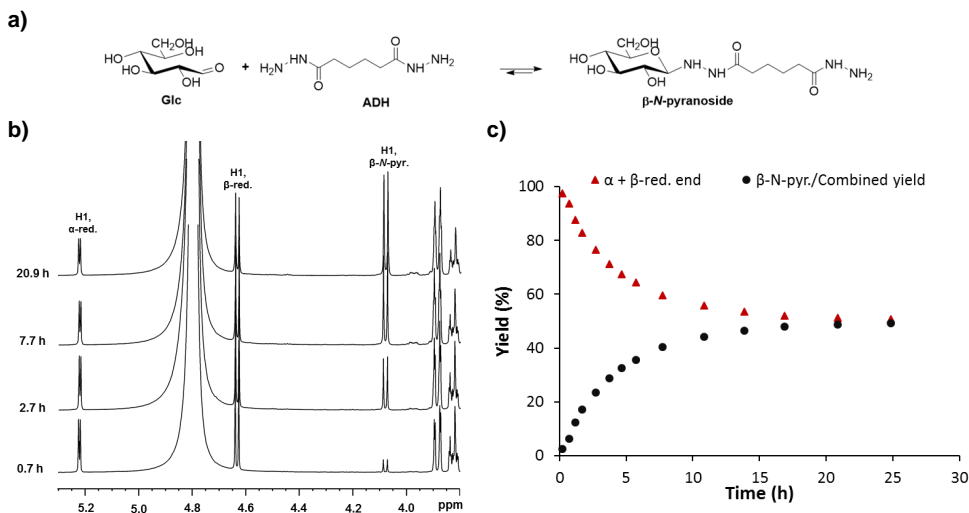
**Figure S40:**  $^1\text{H-NMR}$  characterisation of the mixture of secondary amines, conjugates and unreacted oligomers obtained for the one pot reductive amination with AA, 10 equivalents of ADH and 40 equivalents of PB added in five portions (5 equivalents added at 0, 2, 4 and 6 hours and 20 equivalents added after 8 hours) at 60 °C for 24 hours.

### S14 Conjugation of PDHA and ADH to Dext<sub>1</sub> (Glc) studied by time course NMR

Conjugation of ADH and PDHA to Dext<sub>1</sub> (Glc) was studied by time course NMR. <sup>1</sup>H-NMR spectra at defined time points and the course of the reaction using 2 equivalents of PDHA and ADH at pH 4.0, are given in **Figure S41** and **S42**, respectively. Yields (%) were calculated by relating the integrals (not included) of the resonance resulting from the H1 reducing end unit for the conjugates and unreacted oligomers at specific time points to the sum of these integrals (100 %, theoretical yield).



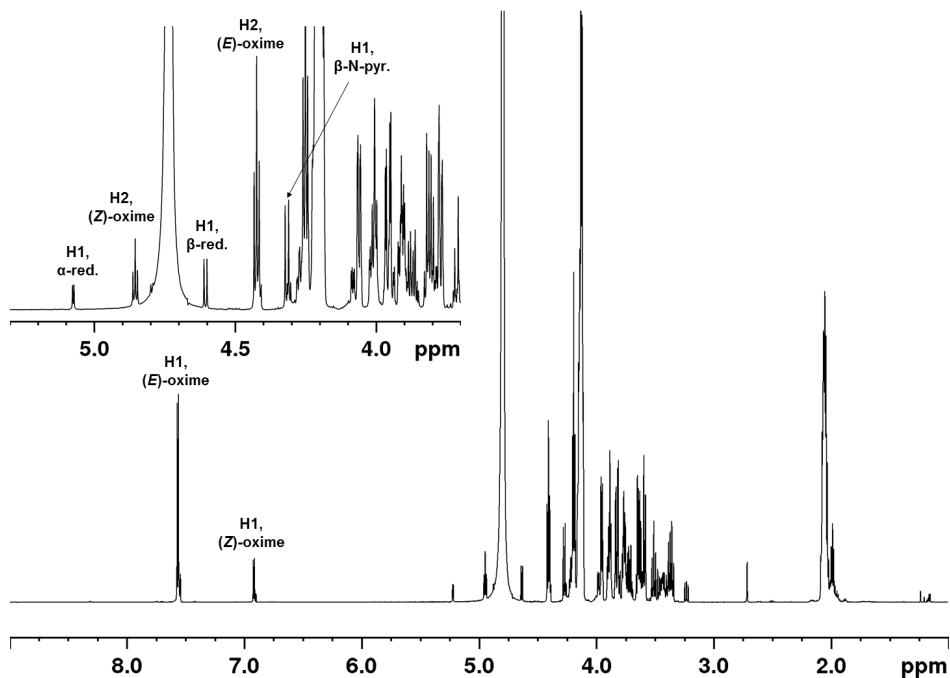
**Figure S41: a)** conjugation of PDHA to Dext<sub>1</sub> (Glc), **b)** <sup>1</sup>H-NMR spectra at defined time points for the conjugation of PDHA (2 equivalents) to Dext<sub>1</sub> (Glc), pH 4.0 **c)** course of the reaction obtained from the integration of the spectra shown in a).



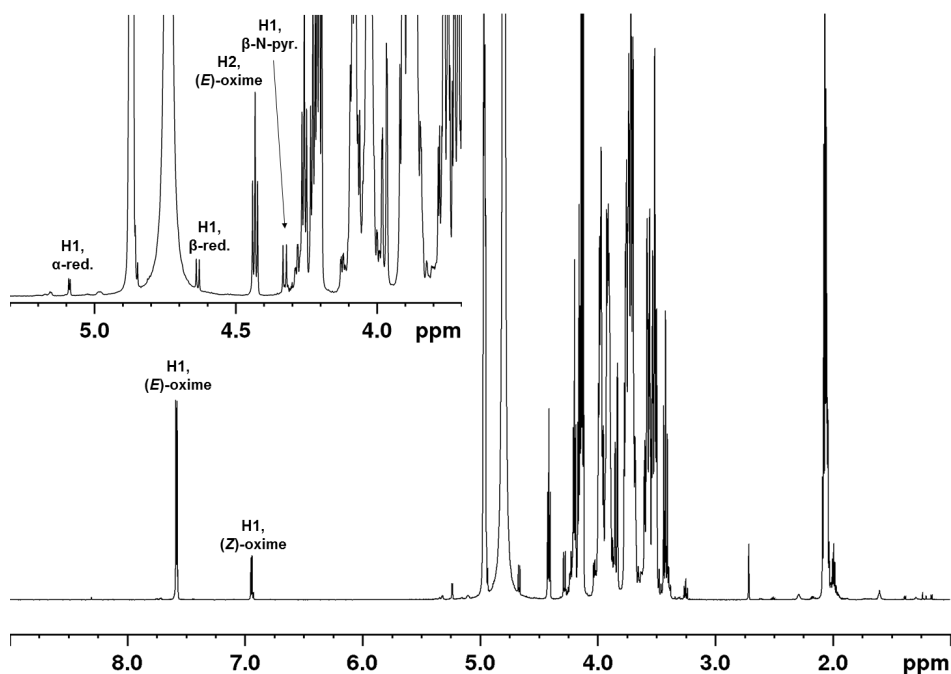
**Figure S42: a)** conjugation of ADH to Dext<sub>1</sub> (Glc), **b)** <sup>1</sup>H-NMR spectra at defined time points for the conjugation of ADH (2 equivalents) to Dext<sub>1</sub> (Glc), pH 4.0 **c)** course of the reaction obtained from the integration of the spectra shown in a).

### S15 <sup>1</sup>H-NMR characterisation of the equilibrium mixtures for the conjugation reactions with Dext<sub>n</sub> oligomers

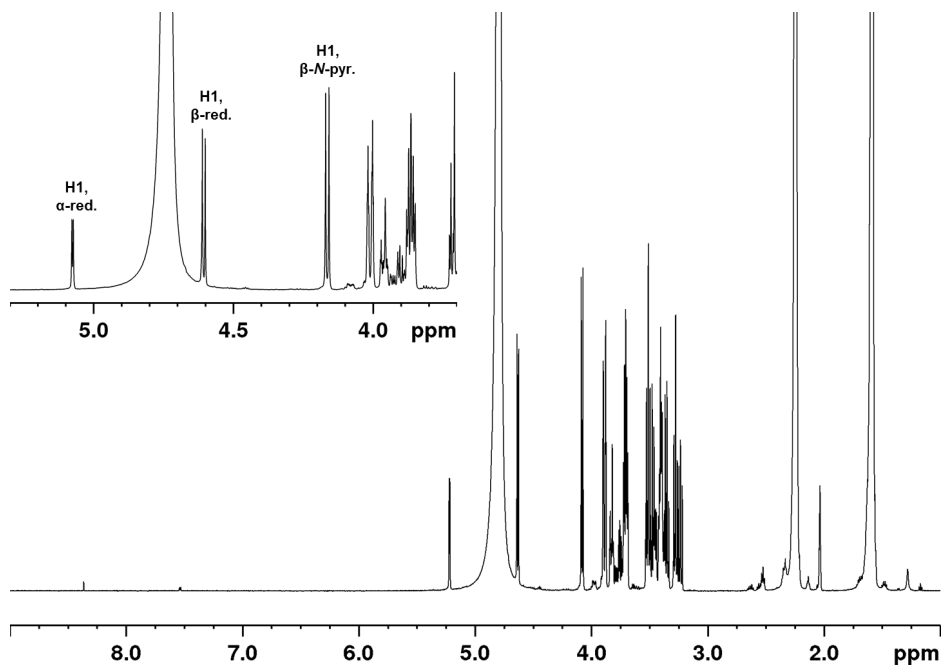
The mixture of conjugates and unreacted oligomers at equilibrium for the reactions of Dext<sub>n</sub> with 2 equivalents PDHA or ADH at pH 4.0 were characterized by <sup>1</sup>H-NMR. The spectra are given in **Figure S43-S46**. The following designations are used in the <sup>1</sup>H-NMR spectra: (*E*)- and (*Z*)-oxime ((*E*)/(*Z*)-configuration of the oxime), β-*N*-pyr. (β-configuration of the *N*-pyranoside) and α- and β- red. (α-/β-configuration of the anomeric proton in the reducing end Glc-unit).



**Figure S43:** <sup>1</sup>H-NMR characterisation of the mixture of conjugates and unreacted oligomers at equilibrium for the reaction of Dext<sub>1</sub> (Glc) with 2 equivalents of PDHA in deuterated NaAc-buffer, pH 4.0. The yield of conjugates at equilibrium was 92 %.

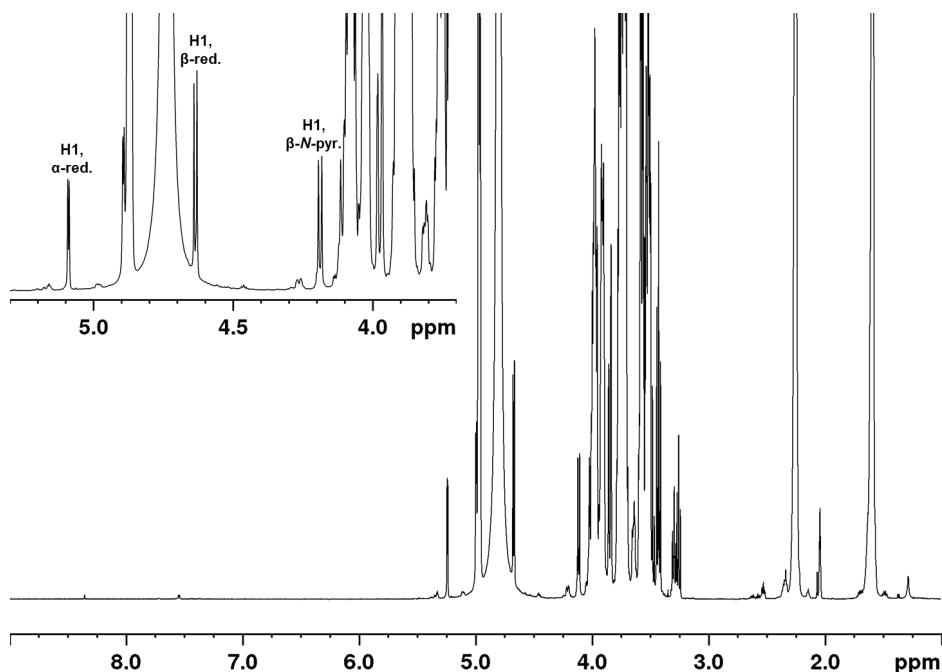


**Figure S44:**  $^1\text{H-NMR}$  characterisation of the mixture of conjugates and unreacted oligomers at equilibrium for the reaction of  $\text{Dext}_5$  with 2 equivalents of PDHA in deuterated NaAc-buffer, pH 4.0. The yield of conjugates at equilibrium was 90 %.



**Figure S45:**  $^1\text{H-NMR}$  characterisation of the mixture of conjugates and unreacted oligomers at equilibrium for the reaction of  $\text{Dext}_1$  (Glc) with 2 equivalents of ADH in deuterated NaAc-buffer, pH 4.0. The yield of conjugates at equilibrium was 49 %.

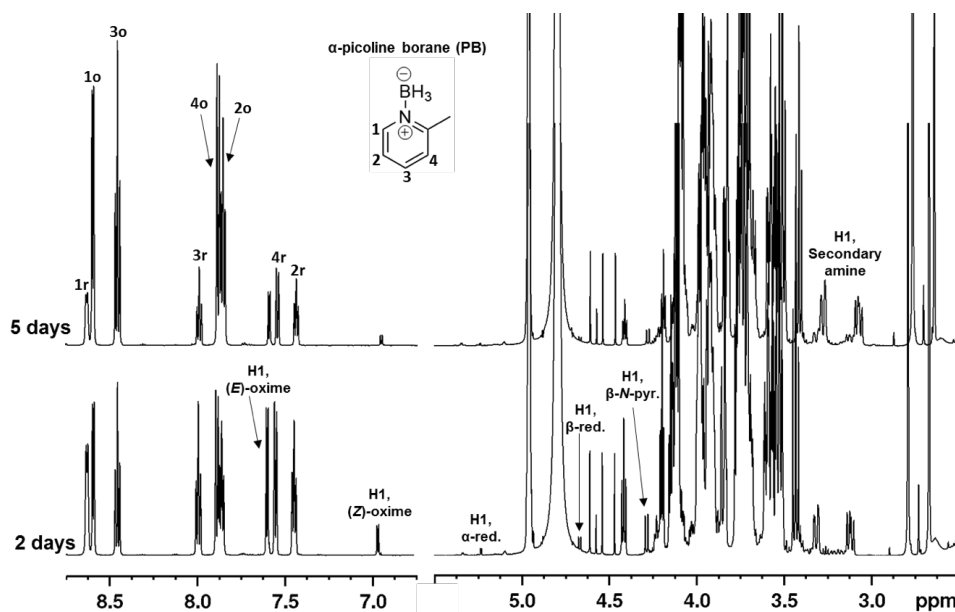




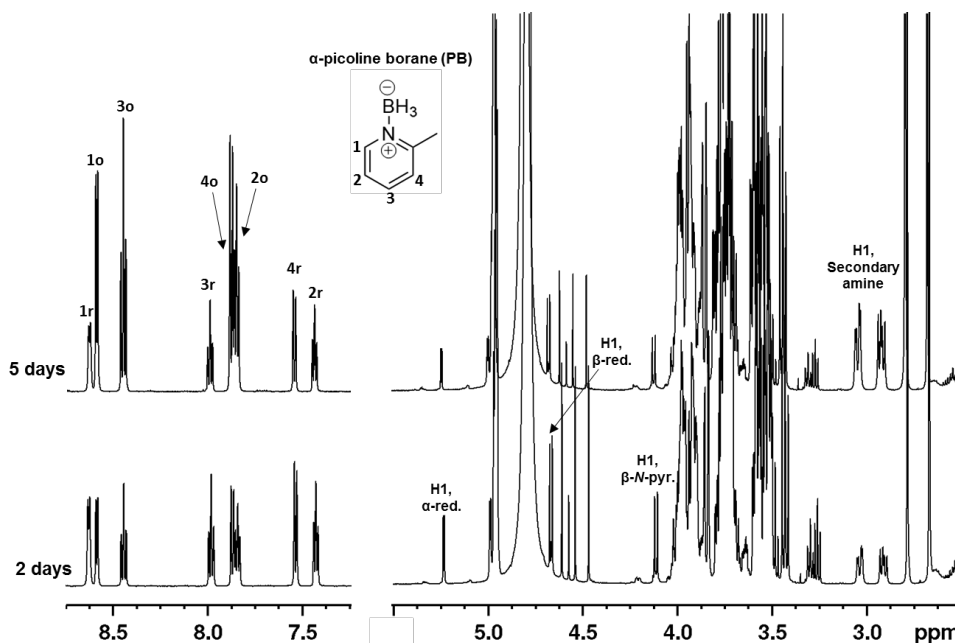
**Figure S46:**  $^1\text{H-NMR}$  characterisation of the mixture of conjugates and unreacted oligomers at equilibrium for the reaction of  $\text{Dext}_5$  with 2 equivalents of ADH in deuterated NaAc-buffer, pH 4.0. The yield of conjugates at equilibrium was 38 %.

#### **S16 $^1\text{H-NMR}$ characterisation of the reaction mixtures for the one pot reductive amination reaction of AA and $\text{Dext}_4$ with PDHA or ADH after 2 and 5 days**

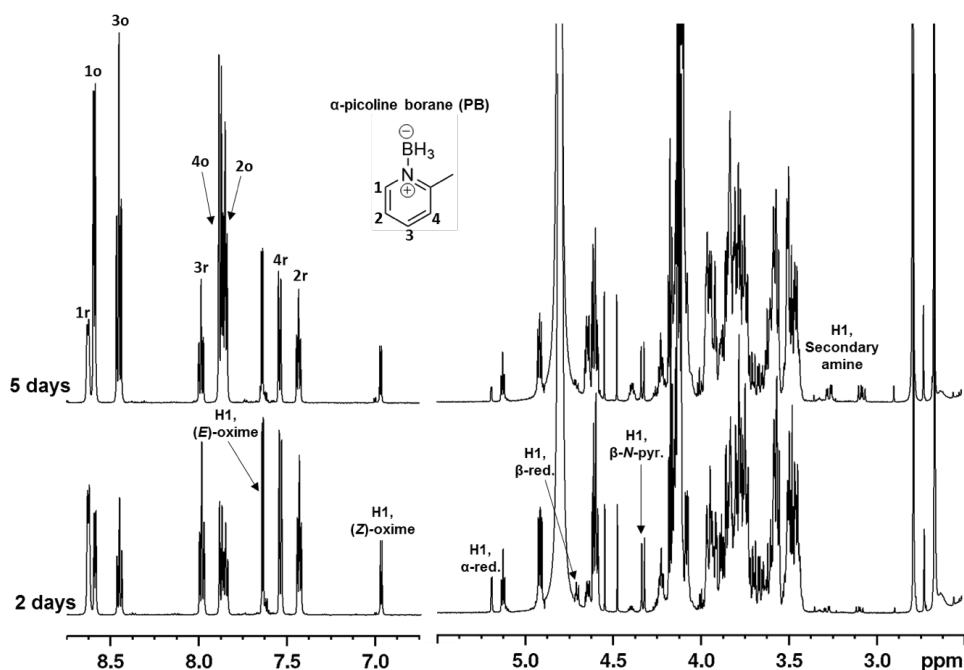
The one pot reductive amination of AA and  $\text{Dext}_4$  with 2 equivalents of ADH or PDHA and 3 equivalents of PB at pH 4.0 was studied by time course NMR. The spectra obtained for the mixture of reduced secondary amine conjugates, non-reduced conjugates (oximes/hydrazones and *N*-glycosides) and unreacted oligomers after 2 and 5 days are given in **Figure S47-S50**. The following designations are used in the  $^1\text{H-NMR}$  spectra: (*E*)- and (*Z*)-oxime ((*E*)/(*Z*)-configuration of the oxime),  $\beta$ -*N*-pyr. ( $\beta$ -configuration of the *N*-pyranoside), *N*-glycoside (unidentified *N*-glycoside conjugate),  $\alpha$ - and  $\beta$ -red. ( $\alpha$ / $\beta$ -configuration of the anomeric protons in the reducing end unit of the unreacted oligomers) and secondary amine (reduced secondary amine conjugates). In addition, resonances resulting from PB both in its reduced (*r*) and oxidized form (in the area 7.3 to 8.7 ppm) are assigned in the spectra. Yields (%) were calculated by relating the integrals (not included) of the resonances resulting from the H1 reducing end unit for the secondary amines, conjugates and unreacted oligomers the sum of these integrals at the start of the reduction (100 %, theoretical yield). The yield of unidentified products was calculated as the difference between the obtained and theoretical yield. The yields (%) obtained after 2 and 5 days of reaction are summarized in **Table S4**.



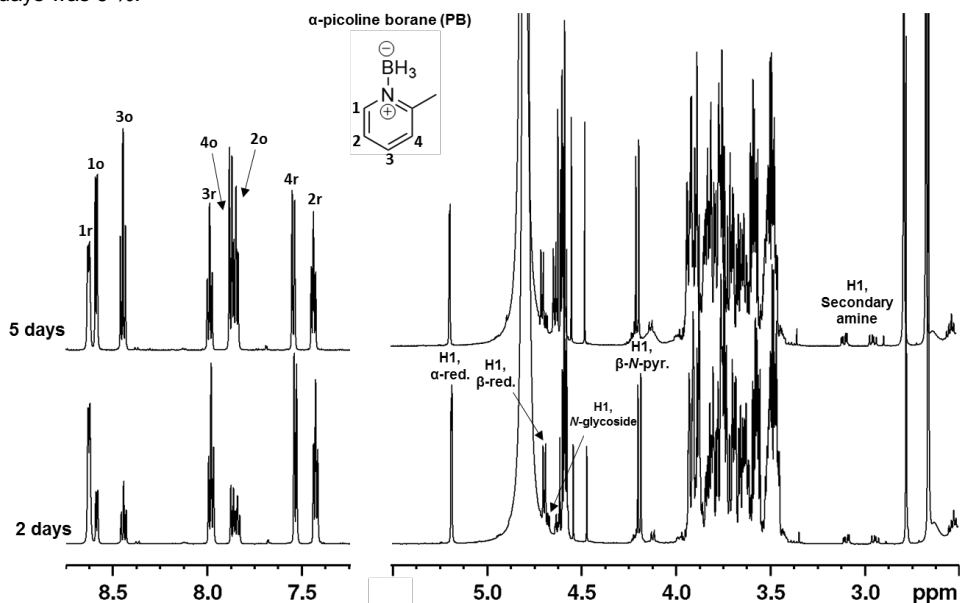
**Figure S47:**  $^1\text{H-NMR}$  characterisation of the mixture of secondary amines, conjugates and unreacted oligomers obtained after 2 and 5 days for the one pot reductive amination of Dext<sub>4</sub> with 2 equivalents PDHA and 3 equivalents PB at pH 4.0. The yield of secondary amines obtained after 5 days was 71 %.



**Figure S48:**  $^1\text{H-NMR}$  characterisation of the mixture of secondary amines, conjugates and unreacted oligomers obtained after 2 and 5 days for the one pot reductive amination of Dext<sub>4</sub> with 2 equivalents ADH and 3 equivalents PB at pH 4.0. The yield of secondary amines obtained after 5 days was 61 %.



**Figure S49:**  $^1\text{H-NMR}$  characterisation of the mixture of secondary amines, conjugates and unreacted oligomers obtained after 2 and 5 days for the one pot reductive amination of AA with 2 equivalents PDHA and 3 equivalents PB at pH 4.0. The yield of secondary amines obtained after 5 days was 9 %.



**Figure S50:**  $^1\text{H-NMR}$  characterisation of the mixture of secondary amines, conjugates and unreacted oligomers obtained after 2 and 5 days for the one pot reductive amination of AA with 2 equivalents ADH and 3 equivalents PB at pH 4.0. The yield of secondary amines obtained after 5 days was 6 %.

**Table S4.** Yields (%) obtained from the <sup>1</sup>H-NMR spectra after 2 and 5 days (**Figure S47-S50**) for the one pot reductive amination reactions of Dext<sub>4</sub> and AA with 2 equivalents PDHA or ADH and 3 equivalents PB at pH 4.0.

Reaction	PDHA/ADH [equivalents]	PB [equivalents]	Time [days]	Reduced conjugates [%]	Non- reduced conjugates [%]	Unreacted oligomers [%]	Unidentified products <sup>[a]</sup> [%]
Dext <sub>4</sub> -PDHA	2	3	2	31	64	5	0
			5	70	28	2	0
Dext <sub>4</sub> -ADH	2	3	2	23	30	47	0
			5	61	17	22	0
AA-PDHA	2	3	2	2	73	19	6
			5	9	56	5	30
AA-ADH	2	3	2	4	37	58	1
			5	6	47	39	8

[a] The yield of unidentified products was calculated as the difference between the formation of reduced (secondary amine) conjugates and the decrease in non-reduced conjugates and unreacted oligomers. Hence, yield of unidentified products (%) = theoretical yield (100 %) – yield of reduced conjugates (%) – yield of non-reduced conjugates (%) – yield of unreacted oligomers (%).

## S16 References

- Sugiyama, Hiroshi, Kanehiko Hisamichi, Kazuo Sakai, Taichi Usui, Jun-Ichi Ishiyama, Hideaki Kudo, Hiroki Ito, & Yasuhisa Senda. (2001). The conformational study of chitin and chitosan oligomers in solution. *Bioorganic & Medicinal Chemistry*, 9, 211-16.
- Sørbotten, Audun, Svein J. Horn, Vincent G. H. Eijsink, & Kjell M. Vårum. (2005). Degradation of chitosans with chitinase B from *Serratia marcescens*. *The FEBS Journal*, 272, 538-49.
- van Aalten, D. M. F., D. Komander, B. Synstad, S. Gåseidnes, M. G. Peter, & V. G. H. Eijsink. (2001). Structural insights into the catalytic mechanism of a family 18 exo-chitinase. *Proceedings of the National Academy of Sciences*, 98, 8979-84.

# Paper II



# 2,5-Anhydro-D-Mannose End-Functionalized Chitin Oligomers Activated by Dioxyamines or Dihydrazides as Precursors of Diblock Oligosaccharides

Ingrid Vikøren Mo, Marianne Øksnes Dalheim, Finn L. Achmann, Christophe Schatz,\* and Bjørn E. Christensen\*

Cite This: *Biomacromolecules* 2020, 21, 2884–2895

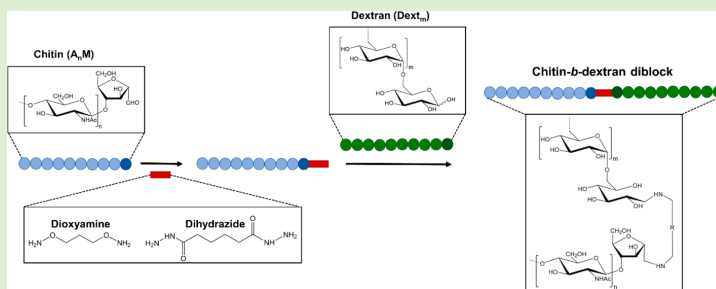
Read Online

ACCESS |

Metrics & More

Article Recommendations

Supporting Information



**ABSTRACT:** Diblock oligosaccharides based on renewable resources allow for a range of new but, so far, little explored biomaterials. Coupling of blocks through their reducing ends ensures retention of many of their intrinsic properties that otherwise are perturbed in classical lateral modifications. Chitin is an abundant, biodegradable, bioactive, and self-assembling polysaccharide. However, most coupling protocols relevant for chitin blocks have shortcomings. Here we exploit the highly reactive 2,5-anhydro-D-mannose residue at the reducing end of chitin oligomers obtained by nitrous acid depolymerization. Subsequent activation by dihydrazides or dioxyamines provides precursors for chitin-based diblock oligosaccharides. These reactions are much faster than for other carbohydrates, and only acyclic imines (hydrazones or oximes) are formed (no cyclic *N*-glycosides).  $\alpha$ -Picoline borane and cyanoborohydride are effective reductants of imines, but in contrast to most other carbohydrates, they are not selective for the imines in the present case. This could be circumvented by a simple two-step procedure. Attachment of a second block to hydrazide- or aminoxy-functionalized chitin oligomers turned out to be even faster than the attachment of the first block. The study provides simple protocols for the preparation of chitin-*b*-chitin and chitin-*b*-dextran diblock oligosaccharides without involving protection/deprotection strategies.

## INTRODUCTION

Block polysaccharides are a new class of engineered polymers based on renewable resources.<sup>1,2</sup> Among these, diblock polysaccharides, which are composed of two different oligo- or polysaccharide blocks (Figure 1), represent the simplest type. By attaching the blocks at the chain termini, their intrinsic properties are minimally perturbed.<sup>3,4</sup> In this respect, they are analogous to synthetic AB-type block copolymers. However, the broad range of chemical, physical, and biological properties of natural and abundant polysaccharides is very different from most synthetic blocks. Examples include solubility, crystallinity, interactions with ions, pH responses, and above all, biodegradability. This work focuses on the preparation of chitin-based diblock oligosaccharides by using the dihydrazide/dioxyamine copper-free and aniline-free conjugation methodology recently applied to chitosan

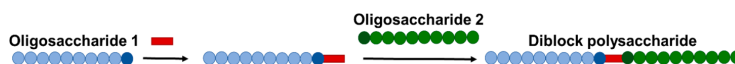
oligosaccharides having a *N*-acetyl-D-glucosamine (GlcNAc) residue at the reducing end.<sup>5</sup> Here we take advantage of chitins with a reactive 2,5-anhydro-D-mannose residue at the reducing end. In contrast to alkyne/azide click chemistry, where each block needs to be modified prior to coupling,<sup>6–9</sup> our methodology takes advantage of the native reducing end for attachment of blocks to bivalent dihydrazides and dioxyamines (Figure 1).

Received: April 23, 2020

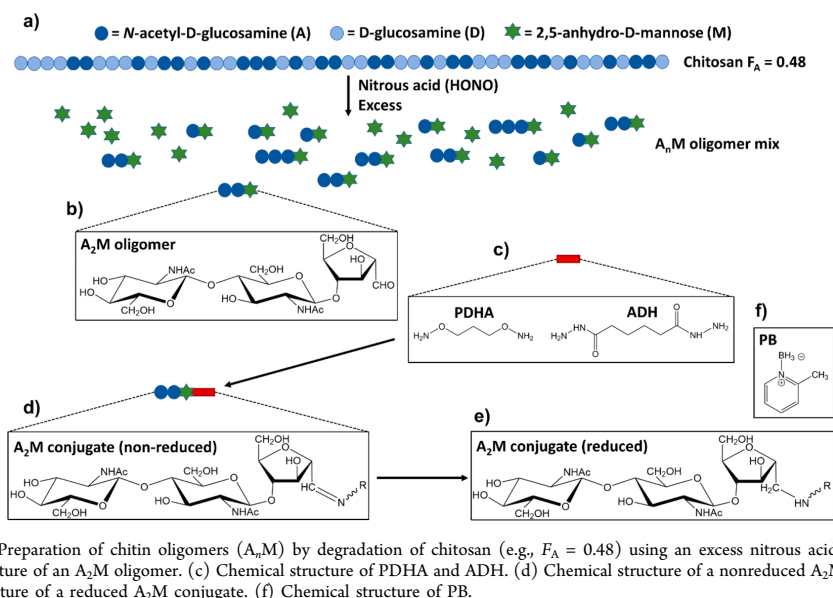
Revised: June 11, 2020

Published: June 15, 2020





**Figure 1.** Preparation of a diblock polysaccharide by a two-step strategy. First, a bivalent linker is attached to the reducing end of oligosaccharide 1. Oligosaccharide 2 is subsequently attached.



**Figure 2.** (a) Preparation of chitin oligomers ( $A_nM$ ) by degradation of chitosan (e.g.,  $F_A = 0.48$ ) using an excess nitrous acid (HONO). (b) Chemical structure of an  $A_2M$  oligomer. (c) Chemical structure of PDHA and ADH. (d) Chemical structure of a nonreduced  $A_2M$  conjugate. (e) Chemical structure of a reduced  $A_2M$  conjugate. (f) Chemical structure of PB.

Chitin is a component of the exoskeleton of shrimp and crabs and is available in large quantities as a byproduct in aquaculture. It is exclusively composed of  $\beta$ -1,4-linked GlcNAc (A) residues and, consequently, the fraction of acetylated units ( $F_A$ ) is 1. Chitin has self-assembly properties and becomes water insoluble and crystalline above DP 6. In contrast to chitosans, which can be obtained by partial de-*N*-acetylation of chitin ( $F_A < 1$ ), it is not responsive to changes in pH. Chitin can be degraded by chitinases or by chemical methods to form chitoooligosaccharides, which may have biological effects, including eliciting defense responses in plants and anticancer properties in animals.<sup>10–13</sup> Enzymatically degradable chitin–cellulose<sup>14</sup> and chitin–poly(propylene glycol)<sup>15</sup> diblocks have been described in the literature. However, their synthesis involved protection/deprotection of hydroxyls and diisocyanate coupling via the natural reducing ends.

Nitrous acid (HONO) depolymerization of chitosan (Figure 2a) is a commonly used alternative to enzymatic degradation or acid hydrolysis to prepare chitoooligosaccharides with a 2,5-anhydro-*D*-mannose (M) residue at the reducing end.<sup>16,17</sup> The HONO only affects the *D*-glucosamine (GlcN, D) residues of the chitosan and, hence, chitin oligomers ( $A_nM$ ) can be obtained by using an excess HONO to the fraction of D residues ( $F_D = 1 - F_A$ ). The pending aldehyde of the M residue (Figure 2b) makes such oligomers particularly reactive. This has been exploited to prepare self-branched chitosans<sup>18</sup> as well as a range of end-activated chitosan oligomers for subsequent preparation of chitosan-based copolymers.<sup>3,19–21</sup> In contrast, block polysaccharides exploiting  $A_nM$  chitin oligomers have to our knowledge not been explored.

Here we report the conjugation of chitin oligomers of the type  $A_nM$  (where  $n$  refers to the number of A residues; hence, the degree of polymerization (DP) =  $n + 1$ ) to adipic acid dihydrazide (ADH) and *O,O'*-1,3-propanediyl-bis(hydroxylamine) (PDHA) as the first step to form activated chitin oligomers ( $A_nM$ -ADH and  $A_nM$ -PDHA; Figure 2b–d). The study includes the irreversible reduction of conjugates to form stable secondary amine conjugates (Figure 2e) using  $\alpha$ -picoline borane (PB) as reductant (Figure 2f).<sup>5,22–25</sup> In the second step, we explore, in a similar way, the attachment of a second oligosaccharide block to both ADH- and PDHA-activated  $A_nM$  to prepare two different chitin-based diblocks with antiparallel chains:  $A_nM$ -*b*- $M_{m_1}$  and  $A_nM$ -*b*-Dext<sub>*m*</sub>. Dext<sub>*m*</sub> refers to dextran oligomers with  $m$  residues. Dextran is a neutral and flexible polysaccharide composed of *D*-glucose residues linked by  $\alpha$ -1,6-linkages, with some short branches.<sup>26,27</sup> The diblocks were purified by gel filtration chromatography (GFC) and characterized by NMR. The outcome of the study includes kinetic and structural data for each conjugation step as well as protocols for preparing activated oligosaccharides and pure diblock polysaccharides, the latter forming a basis for future structure–function studies.

## MATERIALS AND METHODS

**Materials.** High molecular weight chitosan ( $F_A = 0.48$ ,  $[\eta] = 1210$  mL/g) was obtained from Advanced Biopolymers (Norway). The fraction of acetylated units ( $F_A$ ) was confirmed by <sup>1</sup>H NMR spectroscopy.<sup>28</sup> Dextran T-2000 ( $M_w = 2000000$  g/mol) was obtained from Pharmacia Fine Chemicals. Adipic acid dihydrazide (ADH), *O,O'*-1,3-propanediylbis(hydroxylamine) dihydrochloride (PDHA), and 2-methylpyridine borane complex ( $\alpha$ -picoline borane, PB) were



obtained from Sigma-Aldrich. All other chemicals were obtained from commercial sources and were of analytical grade.

**Gel Filtration Chromatography (GFC).** Preparative and analytical gel filtration chromatography (GFC) were used for fractionation of chitin oligosaccharides and fractionation of products, respectively, as described earlier.<sup>5</sup> In brief, both systems were composed of Superdex 30 columns (BPG 140/950 (140 mm × 95 cm) and HiLoad 26/600 (26 mm × 60 cm), respectively) connected in series, continuously eluting ammonium acetate (AmAc) buffer (0.15 M, pH 4.5 and 0.1 M, pH 6.9, respectively). Fractionation was monitored online using a refractive index (RI) detector and fractions were collected and pooled according to elution times. The pooled fractions were reduced to appropriate volumes, dialyzed (MWCO = 100–500 Da) against ultrapure Milli-Q (MQ) water until the measured conductivity of the water was <2  $\mu\text{S}/\text{cm}$  and freeze-dried or freeze-dried directly without dialysis.

**NMR Spectroscopy.** Samples for NMR characterization were dissolved in  $\text{D}_2\text{O}$  (450–600  $\mu\text{L}$ , approx. 10 mg/mL). For some samples, 1% sodium 3-(trimethylsilyl)-propionate- $d_4$  (TSP, 3  $\mu\text{L}$ ) was added as an internal standard. Samples for the time course NMR experiments were prepared in deuterated NaAc buffer (500 mM, pH = 3.0, 4.0, or 5.0, 2 mM TSP).

All homo- and heteronuclear NMR experiments were carried out on a Bruker Ascend 14.1 T 600 MHz or a Bruker Ascend 18.8 T 800 MHz spectrometer (Bruker BioSpin AG, Fällanden, Switzerland), both equipped with Avance III HD electronics and a 5 mm Z-gradient CP-TCI cryogenic probe.

Characterization of oligomers, purified conjugates or other products was performed by obtaining 1D  $^1\text{H}$  NMR spectra at 300 K on the 600 MHz spectrometer. Time-course experiments were performed by obtaining 1D  $^1\text{H}$  NMR spectra at specific time points at 300 K on the 600 MHz spectrometer. Chemical shift assignments were performed at 298 K on the 800 MHz spectrometer by obtaining the following homo- and heteronuclear NMR spectra: 1D proton, 2D double quantum filtered correlation spectroscopy (DQF-COSY), 2D total correlation spectroscopy (TOCSY) with 70 ms mixing time, 2D  $^{13}\text{C}$  heteronuclear single quantum coherence (HSQC) with multiplicity editing, 2D  $^{13}\text{C}$  heteronuclear 2 bond correlation (H2BC), 2D  $^{13}\text{C}$  HSQC- $[^1\text{H}, ^1\text{H}]$  TOCSY with 70 ms mixing time on protons, and 2D heteronuclear multiple bond correlation (HMBC) with BIRD filter to suppress first order correlations.

All spectra were recorded, processed, and analyzed using TopSpin 3.5.pl7 software (Bruker BioSpin).

**Preparation of Chitin Oligomers by Nitrous Acid Degradation.** Chitosan ( $F_A = 0.48$ , 20 mg/mL) was dissolved in acetic acid (AcOH, 2.5 vol %) by stirring overnight. Dissolved oxygen was removed by bubbling the solution with  $\text{N}_2$  gas for 15 min. After cooling the solution to approximately 4  $^\circ\text{C}$ , a freshly prepared  $\text{NaNO}_2$  solution (20 mg/mL, 30% excess mole  $\text{NaNO}_2$ ; mole D-units) was added in three portions with 45 min intervals. The reaction mixture was agitated in the dark at 4  $^\circ\text{C}$  overnight on a shaking device to ensure complete degradation. The degradation mixture was centrifuged using an Allegra X-15R centrifuge (Beckman Coulter) equipped with a SX4750A rotor (30 min, 4750 rpm), and the pellet was washed with AcOH (2.5 vol %). The washing and centrifugation steps were repeated three times to remove insoluble high molecular weight chitin oligomers. The supernatant (containing water-soluble low molecular weight chitin oligomers) was filtered (5 and 45  $\mu\text{m}$ ) and freeze-dried. The water-soluble chitin oligomers (DP < 10) were fractionated according to a degree of polymerization (DP) using the preparative GFC system (0.15 M AmAc, pH 4.5). Oligomer fractions were dialyzed (MWCO = 100–500) against MQ-water until the measured conductivity was <2  $\mu\text{S}/\text{cm}$  and freeze-dried. Purified oligomers were characterized by 1D  $^1\text{H}$  NMR (600 MHz spectrometer).

**Preparation of Dextran Oligomers by Acid Degradation.** Dextran T-2000 ( $M_n = 2000000$ , 50 mg/mL) was dissolved in MQ-water overnight. HCl (0.1 M) was added to give a final concentration of 0.05 M HCl and 25 mg/mL dextran. Degradation was performed at 95  $^\circ\text{C}$  for 12 h. The degradation mixture was fractionated using the

preparative GFC system to obtain dextran oligomers (Dext $_m$ ) of specific DP ( $m = \text{DP}$ ). Dext $_m$  oligomers were purified by dialysis as above and characterized by 1D  $^1\text{H}$  NMR (600 MHz spectrometer).

**Conjugation and Reduction Studied by Time-Course NMR.** Time-course NMR experiments were performed as described earlier.<sup>5</sup> In brief, chitin oligomers ( $A_nM$ ) or dextran oligomers (Dext $_m$ ; 20.1 mM) and 2 equiv ADH or PDHA (40.2 mM) were dissolved separately in deuterated NaAc buffer (500 mM, pH = 3.0, 4.0 or 5.0, 2 mM TSP) and transferred to a 5 mm NMR tube. For the time-course reduction experiments, 3 equiv (60.3 mM) of PB or 3 or 10 equiv (60.3 or 201 mM) of  $\text{NaCNBH}_3$  were added directly to the NMR tube with equilibrium mixtures of conjugates. Concentrations given in parentheses are final concentrations after mixing. Mixing of reagents in the NMR tube or addition of reducing agent served as time zero ( $t = 0$ ). 1D  $^1\text{H}$  NMR spectra were recorded at desired time points (600 MHz spectrometer, 300 K), and the course of the reactions was tracked by integration of the spectra. Samples were held at room temperature between recordings. Equilibrium yields and yields from the reduction of conjugates in the NMR tube were obtained by integration of the  $^1\text{H}$  NMR spectra.

For experiments where a large excess of PB (20 equiv) was used, equilibrium mixtures with nonreduced conjugates were removed from the NMR tube and reduced in a separate vial.

**Preparative Protocol for Reduced Conjugates (Activated Chitin Oligomers).** Chitin oligomers ( $A_nM$ , 20.1 mM) and 10 equiv of ADH or PDHA (201 mM) were dissolved in NaAc buffer (500 mM, pH 4.0) to which 3 or 20 equiv of PB (60.3 or 420 mM), respectively, were added after >6 h. The reduction was performed at room temperature for 24 or 48 h for  $A_nM$ -ADH or  $A_nM$ -PDHA conjugates, respectively. Reactions were terminated by dialysis (MWCO = 100–500 Da) against 0.05 M NaCl until the insoluble PB was dissolved and, subsequently, freeze-dried. Conjugates were purified by GFC (analytical scale) and freeze-dried directly several times to remove the volatile GFC buffer (0.1 M AmAc). Purified conjugates were characterized by NMR spectroscopy (600 MHz spectrometer). Chemical shift assignment for the purified  $A_2M$ -PDHA conjugate was performed by homo- and heteronuclear NMR spectroscopy (800 MHz spectrometer).

**Preparation of Chitin Diblock Structures Using a Substoichiometric Amount of ADH or PDHA.** Chitin oligomers ( $A_nM$ , 20.1 mM) and 0.5 equiv of PDHA or ADH (10.05 mM) were dissolved in deuterated NaAc buffer (500 mM, pH 4.0) and the conjugation was studied by time-course NMR, as described above. Reduction with 3 or 20 equiv PB, fractionation, and characterization of products were performed as described for the preparative protocol, however, with a longer reduction time (96 h) for the diblocks formed with PDHA.

**Preparation of Diblock Structures from Activated Chitin Oligomers.** Purified chitin oligomer conjugates ( $A_nM$ -ADH or  $A_nM$ -PDHA, 20.1 mM) were reacted with equimolar concentrations of chitin oligomers ( $A_nM$ ) or dextran oligomers (Dext $_m$ ) to form diblock structures (in 500 mM deuterated NaAc buffer, pH 4.0, RT). The conjugation of the second block was monitored by time-course  $^1\text{H}$  NMR until equilibrium was reached. Reduction of chitin diblocks ( $A_nM$ - $b$ - $MAn$ ) was performed as described for the preparative protocol using 3 equiv PB. Due to slow reduction of Dext $_m$  conjugates, reduction was performed using 20 equiv (402 mM) PB at 40  $^\circ\text{C}$  for 96 h for the  $A_nM$ -PDHA-Dext $_m$  diblocks and 144 h for the  $A_nM$ -ADH-Dext $_m$  diblocks. Fractionation and characterization of products were performed as above. The relative yield of diblocks was obtained by integration of the GFC chromatogram.

## RESULTS AND DISCUSSION

**Preparation and Characterization of Chitin Oligomers.** Chitin oligomers of the type  $A_nM$  were obtained by degrading chitosan using an excess of nitrous acid (HONO) to the fraction of D residues. The mixture of water-soluble chitin oligomers was fractionated by GFC (Supporting Information, S1). Purified oligomers were characterized by

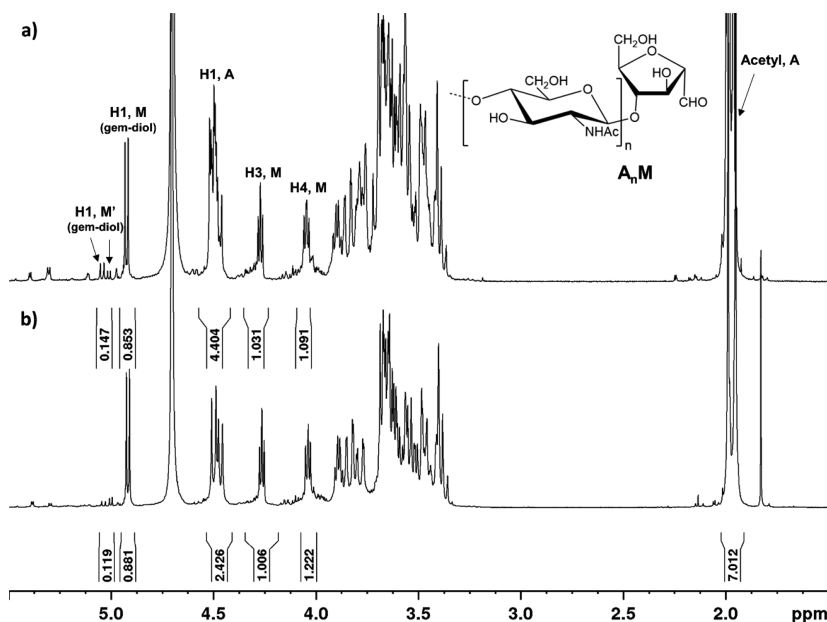


Figure 3.  $^1\text{H}$  NMR characterization of purified (a)  $\text{A}_4\text{M}$  and (b)  $\text{A}_2\text{M}$  oligomers in  $\text{D}_2\text{O}$  (600 MHz).

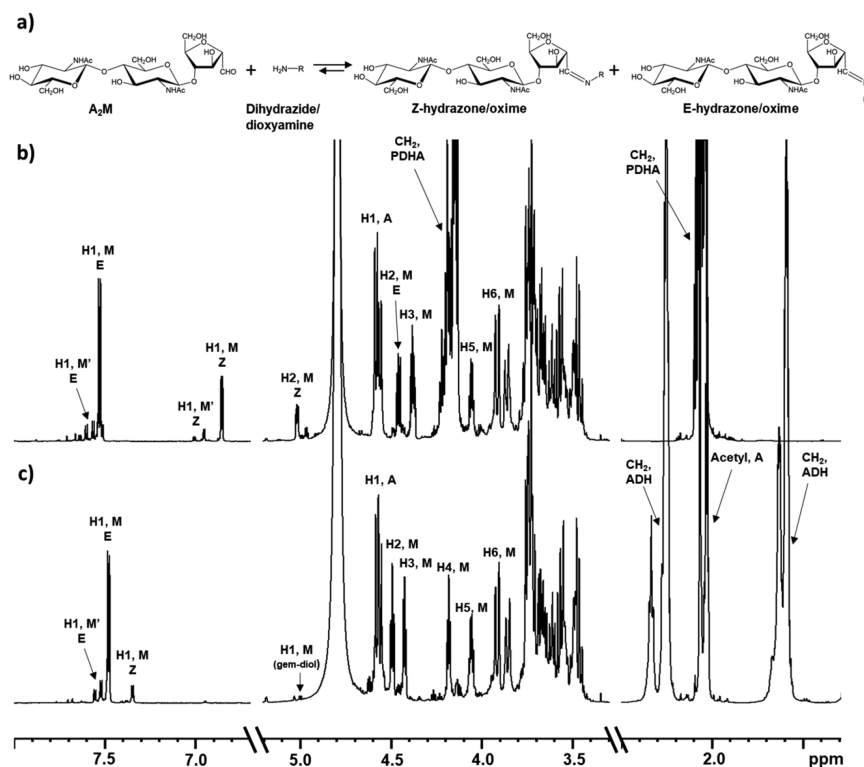
$^1\text{H}$  NMR (Figure 3), and key resonances were annotated according to literature.<sup>17</sup> The reducing end “aldehyde” proton appears as a doublet at 4.9 ppm due to complete hydration in water to the corresponding gem-diol.<sup>17</sup> The minor resonances around 5 ppm (marked as  $\text{M}'$  in Figure 3) were tentatively assigned to alternative forms of the M residue predicted in the literature.<sup>29</sup> These alternative forms (<15%) are not easily detected and, in particular, not quantified for longer oligomers of the  $\text{D}_n\text{M}$  type (where  $n$  is the number of contiguous uninterrupted D residues)<sup>19</sup> due to weak reducing end resonances. Also, a major difference between  $\text{A}_n\text{M}$  and  $\text{D}_n\text{M}$  oligomers is the requirement for excess HONO in the preparation of the former, which may possibly influence the formation of these alternative M forms.

**Reaction with ADH and PDHA.** The conjugation of the trisaccharide  $\text{A}_2\text{M}$  to ADH or PDHA (2 equiv) was studied in detail by time course NMR at pH 3.0, 4.0, and 5.0 (Supporting Information, S2).  $^1\text{H}$  NMR spectra of the equilibrium mixtures for the conjugation reactions at pH 4.0 are given in Figure 4. In agreement with the literature,<sup>19</sup> only *E*-/*Z*-hydrazones or oximes were formed. Minor resonances close to the main resonances for the *E*- and *Z*-hydrazones or oximes were attributed to the conjugation of oligomers with alternative forms of the M residue (marked as H1,  $\text{M}'$  in Figure 4).

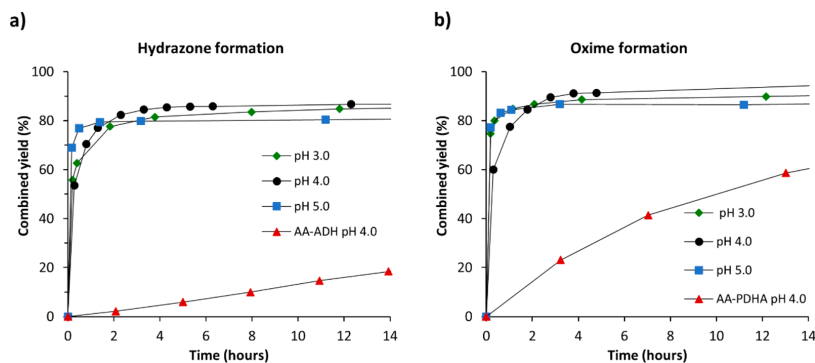
**Kinetics.** Kinetic plots for the conjugation of  $\text{A}_2\text{M}$  to ADH (hydrazone formation) and PDHA (oxime formation) are given in Figure 5a and b, respectively. The combined yield is the sum of *E*- and *Z*-hydrazones/oximes for all the forms of the M residue. Compared to chitosan oligomers with GlcNAc (A) at the reducing end,<sup>5</sup>  $\text{A}_n\text{M}$  oligomers reacted much faster with both ADH and PDHA under otherwise identical conditions (results obtained for AA<sup>5</sup> are included in Figure 5). With 2 equiv of ADH or PDHA, reactions were essentially complete after 4–6 h.

Reaction modeling is a powerful tool to simulate reactions, and to predict the effects of, for example, changing the concentration of reactants. We have previously shown that the conjugation of chitosan oligomers (with A at the reducing end) to ADH and PDHA, was first order with respect to each reactant in the range 2–10 equiv.<sup>5</sup> In contrast to these oligomers, the model for  $\text{A}_n\text{M}$  becomes simpler because cyclic *N*-glycosides are not formed. The model is detailed in Supporting Information, S3. The outcome of the modeling is estimated rate constants for the formation and dissociation of *E*-/*Z*-hydrazones and oximes. Rate constants for best fits are given in Table 1. We also included the times to reach 50% and 90% of the combined equilibrium yields ( $t_{0.5}$  and  $t_{0.9}$ ; Table 1). This provides a clearer picture when comparing different reactions and reaction protocols and also follows the method devised for other conjugation reactions.<sup>5,30</sup> In general, all experimental data gave relatively good fits, except a slight deviation in the range between 85 and 100% conversion, which can tentatively be attributed to the minor population of alternative forms of the M residue reacting somewhat more slowly (Supporting Information, S4). It may also be noted that the rate constants for the dissociation of *E*- and *Z*-conjugates needed to have the same value in order to obtain the good fits for the data to the model. The kinetics, equilibrium constants, and reaction yield depended slightly on pH, with pH 5.0 giving the fastest reactions in both cases (Table 1). However, pH 4.0 was used in further conjugations due to the pH dependence for the reduction step (see below).

The table includes kinetic data for a higher DP, in this case, the hexamer  $\text{A}_6\text{M}$ . As for the chitosan oligomers studied previously,<sup>5</sup> the reaction kinetics appeared to be essentially independent of DP in the range studied. It may be noted that  $\text{A}_n\text{M}$  becomes gradually less soluble in the buffer when  $n > 5$ .



**Figure 4.** (a) General reaction scheme for the conjugation of A<sub>2</sub>M to ADH (dihydrazide) or PDHA (dioxyamine). (b and c) <sup>1</sup>H NMR spectra of the equilibrium mixtures obtained for the conjugation of A<sub>2</sub>M to PDHA and ADH, respectively.



**Figure 5.** Reaction kinetics for the conjugation of A<sub>2</sub>M oligomers (20.1 mM) to 2 equiv of (a) ADH (hydrazone formation) and (b) PDHA (oxime formation) at pH 3.0, 4.0, and 5.0. Kinetics for the conjugation of AA at pH 4.0<sup>9</sup> is included for comparison.

Hence, longer oligomers can therefore not be easily prepared and studied by the present method.

**Reduction.** Most conjugations of this type are combined with an irreversible reduction step to obtain stable secondary amine conjugates. It was recently confirmed that PB can be a good alternative to sodium cyanoborohydride (NaCNBH<sub>3</sub>) for similar conjugations of chitosan oligomers with natural reducing ends,<sup>5</sup> prompting us to attempt a similar approach

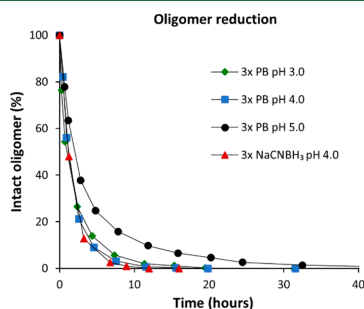
here. Besides being less toxic, PB also spontaneously decomposes more slowly (about 20×) than NaCNBH<sub>3</sub> under the given conditions (Supporting Information, S5). Although PB has low solubility in the aqueous buffer at room temperature, stirring was shown to increase the reduction rate, suggesting the reduction also takes place at the surface of the undissolved particles.<sup>5,31</sup>

**Table 1. Kinetic Parameters Obtained from the Modeling of the Conjugation of A ( $A_nM$ ) to B (ADH, PDHA or  $A_4M$ -ADH) Using Different Equivalents of B<sup>a</sup>**

A	B	equivalents	pH	A + B $\leftrightarrow$ E		A + B $\leftrightarrow$ Z		$t_{0.5}$ (h)	$t_{0.9}$ (h)	equilibrium yield (%)
				$k_1$ ( $h^{-1}$ )	$k_{-1}$ ( $h^{-1}$ )	$k_2$ ( $h^{-1}$ )	$k_{-2}$ ( $h^{-1}$ )			
$A_2M$	ADH	2	3.0	$3.1 \times 10^{-2}$	$4.0 \times 10^{-1}$	$4.1 \times 10^{-3}$	$4.0 \times 10^{-1}$	0.22	0.78	85
$A_2M$	ADH	2	4.0	$1.8 \times 10^{-2}$	$2.0 \times 10^{-1}$	$2.5 \times 10^{-3}$	$2.0 \times 10^{-1}$	0.38	1.37	87
$A_2M$	ADH	2	5.0	$4.1 \times 10^{-2}$	$7.0 \times 10^{-1}$	$5.8 \times 10^{-3}$	$7.0 \times 10^{-1}$	0.16	0.55	81
$A_2M$	PDHA	2	3.0	$2.8 \times 10^{-2}$	$2.5 \times 10^{-1}$	$1.2 \times 10^{-2}$	$2.5 \times 10^{-1}$	0.21	0.75	91
$A_2M$	PDHA	2	4.0	$2.4 \times 10^{-2}$	$2.2 \times 10^{-1}$	$1.0 \times 10^{-2}$	$2.2 \times 10^{-1}$	0.24	0.87	91
$A_2M$	PDHA	2	5.0	$3.5 \times 10^{-2}$	$4.5 \times 10^{-1}$	$1.6 \times 10^{-2}$	$4.5 \times 10^{-1}$	0.16	0.56	88
$A_3M$	ADH	2	4.0	$3.0 \times 10^{-2}$	$3.5 \times 10^{-1}$	$4.0 \times 10^{-3}$	$3.5 \times 10^{-1}$	0.23	0.82	86
$A_3M$	PDHA	2	4.0	$2.3 \times 10^{-2}$	$8.0 \times 10^{-2}$	$1.0 \times 10^{-3}$	$8.0 \times 10^{-2}$	0.27	0.97	96
$A_2M$	ADH	0.5	4.0	$4.0 \times 10^{-1}$	$9.0 \times 10^{-1}$	$5.8 \times 10^{-2}$	$9.0 \times 10^{-1}$	0.06	0.28	73
$A_2M$	PDHA	0.5	4.0	$1.2 \times 10^{-1}$	$6.0 \times 10^{-2}$	$5.2 \times 10^{-2}$	$6.0 \times 10^{-2}$	0.22	1.21	88
$A_4M$	$A_4M$ -ADH	1	4.0	$7.3 \times 10^{-2}$	$1.5 \times 10^{-1}$	$1.1 \times 10^{-2}$	$1.5 \times 10^{-1}$	0.35	1.57	74

<sup>a</sup>E: E-hydrazone/oxime. Z: Z-hydrazone/oxime. Two different models were applied. The first model estimates the individual rate constants for the formation and dissociation of E ( $k_1$  and  $k_{-1}$ ) and Z ( $k_2$  and  $k_{-2}$ ), whereas the second model considers the total (E + Z) as a single reaction product, providing times needed to reach 50% and 90% ( $t_{0.5}$  and  $t_{0.9}$ ) of the equilibrium yield.

The high reactivity of the pending aldehyde (*gem*-diol) of the M residue, prompted us to first investigate possible reduction of  $A_nM$  oligomers, which would render the oligomers unreactive for further conjugation. The reduction by PB was therefore assayed by time course NMR in the pH range 3.0–5.0. Reduction by NaCNBH<sub>3</sub> at pH 4.0 was included for comparison. Kinetic data are shown in Figure 6.



**Figure 6.** Reaction kinetics for the reduction of  $A_nM$  oligomers at pH 3.0, 4.0, and 5.0 using 3 equiv (3 $\times$ ) PB at RT. Reduction at pH 4.0 using 3 equiv NaCNBH<sub>3</sub> at RT, is included in the figure for comparison. NMR spectra are shown in Supporting Information, S6.

NMR spectra are given in the Supporting Information, S6. Complete reduction by PB was obtained after approximately 20, 12, and 40 h for pH 3.0, 4.0, and 5.0, respectively. Data were further fitted to a kinetic model assuming the rate of reduction (assumed irreversible) is proportional to the concentrations of each reactant. The rate constants are given in Table 2. With NaCNBH<sub>3</sub> reduction was complete after less than 12 h at pH 4.0. These results contrast with those of natural reducing ends such as the AA disaccharide, where no detectable reduction was observed under the same conditions (Supporting Information, S6). Hence, both reductants result in significant reduction of the  $A_nM$  oligomers, which directly influences the protocols for reductive amination, as discussed below.

The reduction of  $A_nM$  conjugates (oximes and hydrazones) was subsequently investigated by adding PB (3 equiv) to the

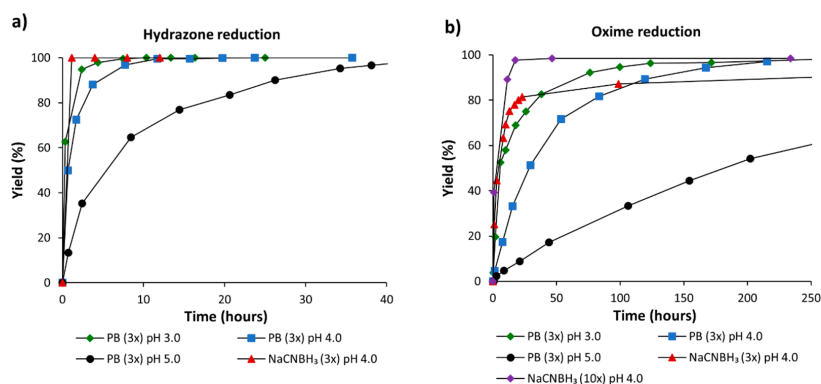
**Table 2. Rate Constants Obtained for the Reduction of Hydrazones and Oximes by PB (3 $\times$ ) Assuming Both Isomers (E-/Z-forms) of the Conjugates Are Reduced with the Same Rate<sup>a</sup>**

pH	rate constants ( $h^{-1}$ )		
	3.0	4.0	5.0
$A_nM$ (unreacted oligomer)	$1.1 \times 10^{-2}$	$1.5 \times 10^{-2}$	$7.0 \times 10^{-3}$
$A_nM$ -ADH (hydrazone)	$4.0 \times 10^{-2}$	$1.5 \times 10^{-2}$	$3.0 \times 10^{-3}$
$A_nM$ -PDHA (oxime)	$1.5 \times 10^{-3}$	$4.2 \times 10^{-4}$	$8.0 \times 10^{-5b}$

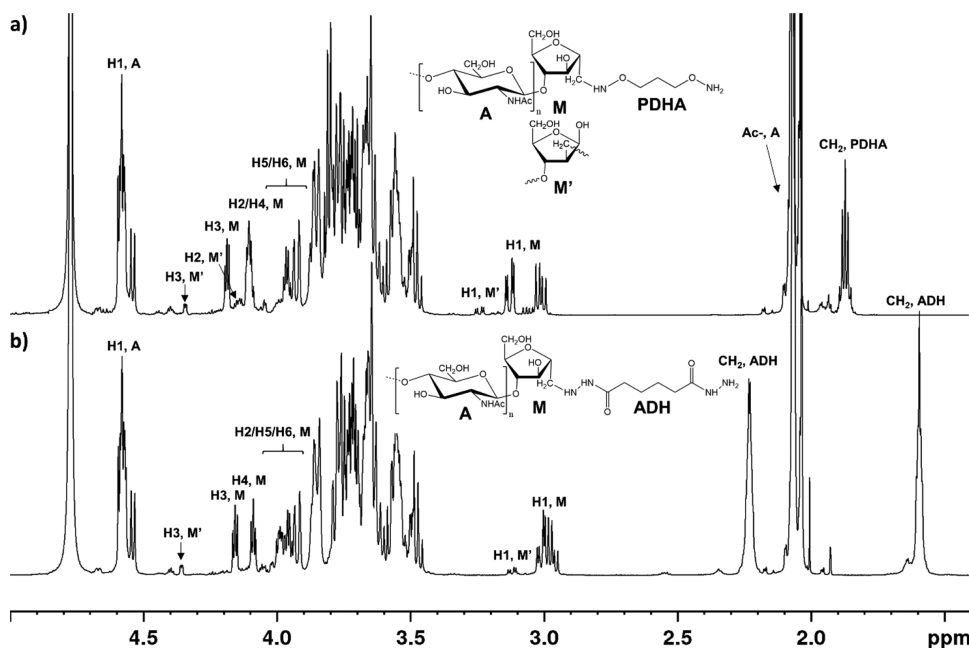
<sup>a</sup>Rate constants for the reduction of oligomers by PB are included for comparison. <sup>b</sup>Inaccurate (initially fast, then slow).

corresponding reaction mixtures after equilibrium was reached (i.e., after >12 h). Bases for the time course NMR analyses were the reduced intensity of the E- and Z-resonances, as well as emergence of methylene proton resonances of the secondary amine in the <sup>1</sup>H NMR spectra (Supporting Information, S7). Kinetic plots are given in Figure 7.

Hydrazone ( $A_nM$ -ADH) reduction with PB (Figure 7a) is indeed very fast in this system, and clearly fastest at pH 3.0, where complete reduction of conjugates is obtained after about 10 h at RT. The reduction here is slightly slower at pH 4.0, and much slower at pH 5.0. The same pH dependence is also observed for oxime ( $A_nM$ -PDHA) reduction (Figure 7b), except that the reduction is generally much slower, being complete after about 150–200 h. The pH-dependence of hydrazone and oxime reduction by PB has to our knowledge not been studied in detail, but we attribute the faster reduction at lower pH to the formation of reducible iminium ions by protonation. Hydrazone and oxime reduction by NaCNBH<sub>3</sub> (pH 4.0) was also investigated. Complete hydrazone reduction was obtained after approximately 1 h with 3 equiv of NaCNBH<sub>3</sub> (Figure 7a). Oxime reduction was slower under the same conditions, however, with an initial rate similar to that of PB at pH 3.0 (Figure 7b). Due to the rapid decomposition of NaCNBH<sub>3</sub> in the buffer, 3 equiv were insufficient to reach completion, leveling off at approximately 90% yield. In contrast to PB, which is poorly soluble at higher concentrations, 10 equiv of NaCNBH<sub>3</sub> could be completely dissolved, enabling monitoring of the oxime reduction. As expected, the rate of reduction increased correspondingly, and resulted in complete reduction in less than 20 h (Figure 7b).



**Figure 7.** Reaction kinetics for the reduction of (a)  $A_nM$ -ADH conjugates (hydrazone reduction) and (b)  $A_nM$ -PDHA conjugates (oxime reduction) at pH 3.0, 4.0, and 5.0 using 3 equiv (3X) PB at RT. Reduction of conjugates at pH 4.0 using 3 or 10 equiv  $\text{NaCNBH}_3$  at RT, is included in the figures for comparison.



**Figure 8.**  $^1\text{H}$  NMR spectra of reduced and purified (a)  $A_3M$ -PDHA and (b)  $A_3M$ -ADH conjugates.

The kinetic data in Figure 7 could be fitted to the model for the reductive amination using the previously obtained rate constants for the formation and dissociation of hydrazones or oximes (Table 1), as well as the rate constants for aldehyde reduction (Table 2). Hence, the rate of hydrazone or oxime reduction (assumed being irreversible and *E*- and *Z*-forms being equally reactive) became the only adjustable kinetic parameter. In general, reasonably good fits were obtained (Supporting Information, S8). The obtained rate constants for the reductions are given in Table 2. Interestingly, somewhat better fits were obtained by lowering the rate constants for

$A_nM$  reduction compared to reactions with  $A_nM$  and PB alone. The reason for this is presently not clear.

#### Preparative Protocols for Reduced $A_nM$ -ADH/PDHA Conjugates.

The results above provide the necessary information to develop protocols for preparative work. The most important is to maximize the conversion, but also to minimize the formation of disubstituted ADH or PDHA, for example,  $A_nM$ -ADH- $\text{MA}_n$ ,<sup>5</sup> as they are not reactive toward a second block. Assuming equal reactivity of both ends of ADH or PDHA, the statistical fraction of disubstituted species ( $f_{\text{DS}}$ ), is given by the expression

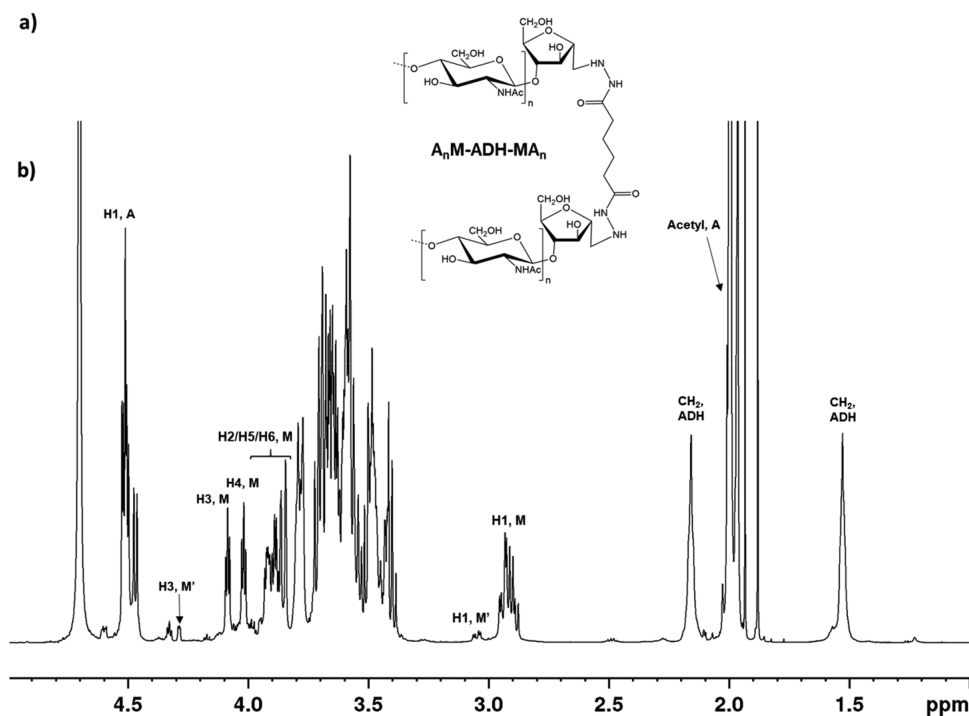


Figure 9. (a) General structure of the  $A_nM$ -ADH- $MA_n$  diblock. (b)  $^1H$  NMR spectrum of the reduced and purified  $A_4M$ -ADH- $MA_4$  diblock.

$$f_{DS} = \left(\frac{b}{2a}\right)^2$$

where  $b$  is the molar fraction of substituted oligosaccharide (from yield in Table 1), and  $a$  is the equivalence of a linker (PDHA or ADH). Derivation of the equation and examples are given in Supporting Information (S9). For example, 2 equiv (40.2 mM) ADH and a  $b$  of 0.87 (from Table 1, at pH 4.0) give 5% disubstituted ADH, which reduces to 0.2% with 10 equiv (201 mM). Hence, a large excess of ADH or PDHA is recommended, even when 2 equiv give acceptable conjugation yields. Although possibly interesting in other contexts, disubstituted species prevent further attachment of a second (different) block. The observation that the second attachment may be faster than the first further emphasizes the need for a high concentration of ADH or PDHA.

Because of the rapid reduction of unreacted  $A_nM$  oligomers, the reducing agent should be added after 4–6 h of conjugation. As shown above, 3 equiv of PB and a reduction time of 24 h (RT) is sufficient for quantitative reduction of  $A_nM$ -ADH conjugates. To overcome the slower reduction of oximes, 20 equiv of PB and a reaction time of 48 h is needed to give complete reduction of  $A_nM$ -PDHA conjugates (Supporting Information, S9). Alternatively, 10 equiv of  $NaCNBH_3$  and a reaction time of 20 h is sufficient for quantitative reduction of PDHA conjugates, whereas 3 equiv and less than 1 h gives complete reduction of ADH conjugates.  $A_3M$ -ADH and  $A_3M$ -PDHA conjugates were prepared by the above-mentioned preparative protocols using PB as the reductant (Supporting Information, S9).  $^1H$  NMR spectra of purified (GFC) and fully

reduced  $A_3M$ -ADH and  $A_3M$ -PDHA conjugates are given in Figure 8. Annotations in the spectra are based on literature data<sup>19</sup> and the NMR characterization of purified and fully reduced  $A_2M$ -PDHA (Supporting Information, S10), where one of the alternative forms of the M residue was structurally elucidated (shown and annotated in Figure 8 as  $M'$ ). In contrast to the main M residue,  $M'$  can appear in equilibrium with the open ring, with two aldehydes at the reducing end. However, conjugates corresponding to the open form were not identified, and hence, it appears that the oligomers with the alternative form of the M residue react with both ADH and PDHA in the same way as oligomers with the main form (with the possible exception of a bit slower kinetics discussed above). The different forms cannot be separated during purification and without further investigation, we assume that the alternative forms cannot be distinguished when part of a diblock polysaccharide.

#### Attaching a Second Block: $A_nM$ - $b$ - $MA_n$ Diblock

**Oligosaccharides.** An efficient protocol to prepare  $A_nM$ -ADH/PDHA conjugates paves the way for attaching a second oligosaccharide in order to prepare chitin-based diblock oligo- or polysaccharides ( $A_nM$ - $b$ - $X$ ). We first investigated the formation of  $A_nM$ -ADH- $MA_n$  diblocks (Figure 9a). To study this, reduced  $A_4M$ -ADH conjugates were prepared and subsequently reacted with an equimolar amount of  $A_4M$  (conditions otherwise as above). The choice of equimolar proportions is based on the general need to use minimum amounts of oligosaccharide and also to simplify the following purification step. The amination was studied by time-course NMR as above, and rate constants are included in Table 1. The

**Table 3. Kinetic Parameters Obtained from the Modeling of the Conjugation of A (Dext<sub>m</sub>) to B (ADH, PDHA or A<sub>3</sub>M-ADH or A<sub>3</sub>M-PDHA) Using Different Equivalents of B<sup>a</sup>**

A	B (2×)	A + B ↔ E		A + B ↔ Z		E ↔ Pyr		Z ↔ Pyr		equilibrium yield (%)
		k <sub>1</sub> (h <sup>-1</sup> )	k <sub>-1</sub> (h <sup>-1</sup> )	k <sub>2</sub> (h <sup>-1</sup> )	k <sub>-2</sub> (h <sup>-1</sup> )	k <sub>3</sub> (h <sup>-1</sup> )	k <sub>-3</sub> (h <sup>-1</sup> )	k <sub>4</sub> (h <sup>-1</sup> )	k <sub>-4</sub> (h <sup>-1</sup> )	
Dext <sub>5</sub>	ADH	1.5 × 10 <sup>-3</sup>	1.0 × 10 <sup>1</sup>	1.5 × 10 <sup>-4</sup>	1.0 × 10 <sup>1</sup>	1.1 × 10 <sup>2</sup>	1.1 × 10 <sup>0</sup>	1.1 × 10 <sup>2</sup>	1.1 × 10 <sup>0</sup>	35
Dext <sub>5</sub>	PDHA	2.9 × 10 <sup>-3</sup>	2.0 × 10 <sup>-3</sup>	4.0 × 10 <sup>-4</sup>	1.5 × 10 <sup>-1</sup>	2.0 × 10 <sup>0</sup>	6.8 × 10 <sup>0</sup>	2.7 × 10 <sup>1</sup>	2.0 × 10 <sup>1</sup>	87
A	B (1×)									
Dext <sub>6</sub>	A <sub>3</sub> M-ADH	3.0 × 10 <sup>-3</sup>	1.7 × 10 <sup>1</sup>	3.0 × 10 <sup>-4</sup>	1.7 × 10 <sup>1</sup>	1.1 × 10 <sup>2</sup>	1.1 × 10 <sup>0</sup>	1.1 × 10 <sup>2</sup>	1.1 × 10 <sup>0</sup>	15
Dext <sub>6</sub>	A <sub>3</sub> M-PDHA	1.1 × 10 <sup>-2</sup>	5.0 × 10 <sup>-2</sup>	1.5 × 10 <sup>-3</sup>	1.0 × 10 <sup>-1</sup>	1.9 × 10 <sup>0</sup>	4.5 × 10 <sup>0</sup>	2.7 × 10 <sup>1</sup>	1.5 × 10 <sup>1</sup>	66

<sup>a</sup>Reactions were performed at pH 4.0, RT. E: E-hydrazone/oxime. Z: Z-hydrazone/oxime. Pyr: N-pyranoside.

total equilibrium yield of hydrazones was as high as 74% with only one equivalent of the second block. To allow a more direct comparison, we used the rate constants for the conjugation of A<sub>2</sub>M and A<sub>3</sub>M to free ADH (2 equiv) to simulate the rate (*t*<sub>0.5</sub> and *t*<sub>0.9</sub>) and yield for the reaction with equimolar proportions of oligomers and amines (Supporting Information, S11). Interestingly, the equilibrium yield was lower, and the rate was lower than for the conjugation of A<sub>4</sub>M to the A<sub>4</sub>M-ADH conjugate, indicating that the reactivity of the free hydrazide group toward terminal M-residues is higher for A<sub>n</sub>M-ADH than for free ADH (Supporting Information, S11). After subsequent reduction with PB (3 equiv) the relative yield of A<sub>n</sub>M-ADH-MA<sub>n</sub> diblocks was approximately 83% (obtained by integration of the GFC chromatogram, Supporting Information, S11). Unreacted A<sub>4</sub>M oligomers were completely reduced, hence, preventing the diblock formation from going to completion. The general structure of the A<sub>n</sub>M-ADH-MA<sub>n</sub> diblocks and <sup>1</sup>H NMR spectrum of the reduced and purified A<sub>4</sub>M-ADH-MA<sub>4</sub> diblock are given in Figure 9.

The diblock formation was further investigated in the special case of 0.5 equiv of ADH or PDHA to A<sub>2</sub>M oligomers. These conditions should at completion give only disubstituted ADH/PDHA, that is, the diblocks A<sub>2</sub>M-ADH-MA<sub>2</sub> and A<sub>2</sub>M-PDHA-MA<sub>2</sub>. Here, faster conjugation was observed, especially for ADH, supporting the theory of different kinetics for the attachment of the second block (Table 1 and Supporting Information, S12). High equilibrium yields of hydrazones and oximes were obtained (73% with ADH and 86% with PDHA). Interesting, the yield of diblocks after reduction was not increased above these values (Supporting Information, S12). Hence, the yield of diblocks corroborates with the statistical amount of disubstituted species expected for the systems (as equimolar concentration of amine and oligomer was used).

**Attaching a Second Block: A<sub>n</sub>M-*b*-Dextran Diblock Oligosaccharides.** The final step was to study the attachment of a second block of a different kind, namely dextran, using purified and reduced A<sub>3</sub>M-ADH and A<sub>3</sub>M-PDHA conjugates to form chitin-*b*-dextran diblocks. Dextran oligomers (Dext<sub>m</sub>) of defined DP (*m* = DP) were obtained by partial hydrolysis of dextran and fractionation of oligomers by gel filtration chromatography (Supporting Information, S13). Reactions were monitored by time course NMR, again using equimolar amounts of the two blocks.

By this strategy the reactivity of the reducing end of Dext<sub>m</sub> governs the conjugation. Therefore, the kinetics of the conjugation of Dext<sub>5</sub> to free ADH and PDHA (2 equiv) was included for comparison (Supporting Information, S14). Importantly, dextran forms N-pyranosides in addition to E- and Z-oximes with PDHA, whereas it forms almost exclusively

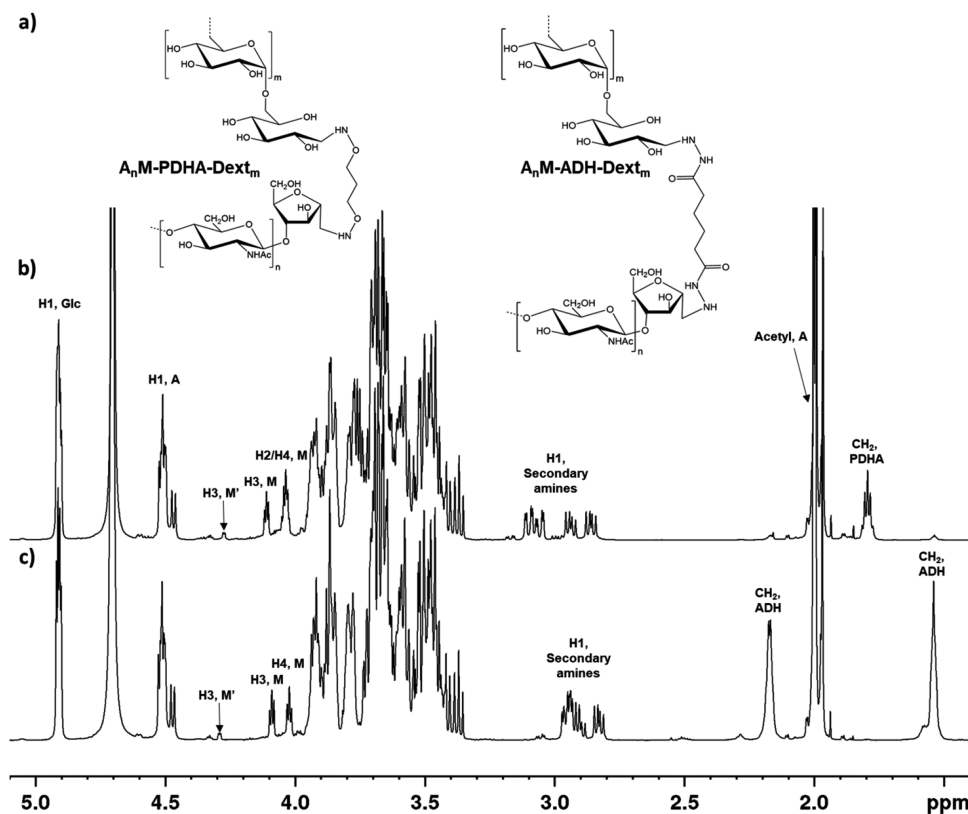
N-pyranosides with ADH.<sup>5,32</sup> Kinetic constants are given in Table 3.

It may first be noted that dextran oligomers, in agreement with previous findings,<sup>5</sup> are much less reactive toward ADH and PDHA compared to A<sub>n</sub>M oligomers (data for A<sub>n</sub>M in Table 1). This is due to the pending aldehyde of the reducing end of the latter being more reactive, as it does not participate in an aldehyde/hemiacetal equilibrium. Second, the rate constants for forming N-pyranosides (*k*<sub>3</sub> and *k*<sub>4</sub>) are 2 orders of magnitude larger for ADH compared to PDHA. For ADH, they are 5–6 orders of magnitude larger than *k*<sub>1</sub> and *k*<sub>2</sub>. Hence, the first step (E- and Z-formation) is rate limiting, although E- and Z-hydrazones are hardly detected during the reaction with ADH.

The rate constants in Table 3 suggest that dextran oligomers react faster with A<sub>n</sub>M-ADH and A<sub>n</sub>M-PDHA compared to free ADH and PDHA. To allow a more direct comparison, we used the rate constants for the conjugation of Dext<sub>5</sub> to free ADH (2 equiv) to simulate the rate (*t*<sub>0.5</sub> and *t*<sub>0.9</sub>) and yield for the reaction with equimolar proportions of Dext<sub>5</sub> and amines (Supporting Information, S15). As observed for the A<sub>n</sub>M oligomers, dextran reacted faster, and resulted in a higher yield, with the A<sub>3</sub>M-ADH or -PDHA conjugates than with free ADH or PDHA. Hence, the second attachment is indeed faster in both cases.

Equilibrium yields obtained with equimolar amounts of dextran and A<sub>3</sub>M-ADH/PDHA were only 15% for ADH, but 66% for PDHA. However, improved yields can be expected during reduction of the equilibrium mixture because of the slow reduction of unreacted dextran. Since dextran-based hydrazones and oximes are slowly reduced by PB at RT,<sup>5</sup> the reduction was performed using 20 equiv PB at increased temperature (40 °C). Reaction products were fractionated by GFC and analyzed by <sup>1</sup>H NMR (Supporting Information, S15).

By integration of the GFC chromatogram, the relative yield of A<sub>3</sub>M-PDHA-Dext<sub>6</sub> diblocks was 92% after 72 h, whereas for A<sub>3</sub>M-ADH-Dext<sub>6</sub>, we obtained about 85% diblocks after 144 h of reduction (Supporting Information, S15). The higher yield and shorter reaction times for PDHA diblocks is partly ascribed to the higher equilibrium yield prior to reduction. Moreover, the almost complete formation of N-pyranosides reduces the reduction rate of dextran-ADH conjugates considerably.<sup>5</sup> It may also be noted that at 40 °C some reduction of unreacted dextran occurred (Supporting Information, S15), but the rate was low compared to reduction of unreacted A<sub>n</sub>M. Hence, an increased yield of diblocks can be obtained after addition of reductant in the dextran systems compared to the A<sub>n</sub>M systems. The general structures of chitin-*b*-dextran diblocks prepared with ADH and PDHA and



**Figure 10.** (a) General structure of chitin-*b*-dextran diblocks prepared with ADH or PDHA.  $^1\text{H}$  NMR spectra of the reduced and purified (b)  $\text{A}_5\text{M}$ -PDHA-Dext $_6$  diblock and the (c)  $\text{A}_5\text{M}$ -ADH-Dext $_6$  diblock.

$^1\text{H}$  NMR spectra of reduced and purified  $\text{A}_5\text{M}$ -*b*-Dext $_6$  diblocks are given in Figure 10.

Based on the results of this study, two strategies for the preparation of  $\text{A}_n\text{M}$ -*b*-dextran block polysaccharides can be proposed. For the strategy where dextran is conjugated to the free end of ADH or PDHA in  $\text{A}_n\text{M}$  conjugates (discussed above), the attachment of the second block is time-consuming since dextran oligomers react more slowly with ADH/PDHA compared to the highly reactive  $\text{A}_n\text{M}$  oligomers. Moreover, the reduction of dextran-based hydrazones and oximes also is slow. However, in contrast to the  $\text{A}_n\text{M}$  oligomers, unreacted dextran oligomers are reduced at a low rate under the given conditions and hence, a high yield of diblocks can be obtained (even under equimolar proportions), even though this strategy requires long reaction times for attachment of the second block.

An alternative strategy is to reverse the protocol and prepare ADH- or PDHA-activated dextran oligomers in the first step. Due to the slow reduction of dextran oligomers, activation using a large excess of ADH or PDHA can be performed as a conventional one-pot reductive amination. The subsequent conjugation of  $\text{A}_n\text{M}$  oligomers to the free end of ADH or PDHA takes advantage of the high reactivity of the terminal M residue of the  $\text{A}_n\text{M}$  oligomers, and the attachment of the

second block (both conjugation and reduction) is time-efficient compared to opposite strategy. However, this strategy is restricted by the rapid reduction of unreacted  $\text{A}_n\text{M}$  oligomers, which will limit the yield of diblocks (if reacted in an equimolar ratio).

An excess of one of the blocks will in both strategies lead to faster kinetics and a higher yield of diblocks. However, an excess of the second block will render some or all the unreacted oligomers inactive after reduction (most relevant for an excess of  $\text{A}_n\text{M}$  oligomers, but also relevant for dextran oligomers, as shown above). An excess of the activated oligomer conjugate will in contrast be beneficial in both strategies as activated oligomers can be recycled. Both the above-mentioned strategies require purification after diblock formation, and in this study, GFC was proven useful. However, purification by block-specific solvents is clearly a possibility deserving future attention. Hence, which strategy is better therefore depends on factors such as which oligomer or conjugate can be used in excess ("value" of reactants) and the available purification steps. It may also be noted that improved equilibrium yields can be obtained by increasing the absolute concentrations of reactants. However, higher concentrations are not compatible with very long chains due to solubility and viscosity issues, and in any case, the reductant (PB) will



certainly be insoluble at very high concentrations. Heterogeneous systems may be worth exploring further, but this is outside the scope of the present work.

The strategies described above should also be relevant for chitosan oligomers prepared by nitrous acid degradation ( $D_nM$  type). However, self-branching is an issue for such oligomers.<sup>18</sup> Hence, the strategy where an excess of activated conjugates is used will be advantageous for such oligomers.

## CONCLUSIONS

In this work we have first studied in detail the activation of chitin oligosaccharides with the highly reactive 2,5-anhydro-D-mannose at the reducing end ( $A_nM$ ) by ADH and PDHA as a basis for the preparation of chitin-based diblock polysaccharides. Kinetic constants for both the formation and dissociation of oximes and hydrazones, as well as for their irreversible reduction to the corresponding secondary amines using PB were determined. Rate constants were essentially independent of the chain length and could be used to model the reactions for a wide range of concentrations of reagents. The high susceptibility to reduction of M residues (by both PB and  $\text{NaCNBH}_3$ ) was circumvented by a two-step procedure thanks to the excellent equilibrium yields prior to reduction. The free ends of ADH or PDHA activated oligomers had higher reactivities compared to free ADH or PDHA. Hence, attachment of a second block to form diblocks was therefore feasible and could easily be modeled kinetically. Examples include  $A_nM$ -*b*- $MA_n$  and  $A_nM$ -*b*-dextran. For the latter, a “reverse” strategy of reacting  $A_nM$  with ADH- or PDHA-activated dextran is also a viable alternative thanks to the high reactivity of the terminal M residue.

Regarding potential applications, water-soluble chitin oligomers activated with PDHA or ADH would be ideally suited for conjugation with biomolecules in aqueous solvents. Strong phase separation of copolymers containing chitin blocks is also expected in solution or in the bulk due to the very high solubility parameter of chitin.<sup>33,34</sup> A wide range of self-assembled structures could then potentially be obtained from chitin-based block copolymers. Chitin, including chitin oligomers, is also known to play important roles in activating immune responses against fungal pathogens in both mammals<sup>35</sup> and in plants<sup>36</sup> and are used in the agricultural industry as plant growth stimulators.<sup>37</sup> Terminally conjugated chitin-based block polymers or block polysaccharides hence offer a wide range of new and possibly bioactive materials. These may, on one hand, take advantage of the uninterrupted chitin sequences needed for interacting with chitin receptors and, on the other hand, have additional bioactivities due to the second chain.

## ASSOCIATED CONTENT

### Supporting Information

The Supporting Information is available free of charge at <https://pubs.acs.org/doi/10.1021/acs.biomac.0c00620>.

Additional data and explanations are given in S1–S15 (PDF)

## AUTHOR INFORMATION

### Corresponding Authors

Christophe Schatz – *Laboratoire de Chimie des Polymères Organiques (LCPO), Université de Bordeaux, 33600 Pessac, France; Email: [schatz@enscbp.fr](mailto:schatz@enscbp.fr)*

Bjørn E. Christensen – *NOBIPOL, Department of Biotechnology and Food Science, NTNU - Norwegian University of Science and Technology, Trondheim, Norway; [orcid.org/0000-0001-9640-0225](https://orcid.org/0000-0001-9640-0225); Email: [bjorn.e.christensen@ntnu.no](mailto:bjorn.e.christensen@ntnu.no)*

## Authors

Ingrid Vikøren Mo – *NOBIPOL, Department of Biotechnology and Food Science, NTNU - Norwegian University of Science and Technology, Trondheim, Norway*

Marianne Øksnes Dalheim – *NOBIPOL, Department of Biotechnology and Food Science, NTNU - Norwegian University of Science and Technology, Trondheim, Norway*

Finn L. Aachmann – *NOBIPOL, Department of Biotechnology and Food Science, NTNU - Norwegian University of Science and Technology, Trondheim, Norway; [orcid.org/0000-0003-1613-4663](https://orcid.org/0000-0003-1613-4663)*

Complete contact information is available at: <https://pubs.acs.org/10.1021/acs.biomac.0c00620>

## Notes

The authors declare no competing financial interest.

## ACKNOWLEDGMENTS

This work was supported by a grant from the Norwegian University of Science and Technology to I.V. Mo, and Grants 268490, 226244, and 221576 from the Research Council of Norway. C.S. wishes to thank the Agence Nationale de la Recherche for its support under the program TANGO (ANR-16-CE09-0020-01).

## REFERENCES

- (1) Volokhova, A. S.; Edgar, K. J.; Matson, J. B. Polysaccharide-containing block copolymers: synthesis and applications. *Mater. Chem. Front.* **2020**, *4*, 99–112.
- (2) Schatz, C.; Lecommandoux, S. Polysaccharide-Containing Block Copolymers: Synthesis, Properties and Applications of an Emerging Family of Glycoconjugates. *Macromol. Rapid Commun.* **2010**, *31* (19), 1664–1684.
- (3) Novoa-Carballeda, R.; Muller, A. H. E. Synthesis of polysaccharide-*b*-PEG block copolymers by oxime click. *Chem. Commun.* **2012**, *48* (31), 3781–3783.
- (4) Bondalapati, S.; Ruvinov, E.; Kryukov, O.; Cohen, S.; Brik, A. Rapid End-Group Modification of Polysaccharides for Biomaterial Applications in Regenerative Medicine. *Macromol. Rapid Commun.* **2014**, *35* (20), 1754–1762.
- (5) Mo, I. V.; Feng, Y.; Dalheim, M. Ø.; Solberg, A.; Aachmann, F. L.; Schatz, C.; Christensen, B. E. Activation of enzymatically produced chito oligosaccharides by dioxyamines and dihydrazides. *Carbohydr. Polym.* **2020**, *232*, 115748.
- (6) Xiao, Y.; Chinoy, Z. S.; Pecaistaings, G.; Bathany, K.; Garanger, E.; Lecommandoux, S. Design of Polysaccharide-*b*-Elastin-Like Polypeptide Bioconjugates and Their Thermoresponsive Self-Assembly. *Biomacromolecules* **2020**, *21* (1), 114–125.
- (7) Rosselgong, J.; Chemin, M.; Almada, C. C.; Hemery, G.; Guigner, J.-M.; Chollet, G.; Labat, G.; Da Silva Perez, D.; Ham-Pichavant, F.; Grau, E.; Grelrier, S.; Lecommandoux, S.; Cramail, H. Synthesis and Self-Assembly of Xylan-Based Amphiphiles: From Bio-Based Vesicles to Antifungal Properties. *Biomacromolecules* **2019**, *20* (1), 118–129.
- (8) Tiwari, V. K.; Mishra, B. B.; Mishra, K. B.; Mishra, N.; Singh, A. S.; Chen, X. Cu-Catalyzed Click Reaction in Carbohydrate Chemistry. *Chem. Rev.* **2016**, *116* (5), 3086–3240.
- (9) Breitenbach, B. B.; Schmid, I.; Wich, P. R. Amphiphilic Polysaccharide Block Copolymers for pH-Responsive Micellar Nanoparticles. *Biomacromolecules* **2017**, *18* (11), 3844–3845.

- (10) Feng, F.; Sun, J.; Radhakrishnan, G. V.; Lee, T.; Bozsoki, Z.; Fort, S.; Gavrin, A.; Gysel, K.; Thygesen, M. B.; Andersen, K. R.; Radutoiu, S.; Stougaard, J.; Oldroyd, G. E. D. A combination of chitoooligosaccharide and lipochitoooligosaccharide recognition promotes arbuscular mycorrhizal associations in *Medicago truncatula*. *Nat. Commun.* **2019**, *10* (1), 5047.
- (11) Ahmed, A. B. A.; Taha, R. M.; Mohajer, S.; Elaagib, M. E.; Kim, S. K. Preparation, properties and biological applications of water soluble chitin oligosaccharides from marine organisms. *Russ. J. Mar. Biol.* **2012**, *38* (4), 351–358.
- (12) Roby, D.; Gabelle, A.; Toppan, A. Chitin oligosaccharides as elicitors of Chitinase activity in melon plants. *Biochem. Biophys. Res. Commun.* **1987**, *143* (3), 885–892.
- (13) Azuma, K.; Osaki, T.; Minami, S.; Okamoto, Y. Anticancer and Anti-Inflammatory Properties of Chitin and Chitosan Oligosaccharides. *J. Funct. Biomater.* **2015**, *6* (1), 33–49.
- (14) Kadokawa, J.-I.; Karasu, M.; Tagaya, H.; Chiba, K. Synthesis of a Block Copolymer Consisting of Oligocellulose and Oligochitin. *J. Macromol. Sci., Part A: Pure Appl. Chem.* **1996**, *33* (11), 1735–1743.
- (15) Kadokawa, U.-I.; Yamashita, K.; Karasu, M.; Tagaya, H.; Chiba, K. Preparation and Enzymatic Hydrolysis of Block Copolymer Consisting of Oligochitin and Poly(Propylene Glycol). *J. Macromol. Sci., Part A: Pure Appl. Chem.* **1995**, *32* (7), 1273–1280.
- (16) Allan, G. G.; Peyron, M. Molecular-Weight Manipulation of Chitosan 0.1. Kinetics of Depolymerization by Nitrous-Acid. *Carbohydr. Res.* **1995**, *277* (2), 257–272.
- (17) Tømmeraaas, K.; Vårum, K. M.; Christensen, B. E.; Smidsrød, O. Preparation and characterisation of oligosaccharides produced by nitrous acid depolymerisation of chitosans. *Carbohydr. Res.* **2001**, *333* (2), 137–144.
- (18) Tømmeraaas, K.; Strand, S. P.; Christensen, B. E.; Smidsrød, O.; Vårum, K. M. Preparation and characterization of branched chitosans. *Carbohydr. Polym.* **2011**, *83* (4), 1558–1564.
- (19) Moussa, A.; Crepet, A.; Ladaviere, C.; Trombotto, S. Reducing-end “clickable” functionalizations of chitosan oligomers for the synthesis of chitosan-based diblock copolymers. *Carbohydr. Polym.* **2019**, *219*, 387–394.
- (20) Pickenhahn, V. D.; Darras, V.; Dziopa, F.; Binięcki, K.; De Crescenzo, G.; Lavertu, M.; Buschmann, M. D. Regioselective thioacetylation of chitosan end-groups for nanoparticle gene delivery systems. *Chem. Sci.* **2015**, *6* (8), 4650–4664.
- (21) Coudurier, M.; Faivre, J.; Crepet, A.; Ladaviere, C.; Delair, T.; Schatz, C.; Trombotto, S. Reducing-End Functionalization of 2,5-Anhydro-d-mannofuranose-Linked Chitoooligosaccharides by Dioxamine: Synthesis and Characterization. *Molecules* **2020**, *25* (5), 1143.
- (22) Ruhaak, L. R.; Steenvoorden, E.; Koeleman, C. A. M.; Deelder, A. M.; Wührer, M. 2-Picoline-borane: A non-toxic reducing agent for oligosaccharide labeling by reductive amination. *Proteomics* **2010**, *10* (12), 2330–2336.
- (23) Cosenza, V. A.; Navarro, D. A.; Stortz, C. A. Usage of  $\alpha$ -picoline borane for the reductive amination of carbohydrates. *ARKIVOC* **2011**, *12*, 182–194.
- (24) Fang, J.; Qin, G.; Ma, J.; She, Y.-M. Quantification of plant cell wall monosaccharides by reversed-phase liquid chromatography with 2-aminobenzamide pre-column derivatization and a non-toxic reducing reagent 2-picoline borane. *J. Chromatogr. A* **2015**, *1414*, 122–128.
- (25) Unterrieser, I.; Mischnick, P. Labeling of oligosaccharides for quantitative mass spectrometry. *Carbohydr. Res.* **2011**, *346* (1), 68–75.
- (26) Chen, J.; Spiering, G.; Mosquera-Giraldo, L.; Moore, R. B.; Edgar, K. J. Regioselective Bromination of the Dextran Nonreducing End Creates a Pathway to Dextran-Based Block Copolymers. *Biomacromolecules* **2020**, *21*, 1729–1738.
- (27) Li, B.; Wang, Q.; Wang, X.; Wang, C.; Jiang, X. Preparation, drug release and cellular uptake of doxorubicin-loaded dextran-*b*-poly( $\epsilon$ -caprolactone) nanoparticles. *Carbohydr. Polym.* **2013**, *93* (2), 430–437.
- (28) Vårum, K. M.; Antohansen, M. W.; Grasdalen, H.; Smidsrød, O. Determination of the degree of N-acetylation and the distribution of N-acetyl groups in partially N-deacetylated chitins (chitosans) by high-field n.m.r. spectroscopy. *Carbohydr. Res.* **1991**, *211* (1), 17–23.
- (29) Lindberg, B.; Lönngrén, J.; Svensson, S., Specific Degradation of Polysaccharides. In *Adv. Carbohydr. Chem. Biochem.*; Tipson, R. S., Derek, H., Eds.; Academic Press, 1975; Vol. 31, pp 185–240.
- (30) Baudendistel, O. R.; Wieland, D. E.; Schmidt, M. S.; Wittmann, V. Real-Time NMR Studies of Oxamine Ligations of Reducing Carbohydrates under Equilibrium Conditions. *Chem. - Eur. J.* **2016**, *22* (48), 17359–17365.
- (31) Gilmore, K.; Vukelić, S.; McQuade, D. T.; Koksche, B.; Seeberger, P. H. Continuous Reductions and Reductive Aminations Using Solid NaBH<sub>4</sub>. *Org. Process Res. Dev.* **2014**, *18* (12), 1771–1776.
- (32) Kwase, Y. A.; Cochran, M.; Nitz, M., Protecting-Group-Free Glycoconjugate Synthesis: Hydrazide and Oxamine Derivatives in N-Glycoside Formation. In *Modern Synthetic Methods in Carbohydrate Chemistry: From Monosaccharides to Complex Glycoconjugates*; Werz, D. B., Vidal, S., Eds.; Wiley, 2013; pp 67–96.
- (33) Ravindra, R.; Krovvidi, K. R.; Khan, A. A. Solubility parameter of chitin and chitosan. *Carbohydr. Polym.* **1998**, *36* (2), 121–127.
- (34) Lehnert, R. J.; Kandelbauer, A. Comments on “Solubility parameter of chitin and chitosan” *Carbohydrate Polymers* 36 (1998) 121–127. *Carbohydr. Polym.* **2017**, *175*, 601–602.
- (35) Fuchs, K.; Cardona Gloria, Y.; Wolz, O.-O.; Herster, F.; Sharma, L.; Dillen, C. A.; Täumer, C.; Dickhöfer, S.; Bittner, Z.; Dang, T.-M.; Singh, A.; Haischer, D.; Schöffel, M. A.; Koymans, K. J.; Sanmuganatham, T.; Krach, M.; Roger, T.; Le Roy, D.; Schilling, N. A.; Frauhammer, F.; Miller, L. S.; Nürnberger, T.; LeibundGut-Landmann, S.; Gust, A. A.; Macek, B.; Frank, M.; Gouttefangeas, C.; Dela Cruz, C. S.; Hartl, D.; Weber, A. N. The fungal ligand chitin directly binds TLR2 and triggers inflammation dependent on oligomer size. *EMBO Rep.* **2018**, *19* (12), e46065.
- (36) Gao, F.; Zhang, B.-S.; Zhao, J.-H.; Huang, J.-F.; Jia, P.-S.; Wang, S.; Zhang, J.; Zhou, J.-M.; Guo, H.-S. Deacetylation of chitin oligomers increases virulence in soil-borne fungal pathogens. *Nature Plants* **2019**, *5* (11), 1167.
- (37) Schmitz, C.; González Auza, L.; Koberidze, D.; Rasche, S.; Fischer, R.; Bortesi, L. Conversion of Chitin to Defined Chitosan Oligomers: Current Status and Future Prospects. *Mar. Drugs* **2019**, *17* (8), 452.

# Supporting Information

## 2,5-Anhydro-D-mannose end-functionalised chitin oligomers activated by dioxyamines or dihydrazides as precursors of diblock oligosaccharides

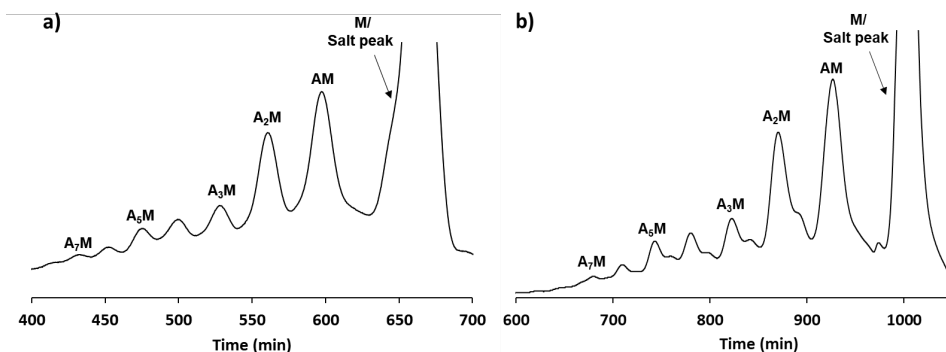
Ingrid Vikøren Mo, Marianne Øksnes Dalheim, Finn L. Aachmann, Christophe Schatz, Bjørn E. Christensen

### Contents

S1 Preparation and characterization of A <sub>n</sub> M oligomers.....	2
S2 Conjugation of A <sub>n</sub> M oligomers to ADH and PDHA studied by time course NMR .....	3
S3 Kinetic modelling of the reductive amination reaction.....	5
S4 Modelling of A <sub>n</sub> M conjugation reactions .....	7
S5 Spontaneous decomposition of reducing agents .....	8
S6 Reduction of A <sub>n</sub> M oligomers .....	10
S7 Reduction of A <sub>n</sub> M conjugates.....	14
S8 Modelling of A <sub>n</sub> M reduction reactions .....	16
S9 Optimisation of preparative protocols .....	16
Statistical distribution of mono-, di- and unsubstituted ADH and PDHA .....	16
Minimisation of disubstituted ADH or PDHA.....	19
Optimisation of reduction conditions for PDHA conjugates .....	20
Preparation of A <sub>n</sub> M conjugates using optimised protocols.....	20
S10 2D NMR characterization of the reduced and purified A <sub>2</sub> M-PDHA.....	22
S11 Preparation of chitin- <i>b</i> -chitin diblocks from activated chitin oligomers (A <sub>4</sub> M-ADH).....	25
S12 Preparation of chitin- <i>b</i> -chitin diblocks using a sub-stoichiometric amount of ADH or PDHA 28	
S13 Preparation and characterization of dextran (Dext <sub>m</sub> ) oligomers .....	32
S14 Conjugation of Dext <sub>m</sub> oligomers to ADH and PDHA studied by time course NMR .....	34
S15 Preparation of chitin- <i>b</i> -dextran diblocks .....	36
References.....	41

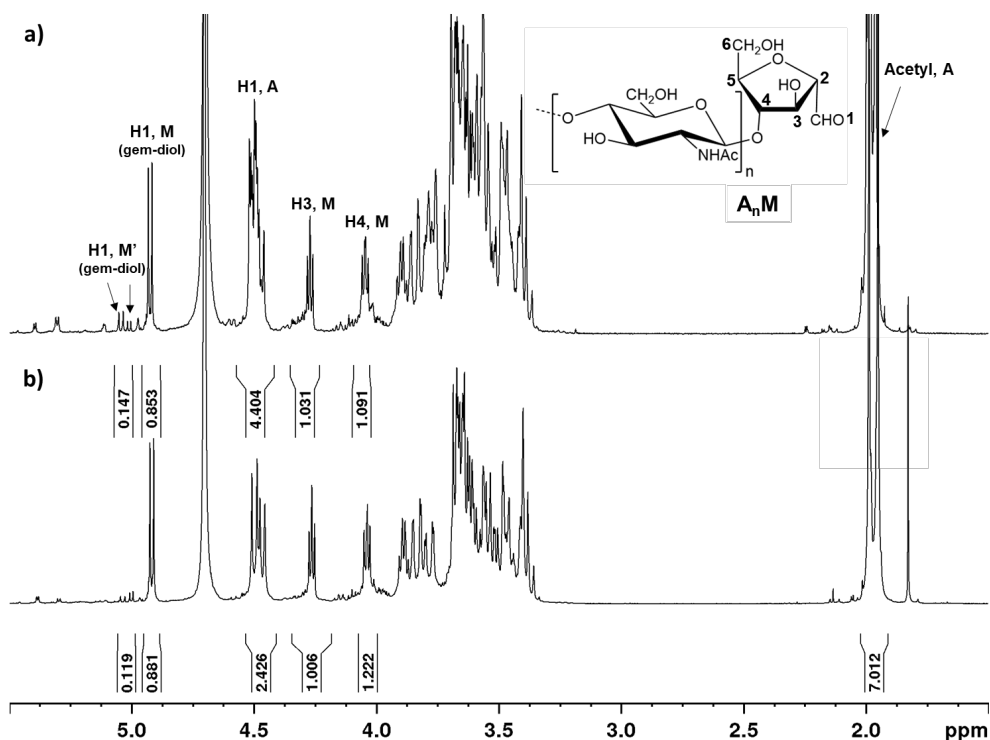
## S1 Preparation and characterization of $A_nM$ oligomers

Chitin oligomers of the type  $A_nM$ , where  $A_n$  represent uninterrupted sequences of *N*-acetyl D-glucosamine (A) residues with a 2,5-anhydro-D-mannose (M) residue at the reducing end, were prepared by nitrous acid (HONO) depolymerisation of chitosan ( $F_A = 0.48$ ), using an excess HONO (1.3 equivalents) to the fraction of D-glucosamine (D) residues<sup>1,2</sup>. The excess of HONO converts all the D residues into M residues, whereas A residues are unaffected, providing solely  $A_nM$  oligomers. The water-soluble oligomers ( $DP < 10$ ) were fractionated by preparative gel filtration chromatography (GFC) to obtain purified low molecular weight  $A_nM$  oligomers of specific DPs (Figure S1a). The chitosan with  $F_A = 0.48$  provided mainly trimers ( $A_2M$ ) and dimers (AM) (Figure S1). Separation of the oligomer mixture by analytical GFC (Figure S1b) showed shoulder peaks for all the oligomer fractions in the chromatogram. Without further investigation, shoulder peaks were suggested to be caused by the alternative forms of M (discussed below).



**Figure S1:** a) preparative and b) analytical GFC fractionation of the mixture of water-soluble  $A_nM$  ( $n = 1-8$ ) oligomers obtained by nitrous acid degradation of chitosan ( $F_A = 0.48$ ) using an excess (1.3x) of nitrous acid.

Oligomers were purified (by dialysis), freeze-dried and characterized by  $^1H$ -NMR (Figure S2). The  $^1H$ -NMR spectra were annotated according to literature<sup>2,3</sup>. The doublet at approximately 4.9 ppm was assigned to the gem-diol (hydrated aldehyde) of the reducing end M residue. Additional doublets in the anomeric region (4.95-5.1 ppm) were assigned to alternative forms of the as M residue suggested in the literature by Lindberg et al<sup>4</sup> marked as  $M'$  in all figures. Purified  $A_nM$  oligomers were slightly polydisperse due to the incomplete baseline separation by the preparative GFC (Figure S1a). The polydispersity of the oligomers was confirmed by the  $^1H$ -NMR characterization of  $A_4M$  and  $A_2M$  in Figure S2a and S2b, respectively, where the integral of H1, A was higher than expected relative to the sum of the integrals of H1, M and H1,  $M'$  (expected ratio 4:1 and 2:1 for  $A_4M$  and  $A_2M$ , respectively).

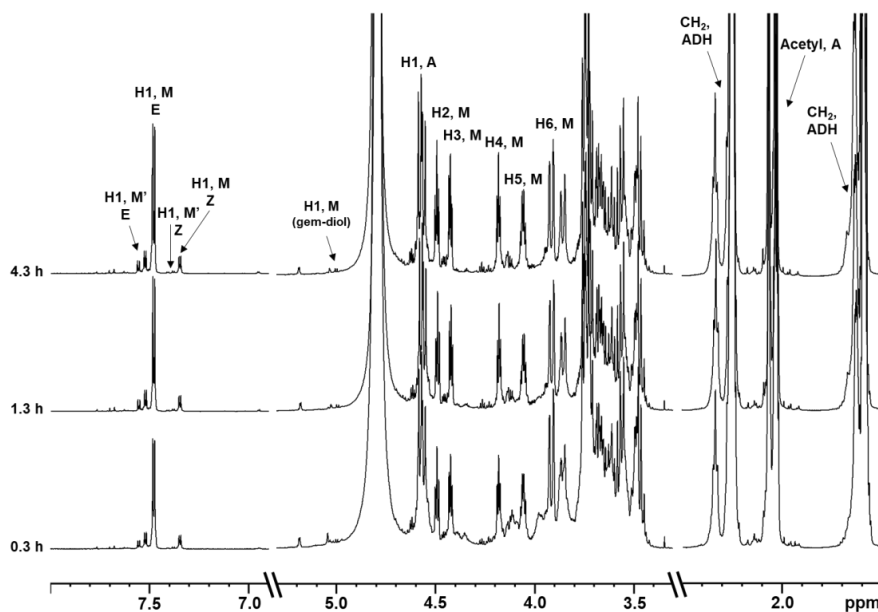


**Figure S2:**  $^1\text{H-NMR}$  characterization of fractionated and purified **a)**  $\text{A}_4\text{M}$  and **b)**  $\text{A}_2\text{M}$  in  $\text{D}_2\text{O}$  including annotations and integrals (600 MHz). M' refers to alternative (minor) forms of M (see S2).

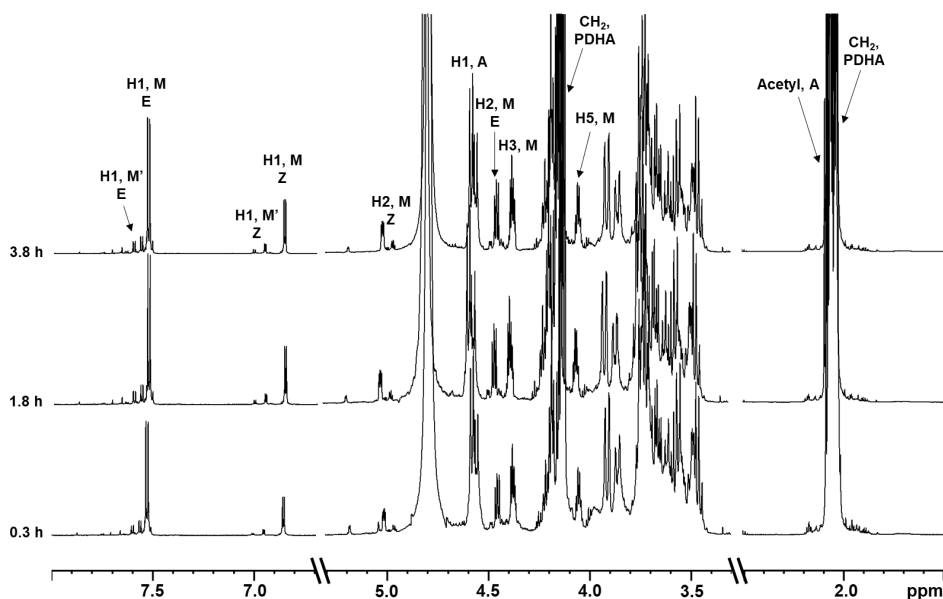
## S2 Conjugation of $\text{A}_n\text{M}$ oligomers to ADH and PDHA studied by time course NMR

Conjugation of  $\text{A}_n\text{M}$  oligomers to ADH and PDHA was monitored by time course NMR as described earlier<sup>5</sup>. In brief, conjugation reactions were performed in deuterated NaAc-buffer (with TSP added as internal standard) at pH 3.0, 4.0 or 5.0 using 2 equivalents of ADH or PDHA relative to the concentration of oligomers (20.1 mM).  $^1\text{H-NMR}$  spectra were recorded at specific time points (Figure S3 and S4) and yields of conjugates were determined by integration of the obtained spectra. Minor resonances close to the major resonances from the hydrazones/oximes (H1, M E or Z) were attributed to the conjugation of oligomers with alternative forms of the M residue (H1, M' E or Z) (assigned in Figure S3 and S4). Both the major and minor resonances from the E and Z hydrazones or oximes were integrated to obtain the yield of conjugates. Due to overlapping resonances (e.g. H2, M Z overlapping with H1, M (gem-diol) in Figure S4), yields could not be calculated from the sum of integrals from the H1 reducing end proton resonances in each individual spectrum. Due to the slight polydispersity of the oligomers, the yields could not be calculated from the integrals of the resonances resulting from

the oligomers. Therefore, the integral of the resonance from the internal standard (TSP, 0 ppm) was used as reference to calculate yields. As the conjugates were reduced in a subsequent step (see below) the integral value of the TSP resonance was related to the integrals of the resonances from the completely reduced conjugates (for each individual reaction mixture). The TSP integral value was set to this specific value in all the spectra obtained during the time course NMR study for the conjugation and reduction to calculate the yields of conjugates and subsequently reduced secondary amine conjugates during the reactions. The yields were calculated based on the assumption of 100 % yield of reduced secondary amine conjugates. Integrals of overlapping resonances were calculated by subtraction.



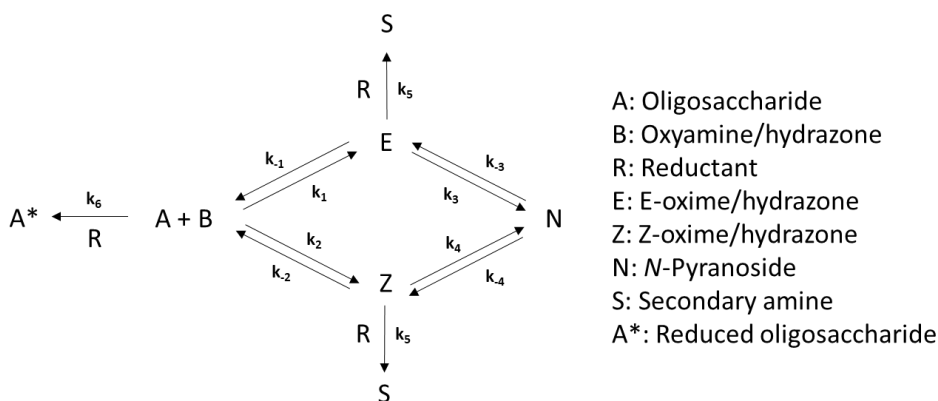
**Figure S3:** <sup>1</sup>H-NMR spectra obtained at defined time points for the conjugation reaction with A<sub>2</sub>M (20.1 mM) and 2 equivalents ADH at pH 4.0, RT.



**Figure S4:**  $^1\text{H}$ -NMR spectra obtained at defined time points for the conjugation reaction with  $\text{A}_2\text{M}$  (20.1 mM) and 2 equivalents PDHA at pH 4.0, RT.

### S3 Kinetic modelling of the reductive amination reaction

The reductive amination of oligosaccharides with different amines (e.g. oxyamines (PDHA) or hydrazides (ADH)) is comprised of several individual reactions with independent rates and rate constants. The overall reaction involves the conjugation (amination) of the oligosaccharide, where E- and Z- oximes or hydrazones (Schiff bases) are formed for oxyamines or hydrazides, respectively. For oligosaccharides where the reducing end aldehyde is in equilibrium with a hemiacetal (normal reducing end), the acyclic Schiff bases are in equilibrium with cyclic *N*-glycosides (e.g. *N*-pyranosides). By adding a reducing agent, the Schiff bases will be irreversibly reduced forming secondary amine conjugates. Irreversible reduction of oligosaccharides by the reducing agent will prevent the reductive amination reaction from going to completion. The general reaction scheme is shown in Figure S5.



**Figure S5:** General reaction scheme for the reductive amination of oligosaccharides with normal reducing ends including assigned rate constants for each independent reaction involved. Reversible reactions are described by two rate constants (forward and reverse), whereas irreversible reactions are described by one rate constant (the scheme indicates the assumption that reduction of E and Z had the same rate constant ( $k_5$ )).

When considering the reactions to be *first order* with respect to each reactant, reaction rates can be determined by the following equations

$$\frac{d[A]}{dt} = -k_1[A][B] + k_{-1}[E] - k_2[A][B] + k_{-2}[Z] - k_6[A][R]$$

$$\frac{d[B]}{dt} = -k_1[A][B] + k_{-1}[E] - k_2[A][B] + k_{-2}[Z]$$

$$\frac{d[R]}{dt} = -k_5[E][R] - k_5[Z][R] - k_6[A][R]$$

$$\frac{d[E]}{dt} = k_1[A][B] - k_{-1}[E] - k_3[E] + k_{-3}[N] - k_5[E][R]$$

$$\frac{d[Z]}{dt} = k_2[A][B] - k_{-2}[Z] - k_4[Z] + k_{-4}[N] - k_5[Z][R]$$

$$\frac{d[N]}{dt} = k_3[E] - k_{-3}[N] + k_4[Z] - k_{-4}[N]$$

$$\frac{d[A^*]}{dt} = k_6[A][R]$$

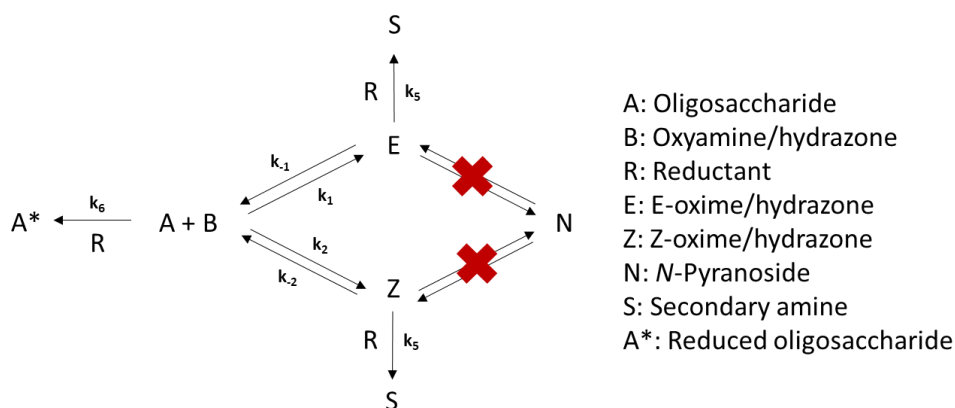
The concentration of each reactant or product at specific time points,  $[X]_t$ , can be obtained from the reaction rates by the following equation

$$[X]_t = [X]_{t-\Delta t} + \frac{d[X]}{dt} \Delta t$$



where,  $t$  is the time, and  $\Delta t$  is the time difference from last modelled time point. The numeric modelling was carried out using Excel, generally substituting differentials of the type  $d[X]/dt$  with  $\Delta[X]/\Delta t$ . From starting concentrations  $[A]_0$ ,  $[B]_0$  etc, the concentrations at successive time increments  $t_{i+1} = t_i + \Delta t$  were inductively calculated as  $[X]_{i+1} = [X]_i + (\Delta[X]_i/\Delta t)\Delta t$ . The time interval ( $\Delta t$ ) was chosen sufficiently small to result in a simulation which did not further change when choosing an even smaller time interval. All reactions were modelled using this approach, and the model was fitted to the experimental data by adjusting the rate constants to give the minimum sum of squares.

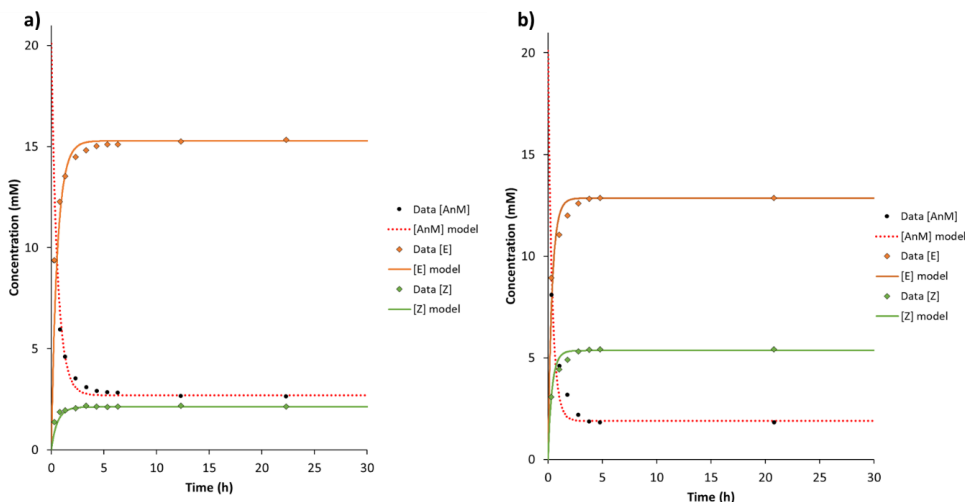
In the special case of reductive amination with chitin or chitosan oligosaccharides prepared by nitrous acid degradation, only Schiff bases (oximes/hydrazones) can be formed. Hence, the general reaction scheme for these reactions is simplified as showed in Figure S6.



**Figure S6:** General reaction scheme for the reductive amination of oligosaccharides with M residue at the reducing end including assigned rate constants for each independent reaction involved.

#### S4 Modelling of $A_nM$ conjugation reactions

Conjugation reactions (no reducing agent present) with  $A_nM$  oligomers were studied by time course NMR (S2). The experimental data obtained for the conjugation reactions were fitted using the model described in S3 (based on the reaction scheme presented in Figure S6). Examples of the data fitting for the conjugation of  $A_2M$  oligomers to ADH and PDHA (2 equivalents) at pH 4.0 are given in Figure S7.



**Figure S7:** Model fitting of experimental data obtained at pH 4.0, RT for the reactions with  $A_2M$  and 2 equivalents of a) ADH or b) PDHA.

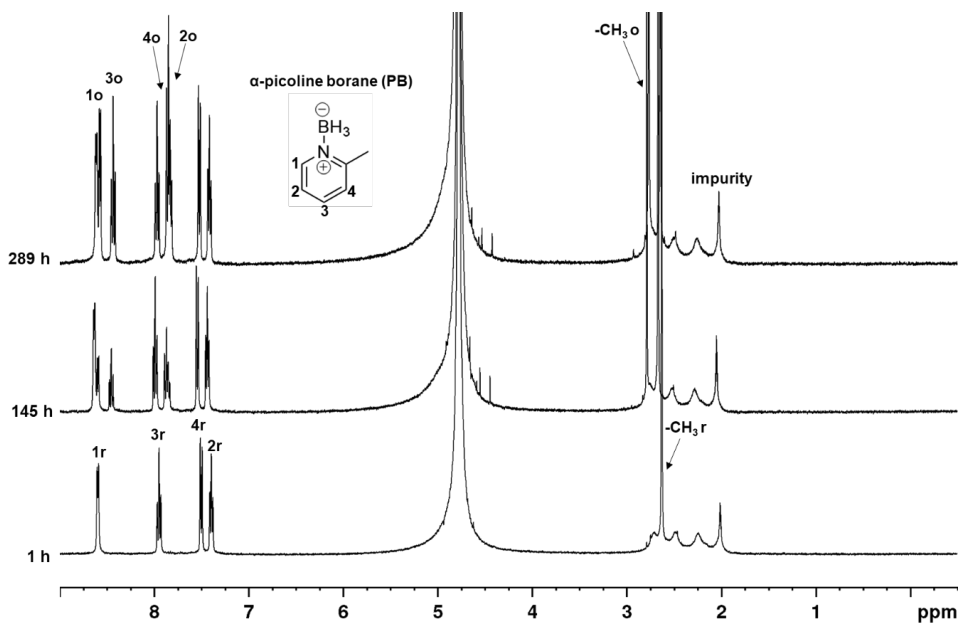
### S5 Spontaneous decomposition of reducing agents

The decomposition of  $\alpha$ -picoline borane (PB) and sodium cyanoborohydride ( $NaCNBH_3$ ) in 500 mM deuterated NaAc-buffer, pH 4.0, was monitored by NMR. The two reducing agents have distinct resonances in the  $^1H$ -NMR spectrum and hence, their decomposition was studied. In contrast to  $NaCNBH_3$ , which is completely dissolved in the buffer, PB has low initial solubility, but dissolves slowly over time (observed by increased intensity of the resonances over time).

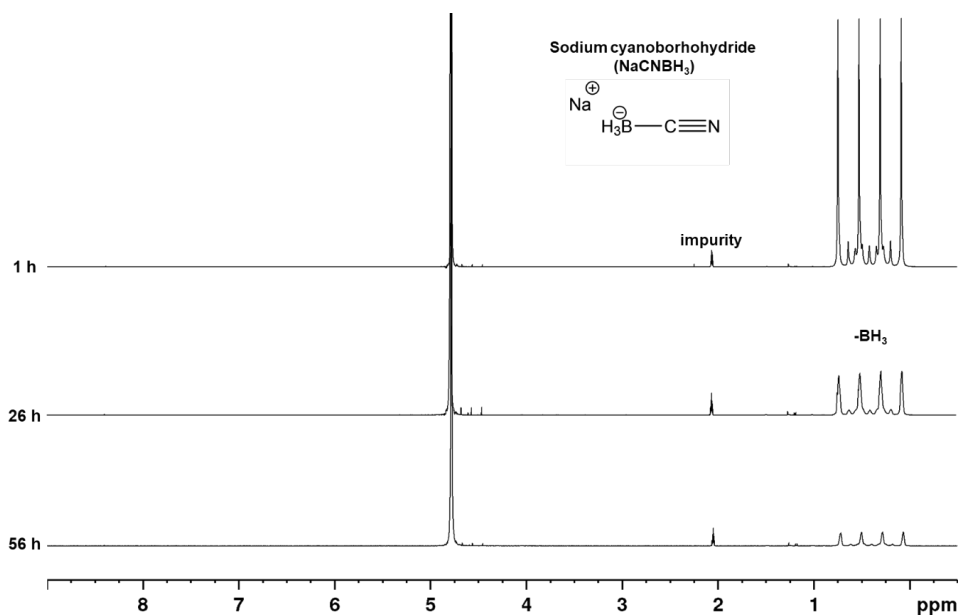
The protons of the pyridine ring in PB give resonances with chemical shifts in the range 7.2 to 8.7 ppm, whereas the protons of the methyl group give one resonance with a chemical shift of approximately 2.6 ppm (Figure S8). The protons of the  $-BH_3$  group are not visible in the  $^1H$ -NMR spectrum due to negative chemical shifts. When PB is oxidised (o), the proton resonances are moved slightly downfield as seen in Figure S8. The relative reductive power (%) for PB over time was calculated by relating the intensity of the protons resulting from the reduced form of PB (r) to the total amount of dissolved PB (r+o) (Figure S8).

In contrast to PB, the proton resonances of the  $-BH_3$  group in  $NaCNBH_3$  are within the NMR scale (0 – 8 ppm).  $NaCNBH_3$  lacks other protons and hence, it was not possible to study the oxidation of this reducing agent. Therefore, the decomposition was related to the reduced intensity of the resonances from the protons in the  $-BH_3$  group relative to an impurity in the buffer (Figure S9). As the first spectrum was obtained after one hour, the intensity of the resonances at  $t = 0$  was obtained by extrapolation. The relative reductive power (%) for  $NaCNBH_3$  was related to the decomposition of the reducing agent. By comparing the change in relative reductive power (%) for the two reducing agents

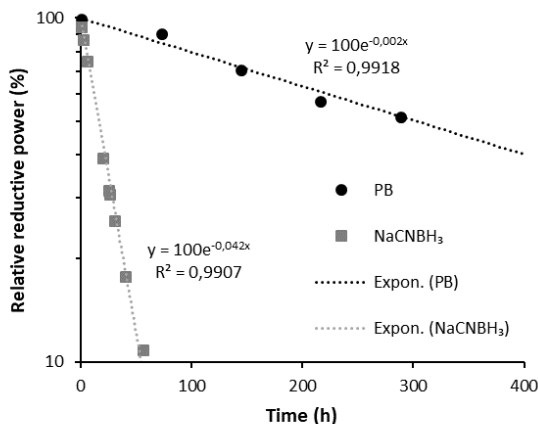
over time (Figure S10), NaCNBH<sub>3</sub> was shown to decompose approximately 20 times faster than PB in the buffer.



**Figure S8:** Spontaneous decomposition of PB in deuterated acetate buffer (500 mM, pH 4.0, RT) monitored by time course NMR.



**Figure S9:** Spontaneous decomposition of NaCNBH<sub>3</sub> in deuterated NaAc-buffer (500 mM, pH 4.0, RT) monitored by time course NMR.

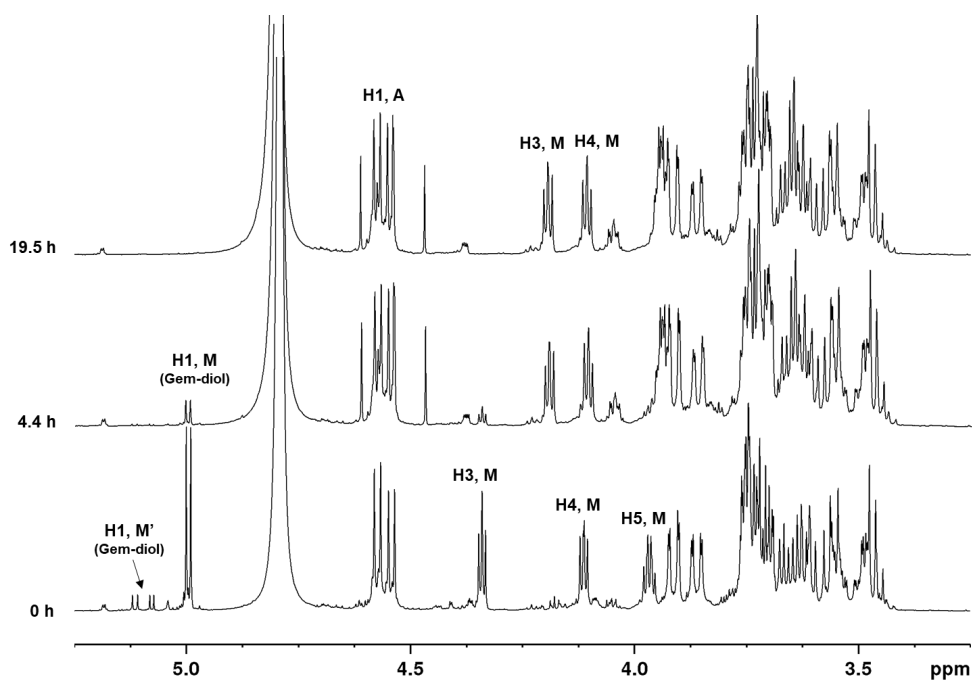


**Figure S10:** Change in relative reductive power (%) of PB and NaCNBH<sub>3</sub> over time in deuterated NaAc-buffer (500 mM, pH 4.0, RT).

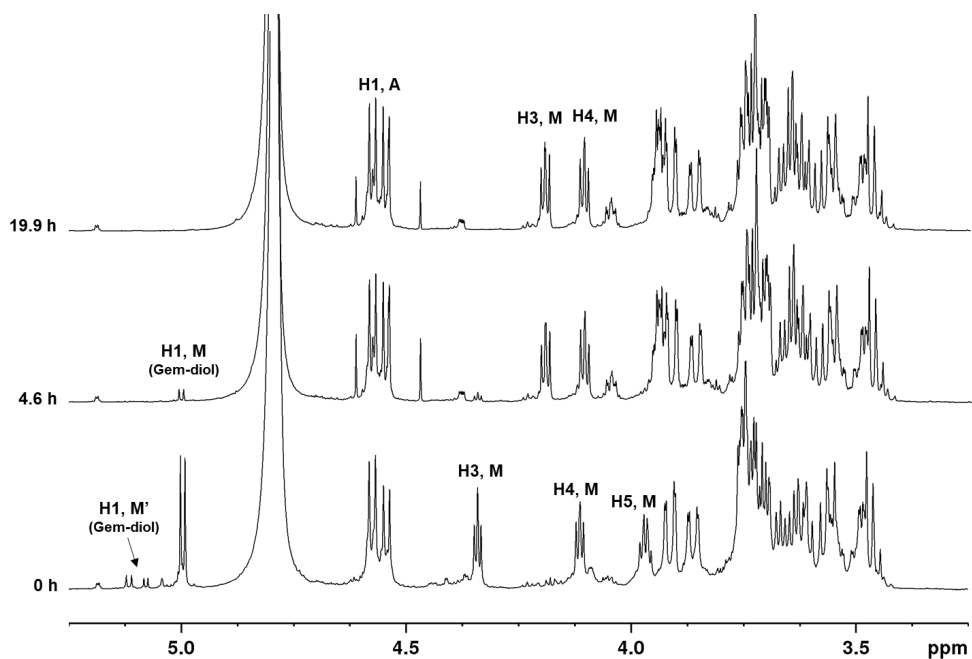
### S6 Reduction of A<sub>n</sub>M oligomers

Reduction of A<sub>n</sub>M oligomers was performed by adding 3 equivalents reducing agent (PB or NaCNBH<sub>3</sub>) to oligomers dissolved in deuterated NaAc-buffer. The course of the reduction was studied by monitoring the disappearance of reducing end gem-diol resonances (H1, M and H1, M'). Resonance intensities were related to the internal standard (TSP). Reduction of A<sub>n</sub>M oligomers by PB was studied at pH 3.0, 4.0 or 5.0 (Figure S11-S13) or by NaCNBH<sub>3</sub> at pH 4.0 (Figure S14).

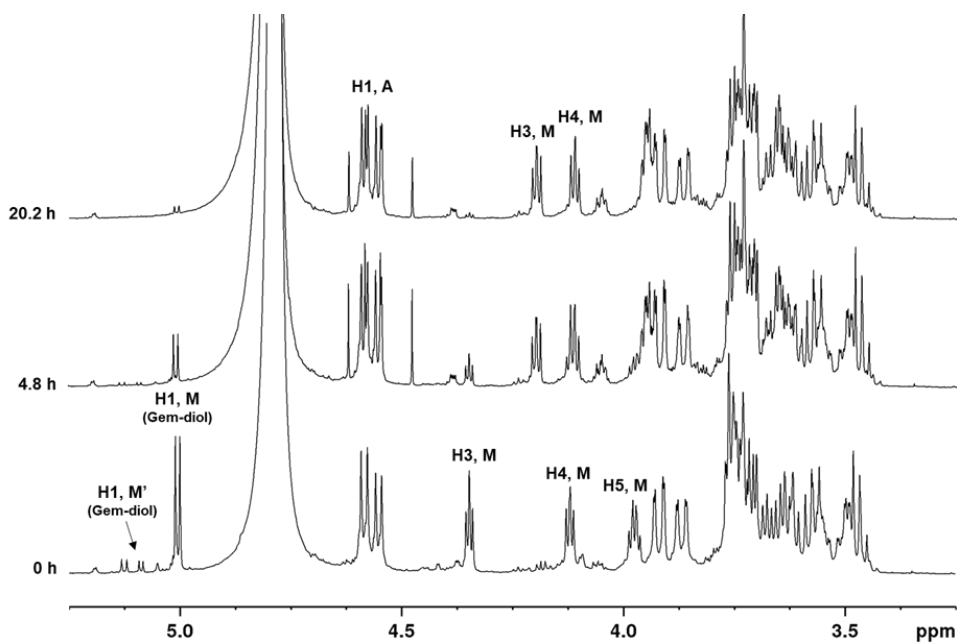
For comparison, reduction of AA oligomers (normal reducing end) was studied using 3 equivalents PB (Figure S15) or NaCNBH<sub>3</sub> (Figure S16) at pH 4.0. In contrast to the A<sub>n</sub>M oligomers, no detectable reduction in the intensity of the reducing end resonances for AA was observed. However, the relative ratio of the α- to β- reducing end resonances gradually changed (Figure S15). For this experiment AA was dissolved in the buffer shortly before PB was added and the first spectrum was obtained.



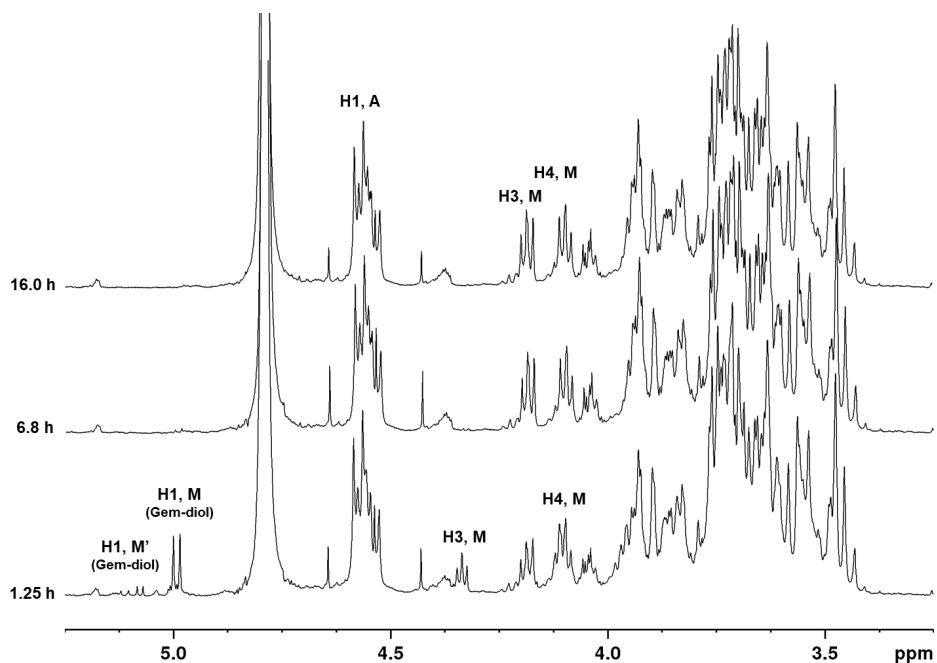
**Figure S11:** <sup>1</sup>H-NMR spectra obtained at defined time points for the reduction of A<sub>2</sub>M oligomers (20.1 mM) in deuterated acetate buffer, pH 3.0, RT using 3 equivalents PB (60.3 mM).



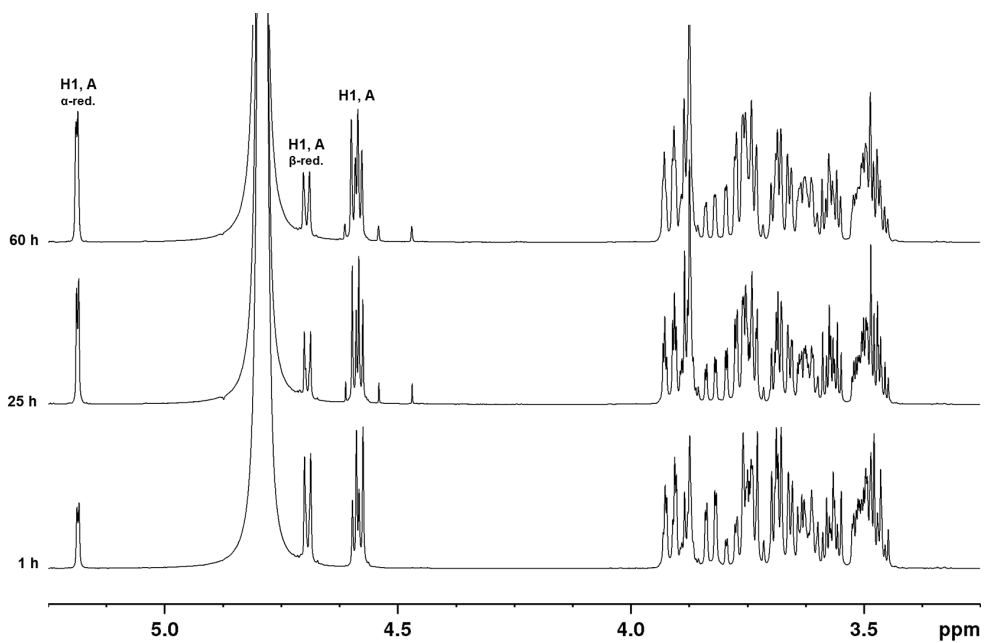
**Figure S12:** <sup>1</sup>H-NMR spectra obtained at defined time points for the reduction of A<sub>2</sub>M oligomers (20.1 mM) in deuterated acetate buffer, pH 4.0, RT using 3 equivalents PB (60.3 mM).



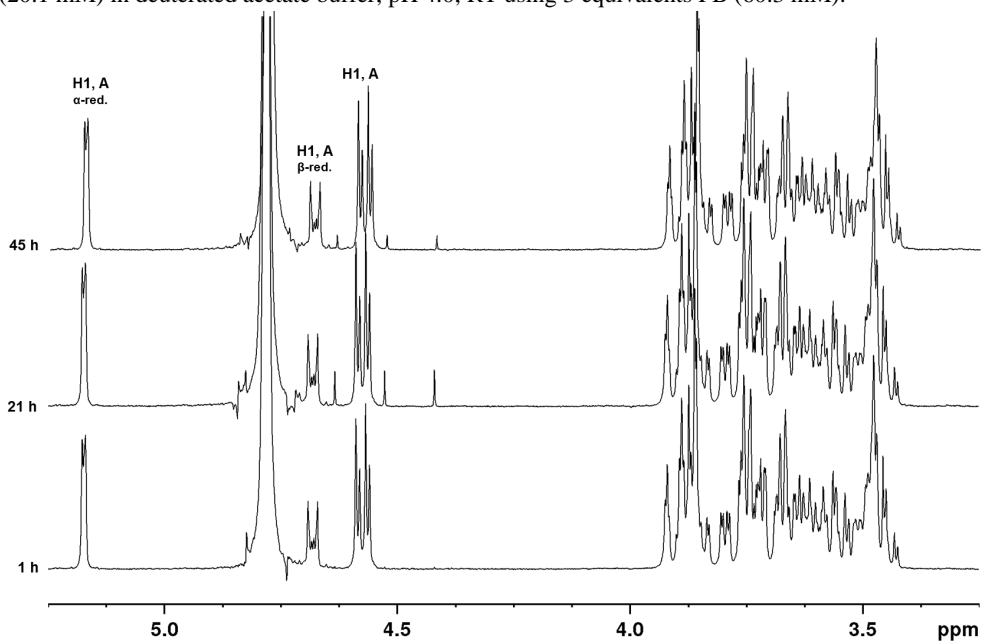
**Figure S13:** <sup>1</sup>H-NMR spectra obtained at defined time points for the reduction of A<sub>2</sub>M oligomers (20.1 mM) in deuterated acetate buffer, pH 5.0, RT using 3 equivalents PB (60.3 mM).



**Figure S14:** <sup>1</sup>H-NMR spectra obtained at defined time points for the reduction of A<sub>3</sub>M oligomers (20.1 mM) in deuterated acetate buffer, pH 4.0, RT using 3 equivalents NaCNBH<sub>3</sub> (60.3 mM).



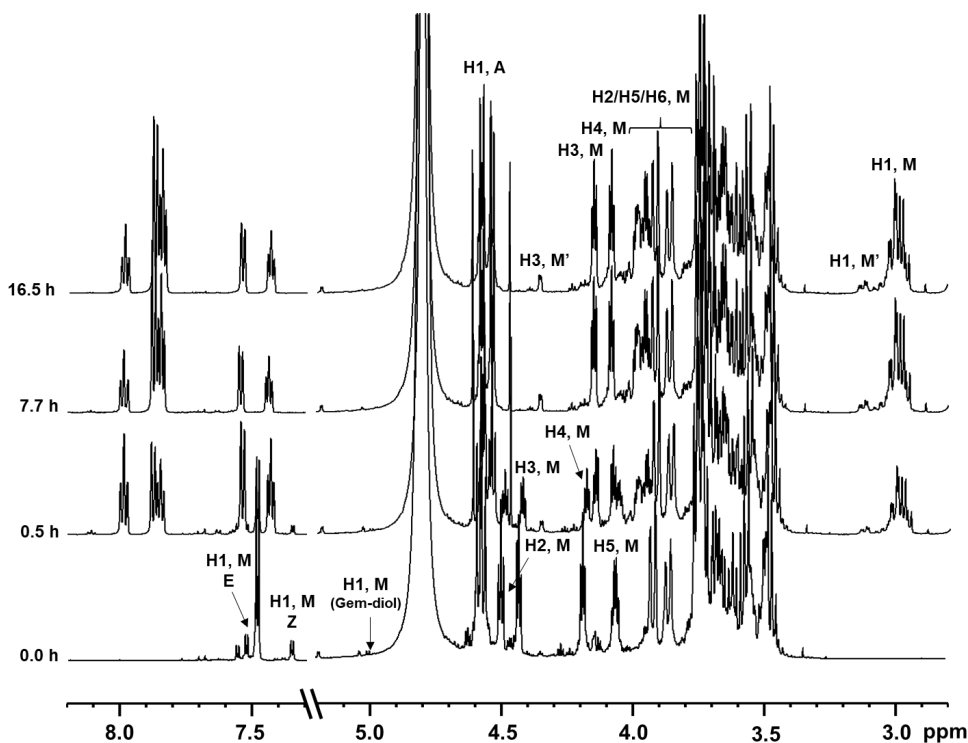
**Figure S15:** <sup>1</sup>H-NMR spectra obtained at defined time points for the reduction of AA oligomers (20.1 mM) in deuterated acetate buffer, pH 4.0, RT using 3 equivalents PB (60.3 mM).



**Figure S16:** <sup>1</sup>H-NMR spectra obtained at defined time points for the reduction of AA oligomers (20.1 mM) in deuterated acetate buffer, pH 4.0, RT using 3 equivalents NaCNBH<sub>3</sub> (60.3 mM).

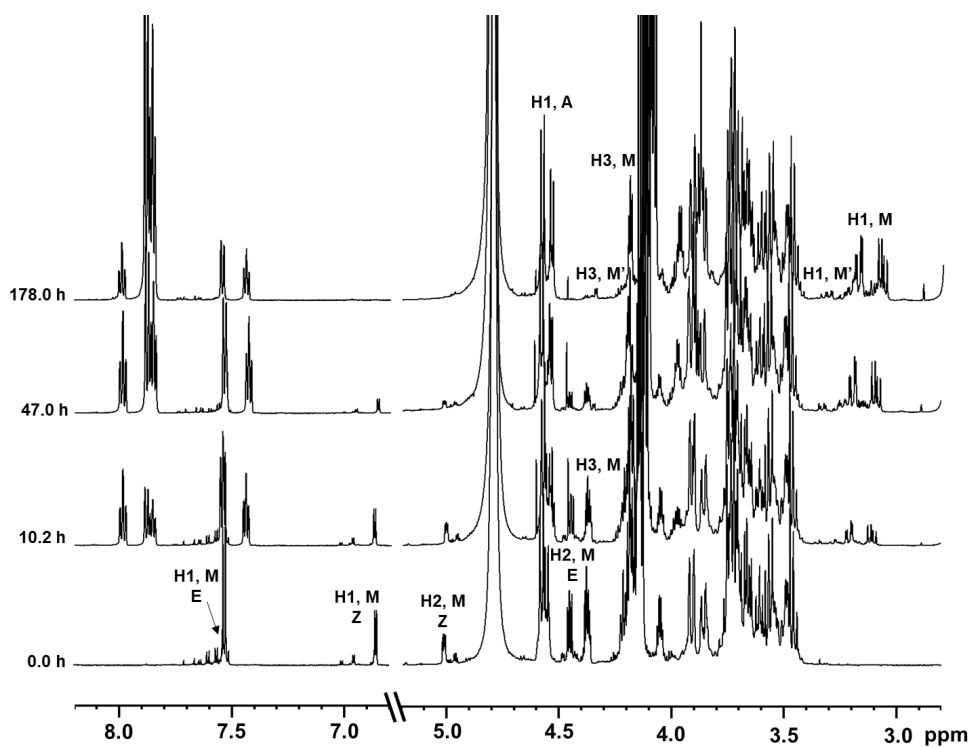
## S7 Reduction of A<sub>n</sub>M conjugates

Reduction of A<sub>n</sub>M conjugates was studied by adding 3 equivalents reducing agent (PB or NaCNBH<sub>3</sub>) to the equilibrium mixtures of conjugates (pH 3.0, 4.0 or 5.0). The course of the reduction was studied by monitoring the disappearance of hydrazone or oxime proton resonances and the appearance methylene proton resonances from the reduced secondary amine conjugates (at approximately 3 ppm) over time. Due to the overlap of the methylene proton resonances from the different forms of the M residue after reduction, the total resonance area (2.9 – 3.35 ppm) was integrated to give the yield of reduced conjugates. <sup>1</sup>H-NMR spectra obtained at different time points for the reduction of A<sub>2</sub>M-ADH and A<sub>2</sub>M-PDHA conjugates by 3 equivalents PB at pH 4.0 are given in Figure S17 and S18, respectively. The kinetics of the reduction is given in Figure S19 a and b, respectively. For the reduction of A<sub>n</sub>M-PDHA conjugates, E-oxime resonances (H1, M E) overlapped with one of the resonances from the reduced form of PB (Figure S18). Hence, this integral was obtained by subtraction.

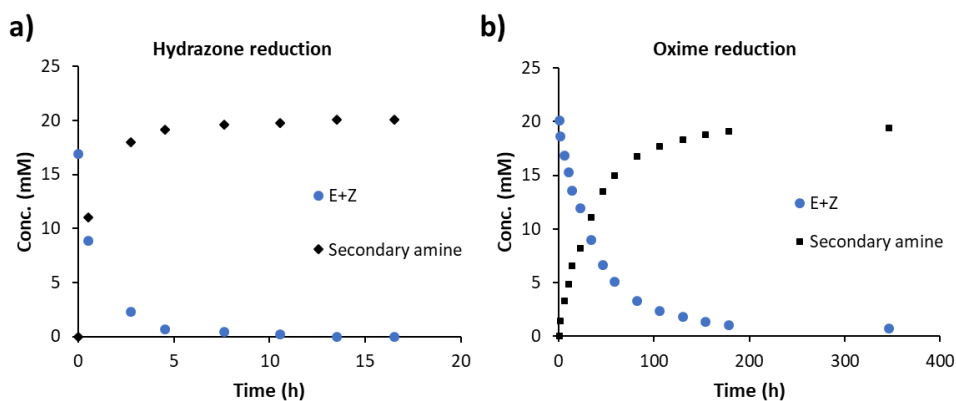


**Figure S17:** <sup>1</sup>H-NMR spectra obtained at defined time points for the reduction of A<sub>2</sub>M-ADH conjugates (prepared using 2 equivalents ADH) by 3 equivalents (60.3 mM) PB at pH 4.0, RT. Resonances from the unreduced conjugate and unreacted oligomer are annotated in the first two spectra, whereas resonances from the reduced secondary amine conjugate are annotated in the last obtained spectrum (16.5 h).





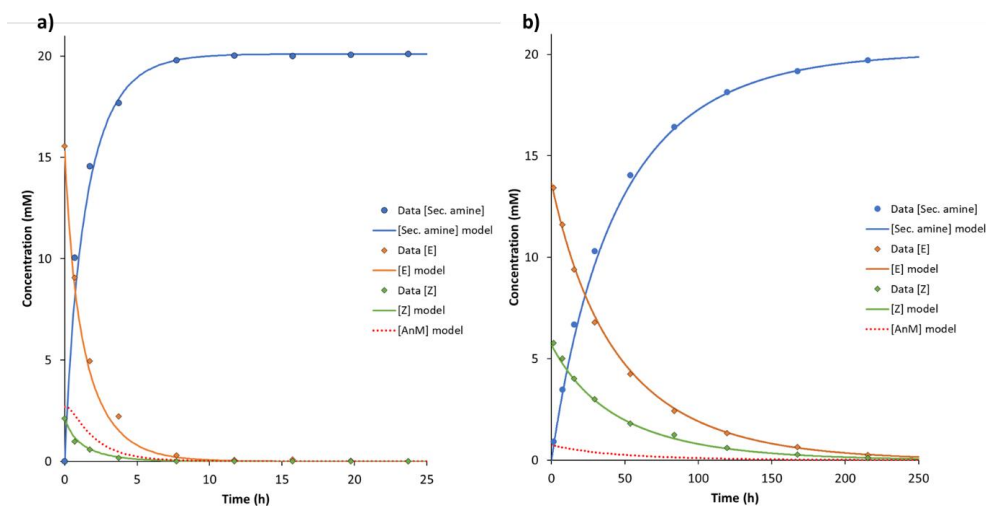
**Figure S18:**  $^1\text{H}$ -NMR spectra obtained at defined time points for the reduction of  $\text{A}_2\text{M}$ -PDHA conjugates (prepared using 2 equivalents PDHA) by 3 equivalents (60.3 mM) PB at pH 4.0, RT. Resonances from the unreduced conjugate and unreacted oligomer are annotated in the first two spectra, whereas resonances from the reduced secondary amine conjugate are annotated in the last obtained spectrum (178 h).



**Figure S19:** Kinetics of the reaction obtained from the spectra in Figure S17 and S18 for the reduction of **a)**  $\text{A}_2\text{M}$ -ADH (hydrazone) conjugates and **b)**  $\text{A}_2\text{M}$ -PDHA (oxime) conjugates by 3 equivalents PB at pH 4.0, RT, respectively.

## S8 Modelling of $A_nM$ reduction reactions

Using the rate constants and equilibrium yields obtained for the conjugation of  $A_nM$  to 2 equivalents ADH or PDHA, the experimental data obtained for the reduction of conjugates (studied by time course NMR, S7) were fitted using the model described in S3 (based on the reaction scheme presented in Figure S6). Examples for the data fitting for the reduction  $A_2M$ -ADH or  $A_2M$ -PDHA conjugates using 3 equivalents PB at pH 4.0 (RT) are given in Figure S20 a and b, respectively. The addition of reducing agent to the equilibrium mixture of conjugates was set as  $t = 0$ . Due to overlapping resonances and low resolution in the NMR spectra, the yield of unreacted oligomers ( $[A_nM]$  in the model) was not monitored. However, the model also predicts the consumption of unreacted oligomers based on the yield of conjugates and the rate of reduction (Figure S20).



**Figure S20:** Model fitted to the experimental data obtained for reduction of  $A_2M$ -ADH (a) and  $A_2M$ -PDHA (b) conjugates using 3 equivalents PB at pH 4.0, RT.

## S9 Optimisation of preparative protocols

### Statistical distribution of mono-, di- and unsubstituted ADH and PDHA

The relative amount of unsubstituted, monosubstituted and disubstituted ADH and PDHA can be calculated assuming the reactivities of the two termini are identical. Such estimates are primarily intended to determine how much ADH or PDHA should be used for mono-substitution (activation) without producing too much disubstituted species.

Definitions and main relations:

$[A_nM]_0$ : Initial molar concentration of oligosaccharide

$[L]_0$ : Initial molar concentration of ADH or PDHA

$[-NH_2]_0$ : Initial molar concentration of terminal amine

Let  $a$  be defined as the equivalence of linker (ADH or PDHA) relative to oligosaccharide before reaction. Hence:

$$[L]_0 = a[A_nM]_0$$

Since we treat each terminal amine as a separate and independent reactant we may further write:

$$[-NH_2]_0 = 2[L]_0 = 2a[A_nM]_0$$

Let  $b$  be defined as the fraction of oligosaccharide that has become substituted.  $b$  is obtained directly from the equilibrium yields listed in Table 1. Hence,  $b[A_nM]_0$  becomes the molar concentration of substituted oligosaccharide, which must necessarily equal the molar concentration of substituted amine. The fraction of substituted amines ( $p$ ) thus becomes:

$$p = b \frac{[A_nM]_0}{[-NH_2]_0} = b \frac{[A_nM]_0}{2[L]_0} = \frac{b}{2a}$$

Hence,  $p$  is a simple function of the fraction of substituted oligosaccharide ( $b$ ) and the molar equivalence of linker ( $a$ ). For statistical distributions fractions and probabilities are interchangeable. Hence:

The probability that both ends are substituted, fraction of disubstituted species ( $f_{DS}$ ) =  $p^2$

The probability that none of the ends are substituted, fraction of unsubstituted species ( $f_{US}$ ) =  $(1 - p)^2$

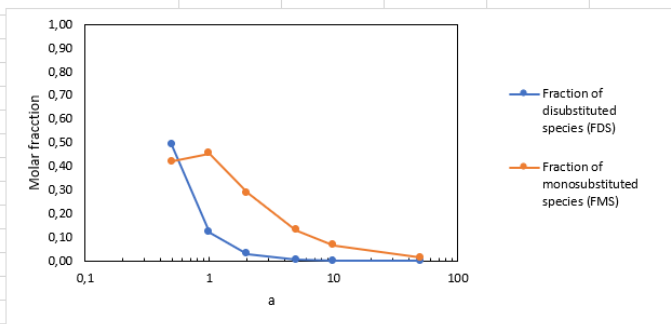
The probability that one end is substituted, fraction of monosubstituted species ( $f_{MS}$ ) =  $1 - p^2 - (1 - p)^2 = 2p - 2p^2 = 2p(1-p)$

$b$  is obtained directly from the equilibrium yields given in Table 1. As an example, the reaction between  $A_2M$  and 2 equivalents of ADH ( $a = 2$ ) at pH 4.0 is considered. The equilibrium yield of substituted oligosaccharides obtained by NMR was 87 % and hence,  $b = 0.87$ . Then  $p$  becomes:

$$p = \frac{0.87}{4} = 0.22$$

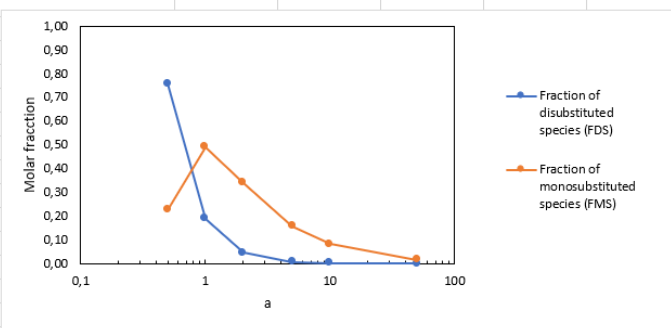
and  $f_{DS}$  is  $(0.22)^2 = 0.0484 = 5\%$ . When 10 equivalents of ADH is used (i.e.  $a = 10$ ) and we assume  $b = 0.87$ ,  $f_{DS}$  is reduced to  $0.002 = 0.2\%$ . Examples of the statistical distribution of mono-, di- and unsubstituted species with different equivalents of linker ( $a$ ) and fractions of substituted oligomer ( $b$ ) are given in Figure S21-S23.

$a$	Equivalents linker	0,5	1	2	5	10	50
$b$	Fraction substituted oligomer	0,70	0,70	0,70	0,70	0,70	0,70
$p$		0,700	0,350	0,175	0,070	0,035	0,007
	Fraction of disubstituted species ( $F_{DS}$ )	0,490	0,123	0,031	0,005	0,001	0,000
	Fraction of monosubstituted species ( $F_{MS}$ )	0,420	0,455	0,289	0,130	0,068	0,014
	Fraction of unsubstituted species ( $F_{US}$ )	0,090	0,423	0,681	0,865	0,931	0,986
	Ratio mono-/disubstituted species	0,86	3,71	9,43	26,57	55,14	283,71



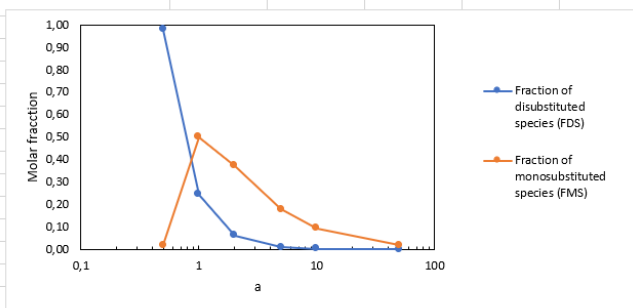
**Figure S21:** Statistical distribution of mono-, di- and unsubstituted species with different equivalents of linker ( $a$ ) and  $b = 0.70$ .

$a$	Equivalents linker	0,5	1	2	5	10	50
$b$	Fraction substituted oligomer	0,87	0,87	0,87	0,87	0,87	0,87
$p$		0,870	0,435	0,218	0,087	0,044	0,009
	Fraction of disubstituted species ( $F_{DS}$ )	0,757	0,189	0,047	0,008	0,002	0,000
	Fraction of monosubstituted species ( $F_{MS}$ )	0,226	0,492	0,340	0,159	0,083	0,017
	Fraction of unsubstituted species ( $F_{US}$ )	0,017	0,319	0,612	0,834	0,915	0,983
	Ratio mono-/disubstituted species	0,30	2,60	7,20	20,99	43,98	227,89



**Figure S22:** Statistical distribution of mono-, di- and unsubstituted species with different equivalents of linker ( $a$ ) and  $b = 0.87$ .

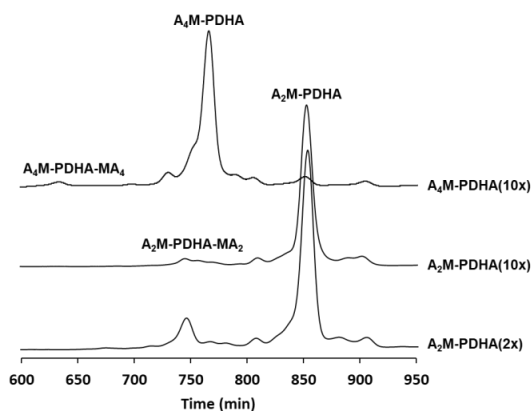
$a$	Equivalents linker	0,5	1	2	5	10	50
$b$	Fraction substituted oligomer	0,99	0,99	0,99	0,99	0,99	0,99
$p$		0,990	0,495	0,248	0,099	0,050	0,010
	Fraction of disubstituted species ( $F_{DS}$ )	0,980	0,245	0,061	0,010	0,002	0,000
	Fraction of monosubstituted species ( $F_{MS}$ )	0,020	0,500	0,372	0,178	0,094	0,020
	Fraction of unsubstituted species ( $F_{US}$ )	0,000	0,255	0,566	0,812	0,903	0,980
	Ratio mono-/disubstituted species	0,02	2,04	6,08	18,20	38,40	200,02



**Figure S23:** Statistical distribution of mono-, di- and unsubstituted species with different equivalents of linker ( $a$ ) and  $b = 0.99$ .

### Minimisation of disubstituted ADH or PDHA

As shown above the statistical amount of disubstituted ADH or PDHA is significant (5-6 %) when 2 equivalents are used, especially for high reaction yields, but decreases below 1% for 10 equivalents. This was qualitatively verified by GFC fractionation of  $A_nM$ -PDHA conjugates prepared with 2 or 10 equivalents of PDHA, respectively (Figure S24). A significant decrease in disubstituted species was observed when 10 equivalents were used. Hence, a large excess ( $\geq 10$  equivalents) is necessary to minimise the amount of disubstituted species.



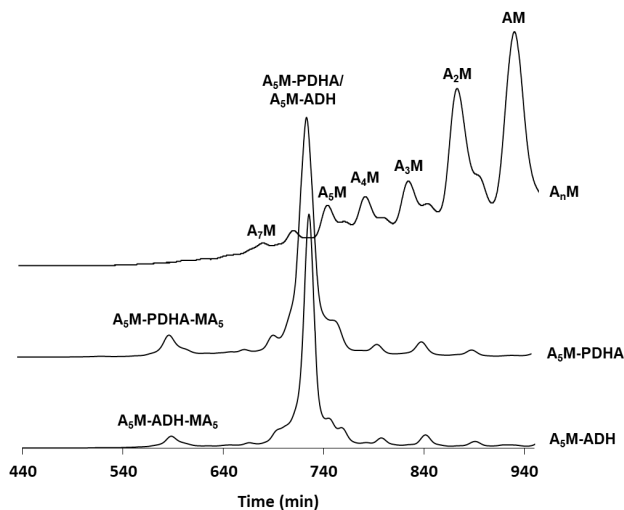
**Figure S24:** GFC fractionation of the reaction mixtures obtained for the conjugation of  $A_nM$  oligomers to 2 or 10 equivalents (2x or 10x, respectively) PDHA under otherwise standard conditions (20.1 mM oligomer, pH 4.0, RT).

### **Optimisation of reduction conditions for PDHA conjugates**

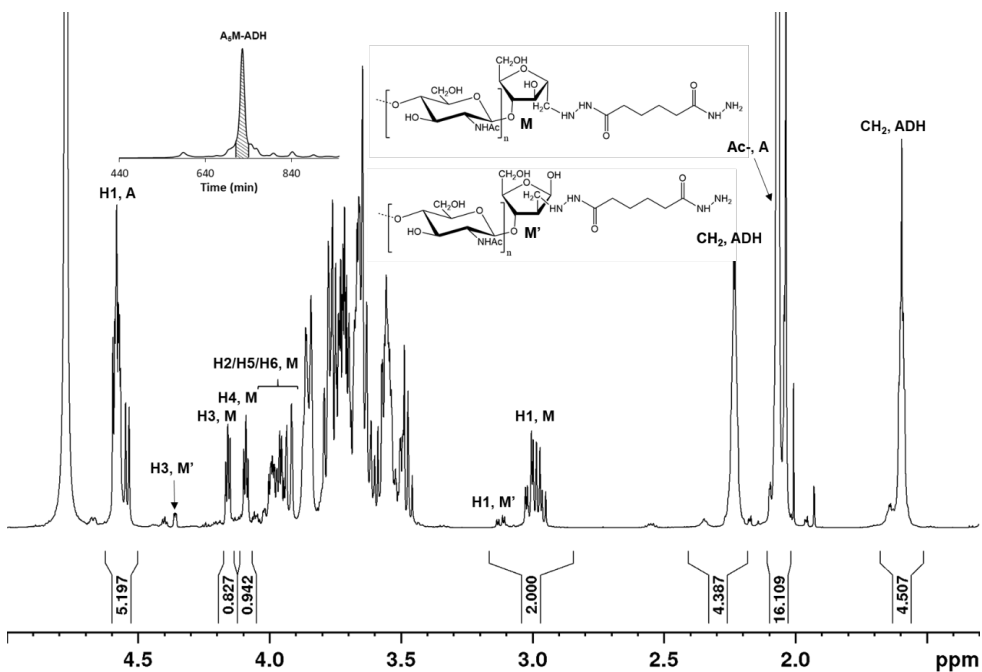
The reduction of PDHA conjugates was optimised by varying the concentration of reducing agent (PB). However, due to the low solubility of PB in the buffer, reduction of A<sub>4</sub>M-PDHA conjugates (equilibrium mixture with 10 equivalents PDHA) using 20 equivalents PB was performed in deuterated buffer in a separate vial (not in the NMR tube). The reaction was performed on a shaking device to increase the collision frequency of undissolved reducing agent and conjugates. NMR spectra of the dissolved phase of the reaction mixture was obtained after 24 and 48 hours revealing complete reduction after 48 hours.

### **Preparation of A<sub>n</sub>M conjugates using optimised protocols**

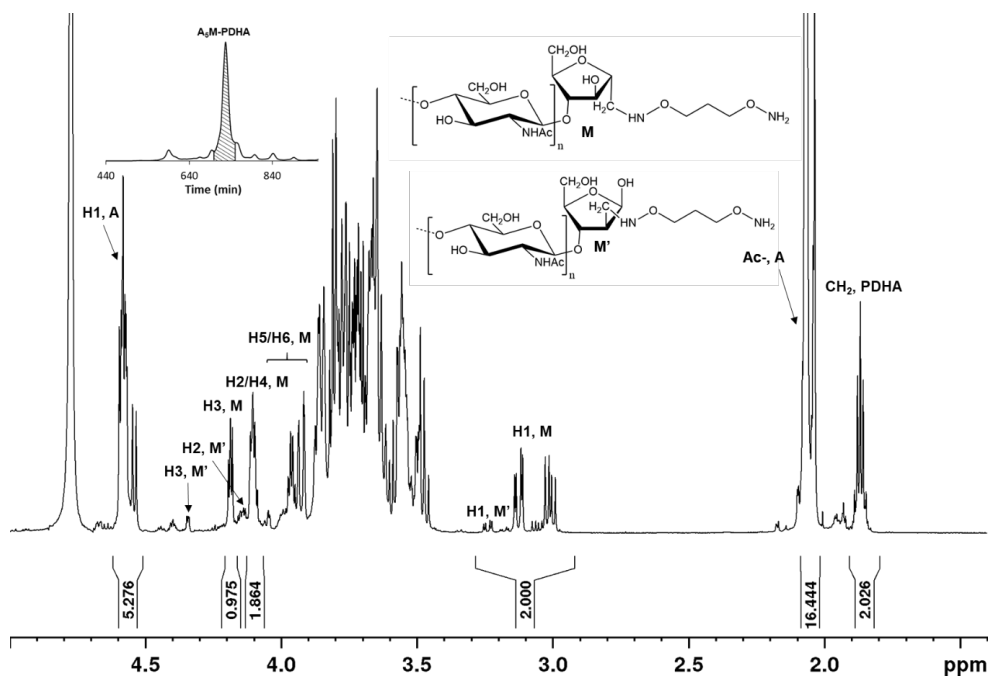
Reduced A<sub>n</sub>M conjugates (A<sub>n</sub>M-ADH and A<sub>n</sub>M-PDHA) were prepared using optimised protocols. In brief, conjugation was carried out for 6 hours at RT using 10 equivalents ADH and PDHA at pH 4.0. For ADH conjugates, reduction was performed for 24 hours at RT by adding 3 equivalents PB to the equilibrium mixture, whereas for the PDHA conjugates, 20 equivalents PB were added to the equilibrium mixture and the reduction was performed for 48 hours at RT to ensure complete reduction. Reaction mixtures were fractionated by GFC and purified conjugates were characterized by <sup>1</sup>H-NMR. Fractionation of reduced A<sub>5</sub>M-ADH and A<sub>5</sub>M-PDHA conjugates is shown in Figure S25. Fractionation of the A<sub>n</sub>M oligomer mixture is included in the figure for comparison. Small amounts of disubstituted ADH/PDHA were formed in both reactions. The relative amount of disubstituted species seemed higher than obtained for the optimised protocol using A<sub>2</sub>M oligomers (Figure S24), which may be a result of higher reactivity of oligomers with higher DP and the higher fraction of substituted amine (equilibrium yield of conjugates). In addition, conjugates with shorter and longer A<sub>n</sub>M oligomers were present in the reaction mixture reflecting a slight polydispersity of the starting oligomer (A<sub>5</sub>M), due to the lower resolution of the preparative GFC system. However, pure A<sub>5</sub>M-ADH/PDHA conjugates were obtained after fractionation, verified by the <sup>1</sup>H-NMR characterization of A<sub>5</sub>M-ADH and A<sub>5</sub>M-PDHA given in Figure S26 and S27, respectively.



**Figure S25:** GFC fractionation of the reaction mixtures obtained for the preparation of  $A_5M$ -ADH and  $A_5M$ -PDHA conjugates using optimised conditions. Fractionation of the mixture of  $A_nM$  oligomers is included for comparison.



**Figure S26:**  $^1H$ -NMR spectrum of the purified  $A_5M$ -ADH conjugate ( $D_2O$ , 300K, 600 MHz)

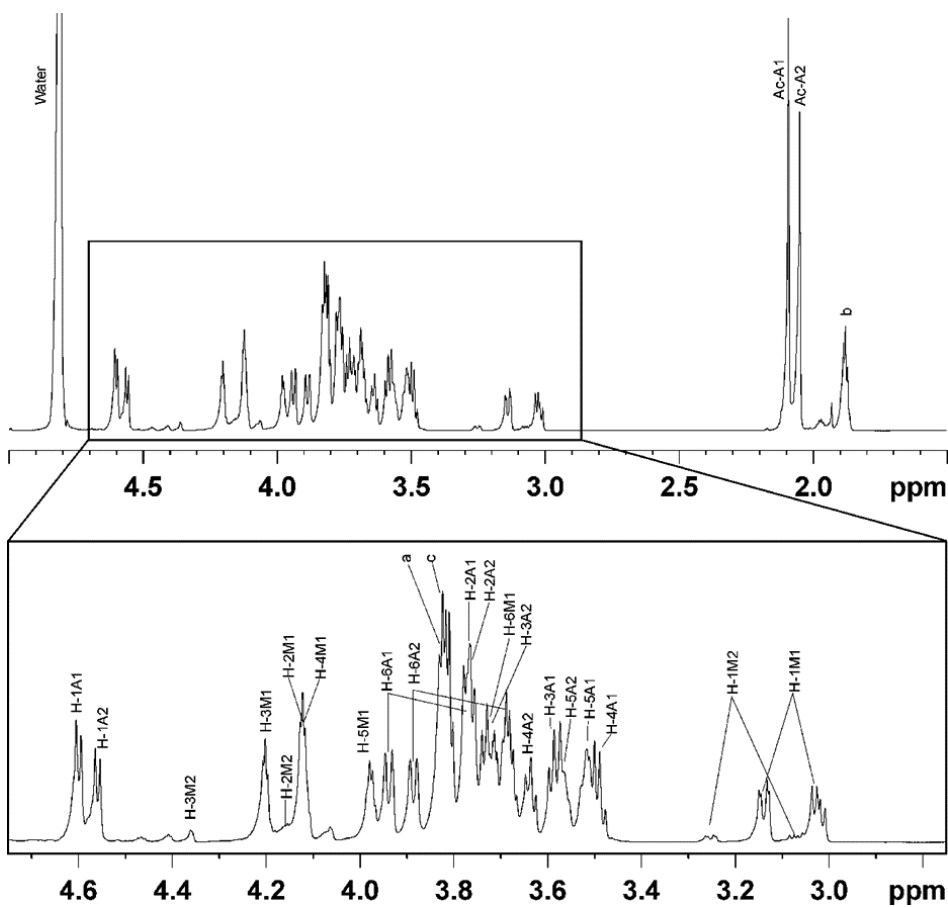


**Figure S27:**  $^1\text{H}$ -NMR spectrum of the purified  $\text{A}_5\text{M}$ -PDHconjugate ( $\text{D}_2\text{O}$ , 300K, 600 MHz)

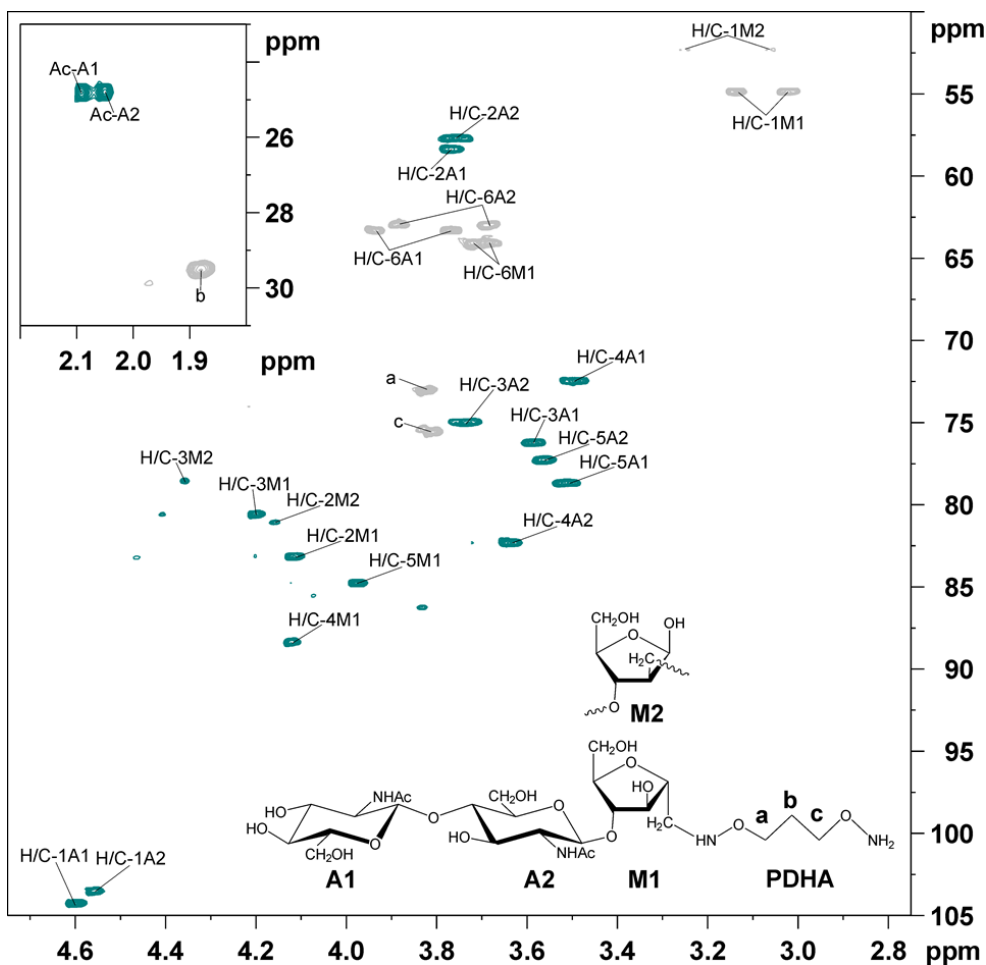
### S10 2D NMR characterization of the reduced and purified $\text{A}_2\text{M}$ -PDHA

The reduced and purified  $\text{A}_2\text{M}$ -PDHA conjugate was characterized by homo- and heteronuclear NMR correlation experiments. The conjugate was dissolved in  $\text{D}_2\text{O}$  and the NMR analysis was carried out using the 800 MHz spectrometer in a 3 mm NMR tube. Resonances were assigned by starting at the anomeric proton signal and then following the proton-proton connectivity using TOCSY, DQF-COSY/IP-COSY,  $^{13}\text{C}$  H2BC and  $^{13}\text{C}$  HSQC- $[\text{H}, \text{H}]$  TOCSY spectra.  $^{13}\text{C}$ -HSQC was used for assigning the carbon chemical shifts. The  $^{13}\text{C}$  HMBC spectrum provided information of connections between the sugars. One of the alternative forms of the M residue was structurally elucidated to be 3,5-anhydro-D-mannose. The following designations are used in the spectra displayed in Figure S28 and S29 and Table S1: A1 (*N*-acetylglucosamine (A) residue at the non-reducing end), A2 (middle *N*-acetylglucosamine (A) residue), M1 (2,5-anhydro-D-mannose (M) residue), M2 (3,5-anhydro-D-mannose (M') residue), -Ac (*N*-acetyl groups of A residues) a, b and c (unique identified methylene groups of PDHA). H/C# refers to the proton-carbon pairs with the ring carbon number for the monosaccharides. TSP was used for chemical shift reference. Chemical shifts are reported in Table S1. The structure of the  $\text{A}_2\text{M}$ -PDHA conjugate is included in Figure S29.





**Figure S28:**  $^1\text{H-NMR}$  spectrum of the reduced and purified  $\text{A}_2\text{M-PDHA}$  conjugate recorded at 298 K. Designations as described above.



**Figure S29:**  $^{13}\text{C}$  HSQC spectrum of the reduced and purified  $\text{A}_2\text{M}$ -PDHA conjugate recorded at 298 K. Designations as described above.

**Table S1:** Chemical shift assignment for the reduced and purified  $\text{A}_2\text{M}$ -PDHA conjugate at 298 K. The chemical shifts are related to TSP. Designations as described above.

Structural unit	Assignment						
	H-1; C-1	H-2; C-2	H-3; C-3	H-4; C-4	H-5; C-5	H-6; C-6	Ac-H; C
A1	4.60;104.2	3.75;57.5	3.59;76.2	3.49;72.4	3.51;78.6	3.93;3.77;63.2	2.09; 24.8
A2	4.56; 103.4	3.77;58.2	3.74;74.9	3.98;84.7	3.56;77.2	3.88;3.69;62.9	2.05; 24.8
M1	3.14;3.02;54.8	4.11;83.1	4.20;80.5	4.12;88.3	3.98;84.7	3.73;3.69;64.0	-
M2	3.25;3.07;52.2	4.16;80.9	4.36; 78.4	3.62; 82.3	n.d	n.d	-
PDHA	3.82;72.9	1.88;29.6	3.81;75.6	-	-	-	-

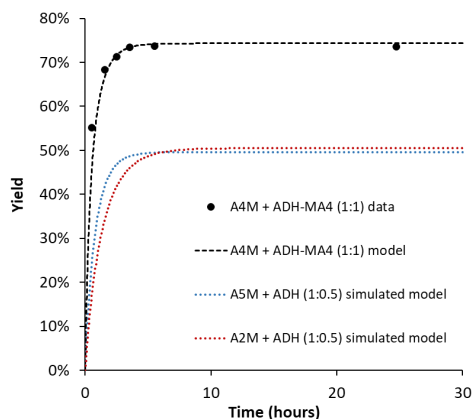
n.d: Not determined.

## S11 Preparation of chitin-*b*-chitin diblocks from activated chitin oligomers (A<sub>4</sub>M-ADH)

Chitin-*b*-chitin diblocks were prepared by reacting A<sub>4</sub>M-ADH conjugates (reduced and purified) with A<sub>4</sub>M oligomers in an equimolar molar ratio. The conjugation of the second block (A<sub>4</sub>M) was monitored by NMR (as described in S2). The kinetics was compared to simulated values for the corresponding reaction using rate constants obtained for the conjugation of A<sub>2</sub>M and A<sub>5</sub>M to free ADH. The results are summarised in Table S2 and kinetic plots are given in Figure S30. The comparison suggests the second conjugation proceeds somewhat faster than the first.

**Table S2:** Kinetic parameters obtained from the modelling of the reaction of A<sub>4</sub>M with an equimolar proportion of A<sub>4</sub>M-ADH. Simulated parameters for the corresponding reactions with equimolar proportions of oligomers and amines (0.5 equivalents ADH) using rate constants obtained for the conjugation of A<sub>2</sub>M and A<sub>5</sub>M to free ADH are given in italics.

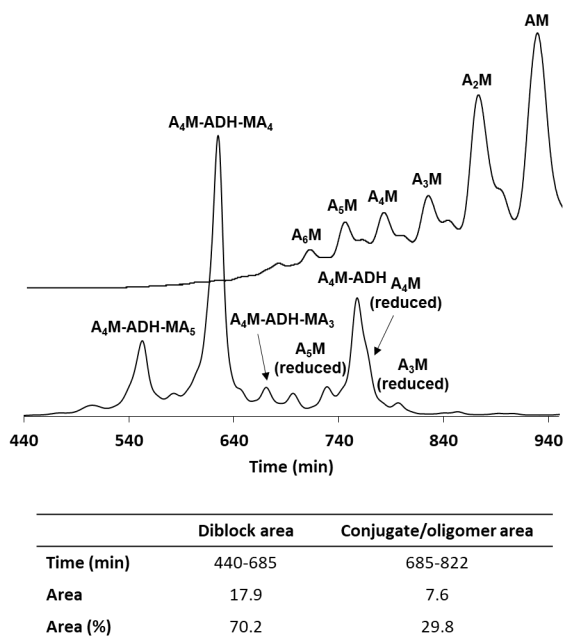
Equivalents				A+B ↔ E		A+B ↔ Z		A+B ↔ E + Z		Equilibrium yield [%]
A	B	B	pH	<i>k</i> <sub>1</sub> [h <sup>-1</sup> ]	<i>k</i> <sub>-1</sub> [h <sup>-1</sup> ]	<i>k</i> <sub>2</sub> [h <sup>-1</sup> ]	<i>k</i> <sub>-2</sub> [h <sup>-1</sup> ]	<i>t</i> <sub>0.5</sub> [h]	<i>t</i> <sub>0.9</sub> [h]	
A <sub>4</sub> M	A <sub>4</sub> M-ADH	1	4.0	7.3 × 10 <sup>-2</sup>	1.5 × 10 <sup>-1</sup>	1.1 × 10 <sup>-2</sup>	1.5 × 10 <sup>-1</sup>	0.35	1.57	74
A <sub>2</sub> M	ADH	0.5	4.0	<i>1.8 × 10<sup>-2</sup></i>	<i>2.0 × 10<sup>-1</sup></i>	<i>2.5 × 10<sup>-3</sup></i>	<i>2.0 × 10<sup>-1</sup></i>	<i>0.91</i>	<i>3.34</i>	<i>51</i>
A <sub>5</sub> M	ADH	0.5	4.0	<i>3.0 × 10<sup>-2</sup></i>	<i>3.5 × 10<sup>-1</sup></i>	<i>4.0 × 10<sup>-3</sup></i>	<i>3.5 × 10<sup>-1</sup></i>	<i>0.54</i>	<i>1.96</i>	<i>50</i>



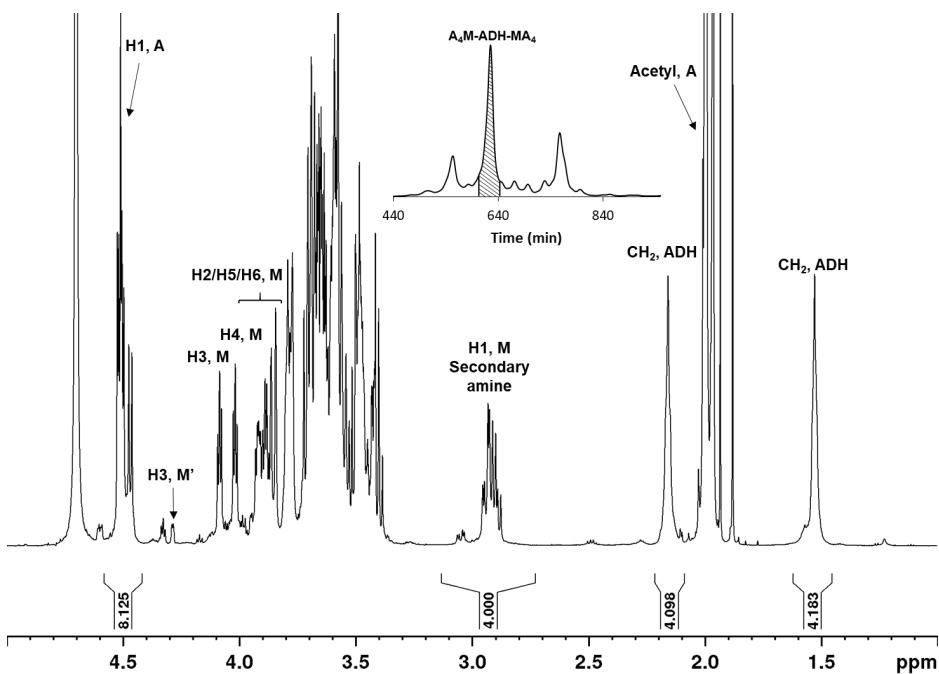
**Figure S30:** Kinetics of the reaction of A<sub>4</sub>M with an equimolar proportion of A<sub>4</sub>M-ADH. Simulated data for the corresponding reactions of A<sub>2</sub>M and A<sub>5</sub>M with free ADH and PDHA (0.5 equivalents, equimolar proportions of oligomers and amines) is included for comparison.

Reduction of the obtained equilibrium mixture was performed using 3 equivalents PB for 24 hours (RT). The reaction mixture was fractionated by GFC (Figure S31) and main products were purified. <sup>1</sup>H-NMR characterization of the main fraction (Figure S32) confirmed formation of the completely reduced A<sub>4</sub>M-ADH-MA<sub>4</sub> diblock. Due to slight polydispersity of the A<sub>4</sub>M oligomer (containing

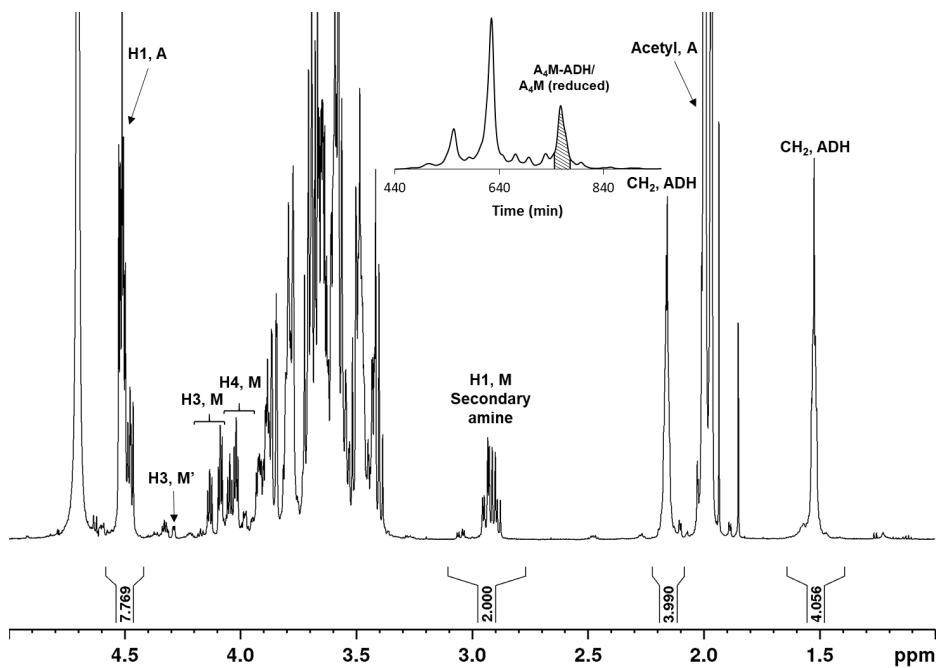
oligomers of lower and higher DP), some longer and shorter diblocks were consequently formed.  $^1\text{H}$ -NMR characterization of the fraction holding unreacted  $\text{A}_4\text{M}$  oligomers and  $\text{A}_4\text{M}$ -ADH conjugates (Figure S33) revealed complete reduction of the unreacted oligomers (no H1, M reducing end resonances). Hence, the fast reduction of oligomers prevented the diblock formation from going to completion. By integration of the chromatogram (Figure S31), the chitin-*b*-chitin diblock ( $\text{A}_4\text{M}$ -ADH- $\text{MA}_n$ ) area was found to account for 70 % of the total area, whereas unreacted conjugates ( $\text{A}_4\text{M}$ -ADH) and unreacted oligomers ( $\text{A}_n\text{M}$ ) accounted for the remaining 30 % of the area. By assuming an equimolar ratio of oligomers and conjugates, the weight yield of diblocks in the reaction was 82.5 %.



**Figure S31:** GFC fractionation of the reaction mixture obtained for the preparation of chitin diblocks by reacting  $\text{A}_4\text{M}$ -ADH with  $\text{A}_4\text{M}$  oligomers in an equimolar ratio. Fractionation of the mixture of  $\text{A}_n\text{M}$  oligomers is included for comparison.



**Figure S32:**  $^1\text{H-NMR}$  spectrum of the purified  $\text{A}_4\text{M-PDHA-MA}_4$  diblock fraction ( $\text{D}_2\text{O}$ , 300K, 600 MHz) from the chromatogram in Figure S31.



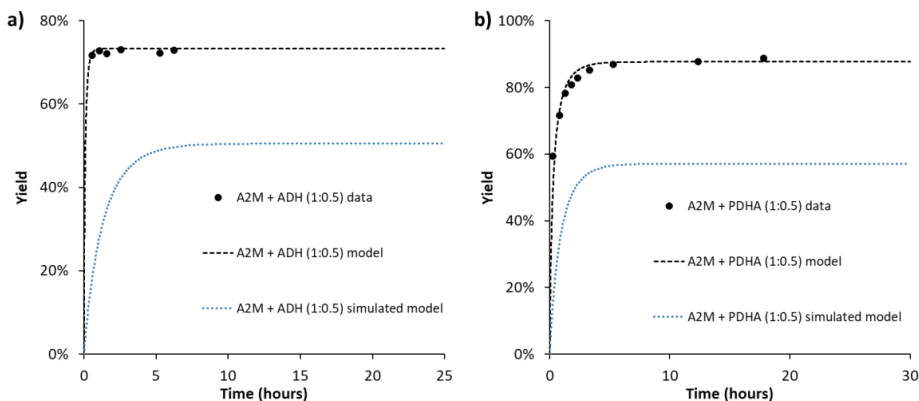
**Figure S33:**  $^1\text{H-NMR}$  spectrum of the  $\text{A}_4\text{M-PDHA/A}_4\text{M (reduced)}$  fraction ( $\text{D}_2\text{O}$ , 300K, 600 MHz) from the chromatogram in Figure S31.

## S12 Preparation of chitin-*b*-chitin diblocks using a sub-stoichiometric amount of ADH or PDHA

Chitin-*b*-chitin diblocks were prepared using A<sub>2</sub>M oligomers and a sub-stoichiometric amount of ADH or PDHA (0.5 equivalents). The conjugation of oligomers was monitored by NMR. The kinetics was compared to simulated values using rate constants obtained for the conjugation of A<sub>2</sub>M to free ADH or PDHA (2 equivalents). The results are summarised in Table S3 and the kinetic plots are given in Figure S34.

**Table S3:** Kinetic parameters obtained from the modelling of the reaction of A<sub>2</sub>M with 0.5 equivalents of ADH or PDHA (equimolar proportions of oligomers and amines). Simulated parameters for the corresponding reactions using rate constants obtained for the conjugation of A<sub>2</sub>M to free ADH or PDHA are given in italics.

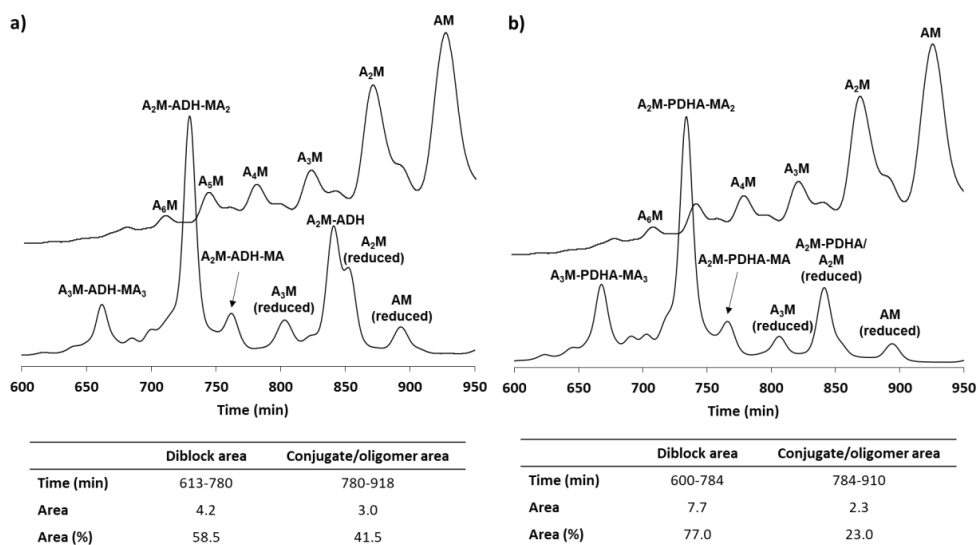
Equivalents				A+B ↔ E		A+B ↔ Z		A+B ↔ E + Z		Equilibrium yield [%]
A	B	B	pH	k <sub>1</sub> [h <sup>-1</sup> ]	k <sub>-1</sub> [h <sup>-1</sup> ]	k <sub>2</sub> [h <sup>-1</sup> ]	k <sub>-2</sub> [h <sup>-1</sup> ]	t <sub>0.5</sub> [h]	t <sub>0.9</sub> [h]	
A <sub>2</sub> M	ADH	0.5	4.0	4.0x10 <sup>-1</sup>	9.0x10 <sup>-1</sup>	5.8x10 <sup>-2</sup>	9.0x10 <sup>-1</sup>	0.06	0.28	73
<i>A<sub>2</sub>M</i>	<i>ADH</i>	<i>0.5</i>	<i>4.0</i>	<i>1.8x10<sup>-2</sup></i>	<i>2.0x10<sup>-1</sup></i>	<i>2.5x10<sup>-3</sup></i>	<i>2.0x10<sup>-1</sup></i>	<i>0.91</i>	<i>3.35</i>	<i>51</i>
A <sub>2</sub> M	PDHA	0.5	4.0	1.2x10 <sup>-1</sup>	6.0x10 <sup>-2</sup>	5.2x10 <sup>-2</sup>	6.0x10 <sup>-2</sup>	0.22	1.21	88
<i>A<sub>2</sub>M</i>	<i>PDHA</i>	<i>0.5</i>	<i>4.0</i>	<i>2.4x10<sup>-2</sup></i>	<i>2.2x10<sup>-1</sup></i>	<i>1.0x10<sup>-2</sup></i>	<i>2.2x10<sup>-1</sup></i>	<i>0.64</i>	<i>2.41</i>	<i>57</i>



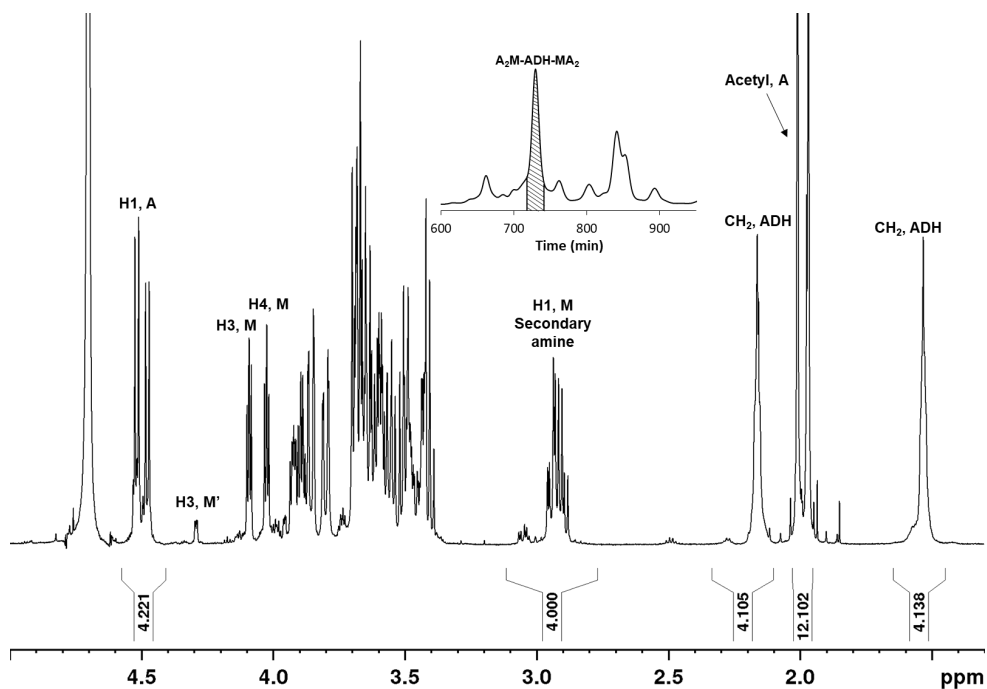
**Figure S34:** Kinetics of the reactions of A<sub>2</sub>M with 0.5 equivalents of **a)** ADH and **b)** PDHA. Simulated data for the corresponding reactions of A<sub>2</sub>M with free ADH and PDHA (0.5 equivalents, equimolar proportions of oligomers and amines) is included for comparison.

Reduction of the equilibrium mixtures was performed using 3 equivalents PB for 24 hours or 20 equivalents PB for 48 hours at room temperature for the reaction with ADH and PDHA, respectively. Reaction mixtures were fractionated by GFC (Figure S35) and the main fractions were purified and characterized by <sup>1</sup>H-NMR (Figure S36 – S40). Products from the ADH reaction were completely reduced (no hydrazone resonances in the spectra) whereas minor oxime resonances were observed in

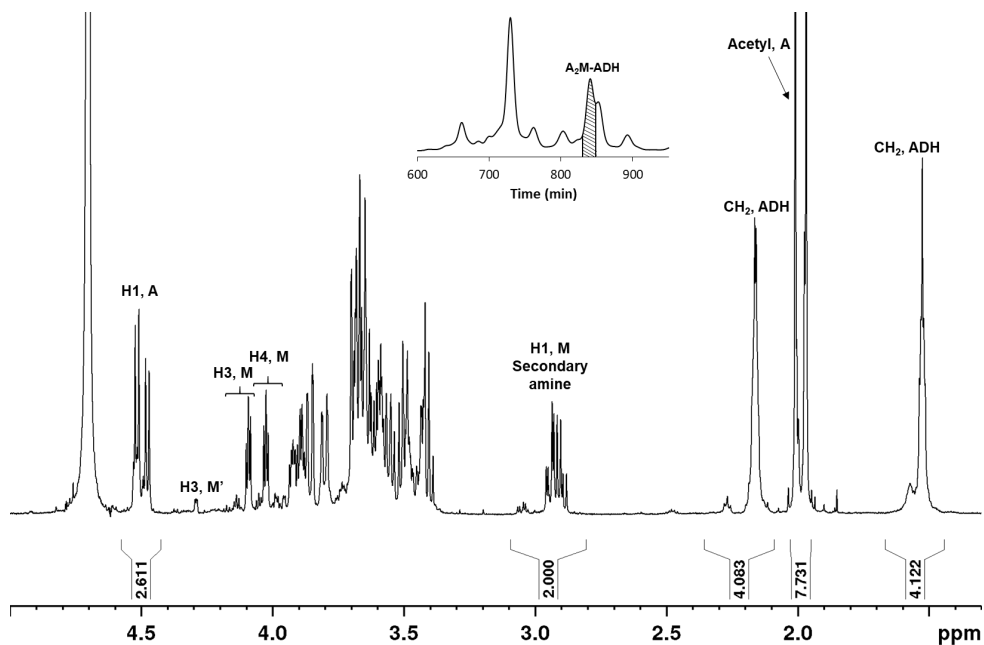
the products from the PDHA reaction, indicating incomplete reduction. Impurity of the  $A_2M$  oligomers gave additional fractions in the GFC chromatograms obtained for both reactions. The yield of diblocks was obtained by integrating the chromatograms (Figure S35) as described above. The weight yield of diblocks was 74 % and 87 % for the reaction with ADH and PDHA, respectively. The weight yield of diblocks corresponds well to the statistical amount of diblocks expected (73 % for ADH and 88 % for PDHA). Unreacted oligomers were completely reduced (no H1, M resonances observed in the  $^1H$ -NMR spectra), confirming the fast reduction of  $A_nM$  oligomers preventing the diblock formation from going to completion.



**Figure S35:** GFC fractionation of the reaction mixture obtained for the preparation of chitin diblocks by reacting  $A_2M$  oligomers with a sub stoichiometric amount (0.5 equivalents) of **a)** ADH or **b)** PDHA. Fractionation of the mixture of  $A_nM$  oligomers is included for comparison.

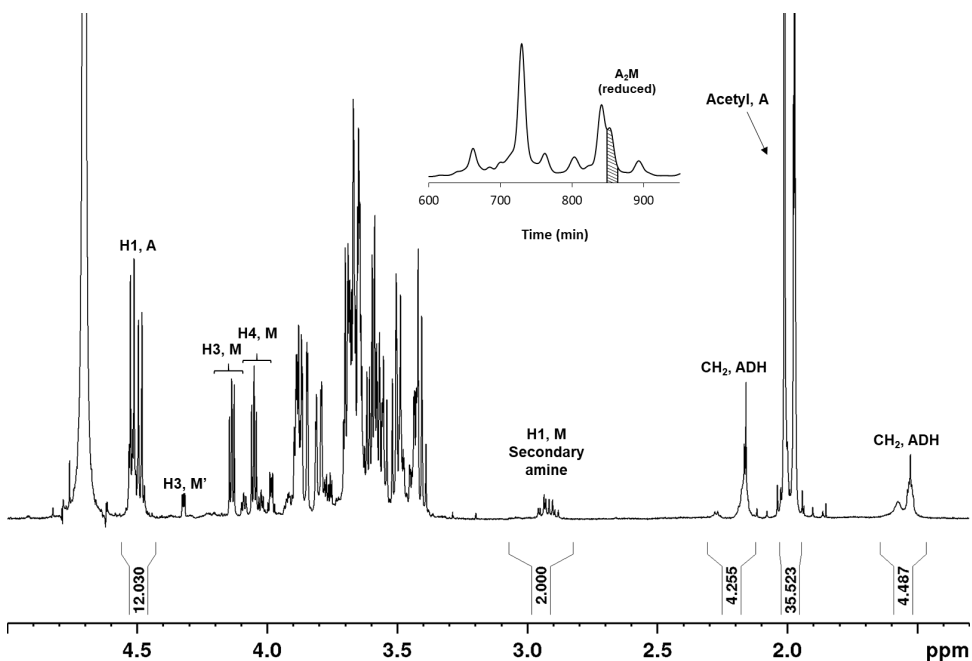


**Figure S36:**  $^1\text{H}$ -NMR spectrum of the purified  $\text{A}_2\text{M-ADH-MA}_2$  diblock fraction ( $\text{D}_2\text{O}$ , 300K, 600 MHz) from the chromatogram in Figure S35a.

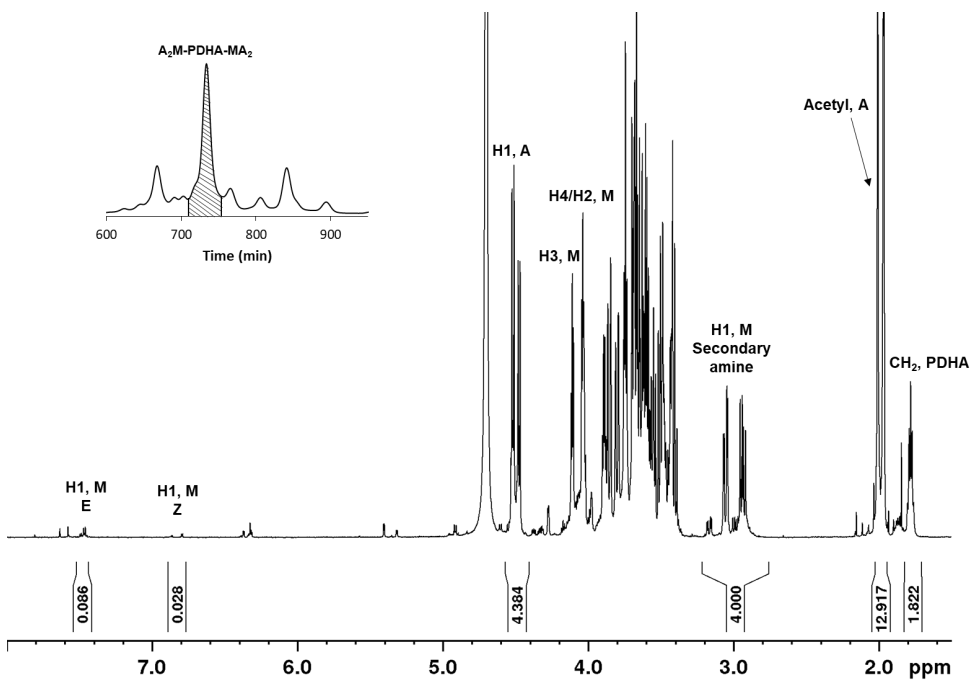


**Figure S37:**  $^1\text{H}$ -NMR spectrum of the  $\text{A}_2\text{M-ADH}$  fraction ( $\text{D}_2\text{O}$ , 300K, 600 MHz) from the chromatogram in Figure S35a.

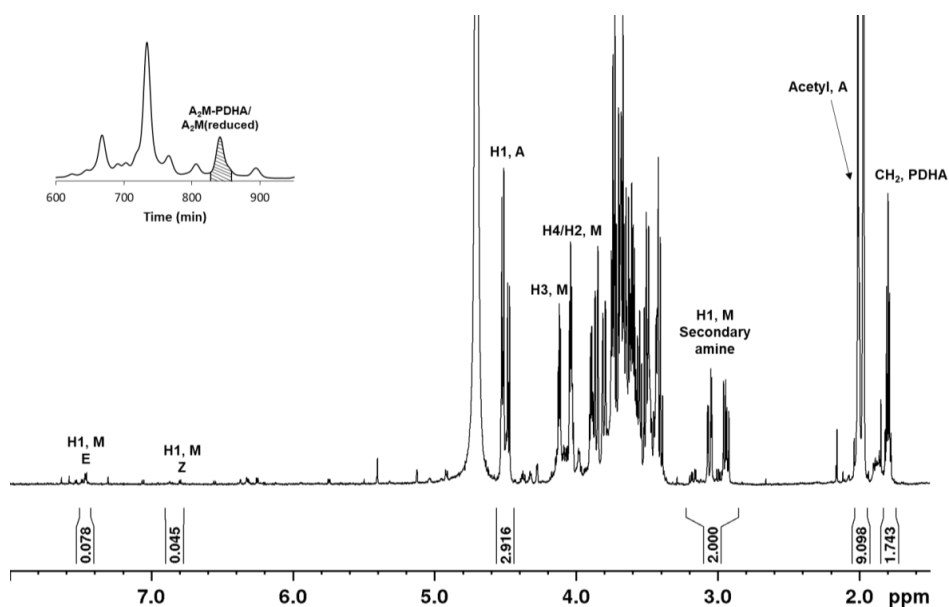




**Figure S38:**  $^1\text{H-NMR}$  spectrum of the  $\text{A}_2\text{M}$  (reduced) fraction ( $\text{D}_2\text{O}$ , 300K, 600 MHz) from the chromatogram in Figure S35a.



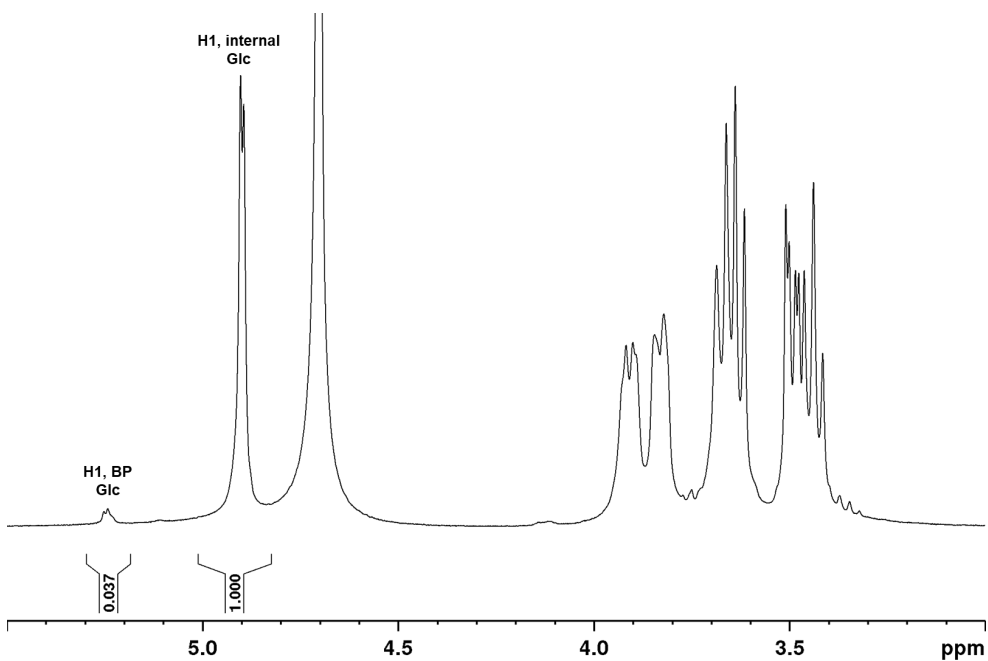
**Figure S39:**  $^1\text{H-NMR}$  spectrum of the purified  $\text{A}_2\text{M-PDHA-MA}_2$  diblock fraction ( $\text{D}_2\text{O}$ , 300K, 600 MHz) from the chromatogram in Figure S35b.



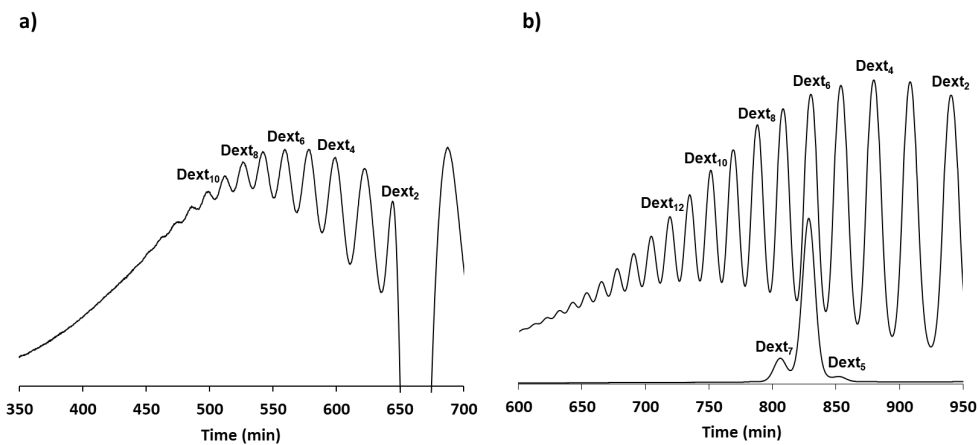
**Figure S40:**  $^1\text{H-NMR}$  spectrum of the  $\text{A}_2\text{M-PDHA}/\text{A}_2\text{M}$  (reduced) fraction ( $\text{D}_2\text{O}$ , 300K, 600 MHz) from the chromatogram in Figure S35b.

### S13 Preparation and characterization of dextran ( $\text{Dext}_m$ ) oligomers

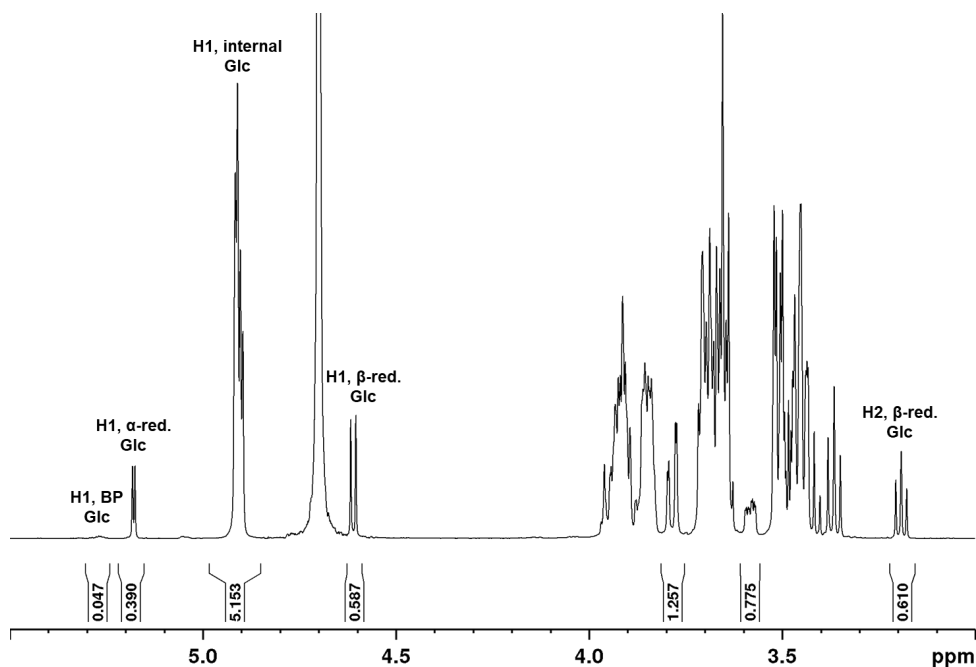
Dextran ( $\text{Dext}_m$ ) oligomers were prepared by acid hydrolysis of dextran (Dextran T-2000,  $M_w = 2,000,000$ ).  $^1\text{H-NMR}$  characterisation of Dextran T-2000 is given in Figure S41. The degree of branching was estimated from the integral of the H1 resonance of internal glucose residues in the main chain and the H1 of the glucose residues at the branching points (BP) to 3.6 %<sup>6</sup>. The degradation mixture was fractionated by preparative GFC to obtain isolated  $\text{Dext}_m$  oligomers (Figure S42a). The isolated  $\text{Dext}_6$  oligomer ( $\text{DP} = 6$ ) was characterized by  $^1\text{H-NMR}$  (Figure S43) and fractionated by analytical GFC (Figure S42b) to show the slight polydispersity of the oligomer. The degree of branching of the oligomer was estimated to approximately 0.8 % showing that the branches are more rapidly hydrolysed than the linkages in the main chain.



**Figure S41:**  $^1\text{H-NMR}$  characterization of Dextran T-2000 ( $\text{D}_2\text{O}$ , 300K, 600 MHz).



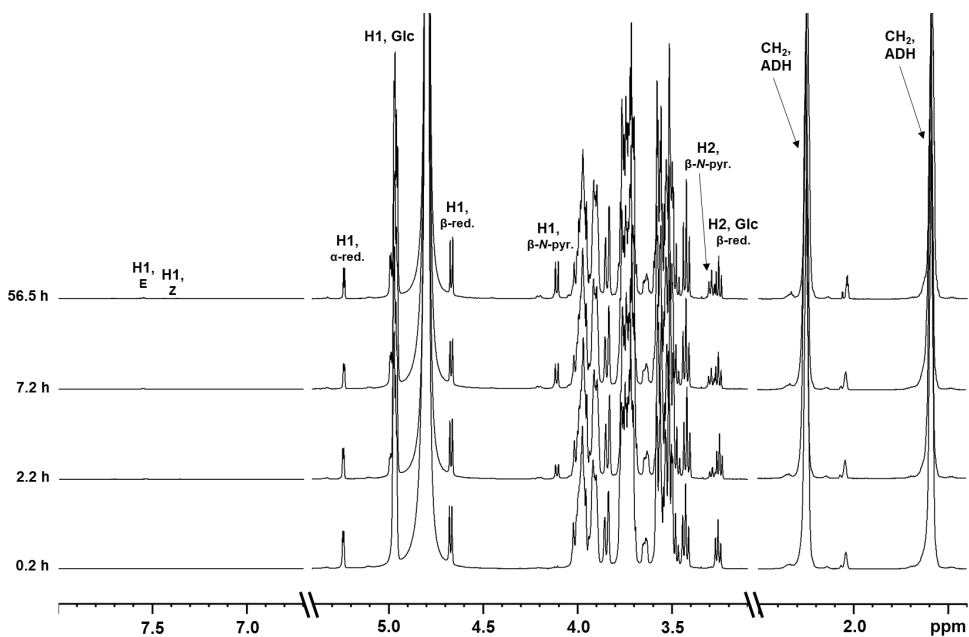
**Figure S42:** **a)** Preparative GFC fractionation of the mixture of  $\text{Dext}_m$  oligomers **b)** analytical GFC fractionation of isolated  $\text{Dext}_6$ . Fractionation of the mixture of  $\text{Dext}_m$  oligomers is included for comparison.



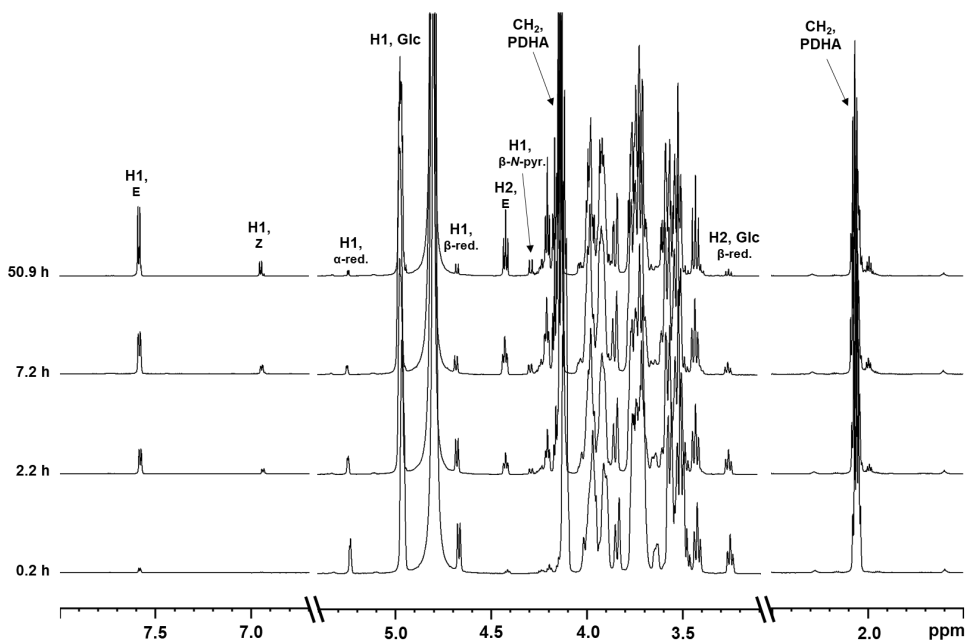
**Figure S43:**  $^1\text{H-NMR}$  spectrum of the isolated  $\text{Dext}_6$  oligomer (in  $\text{D}_2\text{O}$ , 300 K, 600 MHz) obtained from the preparative GFC fractionation in Figure S42a.

#### S14 Conjugation of $\text{Dext}_m$ oligomers to ADH and PDHA studied by time course NMR

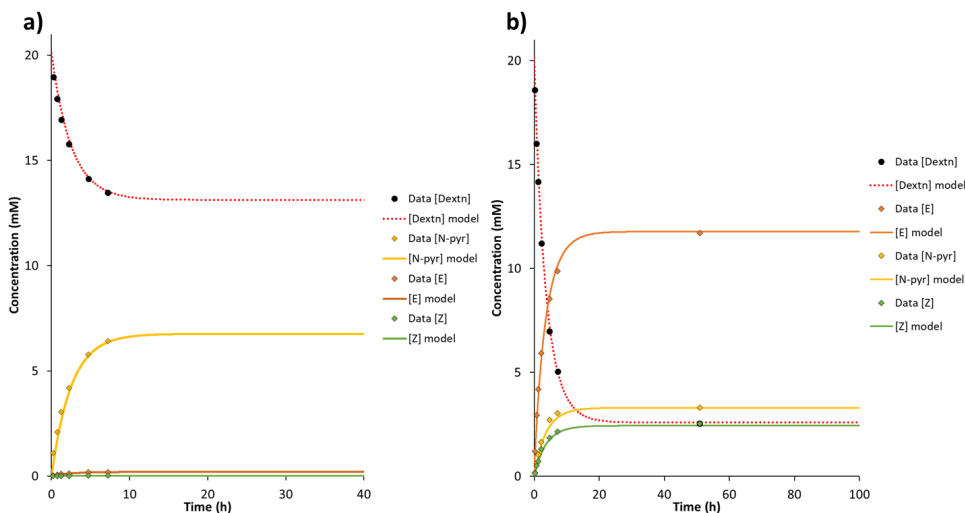
Conjugation of  $\text{Dext}_5$  oligomers ( $\text{DP} = 5$ ) to ADH and PDHA (2 equivalents) at pH 4.0, RT was monitored by NMR (Figure S44 and S45, respectively). Here, the reducing end of dextran (Glc, normal reducing end), governs the conjugation and hence, the acyclic hydrazones and oximes are in equilibrium with cyclic *N*-glycosides. As previously shown<sup>5</sup>, dextran formed almost exclusively *N*-pyranosides with ADH, whereas it formed *N*-pyranosides in addition to *E*- and *Z*-oximes with PDHA. The equilibrium yield of conjugates (*E*-/*Z*-hydrazones or oximes + *N*-pyranosides) obtained for the reactions was 35% for  $\text{Dext}_5$  with ADH and 87% for  $\text{Dext}_5$  with PDHA. The experimental data obtained in the conjugation reactions were fitted using the model described in S3 (based on the reaction scheme presented in Figure S5). The data fitting for the conjugation  $\text{Dext}_5$  oligomers to ADH and PDHA (2 equivalents) at pH 4.0 (RT) are given in Figure S46. Rates ( $t_{0.5}$  and  $t_{0.9}$ ) and equilibrium yields for the total conjugation reaction are given in Table S4.



**Figure S44:**  $^1\text{H-NMR}$  spectra obtained at defined time points for the conjugation reaction with  $\text{Dext}_5$  (20.1 mM) and 2 equivalents ADH at pH 4.0, RT.



**Figure S45:**  $^1\text{H-NMR}$  spectra obtained at defined time points for the conjugation reaction with  $\text{Dext}_5$  (20.1 mM) and 2 equivalents PDHA at pH 4.0, RT.



**Figure S46:** a) Model fitted to the experimental data obtained for the conjugation of Dext<sub>5</sub> to ADH (2 equivalents) at pH 4.0, RT. b) Model fitted to the experimental data obtained for the conjugation of Dext<sub>5</sub> to PDHA (2 equivalents) at pH 4.0, RT.

**Table S4:** Kinetic parameters obtained from the modelling of the reaction of Dext<sub>5</sub> with 2 equivalents ADH or PDHA.

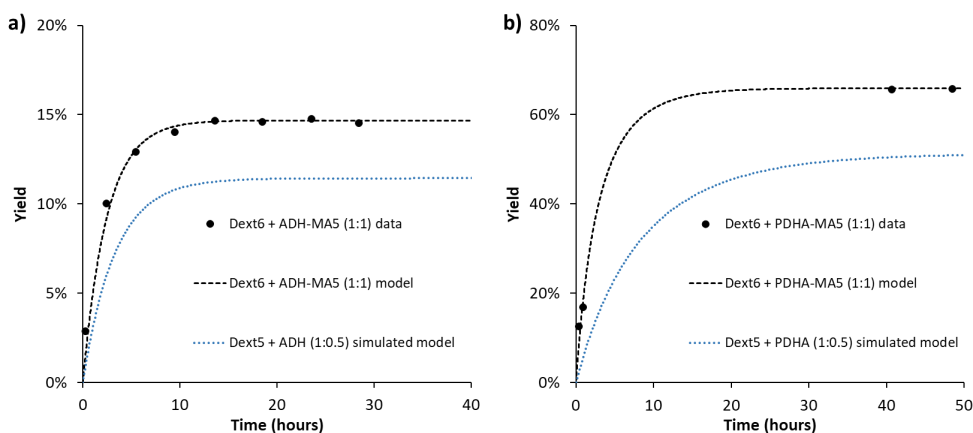
A	B	Equivalents		A+B ↔ E + Z+Pyr		Equilibrium yield [%]
		B	pH	t <sub>0.5</sub> [h]	t <sub>0.9</sub> [h]	
Dext <sub>5</sub>	ADH	2	4.0	1.74	5.84	35
Dext <sub>5</sub>	PDHA	2	4.0	2.38	8.54	87

### S15 Preparation of chitin-*b*-dextran diblocks

Chitin-*b*-dextran diblocks were prepared by reacting A<sub>5</sub>M-ADH or A<sub>5</sub>M-PDHA conjugates (reduced and purified) with dextran oligomers of DP = 6 (Dext<sub>6</sub>) in an equimolar ratio. The conjugation of the dextran block was monitored by NMR (as described in S2) and combined equilibrium yields of 15 and 66 % were obtained for the conjugation to A<sub>5</sub>M-ADH or A<sub>5</sub>M-PDHA, respectively. The kinetics was (as above) compared to simulated values using rate constants ( $k_1$ ,  $k_{-1}$  etc) obtained for the conjugation of Dext<sub>5</sub> to free ADH or PDHA. The results are summarised in Table S5 and the kinetic plots are given in Figure S47. Compared to the model, it appears the second conjugation is faster and gives higher yields than the first.

**Table S5:** Kinetic parameters obtained from the modelling of the reaction of Dext<sub>6</sub> with an equimolar proportion of A<sub>5</sub>M-ADH or A<sub>5</sub>M-PDHA. Simulated parameters for the corresponding reactions with equimolar proportions of oligomers and amine using rate constants obtained for the conjugation of Dext<sub>5</sub> to free ADH or PDHA are given in italics.

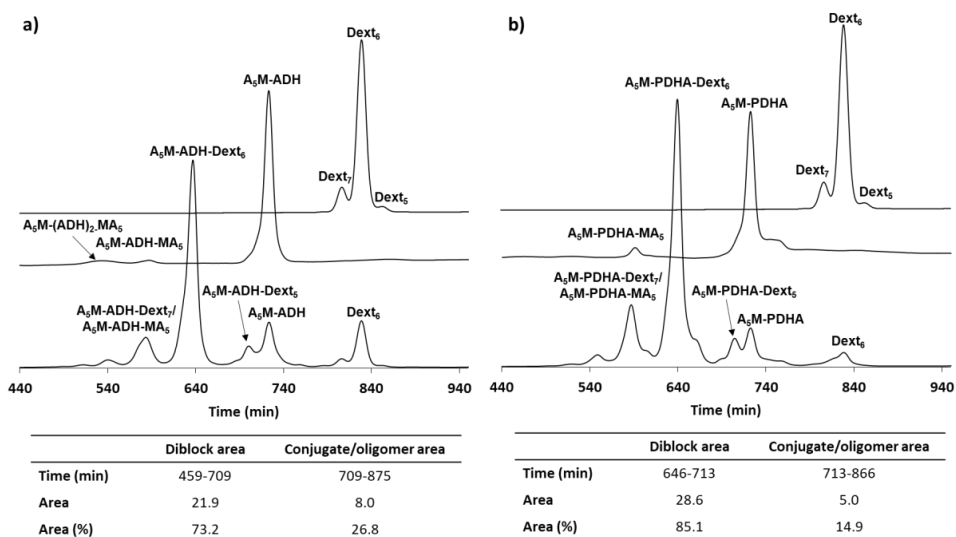
A	B	Equivalents		A+B ↔ E + Z+Pyr		Equilibrium yield [%]
		B	pH	t <sub>0.5</sub> [h]	t <sub>0.9</sub> [h]	
Dext <sub>6</sub>	A <sub>5</sub> M-ADH	1	4.0	1.72	5.74	15
<i>Dext<sub>5</sub></i>	<i>ADH</i>	<i>0.5</i>	<i>4.0</i>	<i>2.27</i>	<i>7.54</i>	<i>11</i>
Dext <sub>6</sub>	A <sub>5</sub> M-PDHA	1	4.0	2.07	8.36	66
<i>Dext<sub>5</sub></i>	<i>PDHA</i>	<i>0.5</i>	<i>4.0</i>	<i>5.76</i>	<i>21.30</i>	<i>51</i>



**Figure S47:** Kinetics of the reactions of Dex<sub>6</sub> with equimolar amounts of **a)** A<sub>5</sub>M-ADH and **b)** A<sub>5</sub>M-PDHA. Simulated data for the corresponding reactions of Dex<sub>5</sub> with free ADH and PDHA (0.5 equivalents) is included for comparison.

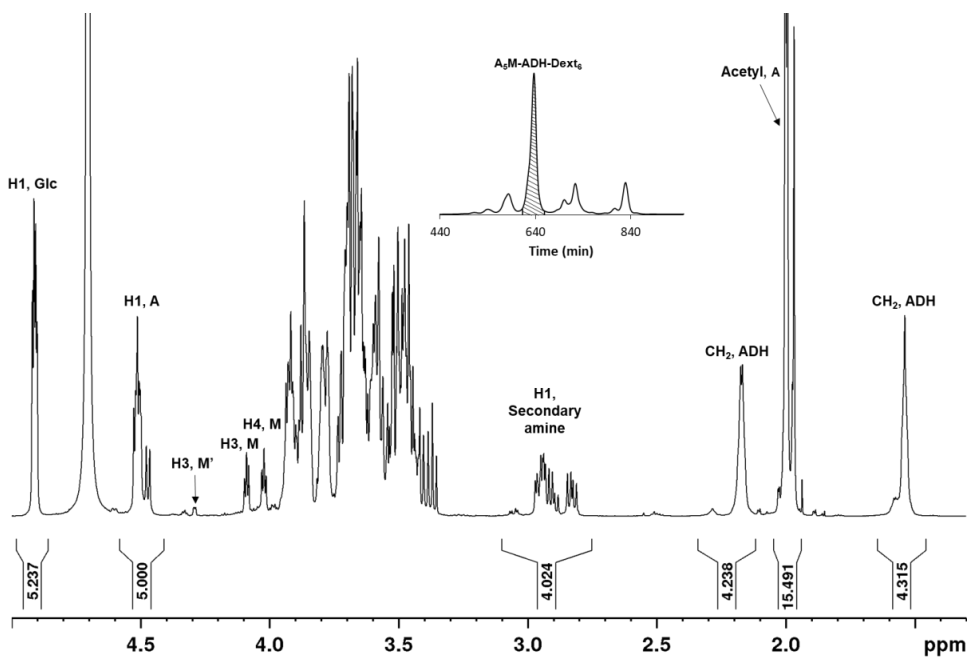
Reduction of the equilibrium mixtures with chitin-*b*-dextran diblocks was performed at 40 °C using 20 equivalents PB due to the slow reduction of conjugates with normal reducing ends<sup>5</sup>. Reduction was terminated after 72 and 144 hours for the preparation A<sub>5</sub>M-PDHA-Dext<sub>6</sub> and A<sub>5</sub>M-ADH-Dext<sub>6</sub> diblocks, respectively, due to the slower reduction of ADH conjugates<sup>5</sup>. The reaction mixtures were fractionated by GFC (Figure S48), and main fractions were purified and characterized by <sup>1</sup>H-NMR (Figure S49-S53). As purified A<sub>5</sub>M conjugates were used for the diblock preparation, the integral for the H1, A resonance was set to 5 in all the <sup>1</sup>H-NMR spectra. The yield of diblocks was obtained by integrating the chromatograms (Figure S48) as described above. Due to the slight polydispersity of the Dext<sub>6</sub> oligomer, some longer and shorter diblocks were also formed. The weight yield of diblocks was 85 and 92 % for chitin-*b*-dextran diblocks with ADH and PDHA, respectively. The amount of remaining unreduced diblock could not be accurately determined because the resonance

corresponding to the unreduced *N*-pyranoside conjugates overlaps with other resonances in the spectra. However, the integral for the secondary amine resonance balanced the integrals of the resonances from both chitin and dextran, suggesting close to complete reduction of diblocks. Approximately 40 % the unreacted dextran oligomers from the reaction with A<sub>5</sub>M-ADH conjugates (20 equivalents PB, 40 °C) were reduced after 144 hours (6 days) (Figure S51). Hence, the dextran oligomers are reduced by PB with a much slower rate than the A<sub>n</sub>M oligomers. The slow reduction of dextran oligomers also explains the higher yield of diblocks obtained compared to the low amination yield, as the dextran oligomers can react further after addition of reducing agent.

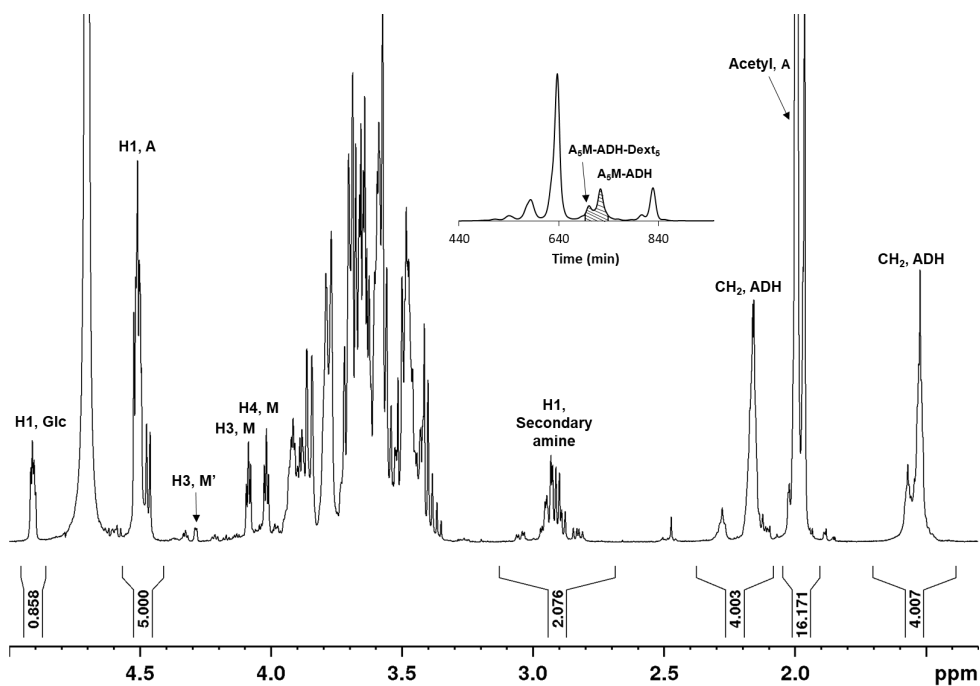


**Figure S48:** GFC fractionation of the reaction mixture obtained for the preparation of diblocks by reacting Dext<sub>6</sub> oligomers with **a)** A<sub>5</sub>M-ADH or **b)** A<sub>5</sub>M-PDHA conjugates in an equimolar ratio. Fractionation of the Dext<sub>6</sub> oligomers and the purified conjugates are included for comparison.

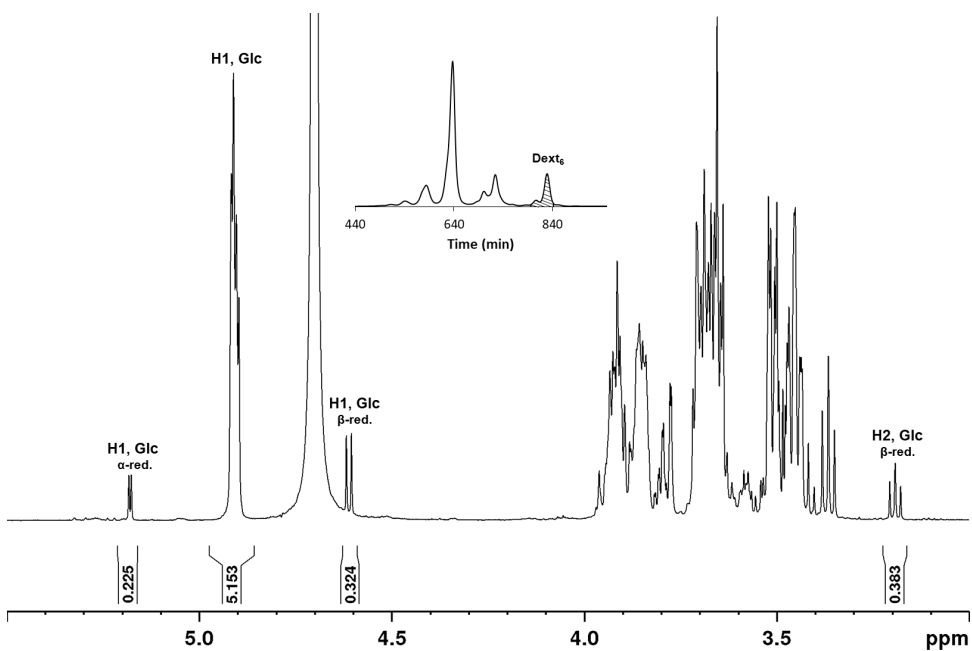




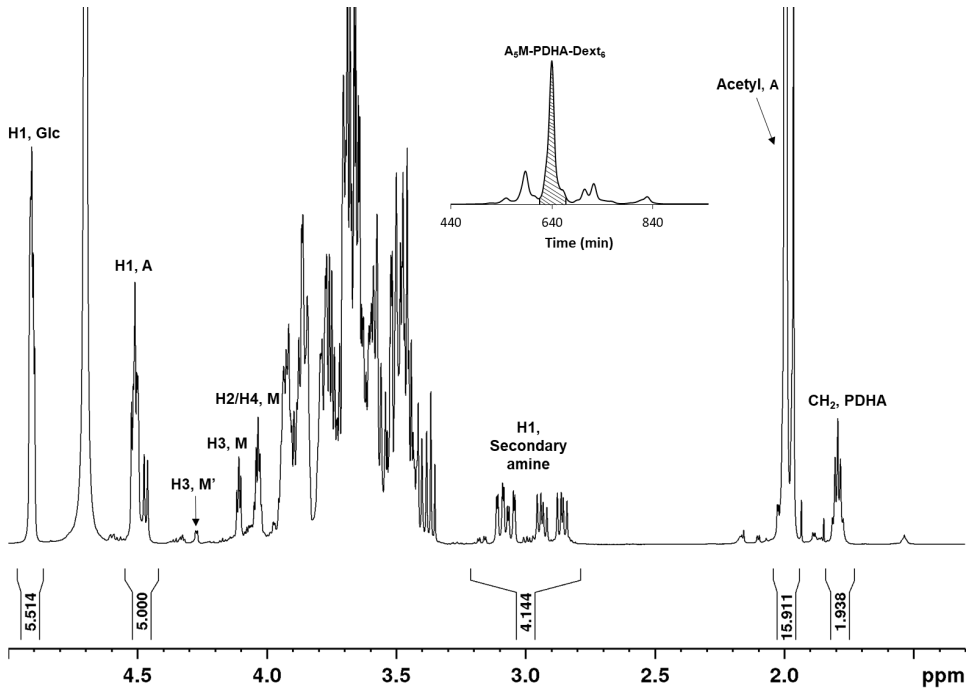
**Figure S49:**  $^1\text{H-NMR}$  spectrum of the  $\text{A}_5\text{M-ADH-Dext}_6$  fraction ( $\text{D}_2\text{O}$ , 300K, 600 MHz) from the chromatogram in Figure S48a.



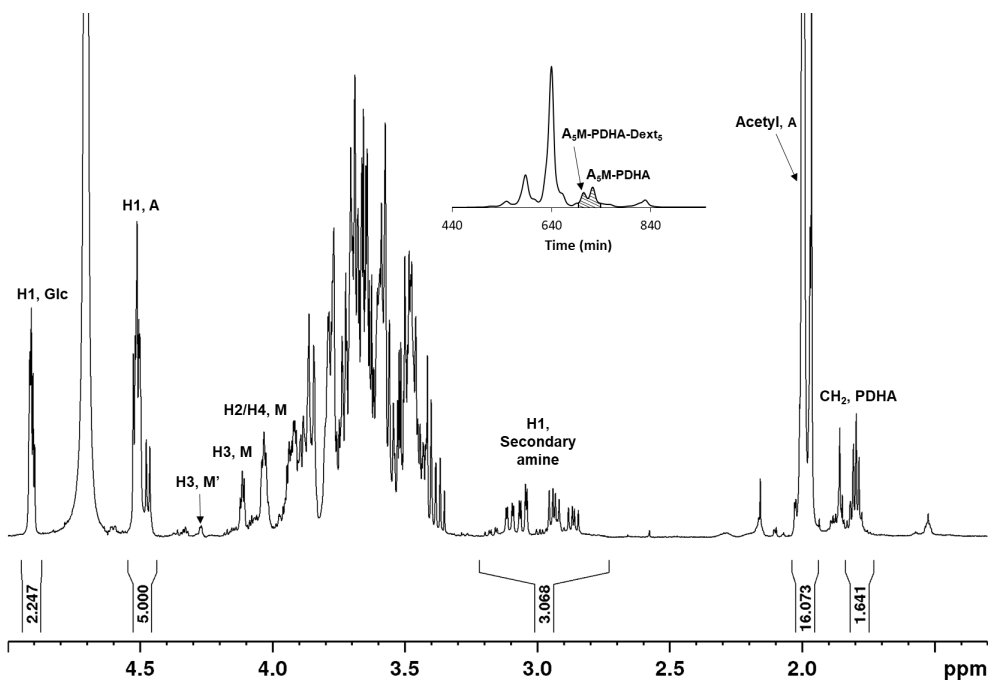
**Figure S50:**  $^1\text{H-NMR}$  spectrum of the  $\text{A}_5\text{M-ADH-Dext}_5/\text{A}_5\text{M-ADH}$  fraction ( $\text{D}_2\text{O}$ , 300K, 600 MHz) from the chromatogram in Figure S48a.



**Figure S51:** <sup>1</sup>H-NMR spectrum of the Dext<sub>6</sub> fraction (D<sub>2</sub>O, 300K, 600 MHz) from the chromatogram in Figure S48a.



**Figure S52:** <sup>1</sup>H-NMR spectrum of the A<sub>5</sub>M-PDHA-Dext<sub>6</sub> fraction (D<sub>2</sub>O, 300K, 600 MHz) from the chromatogram in Figure S48b.



**Figure S53:**  $^1\text{H-NMR}$  spectrum of the  $\text{A}_5\text{M-PDHA-Dext}_5/\text{A}_5\text{M-PDHA}$  fraction ( $\text{D}_2\text{O}$ , 300K, 600 MHz) from the chromatogram in Figure S48b.

## References

- Allan, G. G.; Peyron, M., Molecular-Weight Manipulation of Chitosan .1. Kinetics of Depolymerization by Nitrous-Acid. *Carbohydr. Res.* **1995**, 277, (2), 257-272.
- Tømmeraaas, K.; Vårum, K. M.; Christensen, B. E.; Smidsrød, O., Preparation and characterisation of oligosaccharides produced by nitrous acid depolymerisation of chitosans. *Carbohydr. Res.* **2001**, 333, (2), 137-144.
- Sugiyama, H.; Hisamichi, K.; Sakai, K.; Usui, T.; Ishiyama, J.-I.; Kudo, H.; Ito, H.; Senda, Y., The conformational study of chitin and chitosan oligomers in solution. *Bioorg. Med. Chem.* **2001**, 9, (2), 211-216.
- Lindberg, B.; Lönngrén, J.; Svensson, S., Specific Degradation of Polysaccharides. In *Advances in Carbohydrate Chemistry and Biochemistry*, Tipson, R. S.; Derek, H., Eds. Academic Press: 1975; Vol. Volume 31, pp 185-240.

5. Mo, I. V.; Feng, Y.; Dalheim, M. Ø.; Solberg, A.; Aachmann, F. L.; Schatz, C.; Christensen, B. E., Activation of enzymatically produced chitoooligosaccharides by dioxyamines and dihydrazides. *Carbohydr. Polym.* **2020**, 232, 115748.
6. van Dijk-Wolthuis, W. N. E.; Franssen, O.; Talsma, H.; van Steenbergen, M. J.; Kettenes-van den Bosch, J. J.; Hennink, W. E., Synthesis, Characterization, and Polymerization of Glycidyl Methacrylate Derivatized Dextran. *Macromolecules* **1995**, 28, (18), 6317-6322.

# Paper III



MANUSCRIPT IN PREPARATION

# **Functionalisation of the non-reducing end of chitin: A new approach to form complex block polysaccharides and water-soluble chitin-based block polymers**

*Ingrid Vikøren Mo<sup>†</sup>, Christophe Schatz<sup>‡\*</sup>, Bjørn E. Christensen<sup>†\*</sup>*

<sup>†</sup>NOBIPOL, Department of Biotechnology and Food Science, NTNU - Norwegian University of Science and Technology, Sem Saelands veg 6/8, NO-7491 Trondheim, Norway

<sup>‡</sup>Laboratoire de Chimie des Polymères Organiques (LCPO), Université de Bordeaux, CNRS, Bordeaux INP, UMR 5629, 33600 Pessac, France

\*Corresponding authors

## Abstract

Most polysaccharides used in polysaccharide-containing block copolymers are attached to the second block through the reducing end, due to the few and highly polysaccharide specific non-reducing end functionalisation methods available. However, chitin oligomers prepared by nitrous acid degradation of chitosan, containing the reactive 2,5-anhydro-D-mannose (M) residue at the reducing end ( $A_nM$ ) can be selectively oxidised by periodate at the non-reducing end to form a dialdehyde. Here, we show that the dialdehyde is highly reactive towards bifunctional oxyamine and hydrazide linkers. Sub-stoichiometric amounts of linkers resulted in conjugation of  $A_nM$  oligomers through both chain termini to yield a discrete distribution of 'polymerised'  $A_nM$  oligomers. Such chitin-based block polymers were, in contrast to chitins of the same chain lengths, water-soluble. Oxidised  $A_nM$  oligomers, functionalised at both termini can also enable the preparation of more complex block polysaccharides such as ABA- or ABC-type.

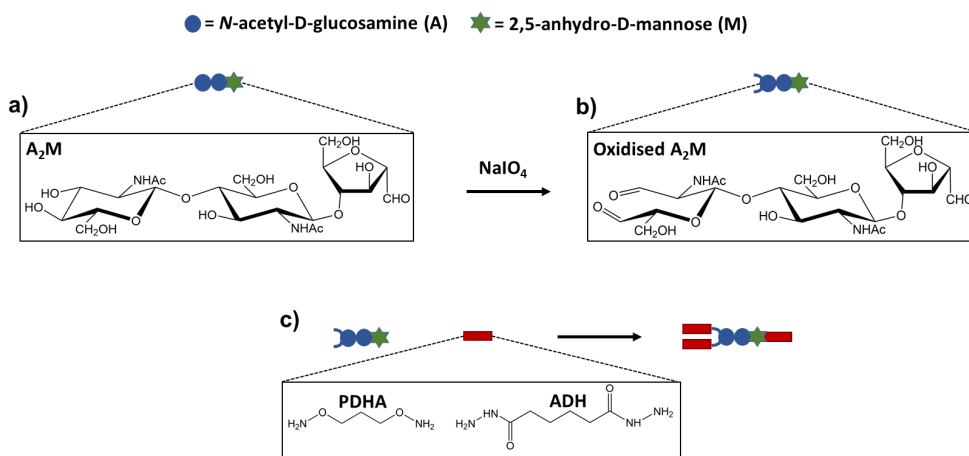
## Introduction

AB-type diblock polysaccharides represent a new class of engineered block polymers, exclusively composed of polysaccharide blocks<sup>1,2</sup>. Coupling of the polysaccharide blocks through their reducing ends, result in structures with antiparallel chains. Preparation of more complex block polysaccharides, such as linear ABA or ABC triblock copolymers, additionally requires reactions at the non-reducing end (NRE) of the B block and only a few polysaccharide specific methods for functionalisation of the NRE are described in the literature. However, NRE reactivity has been demonstrated for dextran<sup>3</sup> and lyase degraded heparin<sup>4</sup> after intermediate functionalisation steps.

Periodate oxidation of polysaccharides converts vicinal diols (and closely related structures) to the corresponding dialdehydes. Hence, the ability of different polysaccharides to be oxidised depends on their chemical composition and linkage geometry<sup>5</sup>. In the special case of fully *N*-acetylated chitin oligomers prepared by nitrous acid degradation of chitosan ( $A_nM$ )<sup>6</sup>, only the NRE residue contains oxidisable, vicinal diols (Figure 1a). Therefore, periodate oxidation of such oligomers should in theory provide oligomers with two aldehydes (C3 and C4) in the oxidised NRE (O-NRE) residue, in addition to the highly reactive pending aldehyde of the 2,5-anhydro-D-mannose (M) residue (Figure 1b). Only a few studies describing the functionalisation of the NRE of chitin by periodate oxidation is reported in the literature<sup>7-9</sup>, and to our knowledge, subsequent reactions with the O-NRE aldehydes have not been investigated. Hence, it is unknown whether both the aldehydes in the O-NRE residue are reactive, but the question is pertinent as only one of the dialdehydes obtained by lateral periodate oxidation of alginate has shown to react with amines through reductive amination<sup>10,11</sup>.



$A_nM$  oligosaccharides have previously been subjected to reducing end (RE) activation a dioxyamine (O,O'-1,3-propanediylbishydroxyamine, PDHA) and a dihydrazide (adipic acid dihydrazide, ADH) to form precursors for AB-type block polysaccharides<sup>12</sup>. Such activated  $A_nM$  oligomers were used to prepare  $A_nM$ -*b*-dextran diblocks by attaching the dextran block to the free end of the linkers. Reaction of *oxidised*  $A_nM$  oligomers with such dioxyamines or dihydrazides may form a range of new complex structures. In the present work we first study the reaction of periodate oxidised  $A_nM$  with an excess PDHA or ADH using the previously developed two-step reductive amination protocol<sup>12</sup> to assess the relative reactivities of aldehydes at the RE and the O-NRE (Figure 1c). Secondly, we reacted oxidised  $A_nM$  oligomers with a sub-stoichiometric amount of PDHA to obtain a discrete distribution of a new type of water-soluble chitin block polysaccharides composed of a progressively increasing number of  $A_nM$  blocks reacted through both termini. The introduction of a dialdehyde in the NRE residue combined with the highly reactive aldehyde at the reducing of  $A_nM$  oligomers enables the preparation of a range of new glycoconjugates, including more complex block polysaccharides.



**Figure 1:** a) chemical structure of an  $A_2M$  oligomer, b) chemical structure of a periodate oxidised  $A_2M$  oligomer, c) conjugation of PDHA or ADH to the RE and NRE of an oxidised  $A_2M$  oligomer.

## Materials and methods

### Materials

High molecular weight chitosan ( $F_A = 0.48$ ,  $[\eta] = 1210$  mL/g) was obtained from Advanced Biopolymers ABC. Adipic acid dihydrazide (ADH), O,O'-1,3-propanediylbishydroxylamine dihydrochloride (PDHA)

and 2-methylpyridine borane complex ( $\alpha$ -Picoline borane, PB) were obtained from Sigma-Aldrich. All other chemicals were obtained from commercial sources and were of analytical grade.

### **Gel filtration chromatography (GFC)**

Preparative and analytical gel filtration chromatography (GFC) were used for fractionation of chitin oligosaccharides and fractionation of products, respectively, as described earlier<sup>12</sup>. In brief, both systems were composed of Superdex 30 columns (BPG 140/950 (140 x 950 mm) and HiLoad 26/600 (26 x 600 mm), respectively) connected in series, continuously eluting ammonium acetate (AmAc) buffer (0.15 M, pH 4.5 and 0.1 M, pH 6.9, respectively). Fractionation was monitored on-line using a refractive index (RI) detector and fractions were collected and pooled according to elution times. The pooled fractions were reduced to appropriate volumes, dialyzed (MWCO = 100-500 Da) against ultrapure Milli-Q (MQ) water until the measured conductivity of the water was  $< 2 \mu\text{S}/\text{cm}$  and freeze-dried or freeze-dried directly without dialysis to remove the volatile mobile phase (AmAc-buffer).

### **NMR spectroscopy**

Water-soluble samples for NMR characterization were dissolved in  $\text{D}_2\text{O}$  (450-600  $\mu\text{L}$ , approx. 10 mg/mL). For some samples, 1% deuterated sodium 3-(trimethylsilyl)-propionate (TSP- $\text{d}_4$ , 3  $\mu\text{L}$ ) was added as an internal standard. Water-insoluble samples were dissolved in deuterated hexafluoro isopropanol (HFIP- $\text{d}_2$ ).

Characterization was performed by obtaining 1D  $^1\text{H}$  NMR spectra at 300K on a Bruker Ascend 14.1 Tesla 600 MHz equipped with Avance III HD electronics and a 5 mm Z-gradient CP-TCI cryogenic probe. All spectra were recorded, processed and analysed using TopSpin 3.5pl7 software (Bruker BioSpin).

### **Mass spectrometry (MS)**

MS characterisation was performed using flow injection analysis (FIA) coupled with quadrupole time of flight (gTOF) MS as described earlier<sup>13</sup>. The mass range was set to 50-2000 Da which limited the characterisation of larger structures.

### **Preparation of chitin oligomers by nitrous acid degradation**

Chitin oligomers ( $A_nM$ ) were prepared by nitrous acid (HONO) degradation as described earlier<sup>12</sup>. In brief, chitosan ( $F_A = 0.48$ ) was degraded using an excess of HONO (1.3 moles of HONO per mole GlcN) overnight in the dark at 4 °C. Washing and centrifugation steps were performed to remove the insoluble fraction, assumed to be water-insoluble chitin oligomers. The water-soluble low molecular weight chitin oligomers were fractionated according to degree of polymerization (DP) by GFC (DP < 10). Isolated oligomers were purified by dialysis, freeze-dried and characterized by  $^1\text{H}$ -NMR.

### **Periodate oxidation**

Chitin oligomers ( $A_nM$ ) or chitin oligomer conjugates ( $A_6M$ -PDHA or  $A_2M$ -ADH- $MA_2$ ) (10 mM) were dissolved in MQ-water. Oxygen was removed by bubbling the solution with  $N_2$  gas for 10 minutes. Freshly prepared and  $N_2$  bubbled  $NaIO_4$  (100 mM) was added to give a final molar ratio of 2:1 or 4:1 ( $NaIO_4$ :  $A_nM$  or conjugates). Reactions were performed in the dark at 4 °C for 24 hours on a shaking device. Ethylene glycol (10 molar equivalents) was added to the reaction mixture and stirred for 30 minutes to terminate the reaction. The reaction mixture was dialyzed (MWCO = 100-500 Da) against MQ-water until the measured conductivity was  $< 2 \mu S/cm$  and freeze-dried.

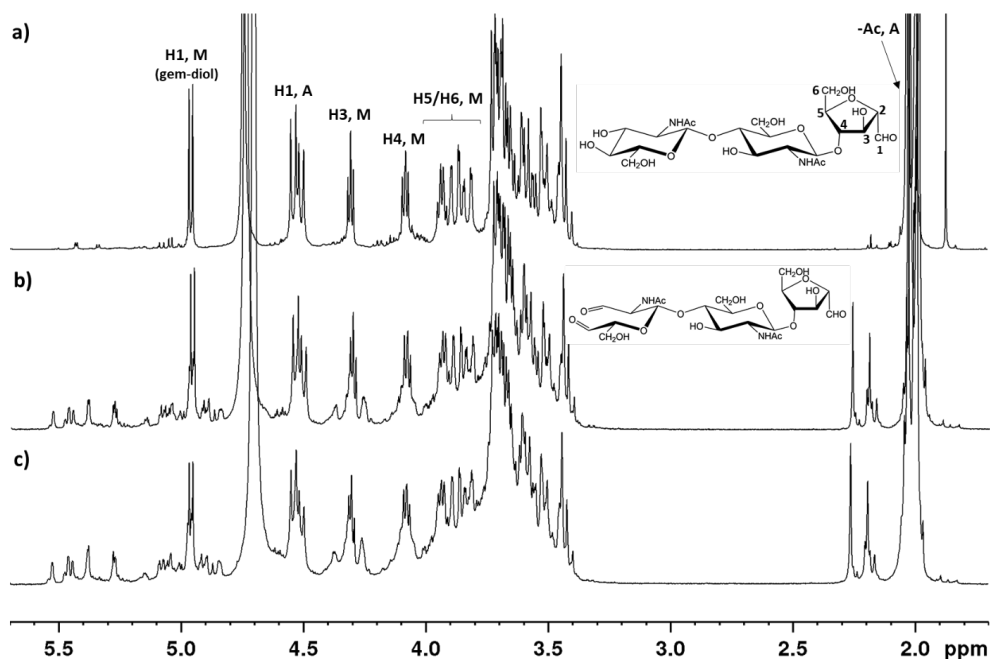
### **Conjugation of oxidised $A_nM$ oligomers to ADH and PDHA**

Oxidised  $A_nM$  oligomers (6.5 mM) and ADH or PDHA (0.5 – 10 equivalents) were dissolved in NaAc-buffer (500 mM, pH 4.0) and reacted for 24 hours at room temperature. PB (20 equivalents) was added to the reaction mixture, and the reduction was allowed to proceed for 72 hours at room temperature. The reaction mixtures were dialysed (MWCO = 100-500 Da) against 0.05 M NaCl until the partly insoluble PB dissolved and subsequently freeze-dried. The mixtures were further fractionated by GFC. Isolated fractions were purified by direct freeze-drying to remove the volatile GFC-buffer (AmAc) and characterised by NMR or MS.

## **Results and discussion**

### **Periodate oxidation of $A_nM$ oligomers**

$A_nM$  oligomers, where n corresponds to DP-1, were prepared by nitrous acid depolymerisation as described earlier<sup>12</sup>. The water-soluble oligomers (n = 0-8) were isolated by GFC fractionation to obtain oligomers of specific DP. Initially,  $A_2M$  oligomers were oxidised using 2 equivalents of periodate, purified by dialysis and characterised by <sup>1</sup>H-NMR (Figure 2b). New resonances appeared in the anomeric region (4.8-5.6 ppm), but the spectrum was otherwise too complex for a complete determination of structure and degree of oxidation. The high complexity can be attributed to inter- or intra-residue hemiacetals readily formed with the dialdehydes after oxidation of the NRE<sup>14,15</sup>. Such hemiacetals are acid stable and difficult to structurally elucidate, but they are reversible and will therefore not represent an issue for further modifications. A reduced intensity was observed for the resonance resulting from H1, M (gem-diol) relative to other resonances in the spectrum after oxidation. The reduced intensity may be caused by the formation of inter-residue hemiacetals with the aldehydes of the O-NRE. The M residue seemed otherwise unaltered as predicted from its structure. Hence, the oxidation only took place at the NRE. Oxidation with 4 equivalents of periodate gave essentially the same result, however, with an even lower intensity of the H1, M resonance suggesting a higher degree of oxidation and more inter-residue hemiacetals formed (Figure 2c). Unless otherwise stated, oligomers oxidised with 2 equivalents periodate were used in the following experiments.

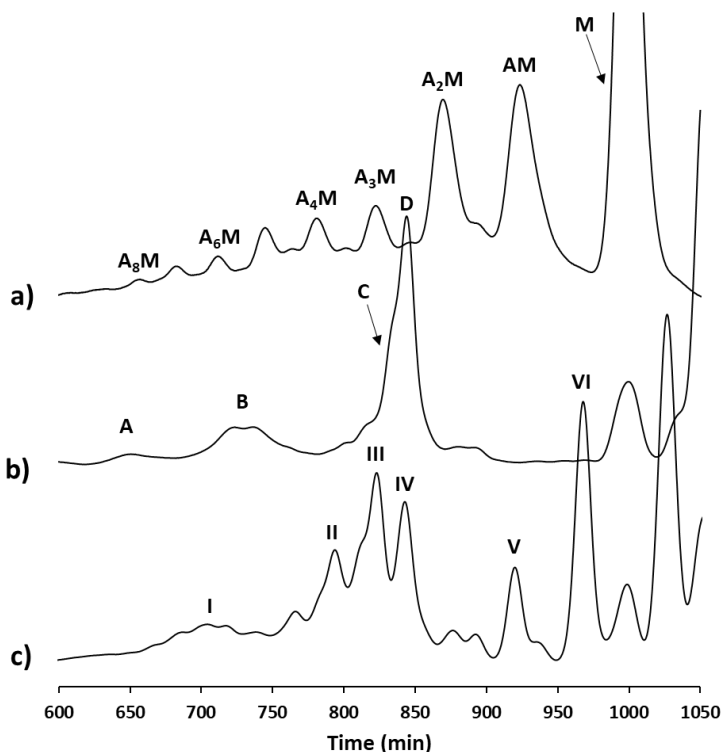


**Figure 2:**  $^1\text{H-NMR}$  spectra of **a)**  $\text{A}_2\text{M}$  (unoxidised), **b)** oxidised  $\text{A}_2\text{M}$  prepared using 2 equivalents  $\text{NaIO}_4$  and **c)** oxidised  $\text{A}_2\text{M}$  prepared using 4 equivalents  $\text{NaIO}_4$ .

### Activation of oxidised $\text{A}_2\text{M}$ oligomers by PDHA and ADH

Even though oxidised  $\text{A}_n\text{M}$  preparations were rather complex mixtures, we decided to proceed without further purification as this most likely could be better obtained after conjugation to PDHA or ADH. Thus, oxidised  $\text{A}_2\text{M}$  oligomers were reacted with 10 equivalents PDHA or ADH using the two-step reductive amination protocols recently developed for  $\text{A}_n\text{M}$  oligomers<sup>12</sup>. Interestingly, the two reaction systems behaved very differently. With ADH an insoluble fraction was formed, while this was not observed for PDHA. The reaction mixtures (soluble fractions) were characterized by  $^1\text{H-NMR}$  (Supporting information, S1). Compared to the corresponding conjugates prepared with unoxidised oligomers, the NMR spectra of the reaction mixtures were more complex. However, resonances resulting from the characteristic secondary amine protons (around 3.0 ppm) appeared, indicating the formation of conjugates. Importantly, the H1 resonances for unreacted M disappeared, confirming complete reaction at the RE, as expected<sup>12</sup>. Incomplete reduction of conjugates formed with PDHA was observed by the presence of resonances in the Schiff base area (6-8 ppm) suggesting unoptimized reduction conditions. Conjugates formed with ADH were in contrast completely reduced (Supporting information, S1). The reaction mixtures were further fractionated

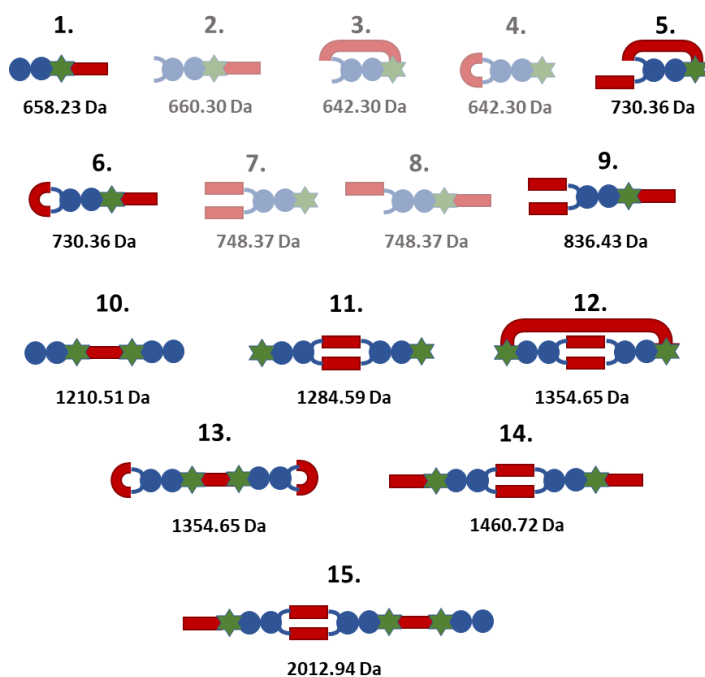
by GFC (Figure 3). Purified fractions were characterised by  $^1\text{H-NMR}$  and MS (Supporting information, S2 and S3 for PDHA and ADH, respectively).



**Figure 3:** Analytical GFC fractionation of **a)** a standard mixture of  $A_nM$  oligomers for GFC calibration, **b)** the mixture following reaction of oxidised  $A_2M$  with 10 equivalents PDHA and 20 equivalents PB and **c)** the water-soluble fraction from the reaction of oxidised  $A_2M$  with 10 equivalents ADH and 20 equivalents PB.

Fractionation of the mixture obtained for the reaction with PDHA resulted in a major fraction with an elution time corresponding to PDHA-activated  $A_2M$  (Fraction D, Figure 3b), with a shoulder fraction (collected separately) with slightly shorter elution time (Fraction C). Both fractions were shown to contain oligomers and PDHA linked by secondary amine or Schiff base linkages by  $^1\text{H-NMR}$  and MS (Supporting information, S2). One oxidised  $A_2M$  oligomer can in principle enable the formation of eight different conjugates with divalent amines (such as PDHA and ADH) as illustrated for PDHA in Figure 4 (2-9). MS was used for determining their presence. **1**, **5**, **6** and **9** (Figure 4) were identified in fraction C and D. **5** and **6** have the same mass and cannot be distinguished by MS. Fraction C consisted predominantly of **9**, which

was the structure aimed for when using an excess of the divalent linkers. The presence of **9** confirms the reactivity of both aldehydes at the O-NRE. This is in contrast to lateral periodate oxidation of alginate, where only one of the aldehydes is reactive towards substitution<sup>10,16</sup>. The absence of conjugates containing unreacted aldehydes (**2-4**, **7** and **8**), indicates high reactivity of all aldehydes, including the possibility to rapidly form intramolecular (cyclic) structures. The presence of **1** confirmed incomplete oxidation of the oligomers under the given conditions.



**Figure 4:** Graphical presentation of possible structures formed when unoxidised and oxidised A<sub>2</sub>M oligomers were reacted with an excess PDHA and the theoretical mass of each structure (fully reduced). For structures with one oligomer (**1-9**) all possible combinations are presented (semi-transparent structures were not identified). For products with two or three oligomers (**10-14** and **15**, respectively), only the identified structures are presented. The symbols used are defined in Figure 1.

The presence of fractions corresponding to a hexamer and a nonamer (Fraction A and B, respectively in Figure 3b based on the calibration with A<sub>n</sub>M oligomers in Figure 3c) indicated conjugation of PDHA to both the RE and O-NRE of the oligomers to form chitin block structures. <sup>1</sup>H-NMR characterisation confirmed the presence of oligomer and PDHA linked by Schiff base or secondary amine linkages (Supporting information, S2). Due to the incomplete oxidation, the block structures were composed of a

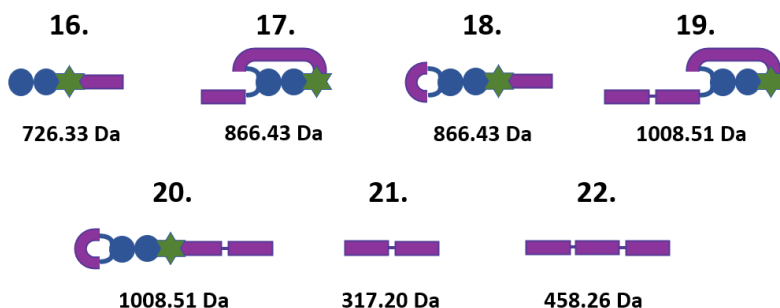
mixture of oxidised and unoxidised A<sub>2</sub>M oligomers. MS characterisation revealed a complex mixture of structures due to the multiple ways of combining oligomers and PDHA. For the block structures composed of two oligomers (Fraction B, Figure 3b), diblocks containing unoxidised oligomers linked by a single PDHA were identified (**10** in Figure 4). Interestingly, diblocks composed of two oxidised oligomers linked by two PDHA molecules through the O-NRE (**11**) were also identified. Their presence suggests similar or even higher reactivities of the O-NRE aldehydes compared to the RE aldehyde. In the opposite case, one would expect the blocks to be predominantly attached through the RE. Importantly, such diblocks could not be identified. Diblocks with intramolecular (cyclic) structures (**12** or **13**) were also detected, in addition to fully substituted diblocks attached through the O-NRE (**14**). For the block structures composed of three oligomers (Fraction A, Figure 3b) we identified block structures composed of two oxidised oligomers and one unoxidised oligomer linked through the RE and O-NRE (**15**). Details regarding the <sup>1</sup>H-NMR and MS characterisation are given in Supporting information, S2. The presence of non-reduced Schiff bases, especially for conjugates linked through the O-NRE suggest the need for longer reduction times and/or higher concentrations of reducing agent (PB) for PDHA based reactions with oxidised oligomers.

Fractionation of the water-soluble fraction obtained for the reaction with ADH revealed a more complex mixture of structures (Figure 3c). The three main fractions (II, III and IV) were confirmed to contain oligomers and ADH linked by secondary amine linkages by <sup>1</sup>H-NMR (Supporting information, S3). Fraction IV (Figure 3c) was mainly composed of A<sub>2</sub>M-ADH conjugates formed with unoxidised oligomers (**16**, Figure 5), confirming the incomplete oxidation of the oligomers discussed above. The presence of intramolecular cyclic structures (**17** or **18**) in fraction III, analogous to those observed with PDHA, confirmed the high reactivity of all the aldehydes. Structures containing multiple ('polymerised') ADH (**19** or **20**) were identified in fraction II, in line with previous experiments with ADH<sup>13</sup>. Fraction VI and V contained free 'polymerised' ADH (**21** and **22**, respectively). In contrast to the PDHA case, complete reduction was obtained for all the conjugates with ADH. This supports our previous observations of faster reduction of hydrazones compared to oximes with PB<sup>12</sup>.

The water-insoluble fraction was dissolved in hexafluoro isopropanol (HFIP) and shown to only contain 'polymerised' ADH by <sup>1</sup>H-NMR (Supporting information, S4). The mechanism for the polymerisation is unknown but seems to be enhanced by the pre-treatment of the oligomers by periodate due to the extensive formation of 'polymerised' insoluble ADH formed after only 96 hours at RT. In a corresponding reaction where 'polymerised' ADH was observed, the reaction proceeded for 40 days at RT without forming an insoluble fraction. The corresponding reaction was performed under the same conditions only differing in reaction time and type of oligomer (*N,N'*-diacetyl chitobiose (AA) instead of oxidised A<sub>2</sub>M)<sup>13</sup>. Oxidised oligomers were only purified by dialysis prior to activation and traces of periodate or ethylene glycol may

have enhanced the ‘polymerisation’ mechanism. We therefore assume that a more thorough purification of the oligomers prior to activation (e.g. by GFC fractionation) can reduce the formation of ‘polymerised’ ADH.

Fully ADH activated oxidised A<sub>2</sub>M conjugates (corresponding to **9** in Figure 4) were not identified in the reaction mixture, in contrast to the reaction with PDHA where a large fraction of this structure was formed. This can be explained by the fast and extensive formation of ‘polymerised’ ADH.



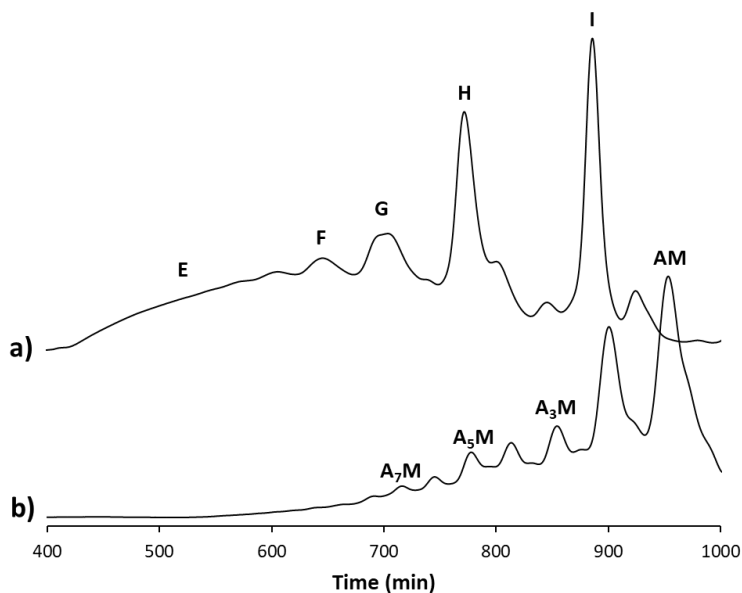
**Figure 5:** Graphical presentation of identified structures from the reaction of oxidised (and unoxidised) A<sub>2</sub>M oligomers with an excess ADH and the mass of each structure (fully reduced).

Although reactions of oxidised A<sub>n</sub>M oligomers with an excess of PDHA or ADH resulted in a range of different structures, including longer block structures (**11- 15**, Figure 4), the results demonstrate that both aldehydes at the O-NRE react avidly. This forms an excellent basis for further reactions towards A<sub>n</sub>M-based block polysaccharides. Even though ADH reacted readily with the oxidised oligomers, further experiments were performed with PDHA to circumvent the complexing factor with the ADH ‘polymerisation’.

#### **Soluble A<sub>2</sub>M-based block polymers**

Based on the results from the initial conjugation experiment with oxidised A<sub>2</sub>M and PDHA, we attempted to form longer chitin block polymers by conjugating oxidised A<sub>2</sub>M using a sub-stoichiometric amount of PDHA (0.5 equivalents). The resulting reaction mixture was completely water soluble. <sup>1</sup>H-NMR characterisation confirmed the presence of secondary amines (Supporting information, S5). The reaction mixture was subsequently fractionated by GFC (Figure 6a).





**Figure 6:** a) GFC fractionation following reaction of oxidised  $A_2M$  with 0.5 equivalents PDHA. b) fractionation of a standard mixture of  $A_nM$  oligomers for GFC calibration.

The reaction resulted in the formation of longer chitin block polymers (up to  $> DP 24$  based on calibration with  $A_nM$  oligomers). Interestingly, all fractions were completely water-soluble, whereas unreacted  $A_nM$  oligomers only are water-soluble up to  $DP 9$  (Figure 6b). Fractions (E-I) were purified and characterised by  $^1H$ -NMR and MS (Supporting information, S6). Fraction I contained oxidised oligomers activated with one PDHA molecule forming intramolecular cyclic structures (**3** or **4**, Figure 4). This fraction also contained a large portion of reduced unreacted  $A_nM$  oligomers. Interestingly, no unreacted *oxidised* oligomers were detected, confirming that the O-NRE aldehydes are more reactive than the aldehyde of the M residue. Fractions G and H corresponded to fraction A and B in Figure 3 with short chitin block structures ( $DP 6$  (e.g. **10-14** Figure 4) and  $9$  (e.g. **15** Figure 4), respectively). However, none of the structures were fully substituted with PDHA as a consequence of the lower equivalence of PDHA used. Due to limitation in the mass detection for larger ions by the MS method, identification of specific block structures in fraction E and F was difficult. However, the obtained  $^1H$ -NMR spectra were identical to the spectrum obtained for fraction G, indicating that these are longer block polymers with otherwise similar structure.

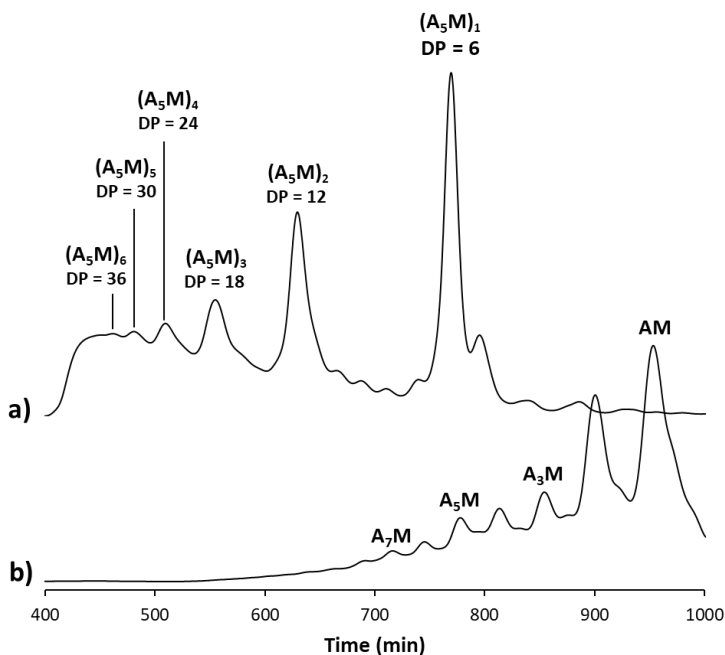
The large amount of reduced unreacted and unoxidised oligomers indicates slow kinetics for the periodate oxidation of the  $A_nM$  oligomers. Less unreacted oligomers were obtained when oxidised  $A_2M$  were prepared using 4 equivalents periodate and reacted under the same conditions (Supporting information, S7). Hence, the degree of oxidation can be increased by using a higher excess of periodate and/or longer reaction (oxidation) time.

#### **Preparation of soluble chitin-based block polymers using longer oxidised $A_nM$ oligomers**

Oxidised  $A_5M$  oligomers (prepared using 2 equivalents  $NaIO_4$ ) were reacted with 0.5 equivalents PDHA and fractionated by GFC (Figure 7a). The resulting chromatogram showed a series of distinct fractions with DP (by extrapolation of the GFC calibration) corresponding to block structures composed of multiple oxidised  $A_5M$  blocks linked by PDHA.

Both the unfractionated sample and the fractions were soluble in water (buffer) even though  $A_5M$  oligomers are close to the solubility limit for chitin. The longest soluble block polymers detected had an apparent DP above 36 (Figure 7a).  $^1H$ -NMR characterisation confirmed the presence of oligomers linked through both the RE and O-NRE by PDHA in all fractions (Supporting information, S8). Due to limitation in mass detection for larger ions by the MS method and the complex mixture of structures formed, the possibilities for precise structure determination of the longer block polymers was limited. However, MS characterisation of the fraction eluting at approx. same time as the parent oligomer turned out to be a mixture of unoxidised oligomers and oxidised oligomers activated with a single PDHA molecule forming an intramolecular cyclic structure, confirming the high reactivity of the O-NRE aldehydes. Hence, the oxidised  $A_5M$  oligomers behaved in the same way as the oxidised  $A_2M$ . We therefore assume the longer block structures to be of the same composition as the structures identified above.

We suggest that the increased solubility is primarily associated with the flexibility of the PDHA linker, contributing to conformational entropy of the block structures as compared to homogenous chitin chains. By increasing the degree of oxidation of the  $A_nM$  oligomers and optimising the conjugation protocol, this method can be used to prepare a new type of soluble chitin block polymers of longer chain length with potential for pharmaceutical and biomaterial applications.

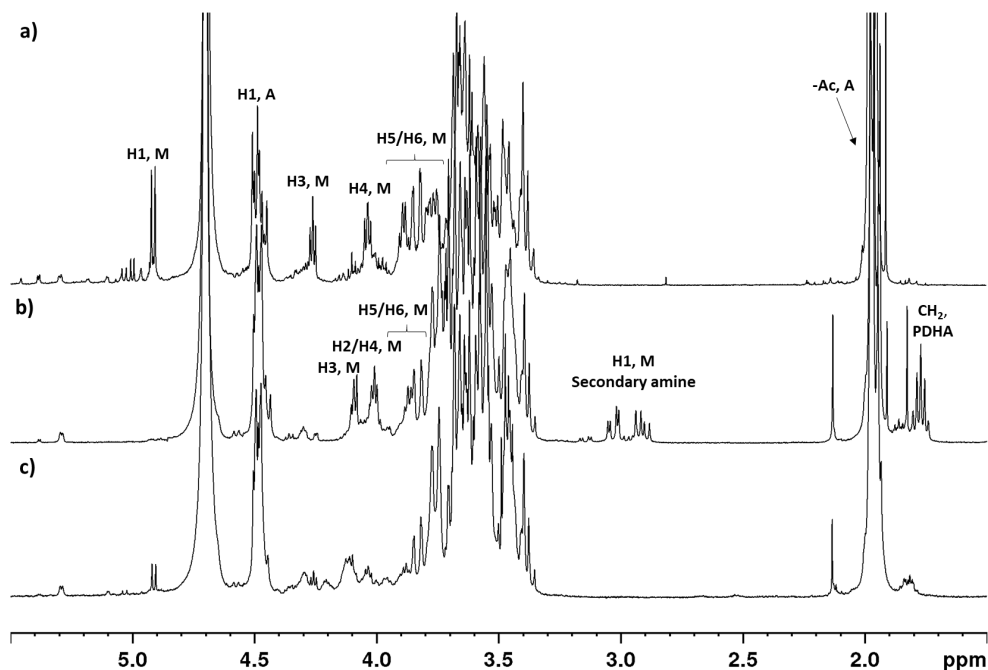


**Figure 7:** a) GFC fractionation following reaction of oxidised  $A_5M$ , prepared using 2 equivalents periodate, with 0.5 equivalents PDHA b) fractionation of a standard mixture of  $A_nM$  oligomers for GFC calibration.

### An alternative approach to NRE functionalisation of chitin oligomers

Reaction with periodate oxidised  $A_nM$  oligomers resulted in a complex mixture of structures. We therefore investigated the oxidation of chitin conjugates ( $A_nM$ -ADH/PDHA) as an alternative approach to functionalise the NRE of chitin oligomers. This approach requires stability of the secondary amine linkage between the oligomers and PDHA or ADH throughout the oxidation step.  $A_nM$  conjugates ( $A_6M$ -PDHA and the diblock  $A_2M$ -ADH- $MA_2$ ) were oxidised using 2 equivalents periodate.  $^1H$ -NMR characterisation after dialysis showed complete disappearance of the resonances resulting from the secondary amines and a drastic change in the proton resonances resulting from the M residue (Figure 8 for  $A_6M$ -PDHA and Supporting information, S9 for  $A_2M$ -ADH- $MA_2$ ). Hence, the results indicate that the secondary amine linkages are destroyed during the oxidation. Interestingly, a minor resonance from H1 M residue reappeared after the treatment with periodate for the  $A_6M$ -PDHA conjugate (Figure 8c). This was not observed for the periodate treatment of  $A_2M$ -ADH- $MA_2$  (Supporting information, S9), suggesting different mechanisms for

the degradation of the conjugates. In any case, this approach is unfortunately not applicable for the preparation of precursors for ABA- or ABC-type block polysaccharides.



**Figure 8:**  $^1\text{H-NMR}$  spectra of **a)** a purified  $\text{A}_3\text{M}$  oligomer, **b)** the purified  $\text{A}_6\text{M-PDHA}$  conjugate prior to oxidation and **c)** the resulting mixture after oxidation and dialysis.

## Conclusions

The vicinal diol in the NRE end residue of  $\text{A}_n\text{M}$  oligomers can be selectively oxidised by periodate, forming the corresponding dialdehydes in addition to the pending aldehyde of the M residue. The dialdehydes are even more reactive towards dioxamines and dihydrazides than the already reactive aldehyde of the M residue. Reactions with an excess of these divalent linkers can provide  $\text{A}_n\text{M}$  oligomers fully substituted at the RE and O-NRE. Such oxidised oligomers are therefore potential precursors for a range of new glycoconjugates, including complex block polysaccharides. The latter was demonstrated by the formation of a discrete distribution of 'polymerised'  $\text{A}_n\text{M}$  oligomers through reactions with sub-stoichiometric amounts of linkers. Importantly, these block polysaccharides were, in contrast to chitins of the same chain lengths, water-soluble. Such soluble chitin-based polymers may be relevant for biomedical and biomaterial applications.

## Acknowledgements

This work was supported by a grant from the Norwegian University of Science and Technology to I. V. Mo. Ranganhild Bardal Roness is thanked for running some preliminary experiments with periodate oxidised A<sub>n</sub>M oligomers during the work with her master thesis (2015-2017). Kåre Kristiansen is thanked for running the MS analysis.

## References

1. Breitenbach, B. B.; Schmid, I.; Wich, P. R. (2017) *Amphiphilic polysaccharide block copolymers for pH-responsive micellar nanoparticles*. *Biomacromolecules* 18 (9), 2839-2848.
2. Breitenbach, B. B.; Steiert, E.; Konhäuser, M.; Vogt, L.-M.; Wang, Y.; Parekh, S. H.; Wich, P. R. (2019) *Double stimuli-responsive polysaccharide block copolymers as green macrosurfactants for near-infrared photodynamic therapy*. *Soft Matter* 15 (6), 1423-1434.
3. Chen, J.; Spiering, G.; Mosquera-Giraldo, L.; Moore, R. B.; Edgar, K. J. (2020) *Regioselective bromination of the dextran nonreducing end creates a pathway to dextran-based block copolymers*. *Biomacromolecules* 21 (5), 1729-1738.
4. Wang, Z.; Shi, C.; Wu, X.; Chen, Y. (2014) *Efficient access to the non-reducing end of low molecular weight heparin for fluorescent labeling*. *Chemical Communications* 50 (53), 7004-7006.
5. Kristiansen, K. A.; Potthast, A.; Christensen, B. E. (2010) *Periodate oxidation of polysaccharides for modification of chemical and physical properties*. *Carbohydrate Research* 345 (10), 1264-1271.
6. Tømmeraaas, K.; Vårum, K. M.; Christensen, B. E.; Smidsrød, O. (2001) *Preparation and characterisation of oligosaccharides produced by nitrous acid depolymerisation of chitosans*. *Carbohydrate Research* 333 (2), 137-144.
7. Hirano, S.; Yagi, Y. (1981) *Periodate oxidation of the non-reducing end-groups of substrates increases the rates of enzymic hydrolyses by chitinase and by lysozyme*. *Carbohydrate Research* 92 (2), 319-322.
8. Huang, G.-L.; Zhang, D.-W.; Zhao, H.-J.; Zhang, H.-C.; Wang, P.-G. (2006) *Chemo-enzymatic synthesis of 1,4-oxazepanyl sugar as potent inhibitor of chitinase*. *Bioorganic & Medicinal Chemistry* 14 (7), 2446-2449.
9. Imai, T.; Watanabe, T.; Yui, T.; Sugiyama, J. (2002) *Directional degradation of  $\beta$ -chitin by chitinase A1 revealed by a novel reducing end labelling technique*. *FEBS Letters* 510 (3), 201-205.
10. Kristiansen, K. A.; Ballance, S.; Potthast, A.; Christensen, B. E. (2009) *An evaluation of tritium and fluorescence labelling combined with multi-detector SEC for the detection of carbonyl groups in polysaccharides*. *Carbohydrate Polymers* 76 (2), 196-205.
11. Dalheim, M. Ø.; Vanacker, J.; Najmi, M. A.; Aachmann, F. L.; Strand, B. L.; Christensen, B. E. (2016) *Efficient functionalization of alginate biomaterials*. *Biomaterials* 80, 146-156.

12. Mo, I. V.; Dalheim, M. Ø.; Aachmann, F. L.; Schatz, C.; Christensen, B. E. (2020) *2,5-anhydro-D-mannose end-functionalized chitin oligomers activated by dioxyamines or dihydrazides as precursors of diblock oligosaccharides*. *Biomacromolecules* 21 (7), 2884-2895.
13. Mo, I. V.; Feng, Y.; Dalheim, M. Ø.; Solberg, A.; Aachmann, F. L.; Schatz, C.; Christensen, B. E. (2020) *Activation of enzymatically produced chitooligosaccharides by dioxyamines and dihydrazides*. *Carbohydrate Polymers* 232, 115748.
14. Ishak, M. F.; Painter, T.; Andersen, V. S.; Enzell, C. R.; Lousberg, R. J. J. C.; Weiss, U. (1971) *Formation of inter-residue hemiacetals during the oxidation of polysaccharides by periodate ion*. *Acta Chemica Scandinavica* 25 (10), 3875-3877.
15. Sharon, N. *Complex carbohydrates. Their chemistry, biosynthesis, and functions*. 1 st. ed., Addison-Wesley Publishing Company (1975).
16. Dalheim, M. Ø.; Ulset, A.-S. T.; Jenssen, I. B.; Christensen, B. E. (2017) *Degradation kinetics of peptide-coupled alginates prepared via the periodate oxidation reductive amination route*. *Carbohydrate Polymers* 157, 1844-1852.

# Supporting information

## Functionalisation of the non-reducing end of chitin: A new approach to form complex block polysaccharides and water-soluble chitin-based block polymers

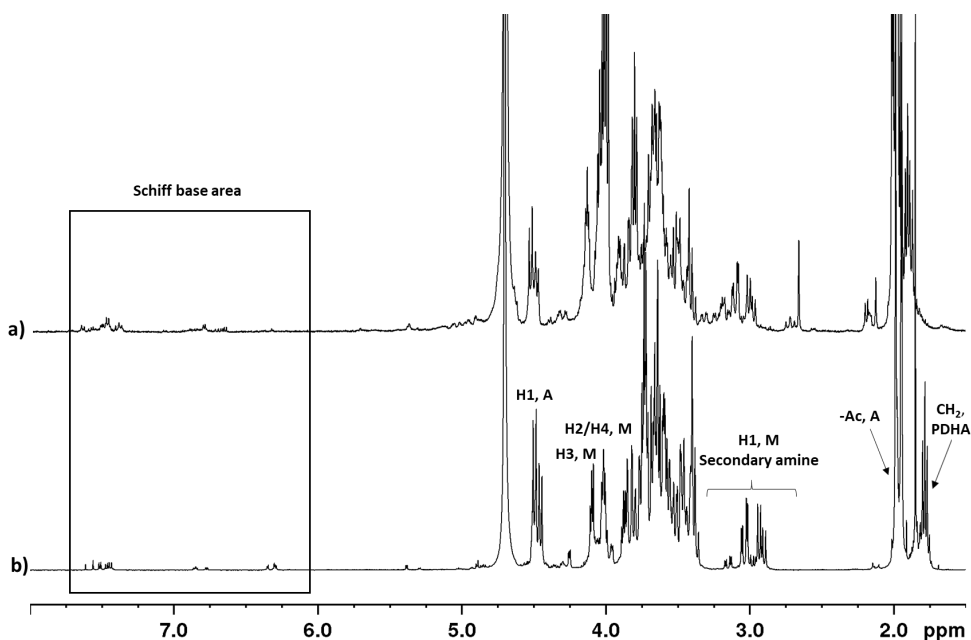
*Ingrid Vikøren Mo, Christophe Schatz, Bjørn E. Christensen*

### Contents

S1 Characterisation of reaction mixtures with oxidised A <sub>2</sub> M oligomers and an excess PDHA or ADH .....	2
S2 Characterisation of fractions from the reaction with oxidised A <sub>2</sub> M oligomers and an excess PDHA ....	3
S3 Characterisation of fractions from the reaction with oxidised A <sub>2</sub> M oligomers and an excess ADH (water-soluble fraction) .....	8
S4 Characterisation of the water-insoluble fraction from the reaction with oxidised A <sub>2</sub> M oligomers and an excess ADH .....	12
S5 Characterisation of the reaction mixture formed with oxidised A <sub>2</sub> M oligomers and a sub-stoichiometric amount of PDHA .....	13
S6 Characterisation of fractions from the reaction with oxidised A <sub>2</sub> M and a sub-stoichiometric amount PDHA.....	14
S7 Reaction of oxidised A <sub>2</sub> M oligomers, obtained using 4 equivalents periodate, with a sub-stoichiometric amount of PDHA .....	17
S8 Characterisation of fractions from the reaction with oxidised A <sub>5</sub> M and a sub-stoichiometric amount PDHA.....	18
S9 Periodate oxidation of A <sub>2</sub> M-ADH-MA <sub>2</sub> diblocks.....	20
S10 References.....	21

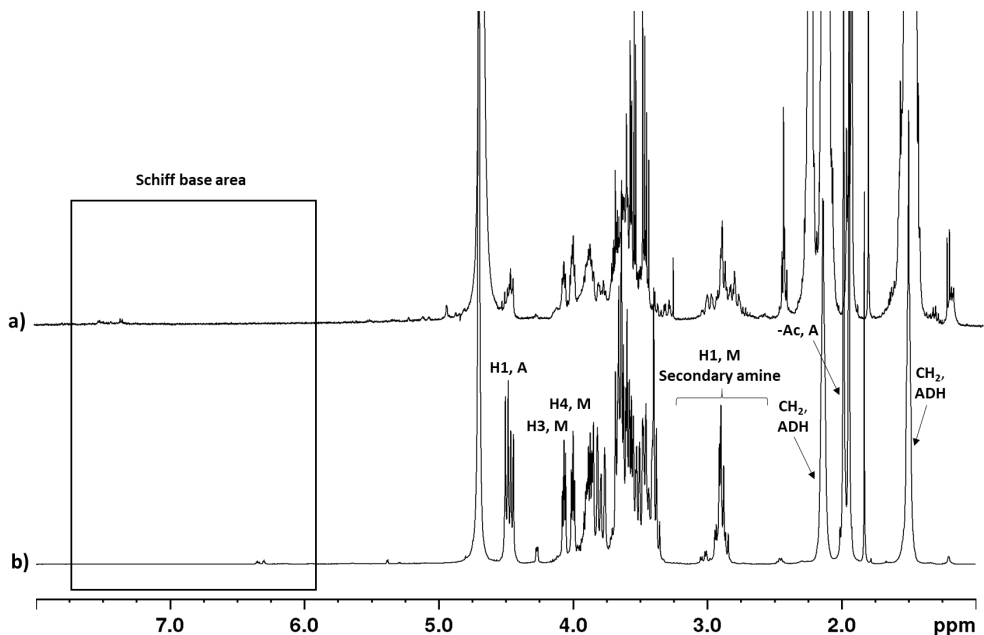
## S1 Characterisation of reaction mixtures with oxidised A<sub>2</sub>M oligomers and an excess PDHA or ADH

The reaction mixtures formed when oxidised A<sub>2</sub>M oligomers were reacted with 10 equivalents PDHA using the two-pot reductive amination procedure (pH 4.0, 20 equivalents PB added after 24 hours, with a total reduction time of 72 hours) and the water-soluble fraction from the corresponding experiment with ADH were characterized by <sup>1</sup>H-NMR and compared to purified A<sub>2</sub>M-PDHA and A<sub>2</sub>M-ADH conjugates prepared using unoxidised oligomers (Figure S1 and S2, respectively). Compared to the latter, the <sup>1</sup>H-NMR spectra of the reaction mixtures formed with oxidised A<sub>2</sub>M oligomers were more complex. However, resonances resulting from the characteristic secondary amine protons (around 3.0 ppm) were present in the samples, confirming formation of conjugates. The resonances were, however, more complex than for the conjugates with unoxidised A<sub>2</sub>M oligomers suggesting more than one type of conjugates formed. Incomplete reduction of conjugates formed with PDHA (Figure S1) was observed by the presence of resonances in the Schiff base area (6-8 ppm). Conjugates formed with ADH were in contrast completely reduced (Figure S2).



**Figure S1:** <sup>1</sup>H-NMR spectra of **a)** the mixture formed upon reaction of oxidised A<sub>2</sub>M oligomers with 10 equivalents PDHA and **b)** the purified A<sub>2</sub>M-PDHA conjugate with annotations of identified resonances<sup>1</sup>.

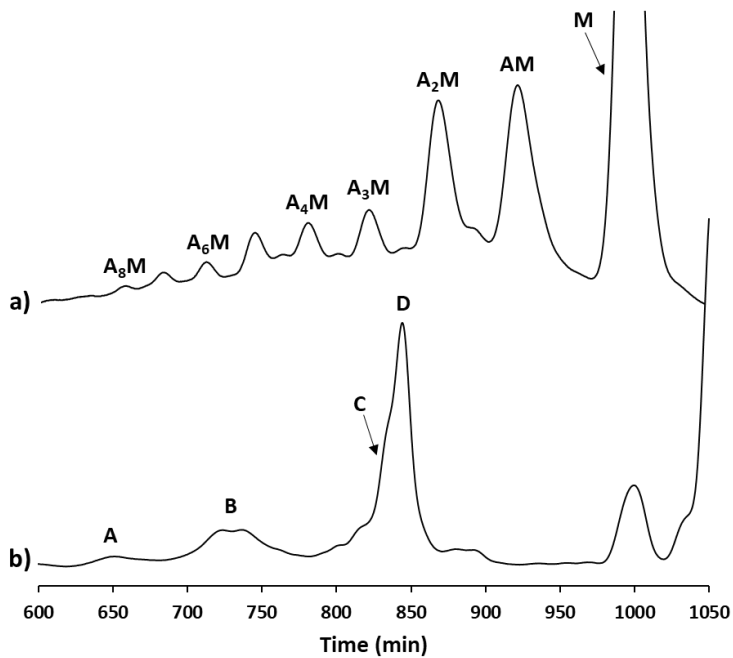




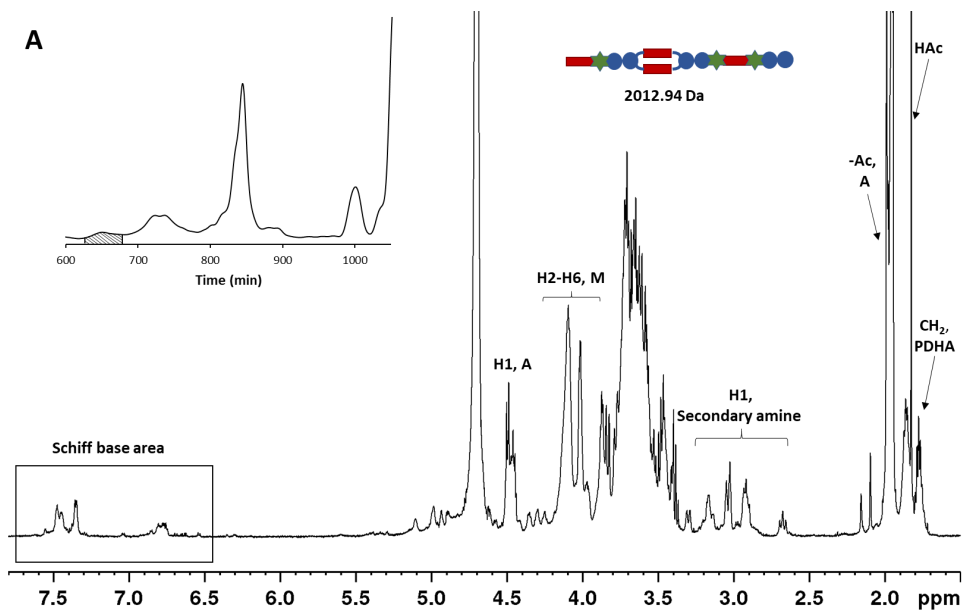
**Figure S2:**  $^1\text{H}$ -NMR spectra of **a)** the mixture formed upon reaction of oxidised  $\text{A}_2\text{M}$  oligomers with 10 equivalents ADH, **b)** purified  $\text{A}_2\text{M}$ -ADH conjugate with annotations of identified resonances<sup>1</sup>.

## S2 Characterisation of fractions from the reaction with oxidised $\text{A}_2\text{M}$ oligomers and an excess PDHA

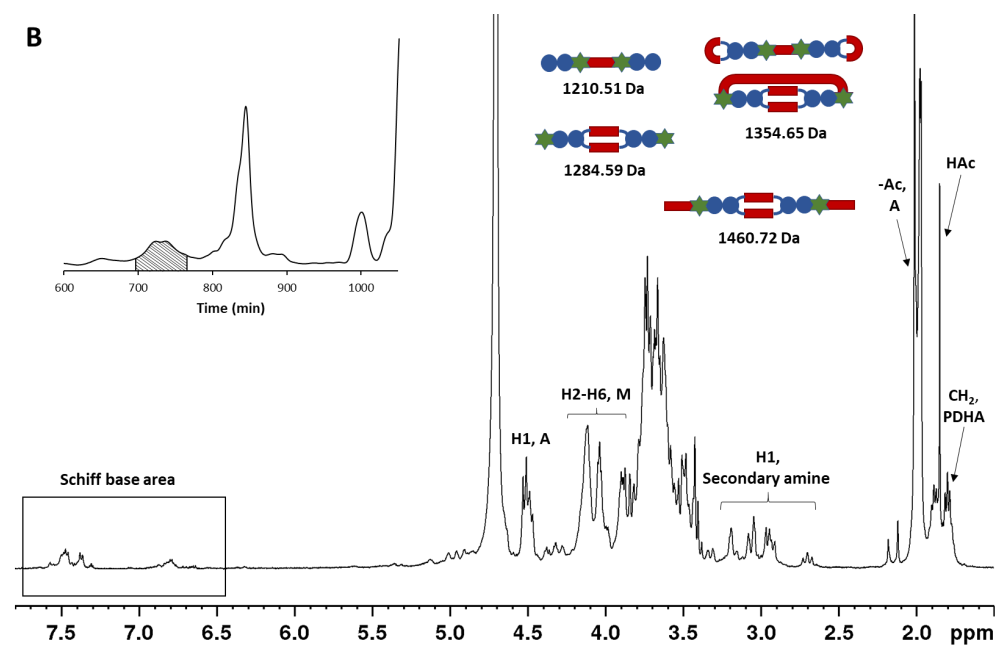
The reaction mixture obtained when oxidised  $\text{A}_2\text{M}$  oligomers were reacted with 10 equivalents PDHA was fractionated by GFC (Figure S3). Collected fractions (A-D) were purified and characterised by  $^1\text{H}$ -NMR and MS. The  $^1\text{H}$ -NMR spectra of the fractions are given in Figure S4-S7. The structures identified by MS and their theoretical mass (Da) are included in the figures. The incomplete reduction of Schiff bases did, however, influence the observed mass of some of the structures. The results from the MS characterisation of the fractions are presented in Table S1.



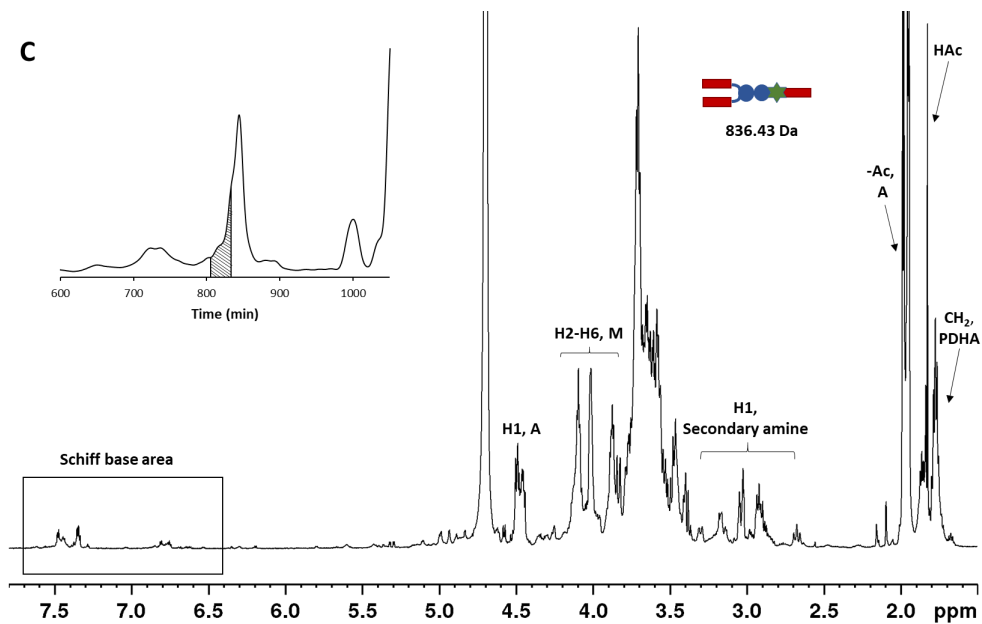
**Figure S3:** GFC fractionation of **a)** a standard mixture of  $A_nM$  oligomers for calibration and **b)** the reaction mixture obtained for oxidised  $A_2M$  oligomers reacted with 10 equivalents PDHA using the two-pot reductive amination protocol.



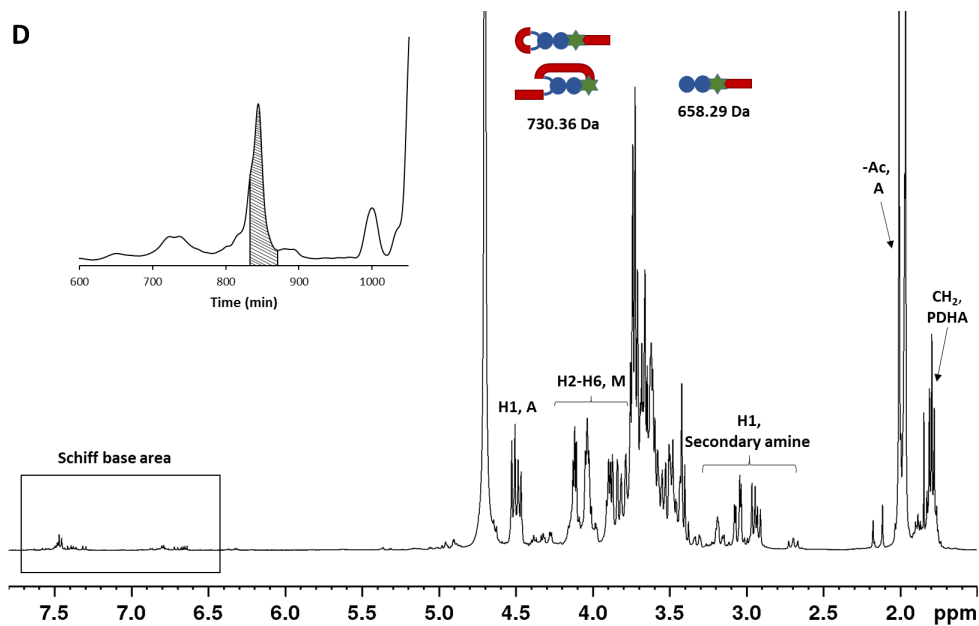
**Figure S4:** <sup>1</sup>H-NMR spectrum of fraction A from Figure S3. The structure identified by MS is included in the figure.



**Figure S5:** <sup>1</sup>H-NMR spectrum of fraction B from Figure S3. The structures identified by MS are included in the figure.










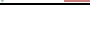












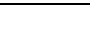










**Figure S6:** <sup>1</sup>H-NMR spectrum of fraction C from Figure S3. The structure identified by MS is included in the figure.



**Figure S7:** <sup>1</sup>H-NMR spectrum of fraction D from Figure S3. The structures identified by MS are included in the figure.

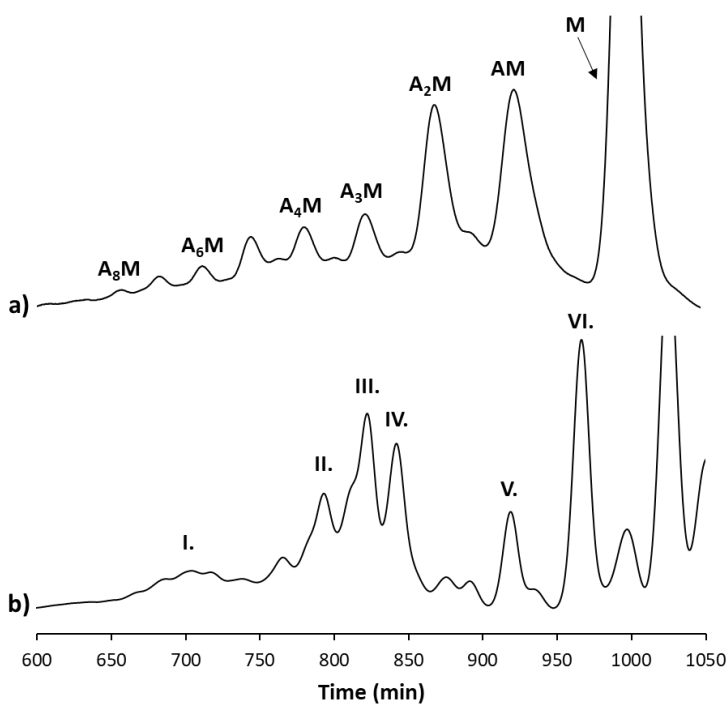
**Table S1:** Results of the MS characterisation of fractions obtained in the reactions with oxidised A<sub>2</sub>M oligomers and 10 (fraction A-D) or 0.5 equivalents (fraction E-I) PDHA. Structures were either identified as fully reduced or with x number (#) of Schiff bases (oximes) due to incomplete reduction. The *m/z* ions in **bold** represent ions identified in the fractions. Semi-transparent structures were not identified in any of the fractions. Fractions E-I are discussed in chapter S6.

Structure	Fraction	Theoretical mass (Da)	# of Schiff bases*	<i>m/z</i>			
				[M+H] <sup>+</sup>	[M+Na] <sup>+</sup>	[M+K] <sup>+</sup>	[M+2H] <sup>2+</sup>
		568.21	-	569.21	591.20	607.17	
	I	570.23	-	571.24	<b>593.22</b>	609.19	
	D	658.29	-	<b>659.30</b>	<b>681.28</b>	697.25	
		660.30	-	661.31	683.29	699.26	
	I	642.30	-	643.31	665.29	681.26	
	D	640.28	1	<b>641.29</b>	<b>663.27</b>	679.24	
	D	730.36	-	<b>731.37</b>	<b>753.35</b>	<b>769.32</b>	
		726.33	2	<b>727.34</b>	<b>749.32</b>	<b>765.29</b>	
		748.37	-	742.38	764.36	780.33	
	C/D	836.43	-	837.44	859.42	<b>875.39</b>	
		834.42	1	<b>835.43</b>	857.41	<b>873.38</b>	
		832.40	2	<b>833.41</b>	855.39	871.36	
	B/H	1210.51	-	<b>1211.52</b>	<b>1233.50</b>	1249.47	
		1208.49	1	<b>1209.50</b>	<b>1231.49</b>	<b>1247.46</b>	
		1284.59	-	1285.60	1307.58	1323.55	643.30
	B/H	1282.58	1	<b>1283.59</b>	1305.57	1321.54	642.30
		1280.56	2	<b>1281.57</b>	<b>1303.55</b>	<b>1319.52</b>	641.29
		1278.54	3	1279.55	<b>1301.53</b>	1317.50	640.28
	B/H	1354.65	-	1355.66	1377.64	1393.61	678.33
		1352.63	1	<b>1353.64</b>	1375.62	1391.59	677.32
		1350.61	2	<b>1351.62</b>	1373.60	1389.57	676.31
		1346.58	4	1347.59	<b>1369.57</b>	1385.54	674.30
		1460.72	-	1461.73	1483.71	1499.68	731.37
	B	1458.70	1	1459.71	1481.69	1497.66	730.36
		1456.68	2	<b>1457.69</b>	<b>1479.67</b>	<b>1495.64</b>	729.35
		1454.66	3	<b>1455.68</b>	1477.65	1493.62	728.34
		1452.64	4	<b>1453.67</b>	1475.63	1491.60	727.33
	G	1924.87	-	1925.88	1947.86	1963.83	<b>963.44</b>
		1922.86	1	<b>1923.87</b>	1945.85	1961.82	<b>962.44</b>
	A	2012.94	-	2013.95	2035.93	2051.90	1007.48
		2008.90	2	2009.91	2031.89	2047.86	<b>1005.46</b>

\* Number (#) of Schiff bases (oximes) in the structure that were not reduced

### S3 Characterisation of fractions from the reaction with oxidised A<sub>2</sub>M oligomers and an excess ADH (water-soluble fraction)

The water-soluble fraction from the reaction of oxidised A<sub>2</sub>M oligomers and 10 equivalents ADH was separated by GFC (Figure S8). Collected fractions (I.-VI.) were purified and characterised by <sup>1</sup>H-NMR and MS. The <sup>1</sup>H-NMR spectra of the fractions are given in Figure S9-S14. The structures identified by MS and their theoretical mass (Da) are included in the figures. All structures were completely reduced as in contrast to the structures from the corresponding reaction with PDHA. The results from the MS characterisation are presented in Table S2.



**Figure S8:** GFC fractionation of **a)** a standard mixture of A<sub>n</sub>M oligomers for calibration and **b)** the water-soluble fraction obtained for oxidised A<sub>2</sub>M oligomers reacted with 10 equivalents ADH using the two-pot reductive amination protocol.

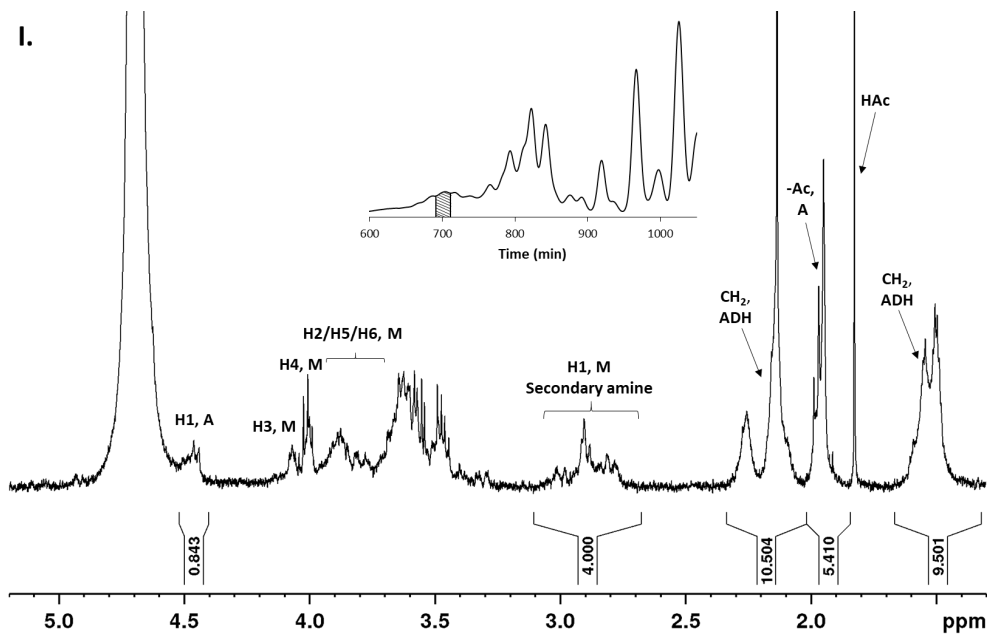


Figure S9: <sup>1</sup>H-NMR spectrum of fraction I. from Figure S8.

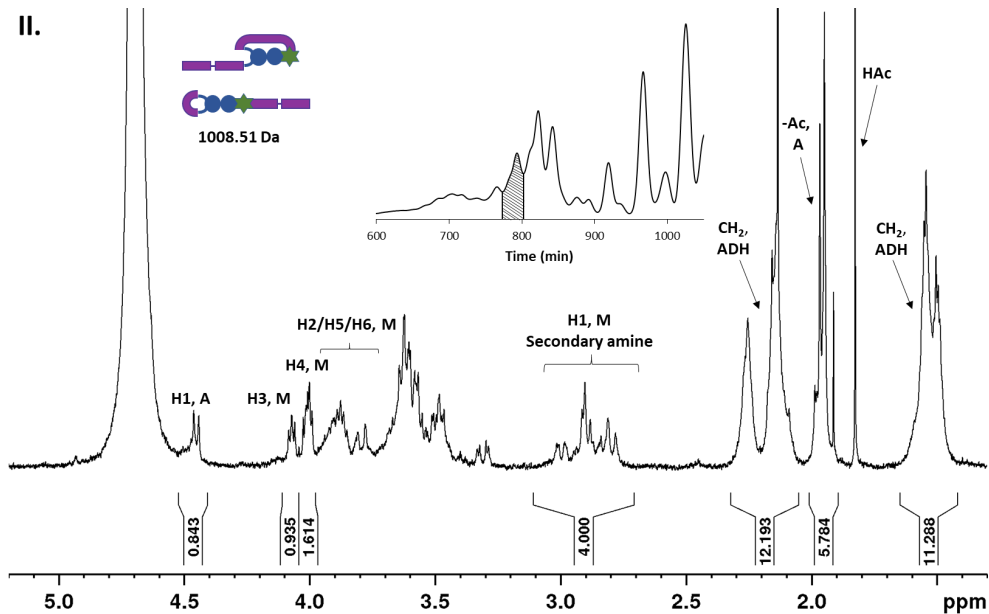
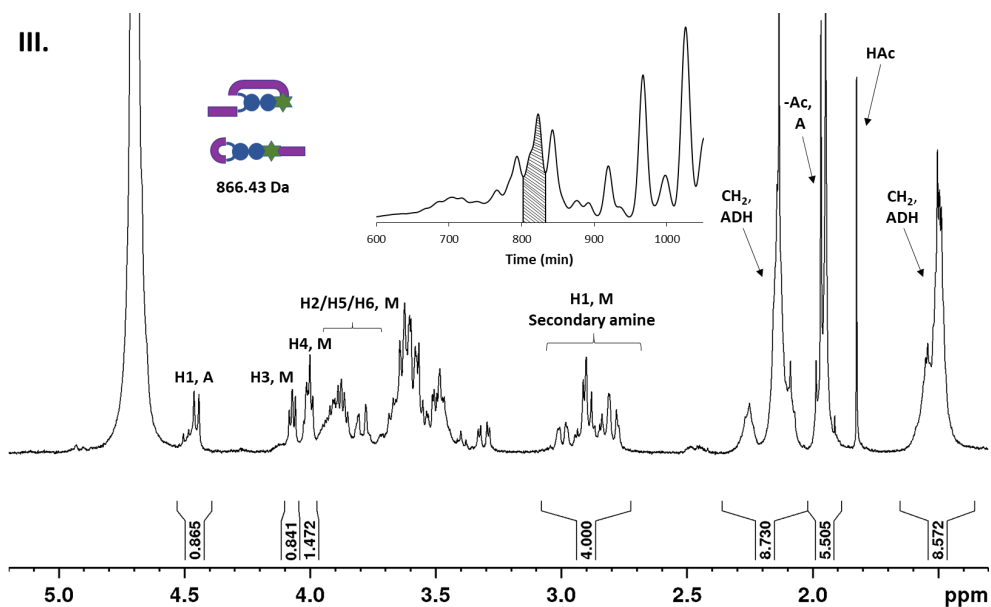
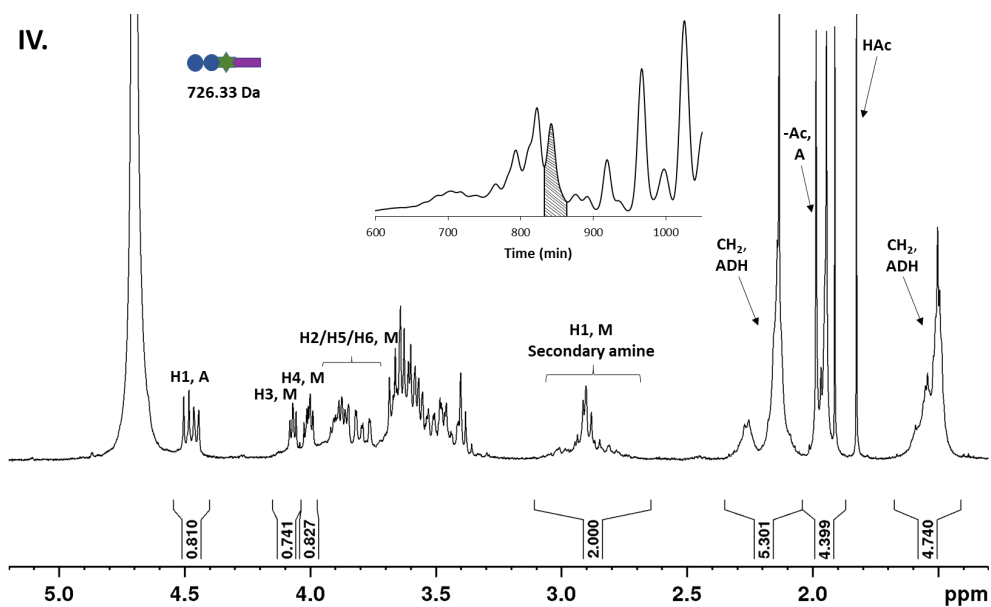


Figure S10: <sup>1</sup>H-NMR spectrum of fraction II. from Figure S8. The structures identified by MS are included in the figure.

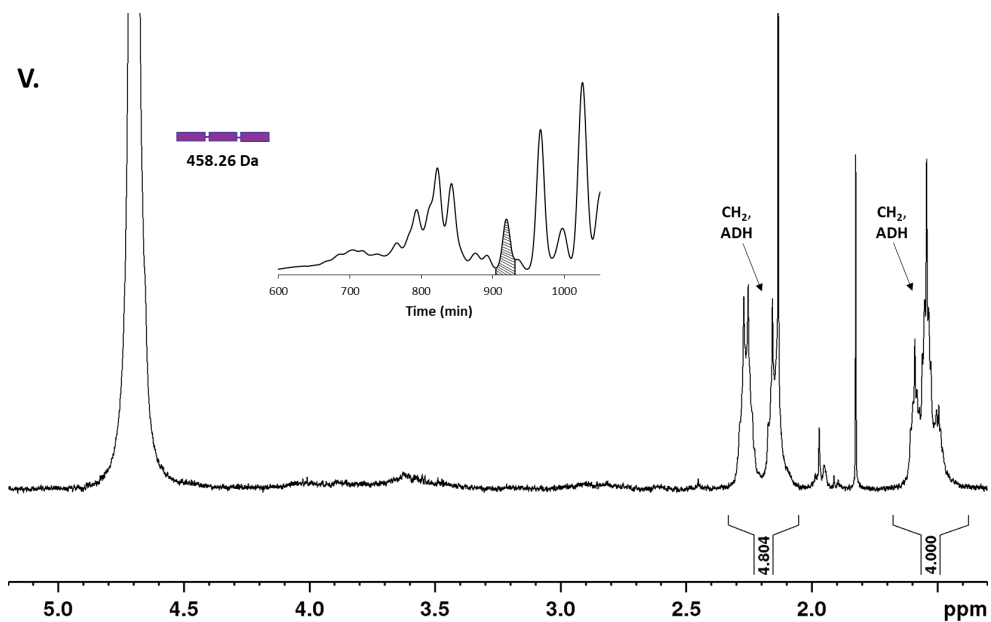


**Figure S11:** <sup>1</sup>H-NMR spectrum of fraction III. from Figure S8. The structures identified by MS are included in the figure.

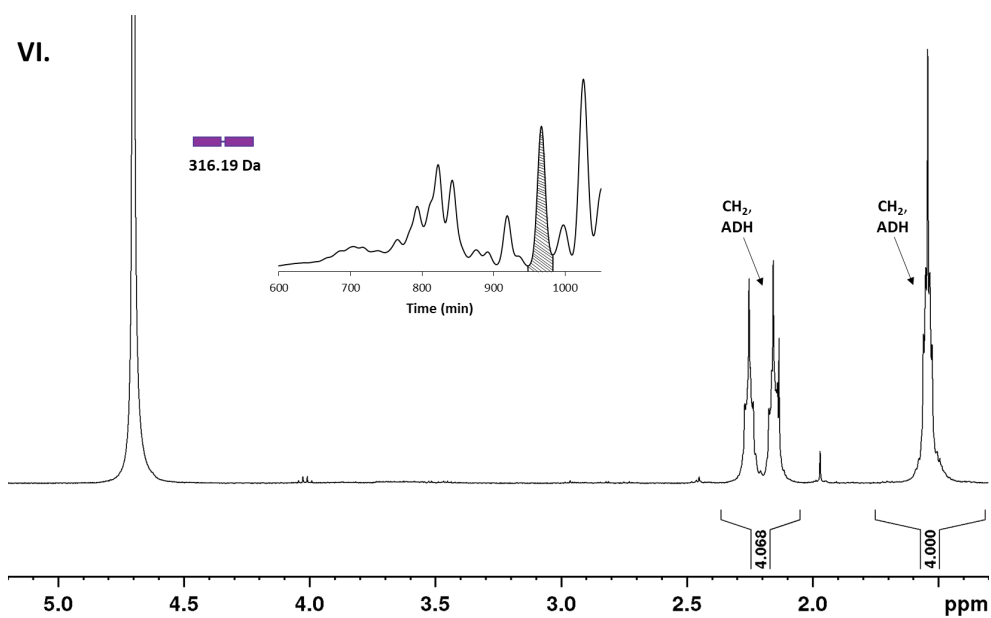


**Figure S12:** <sup>1</sup>H-NMR spectrum of fraction IV. from Figure S8. The structure identified by MS is included in the figure.










**Figure S13:** <sup>1</sup>H-NMR spectrum of fraction V. from Figure S8. The structure identified by MS is included in the figure.



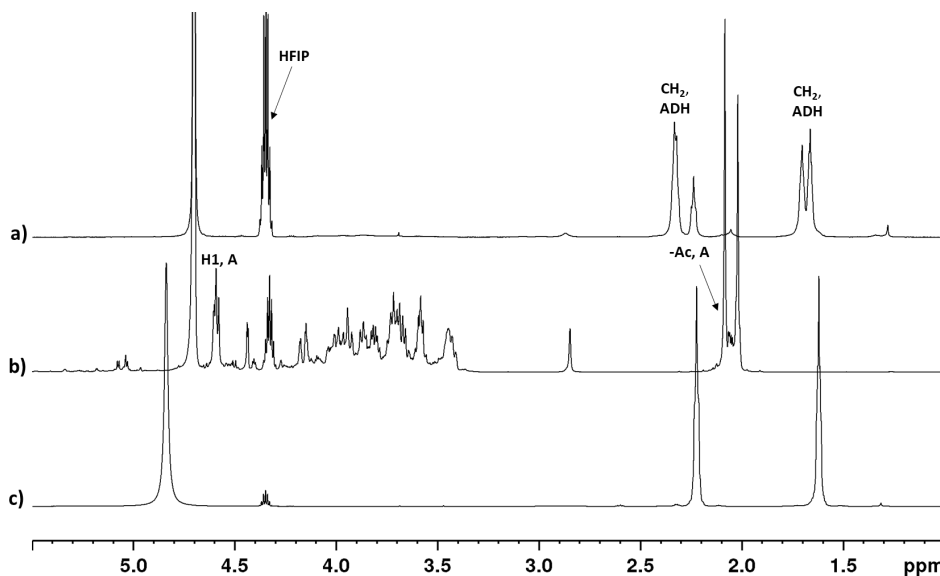
**Figure S14:** <sup>1</sup>H-NMR spectrum of fraction VI. from Figure S8. The structure identified by MS is included in the figure.

**Table S2:** Results of the MS characterisation of fractions obtained in the reaction with oxidised A<sub>2</sub>M oligomers and 10 equivalents ADH (fraction II.-VI.). All structures identified were fully reduced. The *m/z* ions in **bold** represent ions identified in the fractions.

Structure	Fraction	Theoretical mass (Da)	<i>m/z</i>			
			[M+H] <sup>+</sup>	[M+Na] <sup>+</sup>	[M+K] <sup>+</sup>	[M+2H] <sup>2+</sup>
	VI.	316.19	<b>317.20</b>	<b>339.18</b>	<b>355.15</b>	
	V.	458.26	<b>459.27</b>	<b>481.25</b>	<b>497.22</b>	
	IV.	726.33	<b>727.34</b>	<b>749.32</b>	<b>765.29</b>	
	III.	866.43	<b>867.44</b>	<b>889.42</b>	905.39	
	II.	1008.51	<b>1009.52</b>	<b>1031.50</b>	<b>1047.47</b>	<b>505.26</b>

#### S4 Characterisation of the water-insoluble fraction from the reaction with oxidised A<sub>2</sub>M oligomers and an excess ADH

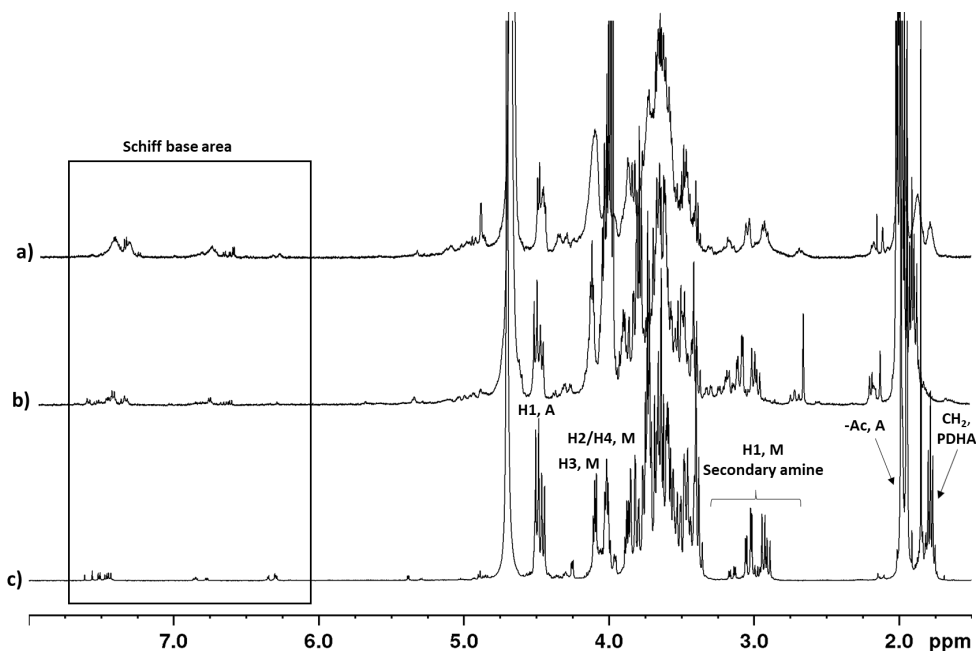
The water-insoluble fraction from the reaction of oxidised A<sub>2</sub>M oligomers with 10 equivalents ADH was dissolved in hexafluoro isopropanol (HFIP) and characterised by <sup>1</sup>H-NMR (Figure S15a). Spectra of A<sub>2</sub>M and ADH dissolved in HFIP is included for comparison (Figure S15b and c, respectively). Only resonances from the protons of ADH was observed in the spectrum obtained for the insoluble fraction, and hence, the sample only contained polymerized ADH.



**Figure S15:** <sup>1</sup>H-NMR spectra of **a)** the insoluble fraction from the reaction of oxidised A<sub>2</sub>M oligomers and 10 equivalents ADH, **b)** A<sub>2</sub>M and **c)** ADH in HFIP.

### S5 Characterisation of the reaction mixture formed with oxidised A<sub>2</sub>M oligomers and a sub-stoichiometric amount of PDHA

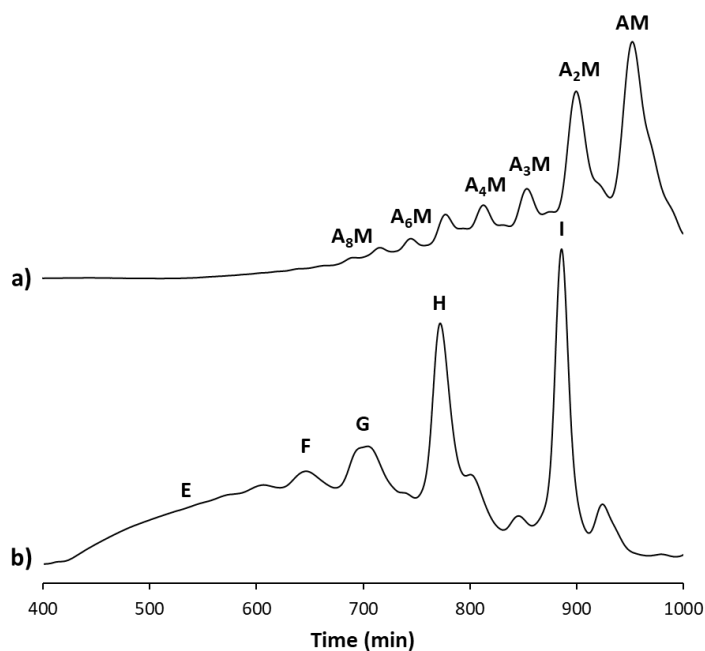
The reaction mixture obtained for oxidised A<sub>2</sub>M oligomers and 0.5 equivalents PDHA was characterized by <sup>1</sup>H-NMR and compared to the spectra obtained for the mixture formed with 10 equivalents PDHA and the purified A<sub>2</sub>M-PDHA conjugate (Figure S16). Compared to latter, the NMR spectra of the reaction mixtures formed with oxidised A<sub>2</sub>M oligomers were more complex. However, resonances resulting from the characteristic secondary amine protons (around 3.0 ppm) were present in the sample, confirming formation of conjugates. The resonances were, however, more complex than for the conjugates with unoxidised oligomers suggesting more than one type of conjugates formed. Compared to the reaction mixture formed with 10 equivalents PDHA (Figure S16b), the sub-stoichiometric amount of PDHA resulted in less defined proton resonances and higher intensity of resonances in the Schiff base area (6-8 ppm), indicating cyclic structures and more unreduced conjugates, respectively.



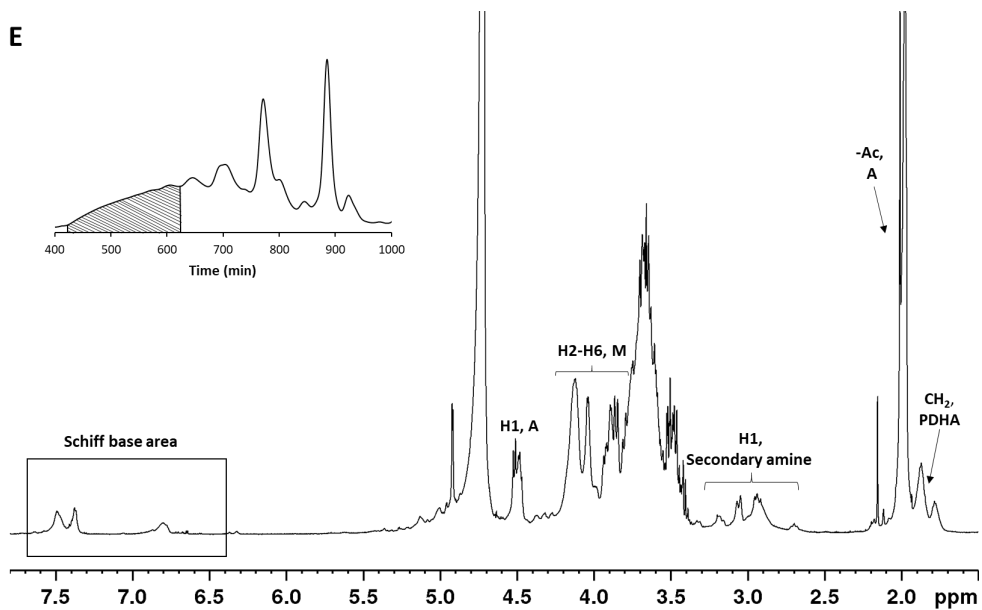
**Figure S16:** <sup>1</sup>H-NMR spectra of a) the reaction mixture formed with oxidised A<sub>2</sub>M oligomers and a sub-stoichiometric amount of PDHA (0.5 equivalents), b) the reaction mixture formed with oxidised A<sub>2</sub>M an excess of PDHA (10 equivalents) and c) the purified A<sub>2</sub>M-PDHA conjugate with annotations of identified resonances<sup>1</sup>.

## S6 Characterisation of fractions from the reaction with oxidised A<sub>2</sub>M and a sub-stoichiometric amount PDHA

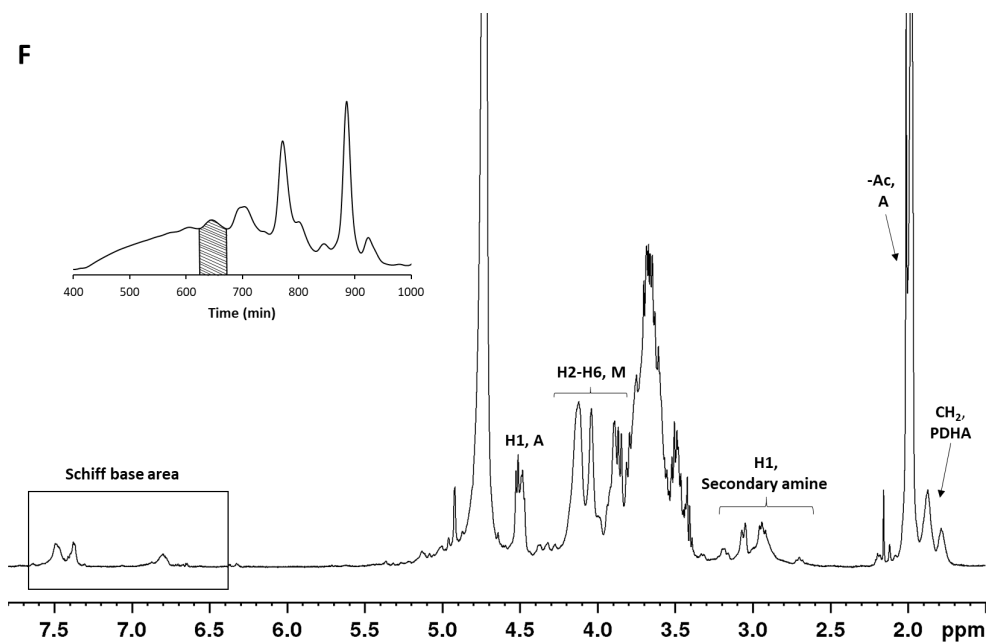
The reaction mixture obtained when oxidised A<sub>2</sub>M oligomers were reacted with 0.5 equivalents PDHA was fractionated by GFC (Figure S17). Collected fractions (E-I) were purified and characterised by <sup>1</sup>H-NMR and MS. The <sup>1</sup>H-NMR spectra of the fractions are given in Figure S18-S22. The structures identified by MS and their theoretical mass (Da) are included in the figures. The incomplete reduction of Schiff bases did, however, influence the observed mass of some of the structures. The results from the MS characterisation of the fractions are included in Table S1 (S2).



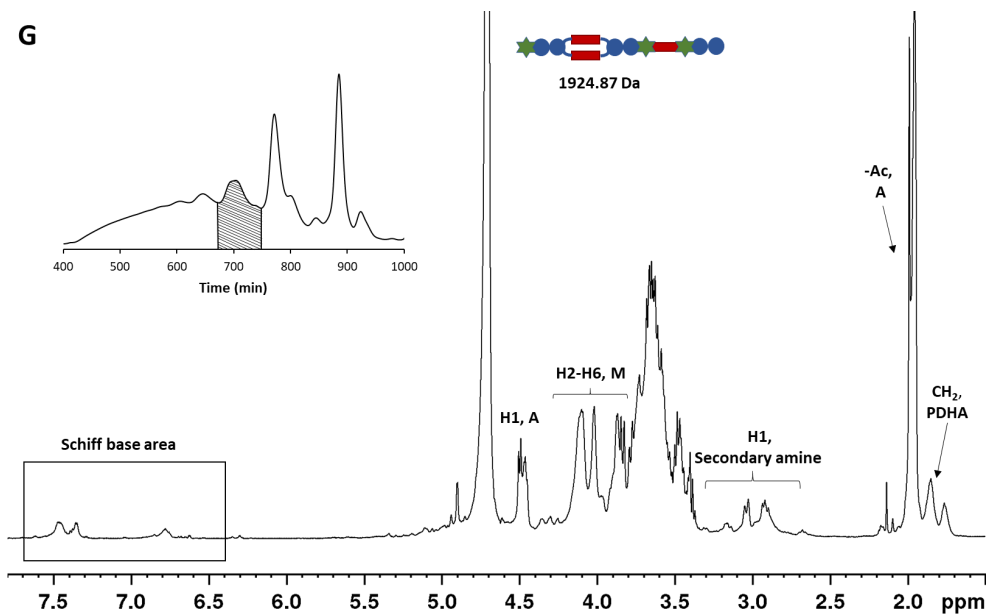
**Figure S17:** GFC fractionation of **a)** a standard mixture of A<sub>n</sub>M oligomers for calibration and **b)** the reaction mixture obtained for oxidised A<sub>2</sub>M oligomers reacted with 0.5 equivalents PDHA using the two-pot reductive amination protocol.



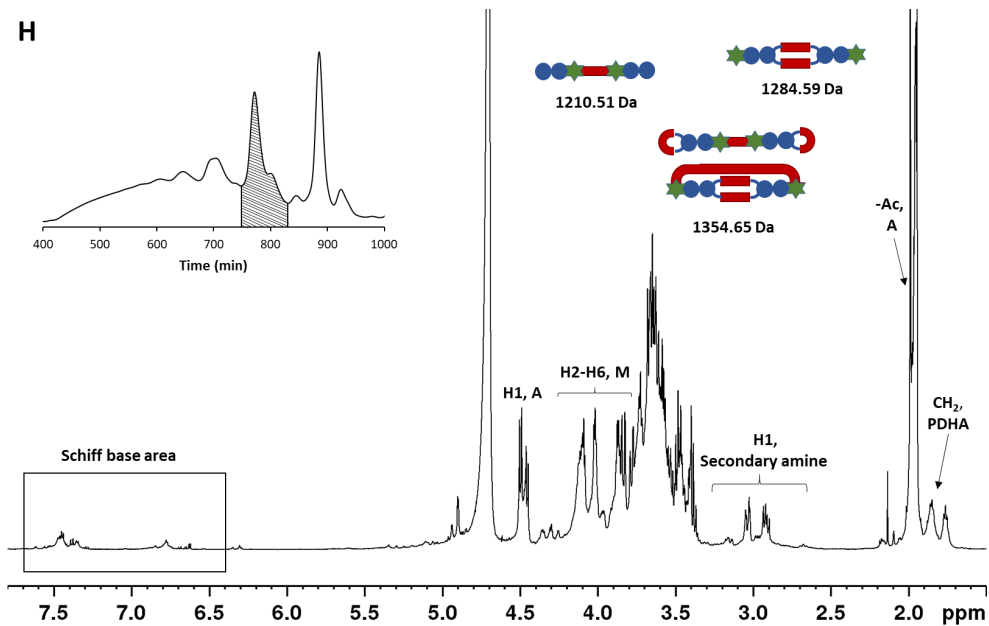
**Figure S18:** <sup>1</sup>H-NMR spectrum of fraction E from Figure S17.



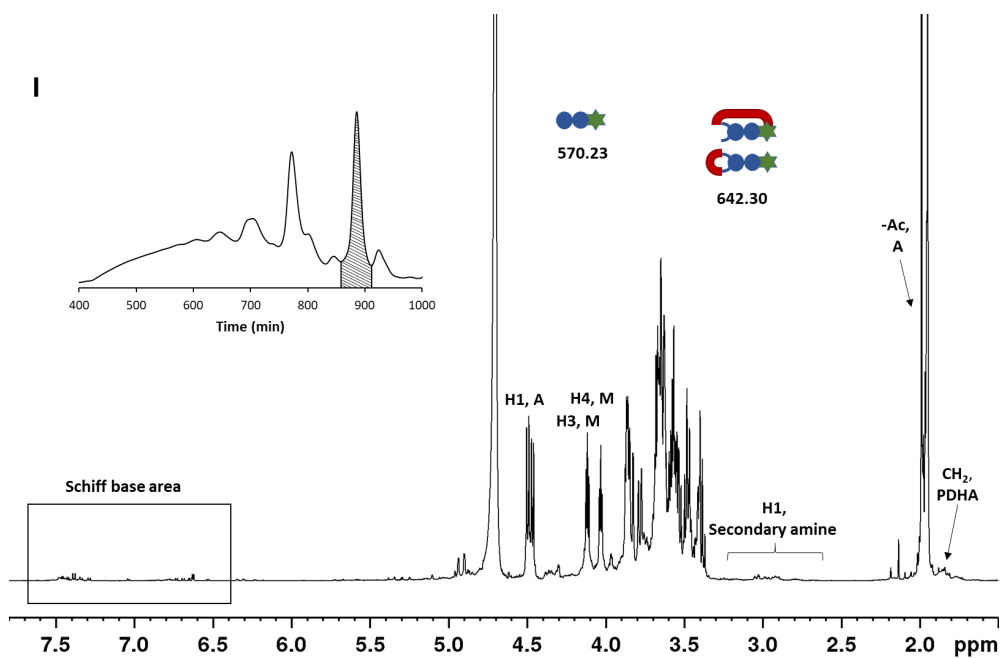
**Figure S19:** <sup>1</sup>H-NMR spectrum of fraction F from Figure S17.



**Figure S20:** <sup>1</sup>H-NMR spectrum of fraction G from Figure S17. The structure identified by MS is included in the figure.



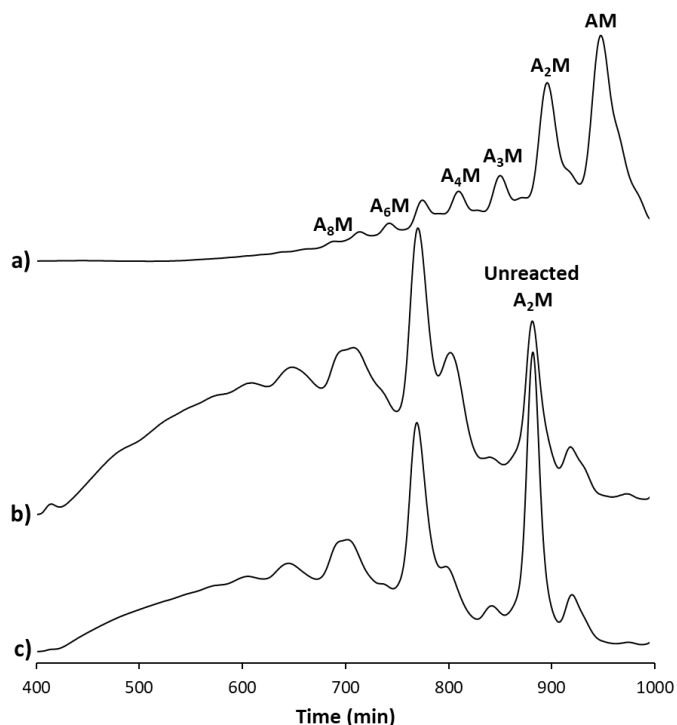
**Figure S21:** <sup>1</sup>H-NMR spectrum of fraction H from Figure S17. The structures identified by MS are included in the figure.



**Figure S22:** <sup>1</sup>H-NMR spectrum of fraction I from Figure S17. The structures identified by MS are included in the figure.

### S7 Reaction of oxidised A<sub>2</sub>M oligomers, obtained using 4 equivalents periodate, with a sub-stoichiometric amount of PDHA

Oxidised A<sub>2</sub>M oligomers, obtained using 4 equivalents periodate, were reacted with 0.5 equivalents PDHA. GFC fractionation of the reaction mixture was compared to the fractionation of the reaction mixture obtained when oxidised A<sub>2</sub>M oligomers, obtained using 2 equivalents periodate, were reacted with PDHA under the same conditions (Figure S23). The fractionation revealed a smaller relative fraction of unreacted oligomers when a higher concentration of periodate was used, indirectly confirming that a higher degree of oxidation was obtained using 4 equivalents periodate. The results also confirm that oxidised oligomers react more rapidly than unoxidised oligomers.

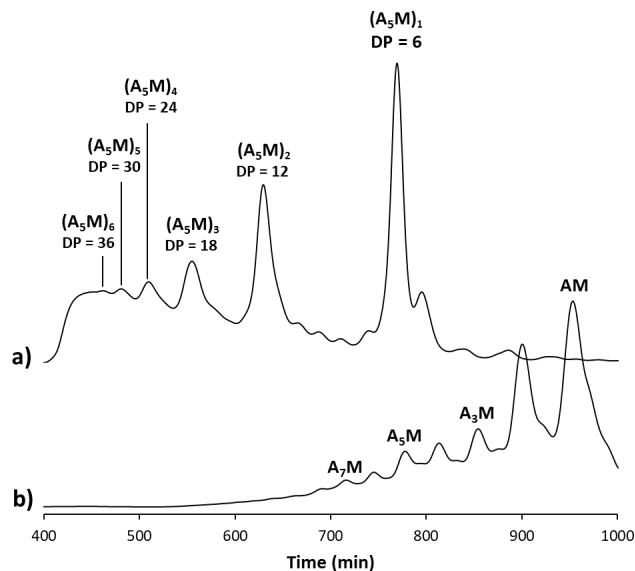


**Figure S23:** GFC fractionation of **a)** a standard mixture of  $A_nM$  oligomers for calibration, **b)** the reaction mixture obtained for  $A_2M$  oligomers, oxidised with 4 equivalents periodate, reacted with 0.5 equivalents PDHA and **c)** the reaction mixture obtained for  $A_2M$  oligomers, oxidised with 2 equivalents periodate, reacted with 0.5 equivalents PDHA using the two-pot reductive amination protocol.

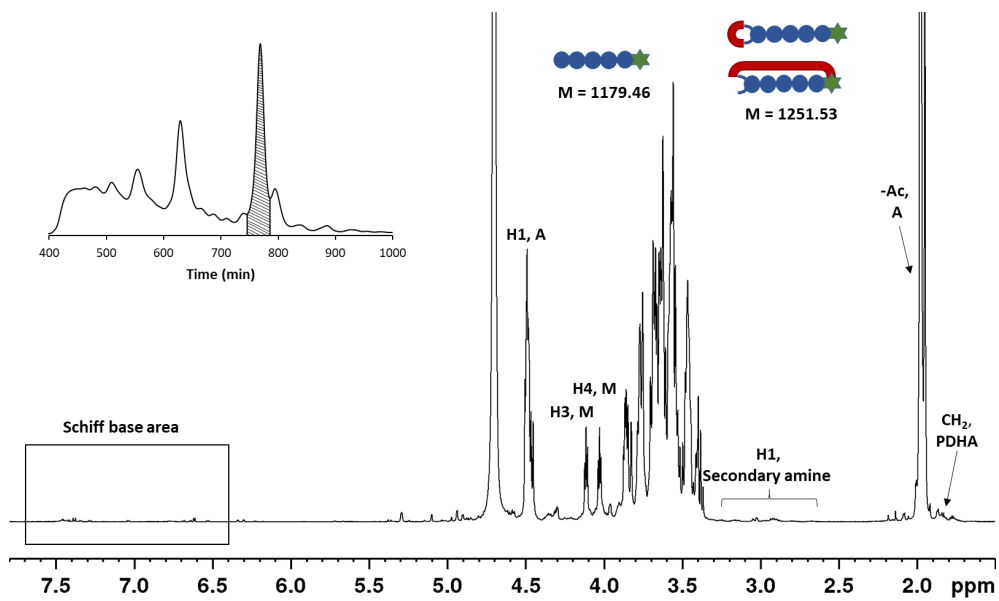
### S8 Characterisation of fractions from the reaction with oxidised $A_5M$ and a sub-stoichiometric amount PDHA

The reaction mixture obtained when oxidised  $A_5M$  oligomers were reacted with 0.5 equivalents PDHA was fractionated by GFC (Figure S24). Collected fractions were purified and characterised by  $^1H$ -NMR (and MS). The  $^1H$ -NMR spectra of the fractions are given in Figure S25 (main fraction) and Figure 26 (the remaining fractions). Structures identified by MS in the main fraction are included in Figure S25. The composition of the polymerised block structures was not identified due to limitations in the MS method for mass detection of larger ions.

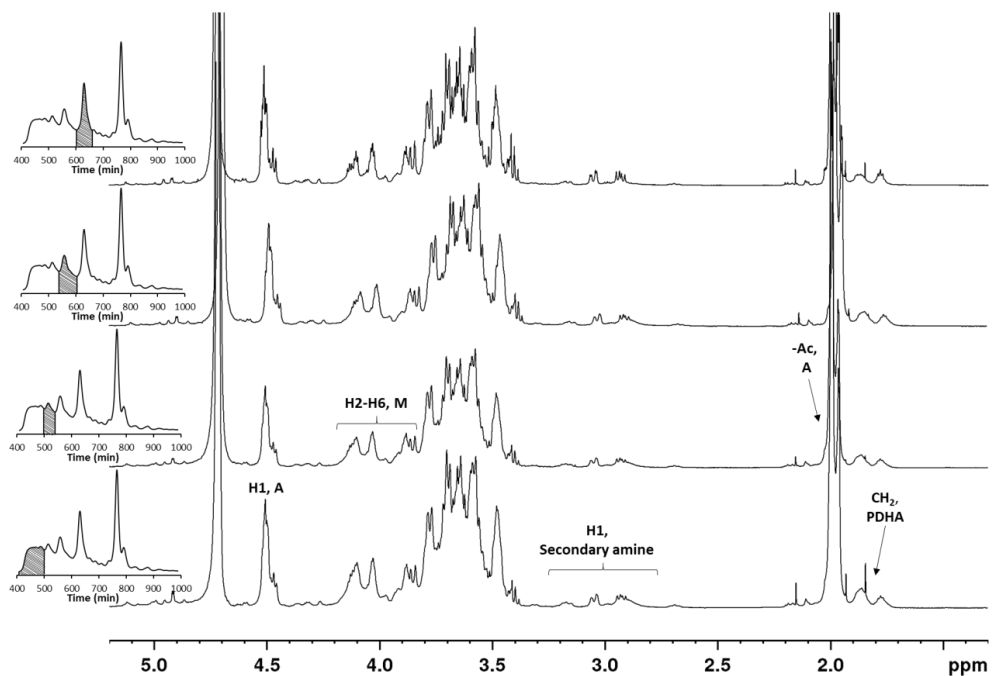




**Figure S24:** GFC fractionation of **a)** the reaction mixture obtained for oxidised  $A_5M$  oligomers reacted with 0.5 equivalents PDHA using the two-pot reductive amination protocol and **b)** a standard mixture of  $A_nM$  oligomers for calibration.



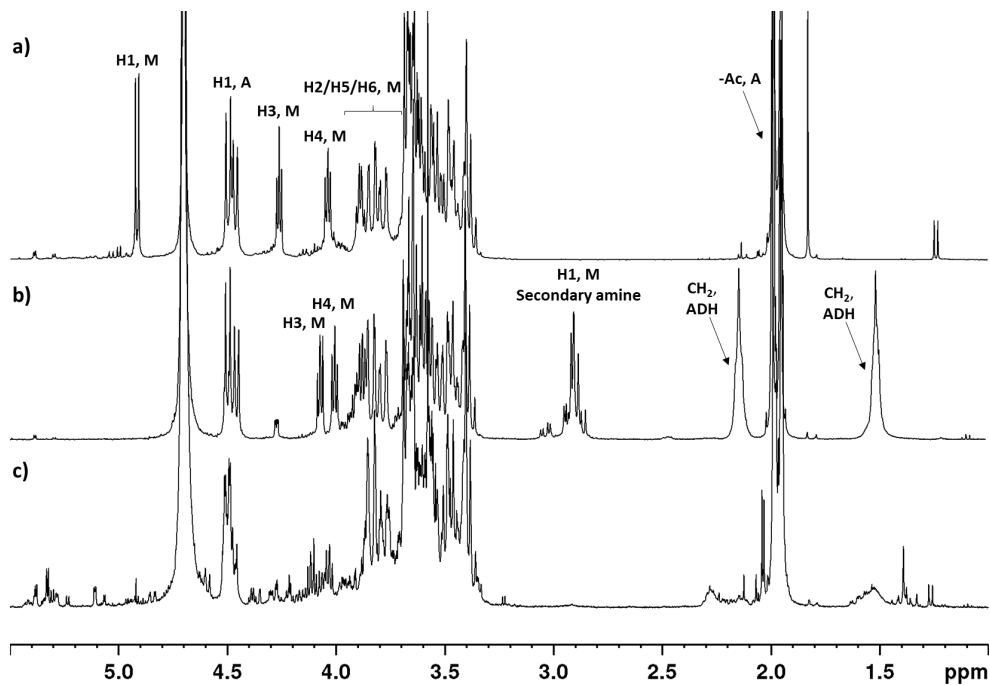
**Figure S25:**  $^1H$ -NMR spectrum of the main fraction from Figure S24. The structures identified by MS are included in the figure.



**Figure S26:**  $^1\text{H-NMR}$  spectra of fractions from Figure S24.

### S9 Periodate oxidation of $\text{A}_2\text{M-ADH-MA}_2$ diblocks

The  $\text{A}_2\text{M-ADH-MA}_2$  diblock was subjected to oxidation using 2 equivalents periodate.  $^1\text{H-NMR}$  spectrum after purification by dialysis is given in Figure S27, revealing complete disappearance of the resonances resulting from the secondary amines and a drastic change in the proton resonances resulting from the reducing end M residue. Hence, the results indicate that the secondary amine linkages of the diblock are destroyed during the periodate oxidation.



**Figure S27:**  $^1\text{H-NMR}$  spectra of **a)** a purified  $\text{A}_2\text{M}$  oligomer, **b)** the purified  $\text{A}_2\text{M-ADH-MA}_2$  diblock prior to oxidation and **c)** the resulting mixture after oxidation and dialysis.

## S10 References

1. Mo, I. V.; Dalheim, M. Ø.; Achmann, F. L.; Schatz, C.; Christensen, B. E. (2020) *2,5-anhydro-D-mannose end-functionalized chitin oligomers activated by dioxyamines or dihydrazides as precursors of diblock oligosaccharides*. *Biomacromolecules* 21 (7), 2884-2895.

ISBN 978-82-326-6212-8 (printed ver.)  
ISBN 978-82-326-6507-5 (electronic ver.)  
ISSN 1503-8181 (printed ver.)  
ISSN 2703-8084 (online ver.)



**NTNU**

Norwegian University of  
Science and Technology